KINEMATICS, DYNAMICS, AND CONTROL OF A PARTICULAR MICRO-MOTION SYSTEM

A Thesis

Submitted to the College of Graduate Studies and Research

in Partial Fulfillment of the Requirements

for the Degree of

Master of Science

in the

Department of Mechanical Engineering

University of Saskatchewan

Saskatoon, Saskatchewan

Canada

by

JING ZOU

July 2000

PERMISSION TO USE

In presenting this thesis in partial fulfillment of the requirements for a Master of Science degree from the University of Saskatchewan, the author agrees that the Libraries of this University may make it freely available for inspection. The author further agrees that permission for copying of this thesis in any manner, in whole or in part, for scholarly purposes may be granted by the professors who supervised the thesis work or, in their absence, by the Head of the Department or the Dean of the College in which the thesis work was done. It is understood that any copying or publication or use of this thesis or parts thereof for financial gain shall not be allowed without the author's written permission. It is also understood that due recognition shall be given to the author and to the University of Saskatchewan in any scholarly use which may be made of any material in this thesis.

Requests for permission to copy or to make other use of material in this thesis in whole or part should be addressed to:

Head of the Department of Mechanical Engineering,
University of Saskatchewan,
Saskatoon, Saskatchewan, Canada S7N 5A9

Abstract

In many applications such as chip assembly in the semiconductor industry, cell manipulation in biotechnology, and surgery automation in medicine, there is a need for devices which can perform very small motions (less than 100 μm) with very high positioning accuracy (in the submicron range) and complex trajectories. This range of motion is known as micro-motion. In this thesis, the research is described concerning the design of micro-motion systems. A particular interest of this research lies in a particular system that produces planar micro-motions and has been found useful in semi-conductor industries.

The general methodology of designing such systems is based on an observation made by the author. It is not difficult to find that most of the micro-motion systems commercially available were developed based on the ball-screw and DC-servo or stepper motor component systems. These systems have their inherent problems, such as backlash, friction, and assembly errors, which usually call for high precision manufacturing technologies and, thus, cause high cost. The compliant mechanism concept, which suggests generating motions based on deformations in a member of compliant material, was proposed around the 1990s. The compliant mechanism concept has been used in mechanism design for years; however, it has not been used for systems with a feedback control need. Therefore, using the compliant mechanism concept for building micro-motion systems appears to be a promising methodology and worth studying.

The goal of the research described in this thesis is to develop an understanding of and a design tool for a particular planar micro-motion system (called the *RRR compliant mechanism*) which is constructed based on the compliant mechanism concept. This system consists of three PZT actuators and a specially shaped member of compliant material. The structure of this system is symmetrical to the center of the system which serves as the end-effector of the system to perform two translations and one rotation in a

plane. As a result, the following contributions of this research are described in this thesis.

A Constant-Jacobian method for kinematic analysis of the RRR compliant mechanism is developed and verified using the pseudo rigid body model (PRBM) concept. The result of the kinematic calibration based on this method shows an excellent agreement with the experimental result. The PRBM concept leads to a lumped model of materially continuous systems and, hence, to a computationally efficient model.

The finite element analysis of the RRR compliant mechanism, using the ANSYS program, is performed. In this analysis, mesh is directly generated on a compliant material, which differs from the lumped approximation procedure associated with PRBM. This finite element model is a parametric one and is completely determined by nine parameters. A change in any one of these parameters will update the mesh automatically. This is very useful for an optimal selection of parameters to achieve some set of design objectives. The result of the finite element analysis is compared with those obtained using other methods, including the Constant-Jacobian method and the experiment, which further confirms that the Constant-Jacobian method is an excellent method for kinematic analysis in terms of computational efficiency and modeling accuracy.

A novel dynamic model is further developed based on the Constant-Jacobian kinematics, the PRBM concept, and other simplification procedures that leave out the terms of order $o(\Delta l^2)$ and above (Δl=0-12 μm). Consequently, this dynamic model achieves both computational efficiency and modeling accuracy. This dynamic model is used for feedback control simulation studies for the RRR compliant mechanism.

Acknowledgement

The help from many people has made the present work possible. The research described in this thesis was carried out in the Advanced Engineering Design Laboratory of the University of Saskatchewan, under the supervision of Dr. L.G. Watson and Dr. Chris Zhang. I appreciate Dr. Watson's willingness to give me the freedom to choose a research topic of interest to me. I appreciate Dr. Zhang for allowing the author to work in his research project, that is, micro-motion systems. It is difficult to choose appropriate words to express my thanks for their effective and efficient direction, critical comments, and constructive suggestions.

The author is grateful to other members of her advisory committee: Dr. A. Dolovich, Dr. S. Habibi, Dr. S. Sokhansanj (the external examiner). Their valuable support and constructive suggestions have greatly improved the present work. Assistance from the computing staff of the College of Engineering is gratefully acknowledged.

The author acknowledges Dr. H. M. Morelli from the English as a Second Language (ESL) Centre of the University of Saskatchewan for reviewing the draft version of this thesis and giving the author valuable suggestions in technical English writing.

The author wishes to thank the Natural Sciences and Engineering Research Council (NSERC), Atomic Energy of Canada Limited (AECL), and the College of Graduate Studies and Research for their financial support for this study.

Dedication

To:

my parents, Cai-Ying and Qing-Yuan

TABLE OF CONTENTS

PERMISSION TO USE	i
ABSTRACT	ii
ACKNOWLEDGEMENTS	iv
DEDICATION	v
TABLE OF CONTENTS	vi
LIST OF TABLES	ix
LIST OF FIGURES	x
LIST OF NOTATION AND SYMBOLS	xii
1 INTRODUCTION	1
1.1 Background and Motivation	1
1.2 Literature Review	3
1.3 Research Objectives	7
1.4 General Methodology	9
1.5 Organization of the Thesis	10
2 KINEMATIC DESIGN AND ANALYSIS	12
2.1 Introduction	12
2.2 RRR Compliant Mechanism	13
2.3 Mathematically Exact Kinematic Analysis	18
2.4 Constant-Jacobian Approach - an Approximate Kinematic Analysis	22
2.5 Kinematic Calibration	24
2.6 Results and Discussions	26
2.7 Conclusion	29
3 FINITE ELEMENT MODELING AND SIMULATION	30
3.1 Introduction	30
3.2 Parametric FEM Model of the RRR Compliant Mechanism	31
3.2.1 Identification of Parameters	31

3.2.2 Procedure for Developing an ANSYS Model 31
3.2.3 Acquisition of the End-effector Motion 34
3.3 Results and Discussion 36
3.4 Conclusion 44

4 DYNAMIC MODELING 46
4.1 Introduction 46
4.2 Lagrangian Equation for the RRR Mechanism 47
4.2.1 Kinetic and Potential Energy Equations 47
4.2.2 Calculation of $\Delta\varphi_{Ai}$, $\Delta\varphi_{Bi}$ and $\Delta\varphi_{Ci}$ in the Potential Energy Equation 48
4.2.3 Calculation of Velocity Terms in the Kinetic Energy Equation 54
4.3 Dynamic Model 57
4.4 Implementation of the Dynamic Model 59
4.5 Conclusion 59

5 DYNAMIC CONTROL AND SIMULATION 60
5.1 Introduction 60
5.2 Control Strategies for Robotic Manipulators 60
5.3 CTC Controller for the RRR Compliant Mechanism 62
5.3.1 Introduction of CTC 62
5.3.2 CTC of the RRR Compliant Mechanism 64
5.4 Simulation Results 65
5.5 Conclusion 70

6 CONCLUSION 71
6.1 Introduction 71
6.2 Research Findings and Further Discussion 72
6.2.1 Constant-Jacobian Method 72
6.2.2 Novel Dynamic Model for Real-time Control Applications 73
6.2.3 Finite Element Method for Compliant Mechanisms 74

6.2.4 Unique Planar Micro-Motion Device 74
6.3 Future Work 75

REFERENCES 77

APPENDIX A: EXPERIMENT SET-UP 81

APPENDIX B: PROGRAM FOR THE KINEMATIC CALIBRATION 85

APPENDIX C: FEM MODELING 90

APPENDIX D: DYNAMIC MODEL 106

D.1 Parametric form 106

D.1.1 $\mathbf{W}_i(\mathbf{l})$ and $\mathbf{V}_i(\mathbf{l})$, i=1,2,3 106

D.1.2 $\mathbf{K}(\mathbf{l})$, $\mathbf{C}(\mathbf{l},\dot{\mathbf{l}})$, and $\mathbf{H}(\mathbf{l})$ 114

D.2 Non-parametric form 144

APPENDIX E: CONTROL SIMULATION PROGRAM 148

List of Tables

Table 5.1	Some values of K_P and K_V in an independent-joint PD control law	62
Table 6.1	Comparison of the RRR compliant mechanism with the one developed by Ryu et al. (1997)	75
Table D.1	Initial coordinates (in m) of all the joint points: A_i, B_i and C_i (i=1,2,3)	144
Table D.2	Mass (in kg) and moment of inertia (in kg·m^2) of the end-effector and all the links	144
Table D.3	Other parameter values	144

List of Figures

Figure 1.1	Schematic diagram of a compliant mechanism	3
Figure 1.2	Schematic diagram of a flexure hinge	4
Figure 1.3	Micro-positioning stage (Scire and Teague, 1978)	5
Figure 1.4	Three typical compliant segments	7
Figure 1.5	PRBM of the RRR compliant mechanism	8
Figure 2.1	Initial position of the PRBM of the RRR compliant mechanism	14
Figure 2.2	RRR compliant mechanism	15
Figure 2.3	Schematic diagram of the driving elements	16
Figure 2.4	Schematic diagram of the flexure hinge	17
Figure 2.5	Simulation results versus experimental results	26
Figure 2.6	Difference between the Constant-Jacobian and exact solutions	27
Figure 2.7	Exact results and Constant-Jacobian results versus the experimental results	28
Figure 3.1	FEM model of the RRR compliant mechanism	32
Figure 3.2	Calculation of the yaw angle	35
Figure 3.3	Comparison of FEM results with other results	36
Figure 3.4	Von Mises stress distribution at 12 μm elongation of PZT actuator 1	38
Figure 3.5	Maximum Von Mises stress at 0-12 um elongation of PZT actuator 2	39
Figure 3.6	Von Mises stress distribution at 12 μm elongation of PZT actuator 2	40
Figure 3.7	Maximum Von Mises stress at 0-12 um elongation of PZT actuator 2	41
Figure 3.8	Von Mises stress distribution at 12 μm elongation of PZT actuator 3	42
Figure 3.9	Maximum Von Mises stress at 0-12 um elongation of PZT actuator 3	43
Figure 3.10	Von Mises stress distribution at 12 μm elongation of PZT actuator 1, 2, 3	44
Figure 4.1	Schematic diagram for the potential energy equation	49
Figure 5.1	Independent-joint PD control	61
Figure 5.2	Block diagram of computed torque control	63

Figure 5.3	Computed torque controller for the RRR compliant mechanism	65
Figure 5.4	Desired and actual displacement of PZT actuator 1	66
Figure 5.5	Displacement tracking error of PZT actuator 1	67
Figure 5.6	Desired and actual velocity of PZT actuator 1	68
Figure 5.7	Velocity tracking error of PZT actuator 1	69
Figure 5.8	Actual and theoretical maximum generation force of PZT actuator 1	70
Figure A.1	Assembled RRR compliant mechanism	82
Figure A.2	Manufactured compliant piece	83
Figure A.3	Experimental setup	83
Figure A.4	Measuring method for the motion of the end-effector	84
Figure C.1	Local coordinate system (LCS) and the positioning key points in the modeling of the RRR compliant mechanism	90

List of Notation and Symbols

The most commonly used symbols in this thesis are listed in this section. The numbers in the right hand of this table indicate the page numbers where the corresponding notation or symbol first appears in this thesis.

ROMAN LETTERS

A_i	joint point in RRR mechanism (i=1,2,3)	14
A_i^0	initial position of joint point A_i in RRR mechanism (i=1,2,3)	19
B_i	joint point in RRR mechanism (i=1,2,3)	14
B_i^0	initial position of joint point B_i in RRR mechanism (i=1,2,3)	19
b	thickness of the flexure hinge	16
C_i	joint point in RRR mechanism (i=1,2,3)	14
C_i^0	initial position of joint point C_i in RRR mechanism (i=1,2,3)	19
$\mathbf{C}(\mathbf{l},\dot{\mathbf{l}})$	centrifugal and coriolis terms of the dynamic model of RRR compliant mechanism	58
D_x	domain of the end-effector motion along x direction	24
D_y	domain of the end-effector motion along y direction	24
D_γ	domain of the end-effector motion along γ direction	24
$\mathbf{e}$	displacement tracking error vector in the joints	63
$\dot{\mathbf{e}}$	velocity tracking error vector in the joints	63
E	young's modulus	18
$\mathbf{H}(\mathbf{l})$	gravity term of the dynamic model of RRR compliant mechanism	58
$\mathbf{l}$	actual displacement vector of PZT actuators	64
$\dot{\mathbf{l}}$	Actual velocity vector of the PZT actuators	64
I_{AiBi}	moment of inertia of link A_iB_i (i=1,2,3)	48

I_{BiCi}	moment of inertia of link B_iC_i (i=1,2,3)	48
$\mathbf{l_e}$	displacement error of PZT actuators	64
$\dot{\mathbf{l}}_{\mathbf{e}}$	velocity error of PZT actuators	64
I_o	moment of inertia of the end-effector	48
$J_{\exp}$	experimentally obtained Jacobian matrix	84
J_l	Jacobian Matrix that relates the elongation of PZT actuators to end-effctor motion	22
J_l^0	Jacobian Matrix J_l at initial position	22
J_l^1	first row of J_l^0	55
J_l^2	second row of J_l^0	55
J_l^3	third row of J_l^0	55
J_θ	Jacobian Matrix that relates the rotation of input links to end-effector motion	23
J_θ^0	Jacobian Matrix J_θ at initial position	23
K	kinetic energy	47
	length of link OA_i (i=1,2,3)	21
K_b	stiffness of a torsional spring	16
$\mathbf{K(l)}$	inertia item of the dynamic model of RRR compliant mechanism	58
K_P	proportional gain	61
$\mathbf{K_P}$	proportional gain diagonal matrix	63
K_V	derivative gain	61
$\mathbf{K_V}$	proportional and derivative gain diagonal matrix	63
L	subtraction of kinetic energy and potential energy	47
l_i	generalized displacements of actuators	47
$\dot{l}_i$	generalized velocity of actuators	47
L_{AB}	length of link A_iB_i (i=1,2,3)	13
L_{BC}	length of link B_iC_i (i=1,2,3)	13

L_s	length of the side of equilateral triangular moving platform	53
M	bending moment of a flexure hinge	16
M_{BiCi}	mass of link B_iC_i (i=1,2,3)	48
M_o	mass of the moving platform of RRR mechanism	47
n_y	safety factor of yield stress	38
O	center point of the rigid member of RRR compliant mechanism	2
P	potential energy	47
p_i	design parameters of RRR mechanism (i=1,2,3,...5)	24
p_i^*	optimal p_i (i=1,2,3,...5)	24
$p^l{}_j$	lower bound of p_j (j=1,2,3,...5)	24
$p^u{}_j$	upper bound of p_j (j=1,2,3,...5)	24
P_{Ai}	potential energy of the torsional spring at point A_i (i=1,2,3)	48
P_{Bi}	potential energy of the torsional spring at point B_i (i=1,2,3)	48
P_{Ci}	potential energy of the torsional spring at point C_i (i=1,2,3)	48
Q	force generated by a PZT actuator	67
$\mathbf{Q}$	force vector produced by PZT actuators	64
Q_i	generalized force on the actuators	47
r	radius of the notch in the flexure hinge	16
R	distance between the center and vertex of rigid plate	13
R_0	dimension of the driving element of RRR compliant mechanism	15
$\hat{R}^{-1}$	inverse dynamic model of a plant	63
t	thickness of a flexure hinge	16
V	voltage applied on a PZT actuator (Volt)	67
V_o	velocity of the moving platform	47
W_z	section modulus	17
x	coordinate direction	13
Δx	displacement of end-effector in x direction	19

y	coordinate direction	13
Δy	displacement of end-effector in y direction	19

GREEK LETTERS

θ	Rotational angle	2
$\ddot{\theta}^*$	"corrected" acceleration in CTC control law	63
θ	actual displacement vector in joints	63
$\dot{\theta}$	actual velocity vector in joints	63
$\ddot{\theta}_d$	desired acceleration vectors in joints	63
θ_d	desired displacement vectors in joints	63
$\dot{\theta}_d$	desired velocity vectors in joints	63
ψ_1	a design parameter of the RRR compliant mechanism	23
ψ_2	a design parameter of the RRR compliant mechanism	23
ψ_3	angle dependent on ψ_2	23
$\sigma_{\max}$	maximum stress	17
σ_p	material's proportional limit	17
σ_y	yield stress of a material	38
[σ]	allowable stress	17
$[\sigma]_y$	allowable yield stress of a material	38
γ^0	angle of the rigid piece at the initial position	34
γ'	angle of the rigid piece at any other position	34
ω_{AiBi}	angular velocity of link A_iB_i (i=1,2,3)	48
ω_{BiCi}	angular velocity of link B_iC_i (i=1,2,3)	48
ω_o	angular velocity of the end-effector	48

$\lvert\Delta_{AE}\rvert$	absolute value of the difference between Constant-Jacobian result and experimental result	28
$\lvert\Delta_{EE}\rvert$	absolute value of the difference between mathematically exact result and experimental result	28
Δl	elongation of a PZT actuator	15
Δl_1	elongation of PZT actuator 1	15
Δl_2	elongation of PZT actuator 2	15
Δl_3	elongation of PZT actuator 3	15
$\Delta\varphi_{Ai}$	increment in the relative angle at joint point A_i (i=1,2,3)	48
$\Delta\varphi_{Bi}$	increment in the relative angle at joint point B_i (i=1,2,3)	48
$\Delta\varphi_{Ci}$	increment in the relative angle at joint point C_i (i=1,2,3)	48
$\Delta\gamma$	rotation angle of the rigid piece	35
$\Delta\theta$	angular displacement of RRR mechanism	15
τ	torque applied on the plant	61
τ^*	corrected torque in CTC control law	64
ρ	Density	18
α	thermal expansion ratio	18

ACRONYMS

ANSYS	commercial finite element analysis software (ANSYS®)	9
CTC	computed torque control	60
DOF	degree of freedom	4
FEM	finite element method	9
PD	proportional derivative	10
PRBM	pseudo-rigid-body model	4
PZT	piezoelectric Technology	2
RRR	a particular compliant mechanism	7

Chapter 1
Introduction

1.1 Background and Motivation

In many applications such as chip assembly in the semiconductor industry, cell manipulation in biotechnology, and surgery automation in medicine, there is a need for devices to perform very small motion (less than 100 μm) with very high positioning accuracy (in the submicron range) and complex trajectories. This range of motion is known as micro-motion (Hara and Sugimoto, 1989).

A straightforward approach to developing micro-motion systems is based on conventional servomotors, such as DC-servo or stepper motors and ball screws or other types of rigid linkages. But, these systems have inherent problems, such as backlash, friction and assembly errors, which significantly hinder the development of both cost-effective and functional micro-motion systems.

Another approach to developing such systems is based on the compliant mechanism concept. A compliant mechanism is a flexible monolithic structure. It makes use of flexible elements with notches and holes cut on them to deliver the desired motion as opposed to the use of rigid-body elements and joints. It was reported that systems built based on the compliant mechanism concept make it possible to achieve 0.01 μm positioning accuracy (Hara and Sugimoto, 1989; Her and Chang, 1994). It is, however, noted that the motion range of such systems is small, in the order of 10 μm. In order to achieve a long-range motion with high positioning accuracy and complex motion trajectories, micro-motion systems can be integrated with macro-motion systems, which are designed based on the rigid links and joints concept.

Driving elements for compliant mechanisms are usually unconventional actuators which are developed based on piezoelectric technology (PZT for short), due to their advantages of fast response and smooth and high-resolution displacement characteristics (Lee and Arjunan, 1989). Currently, the displacement generated by a PZT actuator is within the range of 15 μm and the resolution can be sub-nanometer.

A micro-motion system based on the compliant mechanism concept can be constructed as a closed-loop configuration or a parallel manipulator (in the field of robot mechanisms). The closed-loop mechanism configuration can provide better stiffness and accuracy, which should be one of the important design goals for micro-motion systems. Moreover, they allow the actuators to be fixed to the ground, which thus minimizes the inertia of moving parts.

This thesis work is concentrated on the understanding, designing, modeling and controlling of the compliant micro-motion mechanism shown in Figure 1.1. This mechanism consists of a member of compliant material and a member of rigid material which is geometrically an equilateral triangle. The mechanism is driven by three PZT actuators, PZT 1, PZT 2 and PZT 3, and presents its end-effector motion at the center point O of the rigid member, as illustrated in Figure 1.1. This mechanism is a typical one used to produce planar micro-motions with two translations (x and y) and one rotation (θ), and has been found applications in the semiconductor industry (Ryu et al., 1997). It is noted that in industrial applications, the terms *micro-positioning stage* and *single-axis stage* are used. They are to represent a kind of micro-motion system, and thus they are used interchangeably with the term *micro-motion system* in this thesis.

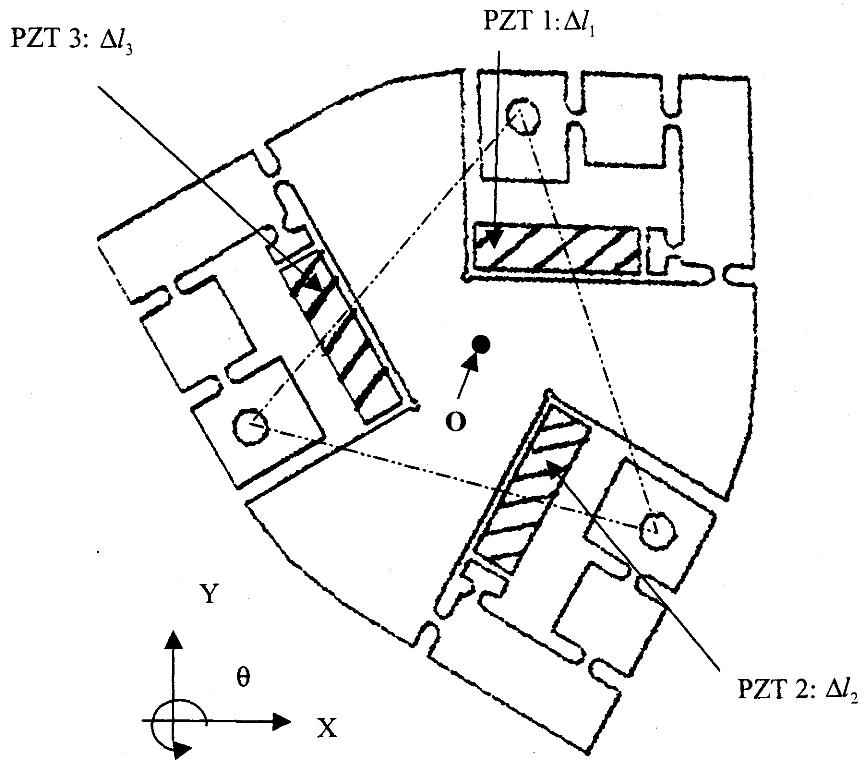

Figure 1.1 Schematic diagram of a compliant mechanism

1.2 Literature Review

Since the 1970s, compliant micro-positioning stages, which consist of piezoelectric actuators and flexure hinges, and which can produce linear motions have been developed,. Figure 1.2 shows a typical type of flexure hinge, where F stands for the force and M for the bending moment; the other symbols are self-explanatory. The flexure hinge allows a relative deflection between the left and right portions, as implied in Figure 1.2. Scire and Teague (1978) designed a compliant single-axis stage (see Figure 1.3a) which combined a PZT actuator and a flexure pivoted lever operating as a displacement amplifier. Figure 1.3b shows a schematic diagram for analysis of this lever operating system. In both figures, the PZT actuator and the end-effector are shown. The labels, R, R_1, R_2, and R_3, describe the correspondence between these two schematic diagrams in this figure. Furukawa and Mizuno (1990) designed a flexure-hinged translation stage, which

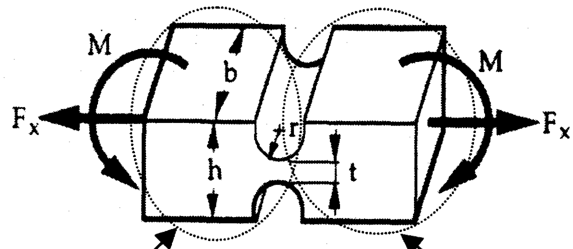

Figure 1.2 Schematic diagram of a flexure hinge

contained a linkage as a mechanical amplifier and a guidance system for rectilinear movement. It is noted that these types of compliant mechanisms were only able to generate linear motions and, hence, their applications are limited.

Since the 1980s, micro-positioning stages that can produce more complex motions than just linear translations have been developed. Lee and Arjunan (1991) designed a spatial 3-DOF (Degree of Freedom) compliant micro-positioning in-parallel stage. The kinematic analysis of this mechanism, based on the pseudo-rigid-body model (PRBM) approach, was studied, and a dynamic model of the piezo-electric actuated link was determined experimentally. Ryu et al. (1997) designed a flexure hinge based XYθ stage and discussed the optimal design of the stage. The objective defined in their optimization problem was to achieve a maximum yaw angle. Their work was based on static analysis only.

The PRBM approach mentioned above is a method used to design and analyze compliant mechanisms. By its nature, the PRBM is an equivalent rigid body description of compliant mechanisms. It is further noted that the stiffness of the flexure hinge in a compliant mechanism will be equivalently represented by a torsional spring on the joint of the PRBM. The relationship or mapping between a compliant mechanism and its PRBM has been extensively studied, which has resulted in some useful mapping formulae (Paros and Weisbord, 1965; Her and Chang, 1994; Jensen et al., 1997; Derderian et al, 1996; Howell and Midha, 1994). Finite element analyses and experiments were performed and their results were compared with the results predicted by the PRBM approach (Jensen et al., 1997; Millar et al., 1996). A good agreement of the results obtained by these approaches was achieved; this validated the PRBM approach.

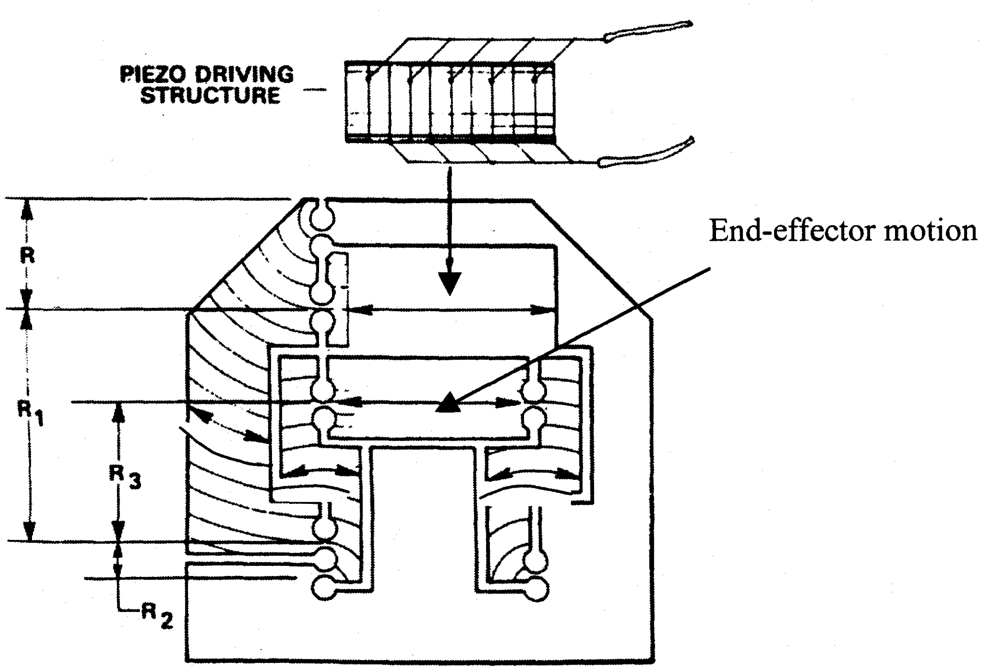

(a) Compliant micro-positioning stage built in 1978

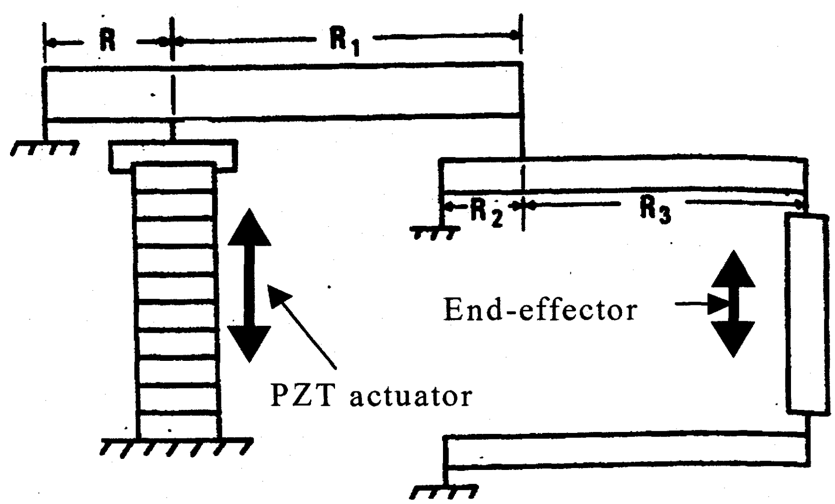

(b) Equivalent lever structure

Figure 1.3 Micro-positioning stage (Scire and Teague, 1978)

Another method of designing a compliant mechanism is topology optimization (Frecker et al., 1999; Nishiwaki et al., 1998). This method provides a procedure to obtain the optimal topology of a structure. This method is generally based on static analysis and requires considerable computation, which limits its suitability to real-time control applications. It is further noted that dynamics and control were not considered in this method.

Micro-motion compliant mechanisms, which use parallel manipulators as their PRBM, have raised substantial research interest. In the literature, the micro-motion compliant mechanisms designed with their PRBM as a parallel manipulator were also called parallel micro-manipulators (Hara and Sugimoto, 1989). The kinematic analysis of parallel manipulators has been extensively studied since the 1980s (Gosselin and Sefrioui, 1991; Ma and Angeles, 1989; Gosselin and Merlet, 1994; Lee and Shah, 1988). In parallel micro-manipulators, as opposed to the use of only rigid-body elements, flexible elements with notches and holes cut on them are used to deliver the desired motion. The rigid revolute pair, prismatic pair, and spherical pair can be implemented with the structures of compliant material, as shown Figure 1.4 (Hara and Sugimoto, 1989). In parallel micro-manipulators, because the motion is very small, the relationship between the input displacements and output displacements can be approximated by a Taylor series expansion, which resulted in a constant matrix (Hara and Sugimoto, 1989). An approximate analysis of the motion of the compliant mechanism shown in Figure 1.1 was also discussed by Zong et al. (1997). Their work led to a constant relationship between the elongation of the PZT actuators and the end-effector motion, but verification of this approximate solution has not been performed. In addition, kinematic parameters need to be calibrated.

The dynamics and control of compliant positioning devices have also been studied. A dynamic model for a spatial 3-DOF compliant positioning stage was obtained experimentally (Lee and Arjunan, 1988). The experimentally obtained dynamic model and the PID feedback control of a vertical motion flexure-hinged micro-positioning stage situated on a pair of X-Y Kinger stages was studied (Jouaneh and Ge, 1997). A dynamic model for a monolithic flexure hinged translation mechanism driven by PZT actuators was derived using the Lagrangian Equation. (Furukawa and Miauno, 1992). Dynamics and control of a compliant planar 3-DOF parallel mechanism based on the PRBM approach were studied by Zhao et al. (1999) and Bi (1997). However, their dynamic model of the system did not account for the stiffness of flexure hinges.

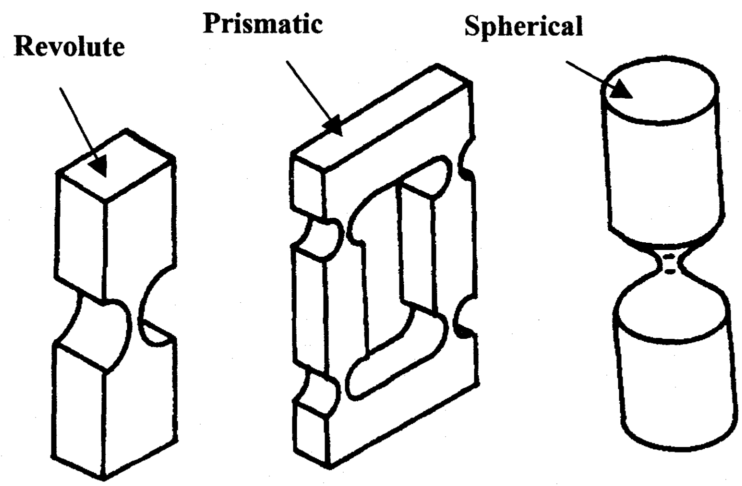

Figure 1.4 Three typical compliant segments

1.3 Research Objectives

Based on the literature review presented above, this thesis work is designed to conduct a comprehensive study of the kinematic, dynamic modeling and control of a particular closed-loop compliant mechanism (see Figure 1.1). The PRBM of this compliant mechanism is shown in Figure 1.5, and is named a *RRR mechanism*, for short, as there are three revolute joints in each closed-loop chain. The compliant mechanism shown in Figure 1.1 is, therefore, named a *RRR compliant mechanism*. It is noted that the torsional spring was not shown in Figure 1.5, and details about the correspondence between Figure 1.1 and Figure 1.5 are discussed in Chapter 2. Furthermore, the RRR compliant mechanism is driven by three PZT actuators, which correspond to θ_1, θ_2 and θ_3 in its PRBM, respectively (see Figure 1.5). In particular, the following research objectives are defined.

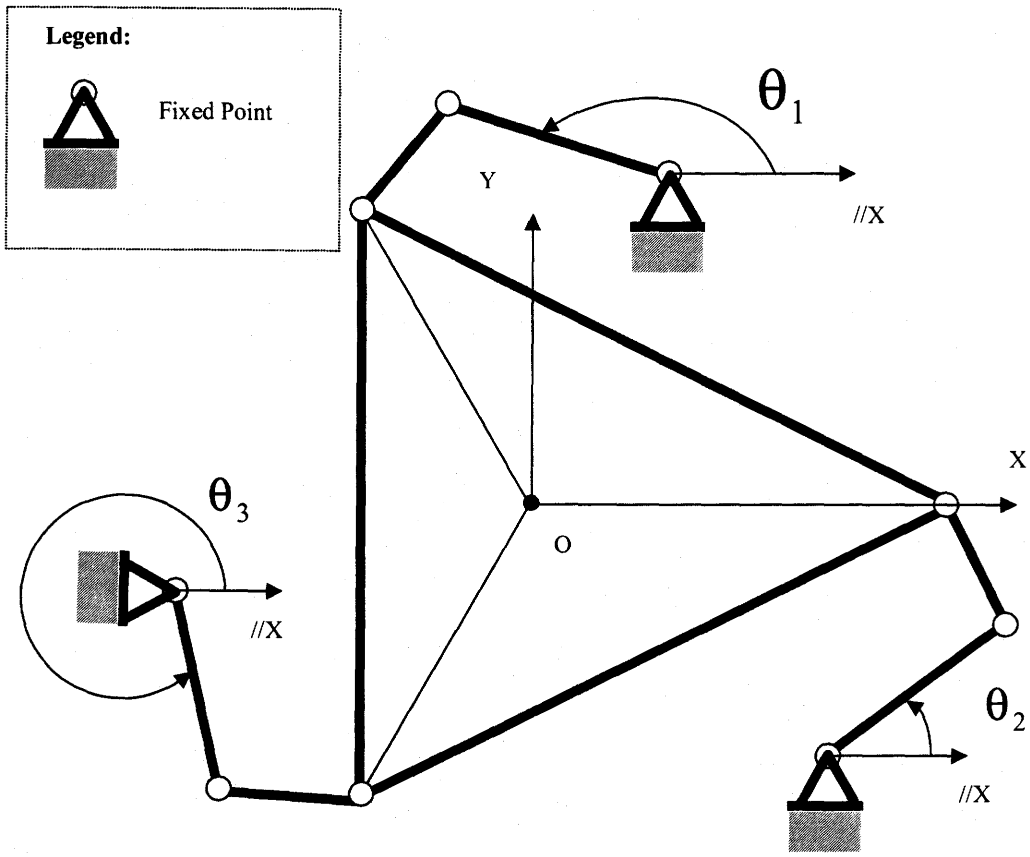

Figure 1.5 PRBM of the RRR compliant mechanism

Objective 1: *To develop an accurate and computationally efficient kinematic model for the RRR compliant mechanism based on the PRBM approach.*

The PRBM approach to compliant mechanisms is suitable to the real-time control of the RRR compliant mechanism based on several significant advantages. *First*, at a low-speed operation, because the inertia terms of the system have a very small influence on the system behavior, the kinematic control (which is based on the kinematic model) suffices. *Second*, the performance of the controlled RRR compliant mechanism is very much related to the quality of a dynamic model. A better kinematic model will contribute to the quality of a dynamic model.

> ***Objective 2:*** *To develop a computationally efficient dynamic model for the RRR compliant mechanism based on the PRBM approach.*

The scope of the dynamic model is such that the internal behavior of PZT actuators is not considered; in other words, the PZT actuator is viewed as a black box. However, effort made in this thesis work should be extendible to situations where the dynamic behavior of the PZT actuators is incorporated.

> ***Objective 3:*** *To perform a preliminary study of control methods for the RRR compliant mechanism based on the PRBM approach.*

Real-time behavior of the RRR compliant mechanism is related to feedback control. The scope of this thesis work is that the behavior of the controlled RRR compliant mechanism should be such that a stable state in simulation study can be reached.

1.4 General Methodology

The accuracy of the kinematic model will be evaluated by comparing the simulation results of the PRBM (of the RRR compliant mechanism) with the experimental results and the simulation results calculated by a finite element package ANSYS. The information about the experimental results will be acquired from the collaborators of this research.

There are several remarks about the PRBM approach versus the finite element method (FEM) approach in this thesis work. The FEM method has the capability to achieve a relatively higher accuracy for compliant mechanisms but requires the availability of a compliant mechanism. At the conceptual design stage, a compliant mechanism is usually not available. This dilemma can be dealt with by the PRBM approach. That is to say, the design process will be as follows: first, the original rigid link mechanism, as shown in Figure 1.5, is proposed and, then, the compliant mechanism is designed, as shown in Figure 1.1. At this point, the kinematic behavior of the compliant mechanism is known based on the kinematic behavior of its original rigid link mechanism. After the compliant mechanism is designed, the stiffness of flexure hinges is known, and then the equivalent torsional spring on its original rigid link mechanism can be determined. It is also noted that the FEM analysis can be further applied to the compliant mechanism.

There are several reasons for choosing the rigid link mechanism shown in Figure 1.5 for development. *First*, this mechanism can produce x, y and θ planar motions, which is the focus of this thesis work. *Second*, this mechanism is one of the simplest parallel mechanisms for planar motions (Hayes et al., 1999). It excludes the actuators in the moving bodies of the mechanism. *Third*, the reported work in the literature on compliant mechanisms for planar motions showed some promise for this mechanism (Ryu et al., 1997). *Last*, if necessary, this mechanism can be extended to a 6-DOF compliant mechanism (Zong et al., 1997).

To develop a dynamic model of the mechanism shown in Figure 1.1, the Lagrangian Equation will be applied. Both the independent-joint proportional-derivative (PD) control law and the model-based PD control law (computed torque control law) (Craig, 1986; An et al., 1988) will be studied and compared.

1.5 Organization of the Thesis

Chapter 2 presents kinematics of the RRR compliant mechanism based on the RRR mechanism (i.e., a pseudo rigid body model of the RRR compliant mechanism), which includes both an exact solution and an approximate solution. Included will also be the evaluation of these two methods. A detailed design of the RRR compliant mechanism is also given in this chapter, including the calculation of the torsional springs for the RRR mechanism based on the flexural hinges in the RRR compliant mechanism. **Chapter 3**

presents the FEM modeling and analysis of the RRR compliant mechanism. The results are then compared with those obtained from both the exact method and approximate method presented in Chapter 2 and with the experimental result. **Chapter 4** presents dynamics of the RRR compliant mechanism based on the RRR mechanism using the Lagrangian Equation. **Chapter 5** presents a study of both an independent-joint PD controller and a model-based PD controller for the RRR compliant mechanism. **Chapter 6** concludes the thesis with discussions of the results, contributions, and future work.

Chapter 2
Kinematic Design and Analysis

2.1 Introduction

Kinematic design and analysis are important tasks which provide a conceptual design of the RRR compliant mechanism. Although a more complete design process should start with the synthesis of a system in conformity with the functional requirements and constraints, the scope of this thesis work, as stated in Chapter 1, is such that the scheme of the rigid body linkage mechanism shown in Figure 1.5 is the starting point. The reasons for this mechanism scheme were explained in Chapter 1 (in particular Section 1.4). This rigid body linkage mechanism is a PRBM of the compliant mechanism shown in Figure 1.1. Therefore, a mapping between them in both topology and geometry should be established. The accuracy of the kinematic model of the RRR compliant mechanism is very important to the eventual controlling of this system. However, in the micro-motion systems, due to the limitation of the current manufacturing technologies, a mathematically exact kinematic model may not describe the actual kinematic behavior of a system better than a mathematically approximate kinematic model. Hence, it is of interest to study a mathematically approximate yet computationally efficient kinematic model. Also, the kinematic parameters need to be calibrated in order to make a kinematic model achieve the best agreement between the simulation result and the experimental result. In the following, Section 2.2 presents a detailed design of the RRR compliant mechanism as well as its PRBM. Section 2.3 derives a mathematically exact kinematic model for the PRBM of the RRR compliant mechanism. A mathematically approximate approach called the Constant-Jacobian approach is described in Section 2.4. Section 2.5 describes the kinematic calibration. A comparative study of various kinematic models versus the experimental results is presented in Section 2.6. Section 2.7 draws conclusions.

2.2 RRR Compliant Mechanism

As stated in Chapter 1 (Section 1.4 in particular), the RRR compliant mechanism is designed based on its PRBM (the RRR mechanism). The configuration and dimensions of the RRR mechanism are shown in Figure 2.1. The RRR mechanism has a symmetric configuration. The end-effector is the center point O of the equilateral triangular platform $C_1C_2C_3$, and its position is represented by variables x, y and γ, respectively. The length of links A_iB_i and B_iC_i (i=1,2,3) are identical, respectively. Five parameters are used to determine the configuration of the mechanism, and they are ψ_1, ψ_2, L_{AB} (the length of links A_iB_i, i=1,2,3); L_{BC} (the length of links B_iC_i, i=1,2,3); R (the length of OC_i, i=1,2,3). Both ψ_1 and ψ_2 are the initial values of the angles defined in Figure 2.1 and Figure 2.2 and, therefore, they do not change with respect to time. The values of these five parameters are given as follows:

$$
\begin{aligned}
&\psi_1 = 1.1733 \text{ rad}, \\
&\psi_2 = 0.81569 \text{ rad}, \\
&L_{AB} = 17.720 \text{ mm}, \\
&L_{BC} = 11 \text{ mm, and} \\
&R = 29.546 \text{ mm}.
\end{aligned}
\tag{2.1}
$$

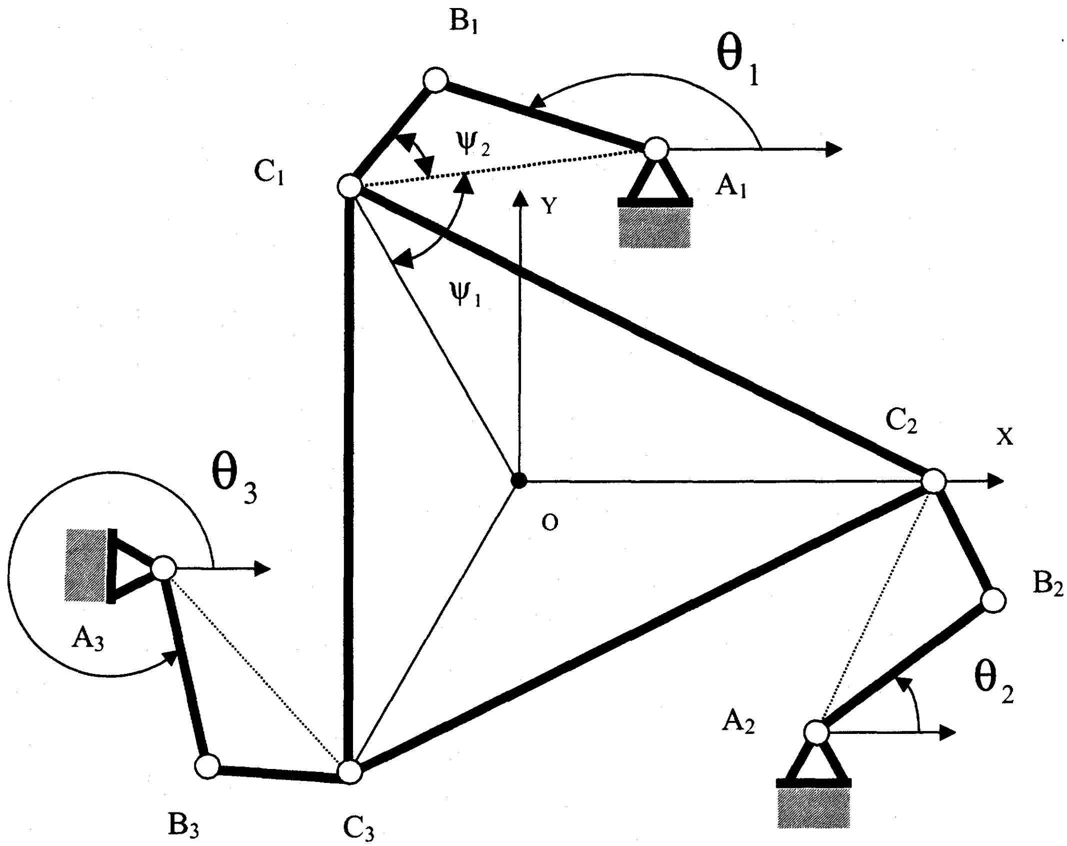

Figure 2.1 Initial position of the PRBM of the RRR compliant mechanism

The RRR compliant mechanism was designed by replacing the revolute joints of the RRR mechanism with the flexure hinges, accordingly. The schematic RRR compliant mechanism is given in Figure 2.2, with the coordinate system defined.

It is noted that the points A_i, B_i, and C_i are the same as those illustrated in Figure 2.1. Therefore, five parameters, which were illustrated in Figure 2.1, are also applied to the RRR compliant mechanism. In Figure 2.2, the coordinate system O-X-Y is coincident with the coordinate system O-X-Y, as shown in Figure 2.1.

The inputs of the system shown in Figure 2.1 are the angular displacements $\Delta\theta_1$, $\Delta\theta_2$ and $\Delta\theta_3$, respectively, but the inputs of the system shown in Figure 2.2 are the elongations of the three PZT actuators Δl_1, Δl_2 and Δl_3, respectively. The relationship between the angular displacement ($\Delta\theta$) and the elongation (Δl) is illustrated in Figure 2.3 and is given as (when $\Delta\theta$ is sufficiently small)

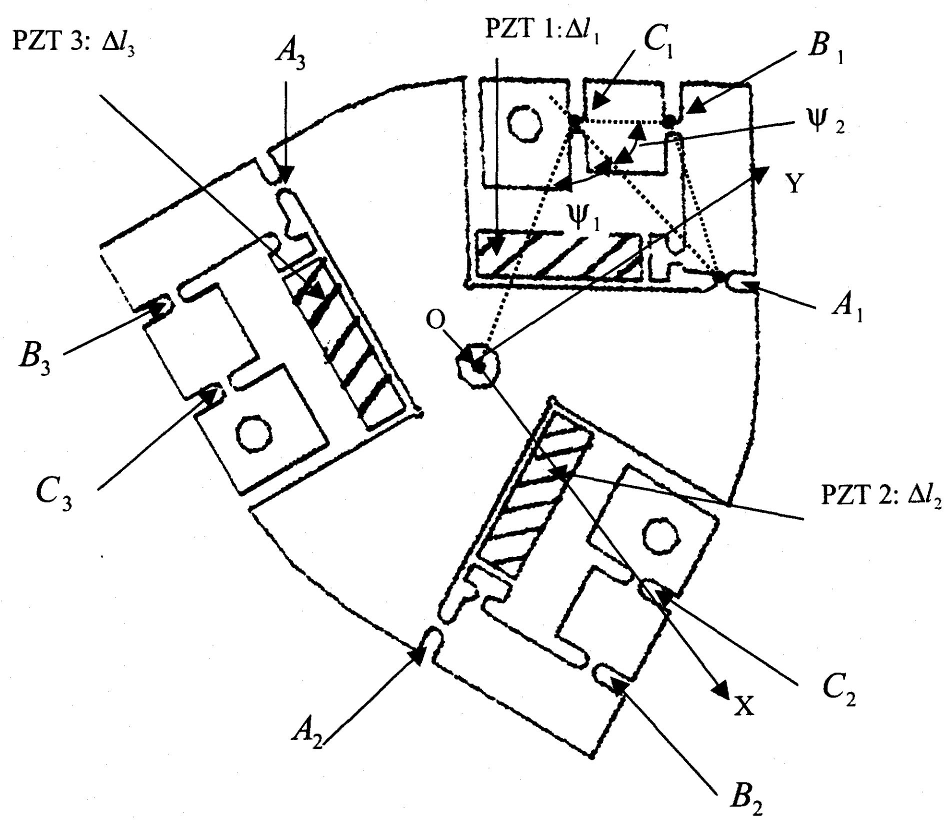

Figure 2.2 RRR compliant mechanism

$$\Delta\theta = \frac{-\Delta l}{R_0} \tag{2.2}$$

where Δl is the elongation of the PZT actuator; Δl is in the range of 0-12 μm,

$\Delta\theta$ is the generated rotation; its direction is clockwise, so it is negative, and

R_0 is shown in this figure.

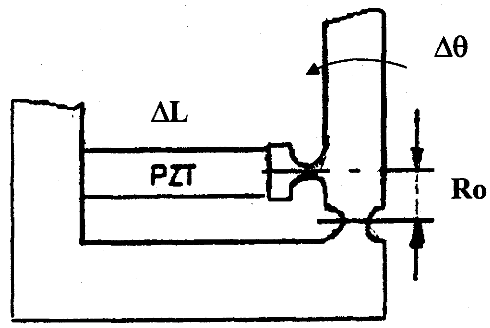

Figure 2.3 Schematic diagram of the driving elements

Flexure hinges at points A_i, B_i, and C_i (in Figure 2.2) are designed to replace the corresponding revolute joints with torsional springs in the PRBM (in Figure 2.1). The relationship between the stiffness of the torsional springs in the RRR mechanism and the dimensions of the flexure hinge can be established (Paros and Weisbord, 1965).

$$K_b = \frac{M}{\delta\theta} = \frac{2Ebt^{5/2}}{9\pi r^{1/2}} \tag{2.3}$$

where K_b is the stiffness of torsional spring,

M is the bending moment,

E is the Young's Modulus,

b, r, and t are the dimensions of the flexure hinge, as shown in Figure 2.4, and

$\delta\theta$ is the change in angle between the left and right portions of the flexure hinge.

If the flexure hinge is only subjected to a moment (Figure 2.4), the maximal stress in the cross-section of the flexure hinge can be calculated by

$$\sigma_{\max} = \frac{M}{W_z} \tag{2.4}$$

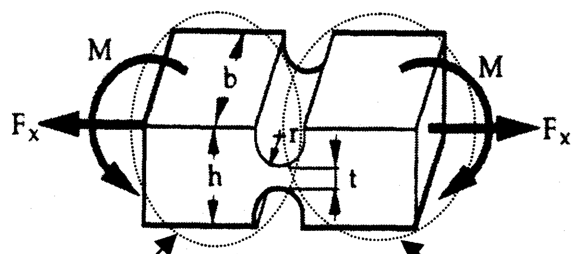

Figure 2.4 Schematic diagram of the flexure hinge

where $W_z = \dfrac{bt^2}{6}$, is the section modulus, and

M is the bending moment applied to the flexure hinge.

The hinge should function as long as

$$\sigma_{\max} \le [\sigma] \tag{2.5}$$

where $[\sigma] = \dfrac{\sigma_p}{n}$, $[\sigma]$ is the allowable stress based on the proportional limit,

σ_p is the material's proportional limit, and

n is the safety factor (in this study, n=2).

Substitution of equations (2.3) and (2.4) into equation (2.5) leads to

$$\delta\theta \le \frac{bt^2}{6K_b}[\sigma] \tag{2.6}$$

Equation (2.6) is a design control equation, which shows that the allowable relative angle of the flexure hinge is determined by the dimensions of the flexure hinge and allowable stress $[\sigma]$. The maximal relative angle of the flexure hinge in the RRR compliant mechanism can be calculated based on the RRR mechanism through kinematic analysis. The dimensions of the flexure hinges are selected to satisfy this equation.

In the above, $[\sigma]$ is dependent on the material chosen. There are several considerations for selecting the material for the micro-motion compliant mechanism, and they are:

(1) to achieve a good stiffness, high E (Young's modulus) should be chosen,
(2) to ensure that the elastic mechanism has good repeatability, high ratio of the yield stress over the Young's Modulus should be chosen, and
(3) to achieve low α (thermal expansion ratio) for small thermal expansion.

In this thesis work, the material QA17 (a sort of Bronze) is chosen. The following are data about QA17 (Cai et al., 1997):

$E=101$ GPa,

$\sigma_p \geq 6$ MPa, and

$\rho = 8.25\times10^3$ kg/m^3, where ρ denotes the density

The dimensions of the flexure hinge are selected based on the discussions above:

$t = 0.8$ mm,

$b = 10$ mm, and

$r = 1$ mm.

It is noted that all the flexure hinges in this RRR compliant mechanism have the same dimensions.

2.3 Mathematically Exact Kinematic Analysis

Mathematically, the task of kinematics is to find equations that relate $[\Delta l_1, \ \Delta l_2, \ \Delta l_3]^T$ with $[\Delta x, \ \Delta y, \ \Delta\gamma]^T$. Note that at the initial position, which also serves as a reference position, $[x, \ y, \ \gamma]^T$ is set to be $[0,0,0]^T$. Therefore, any other position of the end-effector $[x, \ y, \ \gamma]^T$ can be expressed as $[\Delta x, \ \Delta y, \ \Delta\gamma]^T$. The following procedures should lead to the kinematic equation.

Step 1:

At the initial position, the coordinates of A_i, B_i and C_i, (i =1,2,3) are given by

$$A_i^0 = [A_{ix}^0, \ A_{iy}^0, \ 0]^T \tag{2.7}$$

$$B_i^0 = [B_{ix}^0, \ B_{iy}^0, \ 0]^T \tag{2.8}$$

$$C_i^0 = [C_{ix}^0, \ C_{iy}^0, \ 0] = \left[R\cos(\frac{2(2-i)\pi}{3}), \ \ R\sin(\frac{2(2-i)\pi}{3}), \ \ 0 \right]^T \tag{2.9}$$

Step 2:

At any other position, the coordinates of A_i, B_i and C_i are given by

$$A_i = A_i^0 \quad \text{(notice that point A is fixed)} \tag{2.10}$$

$$\begin{aligned} B_i &= \begin{bmatrix} A_{ix}^0 + L_{AB}\cos(\theta_i^0 + \Delta\theta_i) \\ A_{iy}^0 + L_{AB}\sin(\theta_i^0 + \Delta\theta_i) \\ 0 \end{bmatrix}^T \\ &= \begin{bmatrix} A_{ix}^0 + (B_{ix}^0 - A_{ix}^0)\cos\Delta\theta_i - (B_{iy}^0 - A_{iy}^0)\sin\Delta\theta_i \\ A_{iy}^0 - (B_{ix}^0 - A_{ix}^0)\sin\Delta\theta_i + (B_{iy}^0 - A_{iy}^0)\cos\Delta\theta_i \\ 0 \end{bmatrix}^T \end{aligned} \tag{2.11}$$

$$C_i = \begin{bmatrix} x + R\cos(\frac{2(2-i)\pi}{3}+\gamma), & y + R\sin(\frac{2(2-i)\pi}{3}+\gamma), & 0 \end{bmatrix}^T \tag{2.12}$$

Step 3:

At any other position, the following constraint equation on the length of the links B_iC_i (i=1,2,3) should be satisfied, i.e.,

$$(C_{ix} - B_{ix})^2 + (C_{iy} - B_{iy})^2 = L_{BC}{}^2 \tag{2.13}$$

Substitution of C_{ix}, C_{iy}, B_{ix} and B_{iy} into equation (2.13) leads to

$$\begin{aligned}
&x^2 + y^2 + 2x[-A_{1x}^0 - \frac{R\cos\gamma - \sqrt{3}R\sin\gamma}{2} - (B_{1x}^0 - A_{1x}^0)\cos(\frac{\Delta l_1}{R_0}) \\
&- (B_{1y}^0 - A_{1y}^0)\sin(\frac{\Delta l_1}{R_0})] + 2y[-A_{1y}^0 - \frac{Rc\sin\gamma + \sqrt{3}R\cos\gamma}{2} \\
&+ (B_{1x}^0 - A_{1x}^0)\sin(\frac{\Delta l_1}{R_0}) - (B_{1y}^0 - A_{1y}^0)\cos(\frac{\Delta l_1}{R_0})] \\
&+ R[(B_{1x}^0 - A_{1x}^0)\cos(\frac{\Delta l_1}{R_0} + \gamma) + \sqrt{3}(B_{1x}^0 - A_{1x}^0)\sin(\frac{\Delta l_1}{R_0} + \gamma) \\
&+ (B_{1y}^0 - A_{1y}^0)\sin(\frac{\Delta l_1}{R_0} + \gamma) - \sqrt{3}(B_{1y}^0 - A_{1y}^0)\cos(\frac{\Delta l_1}{R_0} + \gamma)] \\
&+ 2[A_{1x}^0(B_{1x}^0 - A_{1x}^0)\cos(\frac{\Delta l_1}{R_0}) + A_{1y}^0(B_{1y}^0 - A_{1y}^0)\cos(\frac{\Delta l_1}{R_0}) \\
&- (B_{1x}^0 A_{1y}^0 - B_{1y}^0 A_{1x}^0)\sin(\frac{\Delta l_1}{R_0})] + L_{AB}{}^2 + K^2 + R^2 - L_{BC}{}^2 = 0
\end{aligned} \tag{2.14}$$

$$
\begin{aligned}
&x^2+y^2+2x[-A_{2x}^0+R\cos\gamma-(B_{2x}^0-A_{2x}^0)\cos(\frac{\Delta l_2}{R_0})\\
&-(B_{2y}^0-A_{2y}^0)\sin(\frac{\Delta l_2}{R_0})]+2y[-A_{2y}^0+R\sin\gamma+(B_{2x}^0-A_{2x}^0)\sin(\frac{\Delta l_2}{R_0})\\
&-(B_{2y}^0-A_{2y}^0)\cos(\frac{\Delta l_2}{R_0}]+2R[-(B_{2x}^0-A_{2x}^0)\cos(\frac{\Delta l_1}{R_0}+\gamma)\\
&-(B_{2y}^0-A_{2y}^0)\sin(\frac{\Delta l_1}{R_0}+\gamma)-A_{2x}^0\cos\gamma-A_{2y}^0\sin\gamma]\\
&+2[A_{2x}^0(B_{2x}^0-A_{2x}^0)\cos(\frac{\Delta l_1}{R_0})+A_{2y}^0(B_{2y}^0-A_{2y}^0)\cos(\frac{\Delta l_1}{R_0})\\
&-(B_{2x}^0A_{2y}^0-B_{2y}^0A_{2x}^0)\sin(\frac{\Delta l_1}{R_0})]+L_{AB}{}^2+K^2+R^2-L_{BC}{}^2=0
\end{aligned}
\tag{2.15}
$$

$$
\begin{aligned}
&x^2+y^2+2x[-A_{2x}^0-\frac{R\cos\gamma+\sqrt{3}R\sin\gamma}{2}-(B_{3x}^0-A_{3x}^0)\cos(\frac{\Delta l_3}{R_0})\\
&-(B_{3y}^0-A_{3y}^0)\sin(\frac{\Delta l_3}{R_0})]+2y[-A_{3y}^0-\frac{R\sin\gamma-\sqrt{3}R\cos\gamma}{2}\\
&+(B_{3x}^0-A_{3x}^0)\sin(\frac{\Delta l_3}{R_0})-(B_{3y}^0-A_{3y}^0)\cos(\frac{\Delta l_3}{R_0})]\\
&+R[(B_{3x}^0-A_{3x}^0)\cos(\frac{\Delta l_3}{R_0}+\gamma)-\sqrt{3}(B_{3x}^0-A_{3x}^0)\sin(\frac{\Delta l_3}{R_0}+\gamma)\\
&+(B_{3y}^0-A_{3y}^0)\sin(\frac{\Delta l_3}{R_0}+\gamma)+\sqrt{3}(B_{3y}^0-A_{3y}^0)\cos(\frac{\Delta l_3}{R_0}+\gamma)]\\
&+2[A_{3x}^0(B_{3x}^0-A_{3x}^0)\cos(\frac{\Delta l_3}{R_0})+A_{3y}^0(B_{3y}^0-A_{3y}^0)\cos(\frac{\Delta l_3}{R_0})\\
&-(B_{3x}^0A_{3y}^0-B_{3y}^0A_{3x}^0)\sin(\frac{\Delta l_3}{R_0})]+L_{AB}{}^2+K^2+R^2-L_{BC}{}^2=0
\end{aligned}
\tag{2.16}
$$

where, K is the length of OA_i.

The equations above have quadratic terms for x, y and γ and are non-linear for Δl_1, Δl_2, and Δl_3.

Note that the forward kinematics means to calculate the end-effector motion from the known motion of the PZT actuators. The inverse kinematics means to calculate the motion of the PZT actuators from the known end-effector motion. From equations (2.14), (2.15), and (2.16), it can be found that the inverse kinematics can be solved explicitly, but the forward kinematics solved with a numerical iteration scheme.

2.4 Constant-Jacobian Approach - an Approximate Kinematic Analysis

In robotics, the relationship between the velocity of an end-effector and the velocity of actuators is described by a general relationship, i.e. (in the case of the RRR mechanism),

$$\begin{bmatrix} \dot{x} \\ \dot{y} \\ \dot{\gamma} \end{bmatrix} = J_l \begin{bmatrix} \dot{l}_1 \\ \dot{l}_2 \\ \dot{l}_3 \end{bmatrix} \tag{2.17}$$

where J_l is called *Jacobian matrix* (Craig, 1986). J_l is a function of Δl_i (i=1,2,3).

When the displacements are sufficiently small, applying the Taylor series expansion to equation (2.17) leads to

$$\begin{bmatrix} \Delta x \\ \Delta y \\ \Delta \gamma \end{bmatrix} \cong J_l^0 \begin{bmatrix} \Delta l_1 \\ \Delta l_2 \\ \Delta l_3 \end{bmatrix} \tag{2.18}$$

where J_l^0 is the Jacobian matrix at the initial position. When the initial coordinate of (x, y, γ) of the end-effector is set as (0,0,0), equation (2.18) can be expressed by

$$\begin{bmatrix} x \\ y \\ \gamma \end{bmatrix} \cong J_l^0 \begin{bmatrix} \Delta l_1 \\ \Delta l_2 \\ \Delta l_3 \end{bmatrix} \tag{2.19}$$

Define J_θ as the Jacobian matrix which relates the motion of the end-effector with $\dot{\theta}_i$, i=1,2,3. Applying the Taylor series expansion to J_θ leads to

$$\begin{bmatrix} \Delta x \\ \Delta y \\ \Delta\gamma \end{bmatrix} \cong J_\theta^0 \begin{bmatrix} \Delta\theta_1 \\ \Delta\theta_2 \\ \Delta\theta_3 \end{bmatrix} \tag{2.20}$$

where J_θ^0 is the Jacobian matrix J_θ at the initial position. J_θ^0 can be derived as

$$J_\theta^0 = L_{AB}\sin(\psi_3)\begin{bmatrix} \frac{-\sqrt{3}}{3}\sin(\psi)-\frac{1}{3}\cos(\psi) & \frac{2}{3}\cos(\psi) & \frac{\sqrt{3}}{3}\sin(\psi)-\frac{1}{3}\cos(\psi) \\ \frac{\sqrt{3}}{3}\cos(\psi)-\frac{1}{3}\sin(\psi) & \frac{2}{3}\sin(\psi) & \frac{-\sqrt{3}}{3}\cos(\psi)-\frac{1}{3}\sin(\psi) \\ \frac{1}{3R\sin(\psi)} & \frac{1}{3R\sin(\psi)} & \frac{1}{3R\sin(\psi)} \end{bmatrix} \tag{2.21}$$

where $\psi = \psi_1 + \psi_2$,

L_{AB} is the length of the link A_iB_i, i=1,2,3,

L_{BC} is the length of the link B_iC_i, i=1,2,3,

R is the length of OC_i, i=1,2,3,

ψ_1 and ψ_2 are illustrated in Figure 2.1, and

ψ_3 is the angle dependent on ψ_2; $\psi_3 = \psi_2 + \arcsin(\frac{L_{BC} \times \sin\psi_2}{L_{AB}})$.

Note that equation (2.21) has corrected some error in the one derived by Zong et al. (1997). According to equation (2.2), the Jacobian matrix, which relates the motion of the end-effector with the motion of the PZT actuators, can be represented by

$$J_l^0 = -\frac{J_\theta^0}{R_0} \tag{2.22}$$

2.5 Kinematic Calibration

The objective of kinematic calibration is to adjust or tune the kinematic parameters in the PRBM to best represent the kinematic behavior of the compliant mechanism. As mentioned earlier, there are five independent parameters, which fully determine the configuration of the PRBM. Let p_i, i=1,2,…,5, stand for these five parameters. The problem of kinematic calibration can be stated as finding an optimal p_i^* around the nominal p_i such that the discrepancy between the simulated behaviors and the measured behaviors is minimized. An optimization model can be developed to solve this problem.

$$\begin{cases} \min\{\max\limits_{D_x \times D_y \times D_\gamma} \{w_x(x_i - x_i^e)^2 + w_y(y_i - y_i^e)^2 + w_\gamma(\gamma_i - \gamma_i^e)^2\}\} \\ p^l{}_j \le p_j \le p^u{}_j, \quad j = 1,2,\ldots,5 \end{cases} \tag{2.23}$$

where x_i, y_i, and γ_i, i=1,2,…, m, are the simulated displacements of the end-effector, respectively, calculated using the developed kinematic model, i.e., equations (2.19) and (2.22).

x_i^e, y_i^e, and γ_i^e, i=1,2,…, m, are the measured displacements of the end-effector,

m is the number of positions of the end-effector for testing,

$p^u{}_j$, $p^l{}_j$ are the upper and lower bounds of p_j,

D_x, D_y and D_z are the domains of the end-effector motion along the x-, y-, and γ-directions, and

$w_x = w_y = 1, w_\gamma = 10^4$ are the weights in the objective function.

In the above model, p_1 stands for L_{AB}, p_2 for L_{BC}, p_3 for R, p_4 for ψ_1, and p_5 for ψ_2, and their nominal values can be found in equation (2.1). p''_j and p'_j are given as follows:

p''_1=10 mm $\quad$ p'_1= 20 mm,

p''_2=10 mm $\quad$ p'_2= 20 mm,

p''_3=20 mm $\quad$ p'_3 = 35 mm,

p''_4=0.6 rads $\quad$ p'_4 = 2.0 rads,

p''_5=0.2 rads $\quad$ p'_5 = 1.5 rads.

The implementation of the above optimization model was done in the Matlab (Ver.5.3) software environment. The measured data were acquired from the collaborators. In Appendix A, there is a brief introduction of the experimental setup and the result. The use of this Matlab program can be found in Appendix B (the program name is '**concalibak_con.m**', and it can also be found in the attached disk).

The result of the kinematic calibration is given as follows (using the Constant-Jacobian approach):

(a) the range of the actuators' motion: 0-12 μm,

(b) the kinematic parameters after the calibration:

L_{AB} = 16.3333 mm,

L_{BC} = 10.7105 mm,

R = 31.2969mm,

ψ_1 = 1.0951 rad, and

ψ_2 = 0.3366 rad;

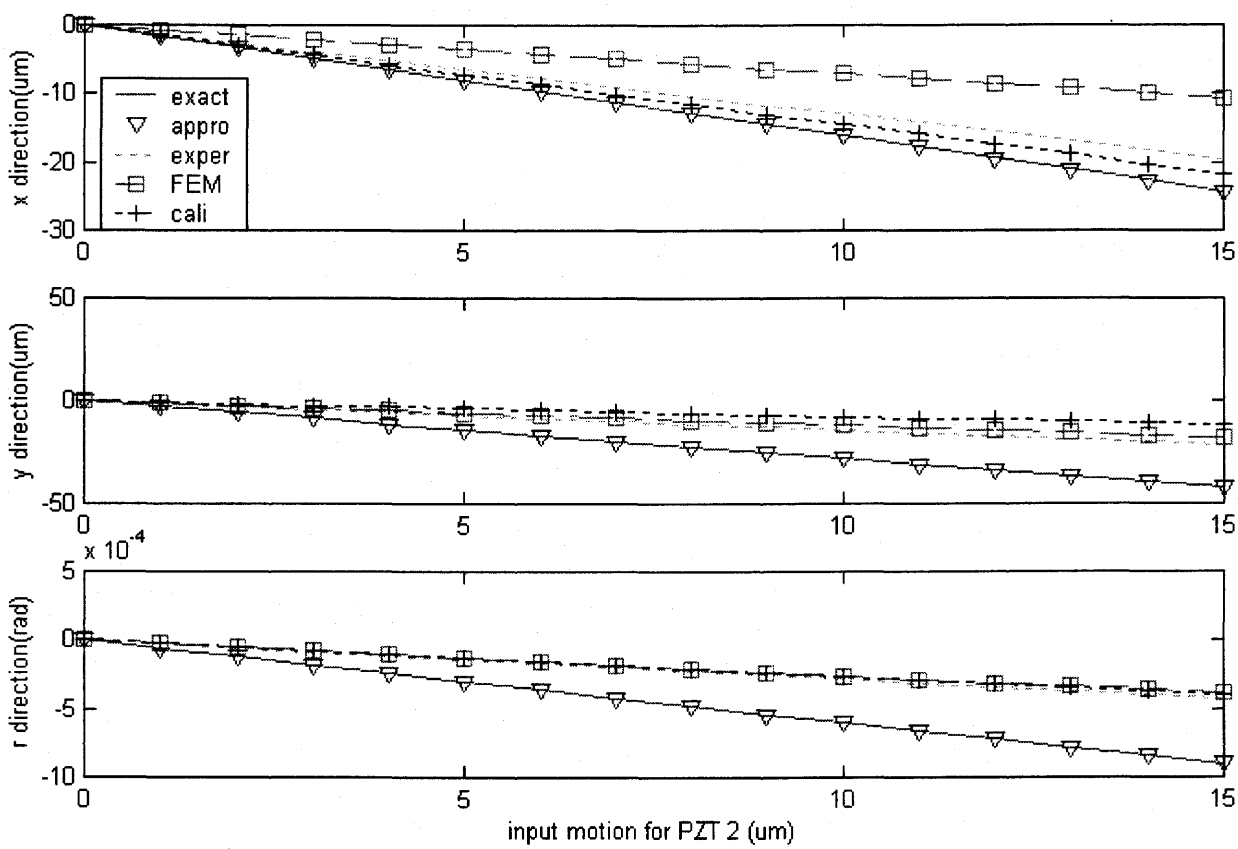

Figure 2.5 Simulation results versus experimental results

2.6 Results and Discussions

The simulation was carried out using the Matlab (Ver.5.3) software. The solving procedure for the forward kinematics has to deal with a system of three non-linear equations, i.e., equations (2.14)-(2.16); in this case the optimization algorithm in Matlab (`SQP, Quasi-Newton, line-search`) is applied (The program is named '**solvefunbak_l.m**', and can also be found in the attached disk)

Figure 2.5 plots the experimental result and all the simulation results (including the mathematically exact solution, the Constant-Jacobian solution, and the calibrated solution). The case used for plotting Figure 2.5 is as follows: PZT2 extends 0-12 μm and

PZT1 and PZT3 extend 0. It is also noted that the r-direction in Figure 2.5 (and in all the following figures) stands for the γ-direction.

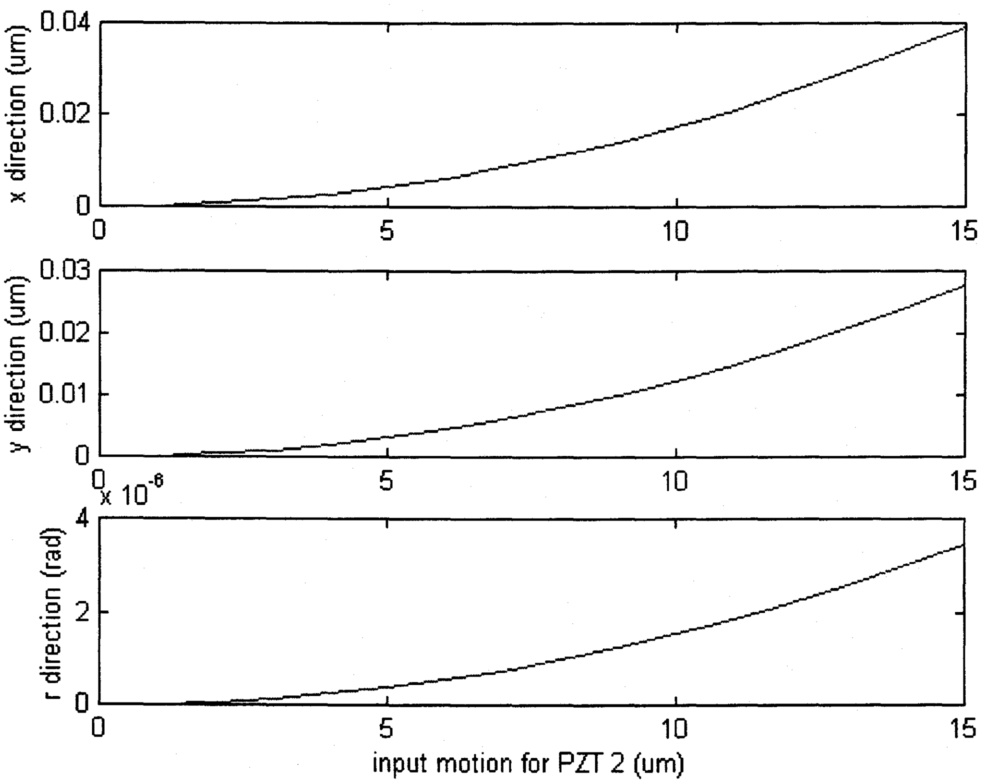

Figure 2.6 Difference between the Constant-Jacobian and exact solutions

From Figure 2.5, it can be seen that the Constant-Jacobian solution is very close to the exact solution. The difference between the exact solution and the Constant-Jacobian solution, when the PZT actuator moves in the range of 12 μm, is further plotted and clarified in Figure 2.6. From Figure 2.6, it can be seen that the difference between these two solutions increases with the increase of the elongation of the PZT actuator; this is reasonable because the Constant-Jacobian solution is an approximation using the first order Taylor series expansion.

It is also shown in Figure 2.5 that even though these two solutions are very close to each other, they are quite far from the experimental results. In order to show this point more clearly, another curve is plotted, as shown in Figure 2.7. The following procedures are taken to plot the curves in Figure 2.7:

Step 1: Calculate the absolute value of the difference between the Constant-Jacobian result and the experimental result, denoted as $|\Delta_{AE}|$.

Step 2: Calculate the absolute value of the difference between the mathematically exact result and the experimental result, denoted as $|\Delta_{EE}|$.

Step 3: Plot $|\Delta_{AE}|$ - $|\Delta_{EE}|$.

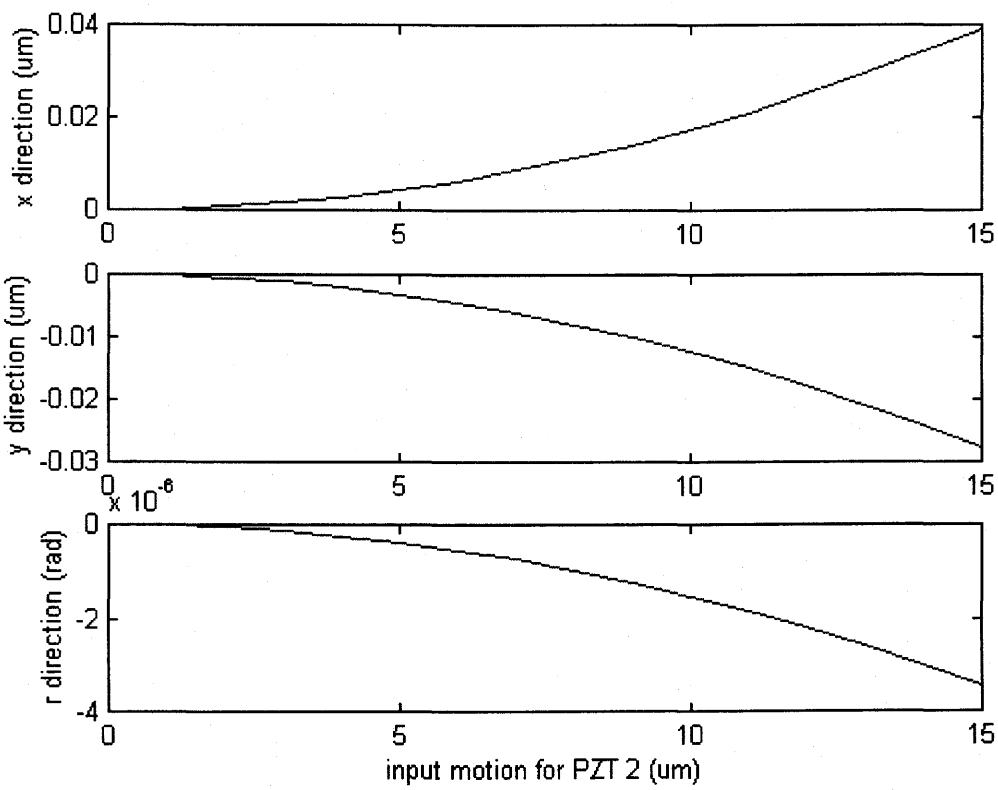

Figure 2.7 Exact results and Constant-Jacobian results versus the experimental results

From Figure 2.7, it can be seen that the Constant-Jacobian solution is even closer to the experimental result in the y- and r- axis directions. Nevertheless, the calibrated result is shown in Figure 2.5 to be far closer to the experimental result than those non-calibrated. It is also found that the computation time for the mathematically exact solution is about 5 times of that of the Constant-Jacobian solution.

2.7 Conclusion

Through simulation, the RRR compliant mechanism is found to have the following properties: the total range of 77.28 μm (when Δl_1=12 μm, Δl_2=12 μm, and Δl_3=0 μm) and 71.02 μm (when Δl_1=12 μm, Δl_2=0 μm, and Δl_3=12 μm) along the x- and y- axis, respectively, and the maximal yaw motion range of 2.16 mrad (when Δl_1=12 μm, Δl_2=12 μm, and Δl_3=12 μm). When the resolution of the PZT actuator is 0.01 μm, the accuracy of motions at the end-effector is 13.2 nm and 3.4 nm along the x- and y-axis, respectively, and the accuracy of the yaw motion is 0.6 μrad.

The Constant-Jacobian approach can provide an excellent model for the kinematic analysis of the RRR compliant mechanism in which the motion range of the PZT actuators is 0-12 μm. This conclusion may be extended to other types of compliant mechanisms for micro-motion manipulation applications. The main reason for this phenomenon, i.e., the mathematically approximate solution could instead represent behaviors of a physical system better than the mathematically exact solution, is that known motion laws, manufacturing, and data processing principles may not apply to this new application, i.e., micro-motion systems using the compliant mechanism concept. Note that known motion laws, manufacturing, and data processing principles are essentially based on the rigid body assumption, small deformation assumption, and component-joint formulation of an assembly. Selection of appropriate methods for kinematic analysis, dynamic analysis, and control of compliant mechanisms is not a straightforward issue.

Chapter 3

Finite Element Modeling and Simulation

3.1 Introduction

This chapter presents a study of the finite element modeling of the RRR compliant mechanism. As stated in Chapter 1 (Section 1.4 in particular), when the specification of a compliant mechanism is available, the finite element method (FEM) could be used to analyze those behaviors and/or properties of the compliant mechanism that are not related to real-time control applications. In this connection, the kinematics of the RRR compliant mechanism (i.e., the translations in both the X- and Y- directions of the centroid of the platform $C_1C_2C_3$, and the orientation of this platform) are analyzed. In the following, Section 3.2 presents the procedure for the FEM modeling of the RRR compliant mechanism. One of the important features of the FEM model to be created is that the model is parametric. This will facilitate a further optimization of the design. Section 3.3 shows the results of the FEM analysis and compares them with the results obtained from both the analytical approaches and the experiment in order to generate a finding of what accuracy level the FEM method could achieve. Some discussion is also given in Section 3.3. Section 3.4 contains the conclusion.

3.2 Parametric FEM Model of the RRR Compliant Mechanism

The FEM modeling was carried out using the ANSYS (Ver. 5.5) software package. One of the important requirements for this task is that the developed model should be parametric. In essence, a parametric FEM model means that the finite element modeling and mesh will depend on a set of parameters. Therefore, a change of the design, i.e., a change in any dimensional parameters, would not need remodeling manually. In other words, after a design change a complete finite element model can be automatically created.

3.2.1 Identification of Parameters

It is known from previous discussion in Chapter 2 that the RRR compliant mechanism has five parameters (L_{AB}, L_{BC}, R, ψ_1, ψ_2, see Figure 2.2 in Chapter 2), which determine the kinematic configuration of the RRR compliant mechanism. These five parameters may also be called the *global parameter*. There are another four parameters (h, r, t, b, see Figure 2.4) which determine the shape and volume of the flexure hinge in the RRR compliant mechanism. These four parameters may be called the *local parameter*.

3.2.2 Procedure for Developing an ANSYS Model

The general procedure for the FEM modeling follows. The first step is to develop a geometric model of the system concerned, the RRR compliant mechanism in this case. The second step is to define a mesh upon the resulting geometric model. The third step is to specify external forces (and/or displacements) and boundary conditions. These steps for the RRR compliant mechanism are described in detail below.

Step 1: developing a geometric model

The physical configuration of the RRR compliant mechanism is such that there are two major components: one compliant member and another rigid member (see Figure 3.1).

The end-effector motion is the x and y translation motions of the center point and the planar rotation of the rigid member. The compliant member is composed of three identical segments, which are symmetrical to the center point of the compliant member. Therefore, one segment is first constructed, and then a coordinate rotation facility provided by ANSYS is applied to construct the other two segments (see Figure 3.1). The geometric construction of the rigid member is straightforward.

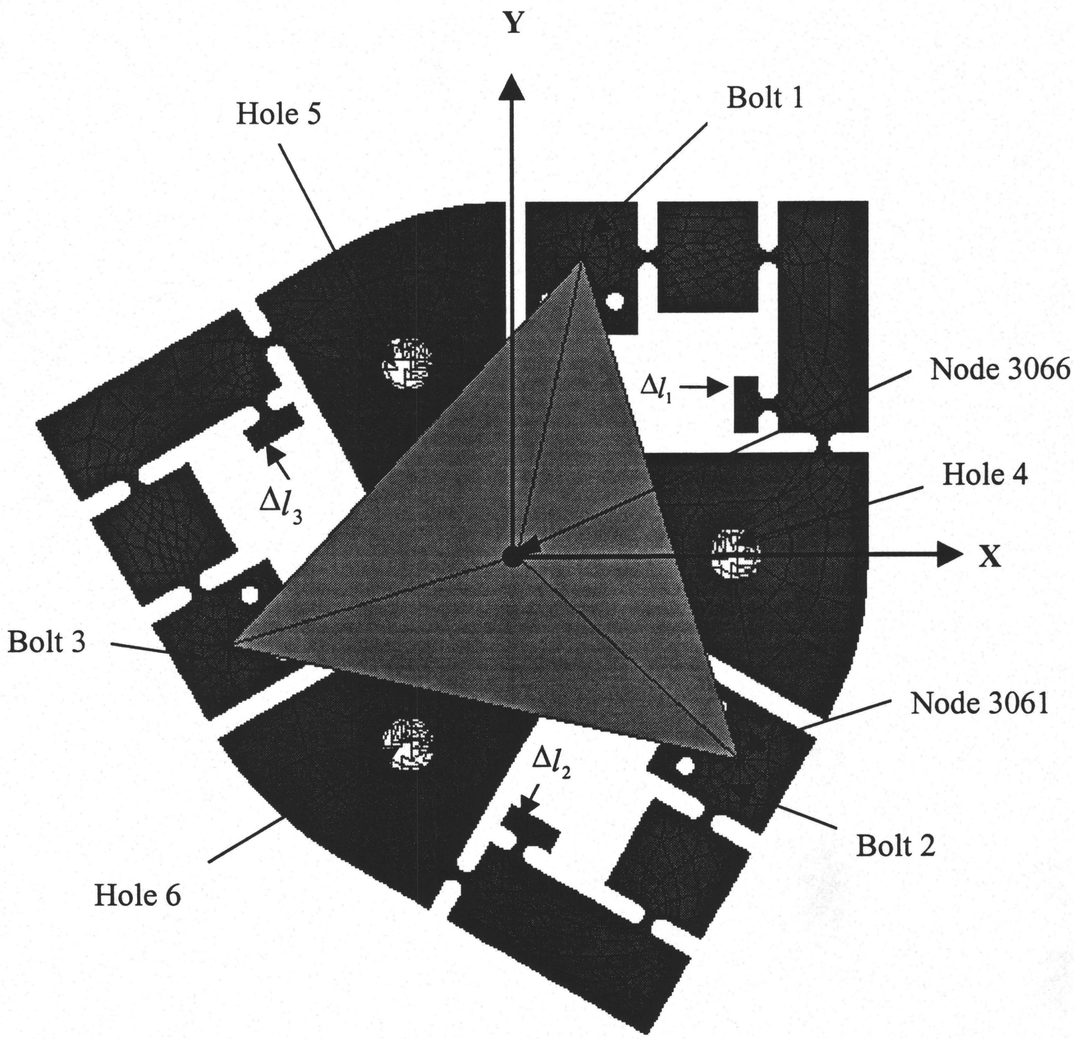

Figure 3.1 FEM model of the RRR compliant mechanism

Step 2: developing a mesh

For the compliant mechanism, a two-dimensional quadrilateral element type with eight nodes (each node having two degrees of freedom) is applied. The modeling procedure is such that an appropriate number of seeds are defined on the relevant geometric edges of the mechanism, and then the element can be automatically generated using the ANSYS tool. Elements with a total number of 838 are generated for the compliant member.

The connection between the rigid and compliant members is made through three bolts, labeled 1, 2 and 3, respectively (see Figure 3.1). The bolts are modeled using a triangular element type with a midpoint node on each edge. Each node in this type of element has two degrees of freedom. The nodes on the boundary of the bolts are made identical to those on the boundary of the compliant member, which enables consistency of the deformation between these two objects. Three conventional triangular elements with a high Young's module are defined for the rigid member in such a way that two of the three nodes of each triangular element are coincident with the nodes at the center of the three bolts (1,2,3), respectively, and the third node of each triangular element is coincident with the center of the rigid member. More specific information such as materials and element types associated with ANSYS are given below.

shape of element	Geometric area	material	E (GPa)	element name in ANSYS
Quadrilateral	the compliant member	bronze	101	plane 82
Triangle	the three bolts	steel	207	plane 82
Triangle	the triangle platform	steel	207	plane 42

Step 3: specifying the boundary condition

Boundary conditions are specified in such a way that the boundaries of the holes (hole 4, 5 and 6, see Figure 3.1) are fixed; that is, the displacements of the nodes on the perimeter of these holes are defined to be zero in both the X- and Y- directions. Note that the input motions of the mechanism are the elongations of the three PZT actuators, denoted by Δl_1, Δl_2, Δl_3, respectively. In this analysis, the physics of the material of the

PZT actuators is not considered. The input motions are, therefore, specified as the prescribed values of the displacements of the nodes of the element contacting the actuators (see Figure 3.1). These prescribed values have a range of 0-12 μm. The following situations of the elongations of the three PZT actuators are considered: the elongations of the 3 PZT actuators individually and the elongations of the 3 PZT actuators simultaneously with the same increment.

3.2.3 Acquisition of the End-effector Motion

The translation displacements of the end-effector, i.e., the center of the rigid member, can be obtained straightforwardly from the X and Y coordinate of the corresponding node, Node 3066 in this case (see Figure 3.1). The yaw motion or orientation of the end-effector can be obtained as follows: choose an element node on the rigid member, Node 3061 in this case (see Figure 3.1); then, calculate the angle change of the line connecting Node 3061 and Node 3066. Figure 3.2 illustrates details of this procedure. In Figure 3.2, for the simplicity of illustration, Node 3061 is denoted as point 1 and Node 3066 as point 6. At any other position of the rigid member, point 1 moves to point 1' and point 6 to point 6'. The rotation angle of the line connecting points 1 and 6 is calculated using the following equations:

$$\gamma^0 = \arctan \frac{C_{1y}}{C_{1x}} \tag{3.1}$$

where C_{1x} and C_{1y} denote coordinates of point 1 at the initial position, and

γ^0 denotes the angle of the rigid member at the initial position.

$$\gamma' = \arctan \frac{C_{1y}'}{C_{1x}'} \tag{3.2}$$

where C_{1x}' and C_{1y}' denote coordinates of point 1 at any other position, and

γ' denotes the angle of the rigid member at any other position.

Further, C_{1y}' and C_{1x}' can be calculated by the following equations:

$$C_{1y}' = (C_{1y} + U_{1y}) - U_{6y} \tag{3.3}$$

$$C_{1x}' = (C_{1x} + U_{1x}) - U_{6x} \tag{3.4}$$

where U denotes the displacement of the node obtained from ANSYS.

Finally, the angle change $\Delta\gamma$ can be found by

$$\Delta\gamma = \gamma' - \gamma^0 \tag{3.5}$$

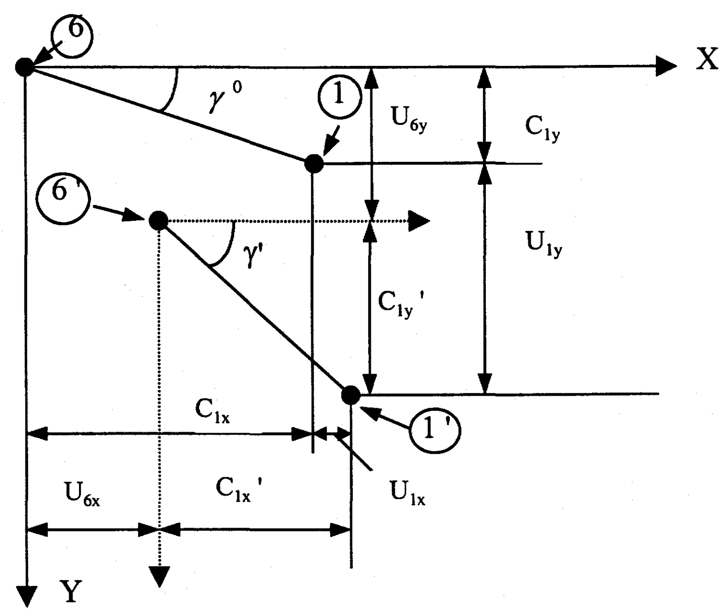

Figure 3.2 Calculation of the yaw angle

3.3 Results and Discussion

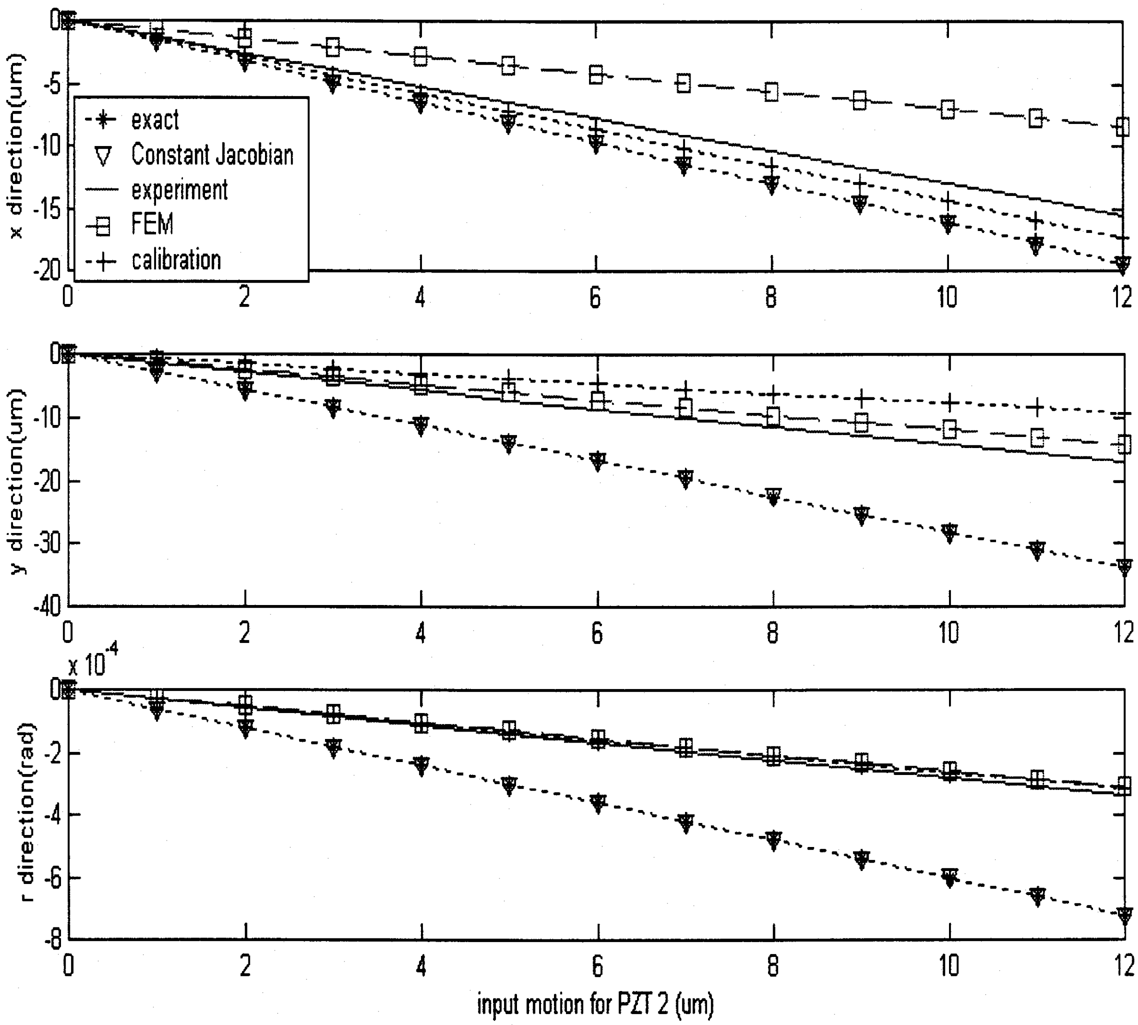

Figure 3.3 Comparison of FEM results with other results

FEM analysis with the ANSYS program requires a computation time 50 times greater than those analytic methods based on PRBM. In Figure 3.3, the FEM results and all the analytic results are plotted for the case where the PZT actuator 2 extends from 0-12 μm while the other two actuators extend 0 μm. It can be seen from this figure that FEM results are not consistently better than the simulation results computed based on the calibrated kinematic model and not even consistently better than the simulation results based on the exact or the Constant-Jacobian result. Nevertheless, the FEM result is generally closer to the experimental result than other results except for the calibrated kinematic result. It can be seen from Figure 3.3 that the calibrated result is very close to the FEM result and sometimes closer to the experimental result than the FEM result. It can be further seen from Figure 3.3 that both the FEM results and the calibrated kinematic results agree very well with the experimental results in the yaw angle, whereas there are relatively large discrepancies between them and the exact and Constant-Jacobian results. This may be explained by the fact that the methods of computing the yaw angle from both the FEM analysis and the experiment are similar, i.e., they are both based on the coordinates of the end nodes of the rigid member and the yaw angle is then calculated using trigonometric relationship (see Appendix A for details of the experiment). Note that the results of the comparative studies of the other settings of the PZT actuators are largely the same.

The fact that FEM analysis is not consistently better than PRBM analysis leads to an important design rule. That is, in micro-motion systems, because the order of the quantities in both the manufacturing and measuring error and the micro-motion is at the same level, the simulation approaches without modeling the manufacturing and measuring errors may not be distinguished from each other in terms of the accuracy achieved in modeling behaviors of micro-motion systems. In other words, for example, the errors presented due to retaining only the first order item of the Taylor series expansion of the Jacobian matrix may offset the errors presented due to neglecting manufacturing and measuring errors in the simulation model.

Stress distribution has been studied to ensure that the maximum Von Mises stress in the deformed mechanism is less than the allowable yield stress of the material, which is calculated by

$$[\sigma]_y = \frac{\sigma_y}{n_y} = \frac{350}{1.5} = 233.3 \text{ (MPa)} \tag{3.6}$$

where $\sigma_y = 350$ MPa, which is the yield stress of the material chosen,

n_y=1.5, which is the safety factor considering application situations, and

$[\sigma]_y$ is the allowable stress based on the yield stress of the material.

The stress distribution of the mechanism has been studied when PZT actuators 1, 2 and 3 elongate in the range of 0-12 μm both individually (i.e., one actuator operates while the other two do not) and simultaneously (i.e., all the actuators operate).

When PZT actuator 1 elongates individually, the maximum stress of the mechanism is found at the flexure hinge 1 (see Figure 3.4). When the elongation of PZT actuator 1 reaches 12 μm, the stress at this flexure hinge is maximal, which is 176.211 MPa, as shown in this figure.

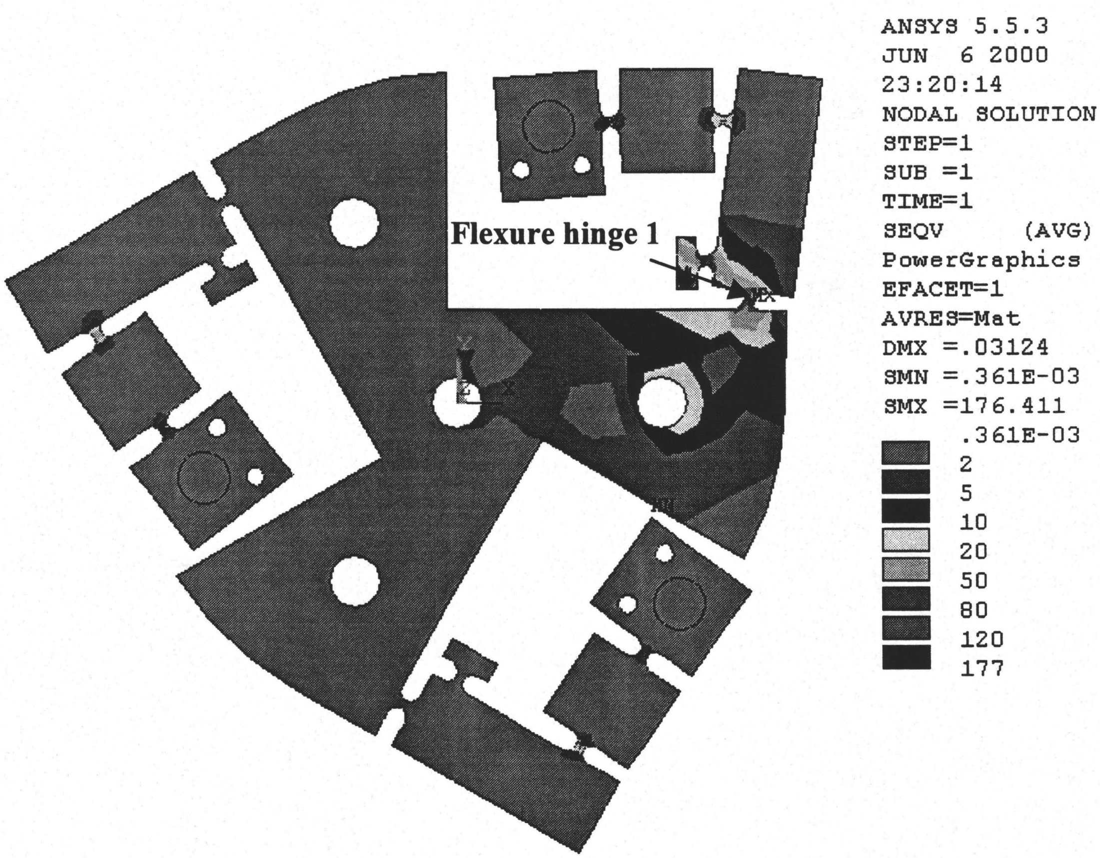

Figure 3.4 Von Mises stress distribution at 12 μm elongation of PZT actuator 1

Figure 3.5 plots the maximum stress of the mechanism versus the elongation of PZT actuator 1 extending from 0 to 12 μm.

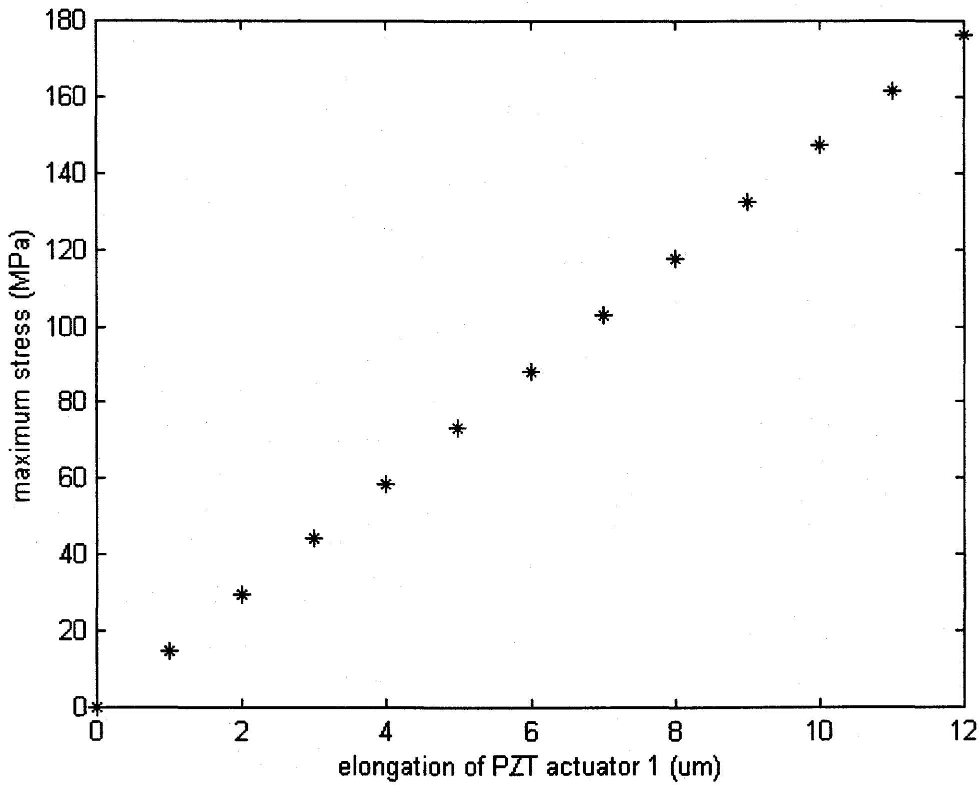

Figure 3.5 Maximum Von Mises stress at 0-12 μm elongation of PZT actuator 2

When PZT actuator 2 elongates individually, the maximum Von Mises stress of the mechanism is found at the flexure hinge 2 (see Figure 3.6). When the elongation of PZT actuator 2 reaches 12 μm, the stress at this flexure hinge is maximal, which is 199.265 MPa, as shown in this figure

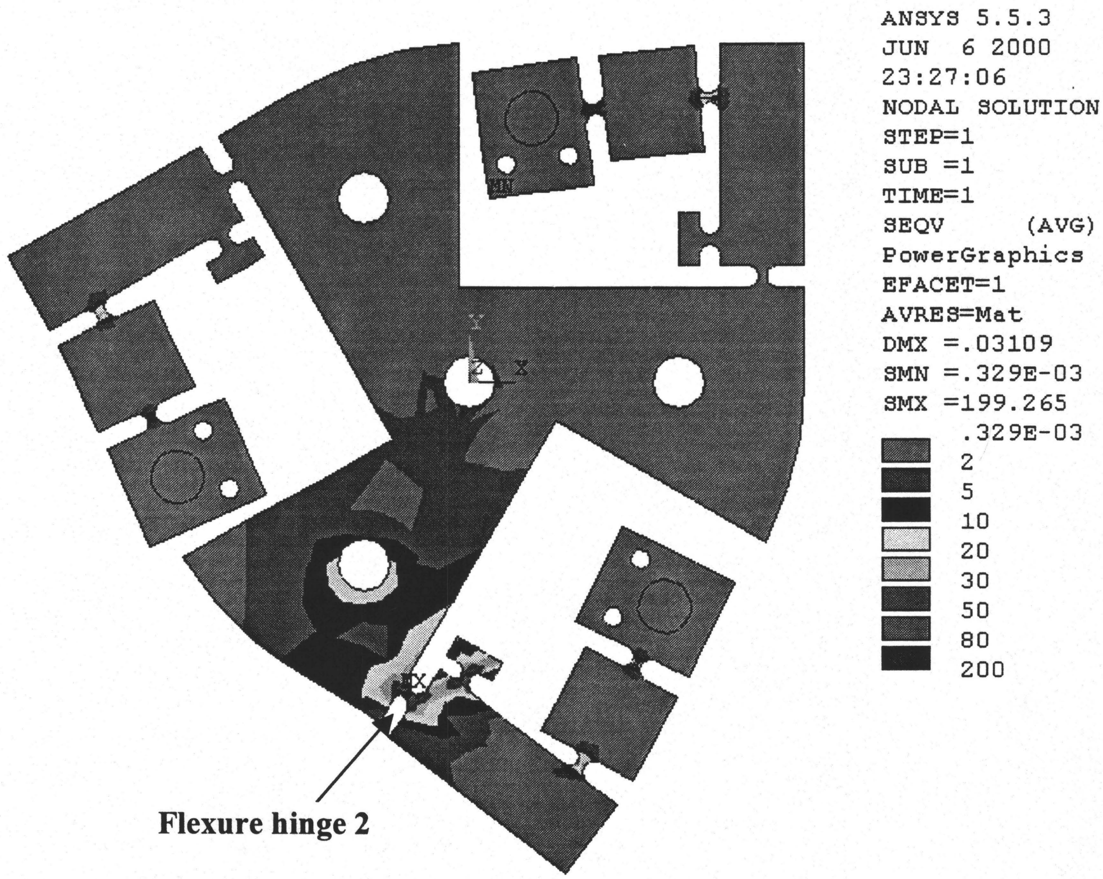

Figure 3.6 Von Mises stress distribution at 12 μm elongation of PZT actuator 2

Figure 3.7 plots the maximum Von Mises stress of the mechanism versus the elongation of PZT actuator 2 extending from 0 to 12 μm.

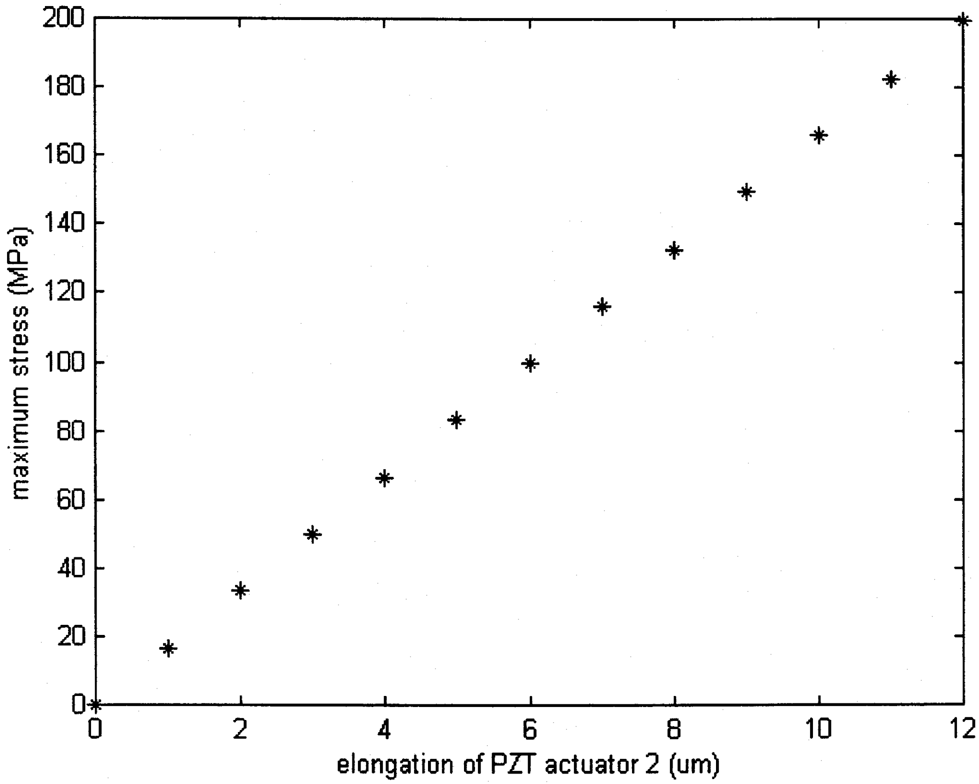

Figure 3.7 Maximum Von Mises stress at 0-12 μm elongation of PZT actuator 2

When PZT actuator 3 elongates individually, the maximum Von Mises stress of the mechanism is at the flexure hinge 3 (see Figure 3.8). When the elongation of PZT actuator 3 reaches 12 μm, the stress at this flexure hinge is maximal, which is 145.658 MPa, as shown in this figure.

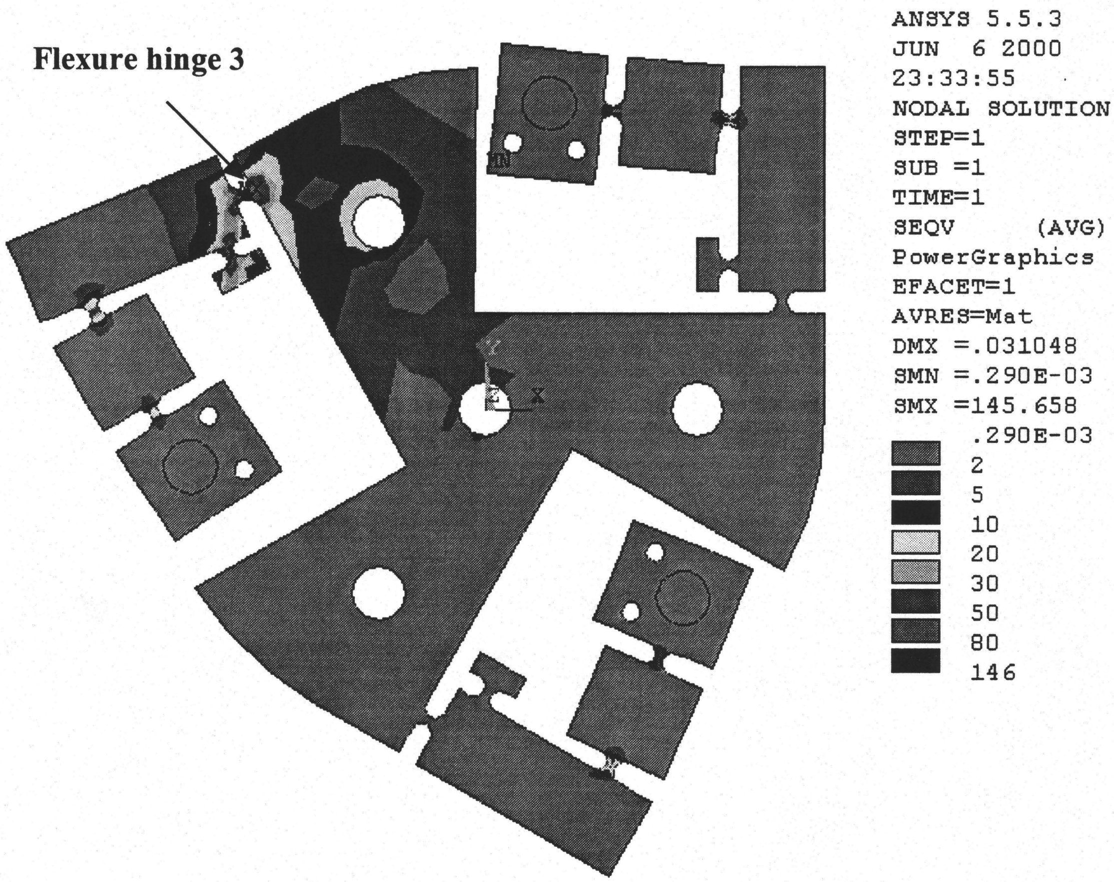

Figure 3.8 Von Mises stress distribution at 12 μm elongation of PZT actuator 3

Figure 3.9 plots the maximum Von Mises stress of the mechanism versus the elongation of PZT actuator 3 extending from 0 to 12 μm.

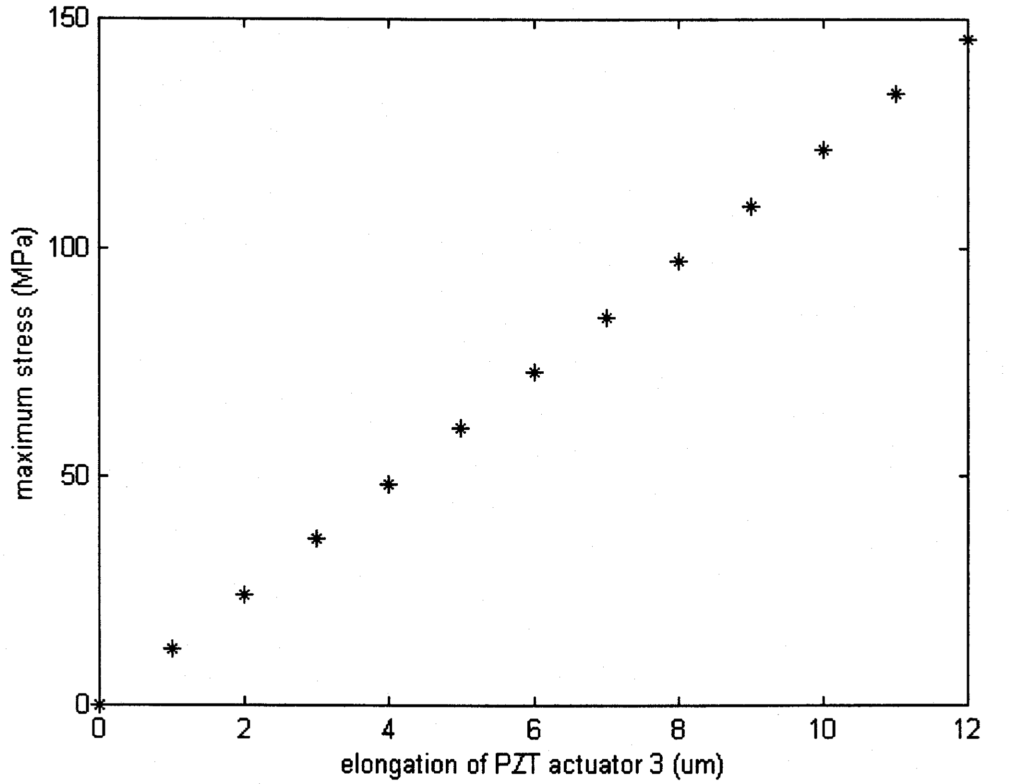

Figure 3.9 Maximum Von Mises stress at 0-12 μm elongation of PZT actuator 3

When PZT actuator 1, 2 and 3 elongate simultaneously, the maximal Von Mises stress of the mechanism is found when the elongations of all the three PZT actuators reach 12 μm. The locations where the maximal Von Mises stress occurs are at the flexure hinge 1, 2 and 3, respectively (see Figure 3.10). The stress at the flexure hinge 2 is the maximum, which is 201.185 MPa, as shown in this figure.

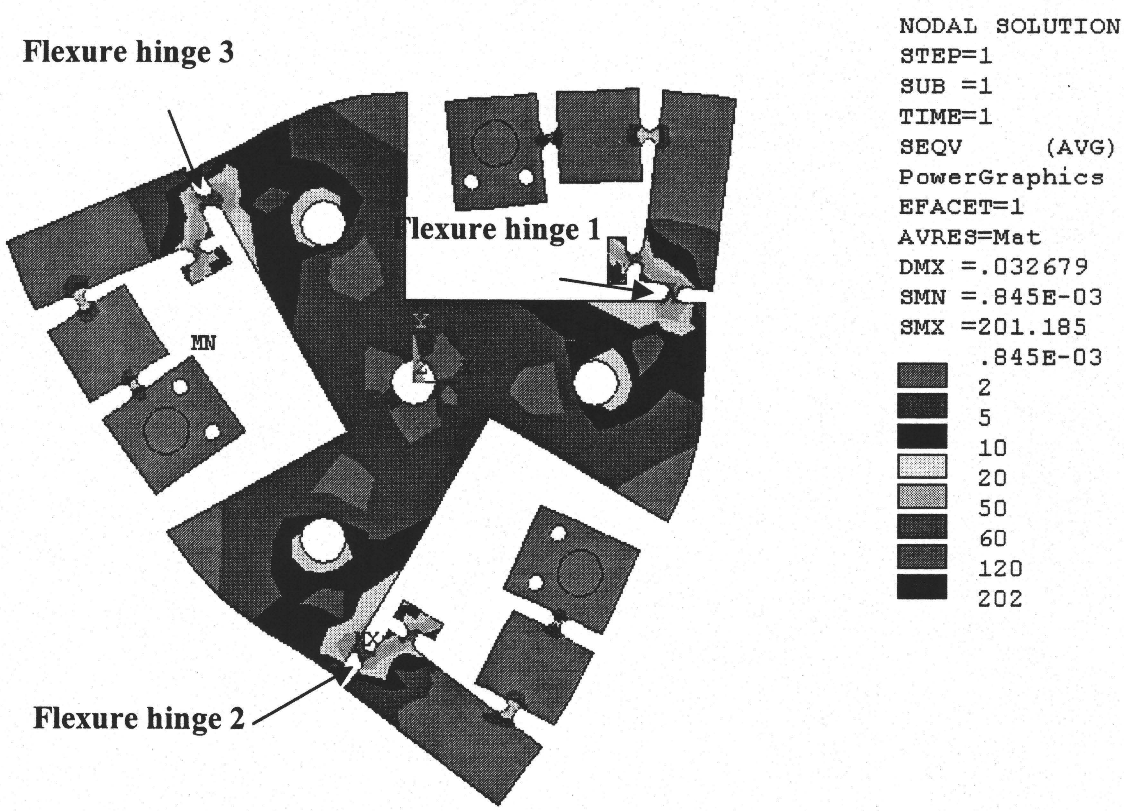

igure 3.10 Von Mises stress distribution at 12 μm elongation of PZT actuators 1, 2, 3

It can be seen from the above discussion that the maximal Von Mises stress of the deformed mechanism is less than the allowable yield strength. It is further noted that there is a noticeable discrepancy in the maximal Von Mises stress between the cases where the actuators operate individually. Some distorted elements which are found in the mesh generated by the ANSYS program may account for this discrepancy. This is worth future work.

3.4 Conclusion

FEM analysis remains to offer the most accurate result in general for the RRR compliant mechanism and is suited to situations without a need for real-time feedback computation. In particular, the facility provided by the ANSYS program for mesh generation for the quadrilateral element type is not computationally stable in the sense that it is possible that a non-symmetrical mesh could be generated on the geometrically symmetrical object and based on the same scheme for mesh generation (by means of seeds specification).

The kinematic calibrated analysis is confirmed to be a necessity for the RRR compliant mechanism and is an excellent replacement for FEM analysis. It is implied that kinematic calibration is an implicit way to take into account the manufacturing and measuring errors in modeling the kinematic behavior of a micro-motion system.

Chapter 4

Dynamic Modeling

4.1 Introduction

This chapter discusses the dynamic modeling of the RRR compliant mechanism based on its PRBM, with the objective to effectively control this system. The task of dynamic modeling is to establish the relationship between the driving force on the actuator and the end-effector motion. This relationship is a system of ordinary differential equations. Because there is a kinematic relationship between the end-effector and the actuator motion, a dynamic model can then be expressed as a relationship between the driving force and the motion of the actuator. One of the common requirements to develop a dynamic model is computational efficiency, and this requirement is addressed in this chapter. The Lagrangian Equation will be applied to derive the dynamic model of the RRR compliant mechanism. It is to be noted that the dynamic model developed will be based on the Constant-Jacobian kinematics, which was developed in Chapter 2. In the following, Section 4.2 presents an efficient way to compute both the kinetic and potential energy terms. Section 4.3 presents the dynamic model. The implementation of this dynamic model is discussed in Section 4.4 with consideration of real-time feed back control application. Section 4.5 concludes this chapter.

4.2 Lagrangian Equation for the RRR Mechanism

The Lagrangian Equation for the RRR mechanism is given by

$$\frac{d}{dt}\left(\frac{\partial L}{\partial \dot{l}_i}\right) - \frac{\partial L}{\partial l_i} = Q_i \tag{4.1}$$

where i=1,2,3,

L= K-P, K and P are kinetic energy and potential energy of the system, respectively,

Q_i is the generalized force, i.e., the driving force on the actuators,

$\dot{l}_i$ is the generalized velocity, i.e., the velocity of the actuators, and

l_i is the generalized displacement, i.e., the displacement of the actuators, and $l_i = \Delta l_i$.

4.2.1 Kinetic and Potential Energy Equations

It is noted that the links A_iB_i (i=1,2,3) perform a pure rotation about the points A_i (i=1,2,3), respectively; while the end-effector platform and the links B_iC_i (i=1,2,3) perform a general planar motion (i.e., one rotation and two translations). The kinetic energy of the RRR mechanism (i.e., the PRBM of the RRR compliant mechanism) can be expressed by

$$K = \frac{1}{2}\left(M_O V_O^{\ 2} + I_O \omega_O^{\ 2} + I_{AiBi}\sum_{i=1}^{3}(\omega_{AiBi})^2 + M_{BiCi}\sum_{i=1}^{3}(V_{BiCi})^2 + I_{BiCi}\sum_{i=1}^{3}(\omega_{BiCi})^2\right) \tag{4.2}$$

where i=1,2,3,

M_O is the mass of the moving platform $C_1C_2C_3$ (see Figure 2.1),

V_O is the velocity of the center of the end-effector (see Figure 2.1),

ω_O is the angular velocity of the end-effector,

I_O is the moment of inertia of the end-effector,

I_{AiBi} is the moment of inertia of the link A_iB_i about joint point A_i,

ω_{AiBi} is the angular velocity of the link A_iB_i,

M_{BiCi} is the mass of the link B_iC_i,

V_{BiCi} is the velocity of the center of the link B_iC_i,

I_{BiCi} is the moment of inertia of the link B_iC_i about its centriod, and

ω_{BiCi} is the angular velocity of the link B_iC_i.

The potential energy of the RRR mechanism is the elastic energy of the nine torsional springs attached at the points A_i, B_i and C_i (i=1,2,3), respectively. Therefore, the potential energy P for the RRR mechanism can be expressed by

$$P = \sum_{i=1}^{3}(P_{Ai} + P_{Bi} + P_{Ci}) = \frac{1}{2}K_b(\sum_{i=1}^{3}\Delta\varphi_{Ai}^{\ 2} + \sum_{i=1}^{3}\Delta\varphi_{Bi}^{\ 2} + \sum_{i=1}^{3}\Delta\varphi_{Ci}^{\ 2}) \qquad (4.3)$$

where i=1,2,3,

K_b is the stiffness of the torsional springs, calculated by equation (2.2),

P_{Ai}, P_{Bi}, and P_{Ci} represent the potential energy of the torsional springs at the points A_i, B_i and C_i, and

$\Delta\varphi_{Ai}$, $\Delta\varphi_{Bi}$, and $\Delta\varphi_{Ci}$ represent the increment in the relative angle at each joint.

4.2.2 Calculation of $\Delta\varphi_{Ai}$, $\Delta\varphi_{Bi}$ and $\Delta\varphi_{Ci}$ in the Potential Energy Equation

Figure 4.1 illustrates the increment in the relative angles. For example, $\Delta\varphi_{A2}$ at the joint A_2 is the increment in the relative angle of the links A_2B_2 at the point A_2. The positive angle is defined to be the one measured counter-clockwise from one line vector to another line vector. $\Delta\varphi_{Ai}$ can be calculated by

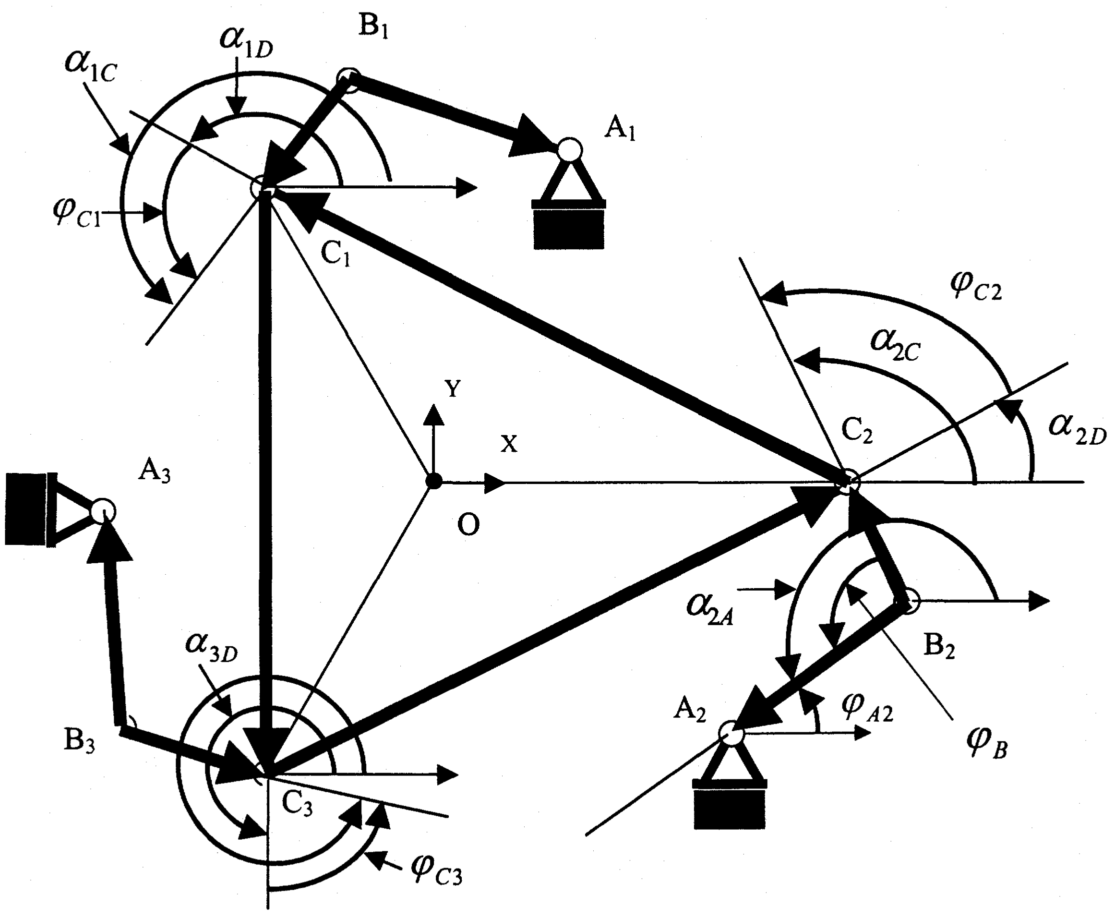

Figure 4.1 Schematic diagram for the potential energy equation

$$\Delta\varphi_{Ai} = \frac{-\Delta l_i}{R_0} \tag{4.4}$$

where Δl_i (i=1,2,3) is the elongation of the ith PZT actuator, and

R_0 was illustrated before in Figure 2.3.

$\Delta\varphi_{Bi}$ (i=1,2,3) is the increment in the relative angle between the links B_iA_i and B_iC_i (i=1,2,3), i.e.,

$$\Delta\varphi_{Bi} = \varphi_{Bi} - \varphi_{Bi}^{0} \tag{4.5}$$

where φ_{Bi}^{0} is the relative angle between the two links B_iA_i and B_iC_i (i=1,2,3) at the initial position, and

φ_{Bi} is the relative angle between the two links B_iA_i and B_iC_i (i=1,2,3) at any other position

φ_{Bi} and φ_{Bi}^{0} can be obtained, respectively, by

$$\varphi_{Bi} = \alpha_{iA} - \alpha_{iC} \tag{4.6}$$

$$\varphi_{Bi}^{0} = \alpha_{iA}^{0} - \alpha_{iC}^{0} \tag{4.7}$$

where α_{iA}^{0} is the angle of the link vector $\overrightarrow{B_iA_i}$ at the initial position,

α_{iC}^{0} is the angle of the link vector $\overrightarrow{B_iC_i}$ at the initial position,

α_{iA} is the angle of the link vector $\overrightarrow{B_iA_i}$ at any other position, and

α_{iC} is the angle of the link vector $\overrightarrow{B_iC_i}$ at any other position.

Substitution of equation (4.6) and (4.7) into equation (4.5) yields

$$\Delta\varphi_{Bi} = (\alpha_{iA} - \alpha_{iC}) - (\alpha_{iA}^{0} - \alpha_{iC}^{0}) = (\alpha_{iA} - \alpha_{iA}^{0}) - (\alpha_{iC} - \alpha_{iC}^{0}) \tag{4.8}$$

Since the displacements are very small, the following simplification is justified.

$$\alpha_{iA} - \alpha_{iA}^{0} \cong \sin(\alpha_{iA} - \alpha_{iA}^{0}) \tag{4.9}$$

$$\alpha_{iC} - \alpha_{iC}{}^{0} \cong \sin(\alpha_{iC} - \alpha_{iC}{}^{0}) \tag{4.10}$$

with $$\sin(\alpha_{iA} - \alpha_{iA}{}^{0}) = \sin\alpha_{iA}\cos\alpha_{iA}{}^{0} - \cos\alpha_{iA}\sin\alpha_{iA}{}^{0} \tag{4.11}$$

$$\sin(\alpha_{iC} - \alpha_{iC}{}^{0}) = \sin\alpha_{iC}\cos\alpha_{iC}{}^{0} - \cos\alpha_{iC}\sin\alpha_{iC}{}^{0} \tag{4.12}$$

As illustrated in Figure 4.1, the following relationships can be found.

$$\sin\alpha_{iA} = \frac{A_{iy}{}^{0} - B_{iy}}{L_{AB}} \tag{4.13}$$

$$\cos\alpha_{iA} = \frac{A_{ix}{}^{0} - B_{ix}}{L_{AB}} \tag{4.14}$$

$$\sin\alpha_{iA}{}^{0} = \frac{A_{iy}{}^{0} - B_{iy}{}^{0}}{L_{AB}} \tag{4.15}$$

$$\cos\alpha_{iA}{}^{0} = \frac{A_{ix}{}^{0} - B_{ix}{}^{0}}{L_{AB}} \tag{4.16}$$

$$\sin\alpha_{iC} = \frac{C_{iy}{}^{0} - B_{iy}}{L_{BC}} \tag{4.17}$$

$$\cos\alpha_{iC} = \frac{C_{ix}{}^{0} - B_{ix}}{L_{BC}} \tag{4.18}$$

$$\sin\alpha_{iC}{}^{0} = \frac{C_{iy}{}^{0} - B_{iy}{}^{0}}{L_{BC}} \tag{4.19}$$

$$\cos\alpha_{iC} = \frac{C_{ix}{}^{0} - B_{ix}{}^{0}}{L_{BC}} \tag{4.20}$$

with $$B_{ix} = A_{ix}^{0} + L_{AB}\cos(\varphi_{Ai}^{0} - \frac{\Delta l_i}{R_0})$$

$$B_{iy} = A_{iy}^{0} + L_{AB}\sin(\varphi_{Ai}^{0} - \frac{\Delta l_i}{R_0})$$

The above procedure for $\Delta\varphi_{Bi}$ can be applied to computing $\Delta\varphi_{Ci}$.

$$\Delta\varphi_{Ci} = \varphi_{Ci} - \varphi_{Ci}^{\ 0} \tag{4.21}$$

where i=1,2,3,

φ_{C1} is the relative angle between the link vectors $\overrightarrow{C_2C_1}$ and $\overrightarrow{B_1C_1}$ at any other position,

φ_{C2} is the relative angle between the link vectors $\overrightarrow{C_3C_2}$ and $\overrightarrow{B_2C_2}$ at any other position,

φ_{C3} is the relative angle between the link vectors $\overrightarrow{C_1C_3}$ and $\overrightarrow{B_3C_3}$ at any other position, and

φ_{ci}^{0} (i=1,2,3) are the angles φ_{Ci} (i=1,2,3) at the initial position.

.

From Figure 4.1, φ_{Ci} and $\varphi_{Ci}^{\ 0}$ can be obtained, respectively, by

$$\varphi_{Ci} = \alpha_{iC} - \alpha_{iD} \tag{4.22}$$

$$\varphi_{Ci}^{\ 0} = \alpha_{iC}^{\ 0} - \alpha_{iD}^{\ 0} \tag{4.23}$$

where α_{1D} is the angle of the link vector $\overrightarrow{C_2C_1}$ at any other position,

α_{2D} is the angle of the link vector $\overrightarrow{C_3C_2}$ at any other position,

α_{3D} is the angle of the link vector $\overrightarrow{C_1C_3}$ at any other position, and

$\alpha_{iD}^{\ 0}$ (i=1,2,3) are the angles α_{iD} (i=1,2,3) at the initial position.

Substitution of equations (4.22) and (4.23) into equation (4.21) yields

$$\Delta\varphi_{Ci} = (\alpha_{iC} - \alpha_{iD}) - (\alpha_{iC}^{\ 0} - \alpha_{iD}^{\ 0}) = (\alpha_{iC} - \alpha_{iC}^{\ 0}) - (\alpha_{iD} - \alpha_{iD}^{\ 0}) \tag{4.24}$$

Since the displacements are very small, the following simplification is justified.

$$\alpha_{iD} - \alpha_{iD}{}^{0} \cong \sin(\alpha_{iD} - \alpha_{iD}{}^{0}) \tag{4.25}$$

with $$\sin(\alpha_{iD} - \alpha_{iD}{}^{0}) = \sin\alpha_{iD}\cos\alpha_{iD}{}^{0} - \cos\alpha_{iD}\sin\alpha_{iD}{}^{0} \tag{4.26}$$

As indicated in Figure 4.1, when i=1,2,

$$\sin\alpha_{iD} = \frac{C_{iy} - C_{(i+1)y}}{L_S} \tag{4.27}$$

$$\sin\alpha_{iD}{}^{0} = \frac{C_{iy}{}^{0} - C_{(i+1)y}{}^{0}}{L_S} \tag{4.28}$$

$$\cos\alpha_{iD} = \frac{C_{ix} - C_{(i+1)x}}{L_S} \tag{4.29}$$

$$\cos\alpha_{iD}{}^{0} = \frac{C_{ix}{}^{0} - C_{(i+1)x}{}^{0}}{L_S} \tag{4.30}$$

when i=3,

$$\sin\alpha_{3D} = \frac{C_{3y} - C_{1y}}{L_S} \tag{4.31}$$

$$\sin\alpha_{3D}{}^{0} = \frac{C_{3y}{}^{0} - C_{1y}{}^{0}}{L_S} \tag{4.32}$$

$$\cos\alpha_{3D} = \frac{C_{3x} - C_{1x}}{L_S} \tag{4.33}$$

$$\cos\alpha_{3D}{}^{0} = \frac{C_{3x}{}^{0} - C_{1x}{}^{0}}{L_S} \tag{4.34}$$

where L_S is the length of the side of the equilateral triangle $\Delta C_1C_2C_3$ and $L_S = \sqrt{3}R$.

From the previous discussion in Chapter 2, in particular from equation (2.12), it can be seen that both C_{ix} and C_{iy} (i=1,2,3) are functions of the displacements (x, y, γ) of the end-effector which are, further, functions of Δl_i (i=1,2,3), see equation (2.19). Therefore, C_{ix} and C_{iy} (i=1,2,3) are functions of Δl_i (i=1,2,3).

It can be seen from the above derivation that all the increment in the relative angles can be expressed as functions of Δl_i (i=1,2,3). Therefore, the potential energy P is a function of Δl_i (i.e. l_i) (i=1,2,3).

4.2.3 Calculation of Velocity Terms in the Kinetic Energy Equation

As shown in equation (4.2), the kinetic energy equation contains the velocity terms: $V_O^{\ 2}$, $\omega_O^{\ 2}$, $\omega_{AiBi}^{\ \ 2}$, $\omega_{BiCi}^{\ \ 2}$ and $V_{BiCi}^{\ \ 2}$. These terms should be expressed as functions of $\dot{l}_i$ and l_i (i.e., Δl_i, i=1,2,3), which will be developed in the following. In order to have a compact form of expression, the matrix notation is applied, wherever possible, based on the observation that these expressions are of quadratic form of $\dot{l}_i$ in nature.

Expressions for $V_O^{\ 2}$, $\omega_O^{\ 2}$, $\omega_{AiBi}^{\ \ 2}$:

$$V_O^{\ 2} = \dot{x}^2 + \dot{y}^2 = \dot{\mathbf{l}}^{\mathrm{T}} \mathbf{V_0} \dot{\mathbf{l}} \tag{4.35}$$

$$\omega_O^{\ 2} = \dot{\gamma}^2 = \dot{\mathbf{l}}^{\mathrm{T}} \mathbf{W_0} \dot{\mathbf{l}} \tag{4.36}$$

$$\sum_{i=1}^{3} \omega_{AiBi}^{\ \ 2} = \sum_{i=1}^{3} (\frac{\dot{l}_i}{R_0})^2 = \dot{\mathbf{l}}^{\mathrm{T}} \mathbf{W_{AB}} \dot{\mathbf{l}} \tag{4.37}$$

with $\dot{x} = \mathbf{J}_l^1 \dot{\mathbf{l}}$,

$\dot{y} = \mathbf{J}_l^2 \dot{\mathbf{l}}$,

$$\dot{\gamma} = \mathbf{J}_l^3 \dot{\mathbf{l}},$$

$$\mathbf{V_O} = \begin{bmatrix} \mathbf{J}_l^1 \\ \mathbf{J}_l^2 \end{bmatrix}^T \begin{bmatrix} \mathbf{J}_l^1 \\ \mathbf{J}_l^2 \end{bmatrix},$$

$$\mathbf{W_O} = [\mathbf{J}_l^3]^T [\mathbf{J}_l^3],$$

$$\mathbf{W_{AB}} = \begin{bmatrix} \frac{1}{R_0} & & \\ & \frac{1}{R_0} & \\ & & \frac{1}{R_0} \end{bmatrix}^T \begin{bmatrix} \frac{1}{R_0} & & \\ & \frac{1}{R_0} & \\ & & \frac{1}{R_0} \end{bmatrix},$$

where $\mathbf{J}_l^1, \mathbf{J}_l^2$ and $\mathbf{J}_l^3$ are the first, second and the third row of the Constant Jacobian Matrix $\mathbf{J}_l^0$ expressed in equation (2.19), respectively.

Expressions for $\omega_{BiCi}{}^2$:

$$\sum_{i=1}^{3} \omega_{BiCi}{}^2 = \dot{\mathbf{l}}^T \sum_{i=1}^{3} \mathbf{W}_i(\mathbf{l}) \dot{\mathbf{l}} \tag{4.38}$$

where ω_{BiCi} (i=1,2,3) is the first order derivative of α_{iC} (i=1,2,3). From Figure 4.1, the following vector equation can be obtained.

$$\overrightarrow{A_i B_i} + \overrightarrow{B_i C_i} + \overrightarrow{C_i O} = \overrightarrow{A_i O} \tag{4.39}$$

The projection of equation (4.39) onto the X- and Y- directions leads to

$$L_{AB} \cos(\varphi_{Ai}^0 - \frac{\Delta l_i}{R_0}) + L_{BC} \cos\alpha_{iC} + R\cos(\frac{2(2-i)\pi}{3} + \gamma + \pi) = x - A_{ix}^0 \tag{4.40}$$

$$L_{AB} \sin(\varphi_{Ai}^0 - \frac{\Delta l_i}{R_0}) + L_{BC} \sin\alpha_{iC} + R\sin(\frac{2(2-i)\pi}{3} + \gamma + \pi) = y - A_{iy}^0 \tag{4.41}$$

The first order derivative of equations (4.40) and (4.41), respectively, leads to

$$\begin{aligned}&L_{AB}(-\sin(\varphi_{Ai}^{0}-\frac{\Delta l_i}{R_0}))(\frac{-\dot{l}_i}{R_0})+L_{BC}(-\sin\alpha_{iC})\omega_{BiCi}\\&+R(-\sin(\frac{2(2-i)\pi}{3}+\gamma+\pi))\omega_O=\dot{x}\end{aligned}\tag{4.42}$$

$$\begin{aligned}&L_{AB}\cos(\varphi_{Ai}^{0}-\frac{\Delta l_i}{R_0})(\frac{-\dot{l}_i}{R_0})+L_{BC}(\cos\alpha_{iC})\omega_{BiCi}\\&+R\cos(\frac{2(2-i)\pi}{3}+\gamma+\pi)\omega_O=\dot{y}\end{aligned}\tag{4.43}$$

Using the relationship $\sin\alpha_{iC}{}^{2}+\cos\alpha_{iC}{}^{2}=1$ leads to the form of equation (4.38), in which $\mathbf{W_i(l)}$ (i=1,2,3) can be derived. With the help of the Maple V software package, elements of $\mathbf{W_i(l)}$ (i=1,2,3) can be found in Appendix D.

Expressions for $V_{BiCi}{}^{2}$:

V_{BiCi} is the velocity of the centroid of the link B_iC_i. Assume that a uniform mass distribution is applied to all these links. The centroid of these links is, therefore, at the midpoint of each of these links, respectively. Let mp_i denote the midpoint of the link B_iC_i. The coordinates of mp_i can be expressed by

$$mp_{ix}=\frac{B_{ix}+C_{ix}}{2}=\frac{1}{2}[A_{ix}^{0}+L_{AB}\cos(\varphi_{Ai}^{0}-\frac{\Delta l_i}{R_0})+x+R\cos(\frac{2(2-i)\pi}{3}+\gamma)]\tag{4.44}$$

$$mp_{iy}=\frac{B_{iy}+C_{iy}}{2}=\frac{1}{2}[A_{iy}^{0}+L_{AB}\sin(\varphi_{Ai}^{0}-\frac{\Delta l_i}{R_0})+y+R\sin(\frac{2(2-i)\pi}{3}+\gamma)]\tag{4.45}$$

The first order derivatives of equations (4.44) and (4.45) with respect to time yield

$$V_{ix} = \frac{1}{2}[\dot{x} - R\sin(\frac{2(2-i)\pi}{3} + \gamma)\dot{\gamma} - L_{AB}\sin(\varphi_{Ai}^{0} - \frac{\Delta l_i}{R_0})(\frac{-\dot{l}_1}{R_0})] \tag{4.46}$$

$$V_{iy} = \frac{1}{2}[\dot{y} + R\cos(\frac{2(2-i)\pi}{3} + \gamma)\dot{\gamma} + L_{AB}\cos(\varphi_{Ai}^{0} - \frac{\Delta l_i}{R_0})(\frac{-\dot{l}_1}{R_0})] \tag{4.47}$$

Therefore

$$\sum_{i=1}^{3} V_{BiCi}{}^{2} = \sum_{i=1}^{3} (V_{ix}{}^{2} + V_{iy}{}^{2}) = \dot{\mathbf{l}}^{\mathrm{T}} \sum_{i=1}^{3} \mathbf{V}_{\mathrm{i}}(\mathbf{l})\dot{\mathbf{l}} \tag{4.48}$$

The elements of $\mathbf{V}_{\mathrm{i}}(\mathbf{l})$ (i=1,2,3) can be found in Appendix D.

The kinetic energy, expressed by equation (4.2), can be written as

$$\begin{aligned} K &= \frac{1}{2}\dot{\mathbf{l}}^{\mathrm{T}}[M_O\mathbf{V_O} + I_O\mathbf{W_O} + I_{AB}\mathbf{W_{AB}} + M_{BiCi}\sum_{i=1}^{3}\mathbf{V}_{\mathrm{i}}(\mathbf{l}) + I_{BiCi}\sum_{i=1}^{3}\mathbf{W}_{\mathrm{i}}(\mathbf{l})]\dot{\mathbf{l}} \\ &= \frac{1}{2}\dot{\mathbf{l}}^{\mathrm{T}}\mathbf{K}(\mathbf{l})\dot{\mathbf{l}} \end{aligned} \tag{4.49}$$

where $\mathbf{K}(\mathbf{l})$ is a 3×3 matrix, the elements of which can be found in Appendix D.

4.3 Dynamic Model

Equation (4.1) can now be written as

$$\frac{d}{dt}(\frac{\partial(K-P)}{\partial \dot{l}_i}) - \frac{\partial(K-P)}{\partial l_i} = Q_i \tag{4.50}$$

where i=1,2,3. In the following, these derivative items in the equation above are written in matrix forms, respectively,

$$\frac{\partial(K-P)}{\partial \dot{l}_i}=\begin{bmatrix} \dfrac{\partial(\frac{1}{2}\dot{\mathbf{l}}^{\mathrm{T}}\mathbf{K}(\mathbf{l})\dot{\mathbf{l}}-P(\mathbf{l}))}{\partial \dot{l}_1} \\ \dfrac{\partial(\frac{1}{2}\dot{\mathbf{l}}^{\mathrm{T}}\mathbf{K}(\mathbf{l})\dot{\mathbf{l}}-P(\mathbf{l}))}{\partial \dot{l}_2} \\ \dfrac{\partial(\frac{1}{2}\dot{\mathbf{l}}^{\mathrm{T}}\mathbf{K}(\mathbf{l})\dot{\mathbf{l}}-P(\mathbf{l}))}{\partial \dot{l}_3} \end{bmatrix}=\mathbf{K}(\mathbf{l})\dot{\mathbf{l}} \tag{4.51}$$

$$\frac{d}{dt}\frac{\partial(K-P)}{\partial \dot{l}_i}=\frac{d}{dt}\mathbf{K}(\mathbf{l})\dot{\mathbf{l}}=\mathbf{K}(\mathbf{l})\ddot{\mathbf{l}}+\mathbf{K}(\dot{\mathbf{l}})\dot{\mathbf{l}} \tag{4.52}$$

$$\begin{aligned}\frac{\partial(K-P)}{\partial l_i}&=\begin{bmatrix} \dfrac{\partial(\frac{1}{2}\dot{\mathbf{l}}^{\mathrm{T}}\mathbf{K}(\mathbf{l})\dot{\mathbf{l}}-P(\mathbf{l}))}{\partial l_1} \\ \dfrac{\partial(\frac{1}{2}\dot{\mathbf{l}}^{\mathrm{T}}\mathbf{K}(\mathbf{l})\dot{\mathbf{l}}-P(\mathbf{l}))}{\partial l_2} \\ \dfrac{\partial(\frac{1}{2}\dot{\mathbf{l}}^{\mathrm{T}}\mathbf{K}(\mathbf{l})\dot{\mathbf{l}}-P(\mathbf{l}))}{\partial l_3} \end{bmatrix}=\begin{bmatrix} \dfrac{\partial(\frac{1}{2}\dot{\mathbf{l}}^{\mathrm{T}}\mathbf{K}(\mathbf{l})\dot{\mathbf{l}})}{\partial l_1} \\ \dfrac{\partial(\frac{1}{2}\dot{\mathbf{l}}^{\mathrm{T}}\mathbf{K}(\mathbf{l})\dot{\mathbf{l}})}{\partial l_2} \\ \dfrac{\partial(\frac{1}{2}\dot{\mathbf{l}}^{\mathrm{T}}\mathbf{K}(\mathbf{l})\dot{\mathbf{l}})}{\partial l_3} \end{bmatrix}-\begin{bmatrix} \dfrac{\partial(P(\mathbf{l}))}{\partial l_1} \\ \dfrac{\partial(P(\mathbf{l}))}{\partial l_2} \\ \dfrac{\partial(P(\mathbf{l}))}{\partial l_3} \end{bmatrix} \\ &=\begin{bmatrix} \frac{1}{2}\dot{\mathbf{l}}^{\mathrm{T}}\dfrac{\partial\mathbf{K}(\mathbf{l})}{\partial l_1}\dot{\mathbf{l}} \\ \frac{1}{2}\dot{\mathbf{l}}^{\mathrm{T}}\dfrac{\partial\mathbf{K}(\mathbf{l})}{\partial l_2}\dot{\mathbf{l}} \\ \frac{1}{2}\dot{\mathbf{l}}^{\mathrm{T}}\dfrac{\partial\mathbf{K}(\mathbf{l})}{\partial l_3}\dot{\mathbf{l}} \end{bmatrix}-\begin{bmatrix} \dfrac{\partial P(\mathbf{l})}{\partial l_1} \\ \dfrac{\partial P(\mathbf{l})}{\partial l_2} \\ \dfrac{\partial P(\mathbf{l})}{\partial l_3} \end{bmatrix}=\mathbf{N}(\mathbf{l},\dot{\mathbf{l}})\dot{\mathbf{l}}-\mathbf{H}(\mathbf{l})\end{aligned} \tag{4.53}$$

Finally, the matrix form of the dynamic model for the RRR mechanism follows.

$$\mathbf{K}(\mathbf{l})\ddot{\mathbf{l}}+\mathbf{C}(\mathbf{l},\dot{\mathbf{l}})\dot{\mathbf{l}}+\mathbf{H}(\mathbf{l})=\mathbf{Q} \tag{4.54}$$

with $\mathbf{C}(\mathbf{l},\dot{\mathbf{l}})=\mathbf{K}(\dot{\mathbf{l}})-\mathbf{N}(\mathbf{l},\dot{\mathbf{l}})$, and

$$\mathbf{Q} = [Q_1, \ Q_2, \ Q_3]^T.$$

The detailed expressions of $\mathbf{C}(\mathbf{l}, \dot{\mathbf{l}})$ and $\mathbf{H}(\mathbf{l})$ can be found in Appendix D.

4.4 Implementation of the Dynamic Model

It is possible that the dynamic model developed above is completely implemented in the Matlab software environment using the SIMULINK tool. This implementation strategy turns out to be complex in the sense that lengthy SIMULINK block diagrams need to be written. Therefore, a strategy which combines the Maple V software and the Matlab SIMULINK software is taken for the current implementation. In this strategy, the Maple V software is used to derive the parametric form of the dynamic model of the RRR compliant mechanism, see Appendix D (D.1 in particular). Furthermore, in the Maple V software environment, these parameters are substituted by their corresponding values; this then leads to a simple non-parametric dynamic model using the Maple V software tool, see Appendix D (D.2 in particular). The non-parametric dynamic model is sufficiently simple to be implemented using the SIMULINK tool. Since the dynamic model is used in conjunction with control of the RRR compliant mechanism, a full implementation using the SIMULINK tool will then be discussed in the next chapter.

4.5 Conclusion

A dynamic model with consideration of computational efficiency has been developed based on the Lagrangian Equation. A compact matrix form eventually describes the model. It is usually a practice that dynamic models for such a complex mechanism can contain a large number of trigonometric terms and this may cause computational problems inherently associated with computer-computation of trigonometric terms. In this development, trigonometric terms are, if possible, substituted by coordinates of the corresponding nodes, see equation (4.13) to (4.20) and equation (4.27) to (4.34). This results in an improvement of computational efficiency.

Chapter 5

Dynamic Control and Simulation

5.1 Introduction

This chapter presents a preliminary study of the control of the RRR compliant mechanism based on its PRBM. A computed torque control (CTC) law for the trajectory tracking of the PZT actuators is developed. In this law, the information of the dynamic model of a system is incorporated into the control law. The dynamic model of the RRR compliant mechanism derived in Chapter 4 will be used in developing this CTC controller. Before discussing this CTC controller, the commonly used control strategies for multi-DOF robotic systems are introduced in Section 5.2. The CTC law for the RRR compliant mechanism will then be presented in Section 5.3. Section 5.4 presents and discusses the simulation results of the trajectory tracking performance of the RRR compliant mechanism. Section 5.5 concludes this chapter.

5.2 Control Strategies for Robotic Manipulators

The independent-joint PD control is the most popular feedback controller for robotic manipulators. The basic structure of this controller is shown in Figure 5.1. It should be noted that in this simulation study, the behavior of actuators is not considered, and this may further imply that a time-invariant perfect linear relationship exists between the actuator input (i.e., the controller output signal) and the actuator output (i.e., the torque). Under these assumptions, the controller shown in Figure 5.1 contains actuators. The output of the controller is torque τ, which drives a robot plant. The output of the plant, i.e., displacement θ and velocity $\dot{\theta}$ of a joint are fed back, compared with the desired joint displacement θ_d and joint velocity $\dot{\theta}_d$. Note that this feedback controller does not include any information of a model of the system, and is driven by the position and velocity errors only. This controller is the same for each joint of a robot, and the control action at one joint is totally independent of control actions at other joints.

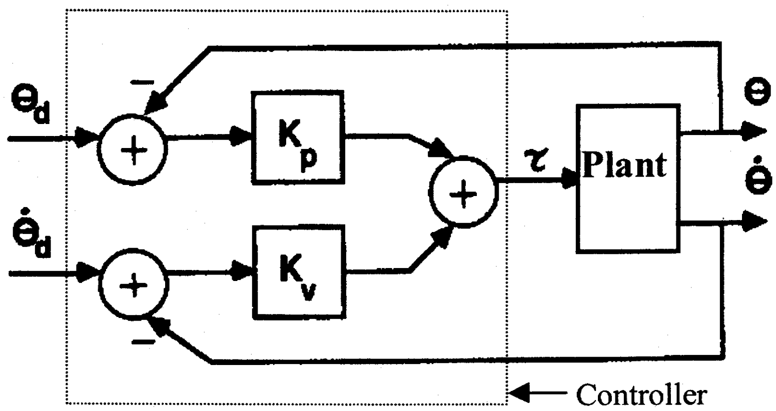

Figure 5.1 Independent-joint PD control

The control law of the independent-joint PD control can be expressed by

$$\tau = K_P(\theta_d - \theta) + K_V(\dot{\theta}_d - \dot{\theta}) \tag{5.1}$$

where K_P is proportional gain, and

K_V is derivative gain.

The previous studies (Guo et al., 1999; Guo et al., 2000) have shown that the simple independent-joint PD control law may not ensure the error convergence in the joints and end-effector of 2-DOF closed-chain mechanical systems. Since the RRR compliant mechanism is a non-linear and coupled 3-DOF closed-chain mechanical system, the independent-joint PD controller may not be applicable. A simulation study with SIMULINK toolbox in Matlab (Ver. 5.3) is performed for this mechanism. In this simulation study, K_P and K_V for each joint are set as the same. Based on a trial-and error approach, several values of K_P and K_V are chosen, as listed in Table 5.1. Unfortunately, the convergence of the trajectory tracking performance has not been achieved. This implies that more advanced control laws need to be considered for the RRR compliant mechanism. In this case, the CTC law will be applied.

Table 5.1 Some values of K_P and K_V in an independent-joint PD control law

K_P	10^2	10^3	10^4	10^5	5×10^5	10^6	3×10^6
K_V	0	0	0	0	0	0	0
K_P	10^9	10^{10}	10^{11}	10^{12}	10^{13}	10^{14}	10^{15}
K_V	0	0	0	0	0	0	0
K_P	10^{17}	10^{17}	10^{17}	10^{17}	10^{17}	10^{17}	10^{17}
K_V	10	100	10^3	10^4	10^5	10^6	3×10^6
K_P	8.5×10^{17}	8×10^{17}	8.6×10^{17}	10^{17}	10^{17}	10^{17}	10^{17}
K_V	3×10^6	3.5×10^6	4×10^6	10^4	10^5	10^6	10^7

5.3 CTC Controller for the RRR Compliant Mechanism

5.3.1 Introduction of CTC (An et al., 1988; Craig, 1986)

The basic idea of CTC is that the information of a dynamic model of a controlled plant system is incorporated in a control law. Figure 5.2 shows a CTC block diagram, where $\hat{R}^{-1}$ is a general representation of the inverse dynamic model of a plant, and is expressed by

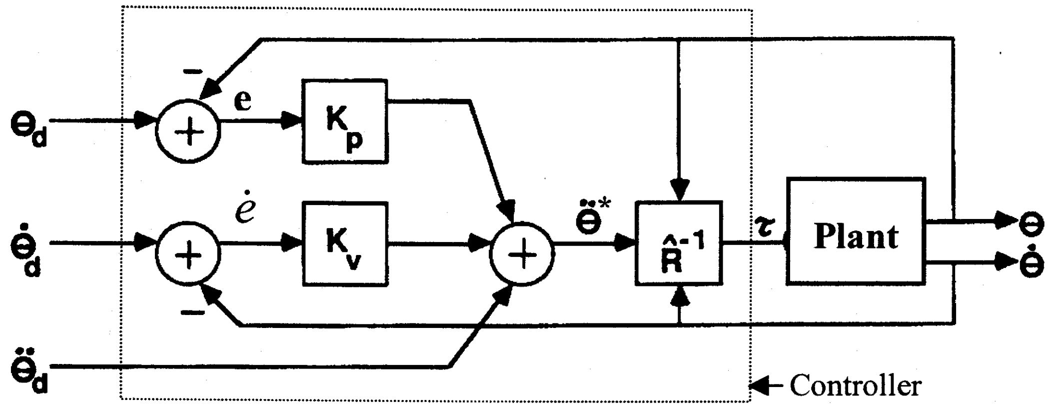

Figure 5.2 Block diagram of computed torque control

$$\mathbf{M}(\theta)\ddot{\theta} + \mathbf{C}(\theta,\dot{\theta})\dot{\theta} + \mathbf{H}(\theta) = \hat{R}^{-1}(\theta,\dot{\theta},\ddot{\theta}) = \tau \tag{5.2}$$

where τ is the torque applied to the joints.

The CTC control law comprises an independent-joint PD controller and the desired acceleration. This yields a "corrected" acceleration $\ddot{\theta}^*$, which is expressed by

$$\ddot{\theta}^* = \ddot{\theta}_d + \mathbf{K}_p(\theta_d - \theta) + \mathbf{K}_V(\dot{\theta}_d - \dot{\theta}) = \ddot{\theta}_d + \mathbf{K}_p\mathbf{e} + \mathbf{K}_V\dot{\mathbf{e}} \tag{5.3}$$

where θ and $\dot{\theta}$ are the actual displacement and velocity vectors in the joints,
θ_d, $\dot{\theta}_d$, and $\ddot{\theta}_d$ are the desired displacement, velocity, and acceleration vectors in the joints, respectively,
$\mathbf{e}$ and $\dot{\mathbf{e}}$ are the displacement and velocity tracking error vectors in the joints,
$\mathbf{K}_P = diag\{K_P\}$ and $\mathbf{K}_V = diag\{K_V\}$ are the proportional and derivative gain diagonal matrices.

This corrected acceleration $\ddot{\theta}^*$ replaces $\ddot{\theta}$ in the inverse dynamic model, and this results in a "corrected" torque, τ^*, i.e.,

$$\tau^* = \hat{R}^{-1}(\theta, \dot{\theta}, \ddot{\theta}^*) \tag{5.4}$$

Substitution of equation (5.3) into equation (5.4), applying equation (5.2), yields:

$$\begin{aligned} \tau^* &= \mathbf{M}(\theta)\ddot{\theta}^* + \mathbf{C}(\theta, \dot{\theta})\dot{\theta} + \mathbf{H}(\theta) \\ &= \mathbf{M}(\theta)(\ddot{\theta}_d + \mathbf{K}_\mathbf{p}\mathbf{e} + \mathbf{K}_\mathbf{V}\dot{\mathbf{e}}) + \mathbf{C}(\theta, \dot{\theta})\dot{\theta} + \mathbf{H}(\theta) \end{aligned} \tag{5.5}$$

Assume that the plant dynamic model "perfectly" represents the dynamics of a plant. The corrected torque τ^*, expressed by equation (5.5), should be equal to the torque τ, expressed by equation (5.2). This yields:

$$\mathbf{M}(\theta)(\ddot{\mathbf{e}} + \mathbf{K}_\mathbf{p}\mathbf{e} + \mathbf{K}_\mathbf{V}\dot{\mathbf{e}}) = \mathbf{0} \tag{5.6}$$

where $\ddot{\mathbf{e}} = \ddot{\theta}_d - \ddot{\theta}$ is the acceleration error vector in the joints.

Since $\mathbf{M}(\theta)$ is a positive definite matrix, the following equation can be obtained:

$$\ddot{\mathbf{e}} + \mathbf{K}_\mathbf{V}\dot{\mathbf{e}} + \mathbf{K}_\mathbf{p}\mathbf{e} = \mathbf{0} \tag{5.7}$$

Equation (5.7) is a linear differential equation which governs the trajectory tracking error. Since this equation is linear, $\mathbf{K}_\mathbf{p}$ and $\mathbf{K}_\mathbf{V}$ can be obtained analytically to make the controlled plant system stable and convergent at $t \to \infty$.

5.3.2 CTC of the RRR Compliant Mechanism

The CTC controller of the RRR compliant mechanism is shown in Figure 5.3. From this figure, the force applied to the joints can be expressed as:

$$\mathbf{Q} = \mathbf{K}(\mathbf{l})(\ddot{\mathbf{l}}_d + \mathbf{K}_\mathbf{V}\dot{\mathbf{l}} + \mathbf{K}_\mathbf{P}\mathbf{l}) + \mathbf{C}(\mathbf{l}, \dot{\mathbf{l}})\dot{\mathbf{l}} + \mathbf{H}(\mathbf{l}) \tag{5.8}$$

where $\mathbf{l}$ and $\dot{\mathbf{l}}$ are the actual displacement and velocity vectors of the PZT actuators,

$\mathbf{l}_d$, $\dot{\mathbf{l}}_d$, and $\ddot{\mathbf{l}}_d$ are the desired displacement, velocity, and acceleration vectors of the PZT actuators, respectively,

$\mathbf{l}_e$, $\dot{\mathbf{l}}_e$ are the displacement and velocity error vectors of the PZT actuators,

$\mathbf{K(l)}$, $\mathbf{C(l,\dot{l})}$ and $\mathbf{H(l)}$ are the items of the dynamic model of the RRR compliant mechanism derived in Chapter 4, and

$\mathbf{Q}$ is the force vector produced by the PZT actuators.

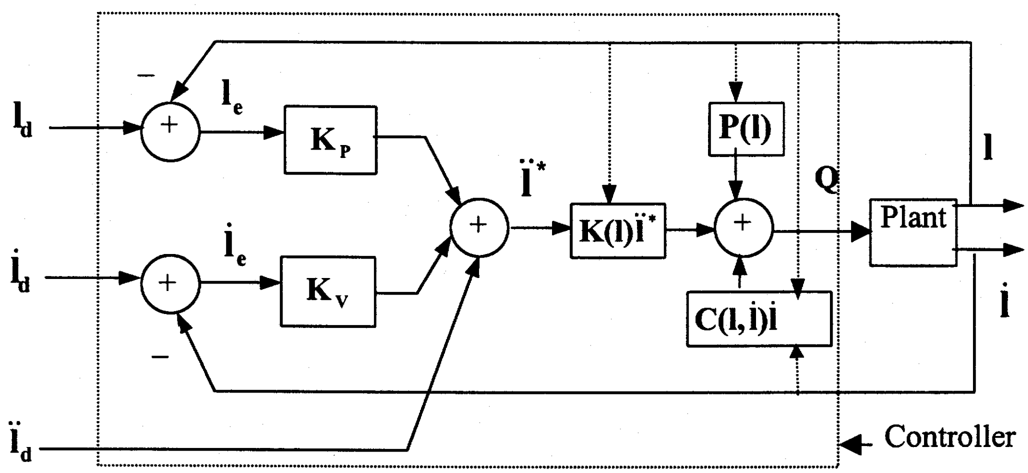

Plant: RRR compliant mechanism

Figure 5.3 Computed torque controller for the RRR compliant mechanism

5.4 Simulation Results

Simulation of the trajectory behavior of the RRR compliant mechanism is carried out with SIMULINK toolbox in Matlab (Ver.5.3). The model is saved in a file called '**dynamics_modelbase.mdl**', which is in the attached disk. Via a trial and error, for each joint, the proportional gain K_P is set as 5×10^{16} and the derivative gain K_V as 6×10^{8}. A solver '**ode23t**' in Matlab is chosen for solving a system of differential equations (three in this case).

For demonstration purpose, desired motions of the three actuators are chosen as a constant velocity motion profile (the constant velocity is 3 μm/s). Convergent trajectory tracking errors are obtained. Figure 5.4 shows the desired and actual displacements of PZT actuator 1 (the other two PZT actuators have the same results as PZT 1); the two results are very close.

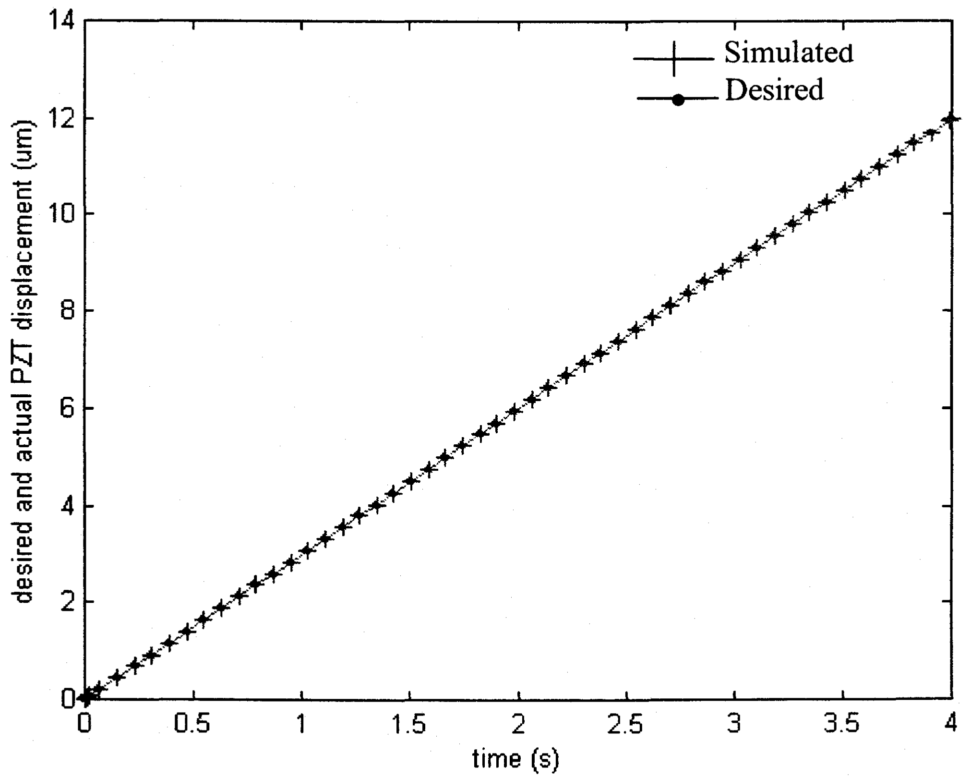

Figure 5.4 Desired and simulated displacement of PZT actuator 1

The displacement tracking error of PZT actuator 1 is plotted in Figure 5.5, where convergence can be seen. The desired and actual velocities of PZT 1 are plotted in Figure 5.6, while the velocity tracking error of PZT actuator 1 is plotted in Figure 5.7. It can be seen from these two figures that convergence is reached.

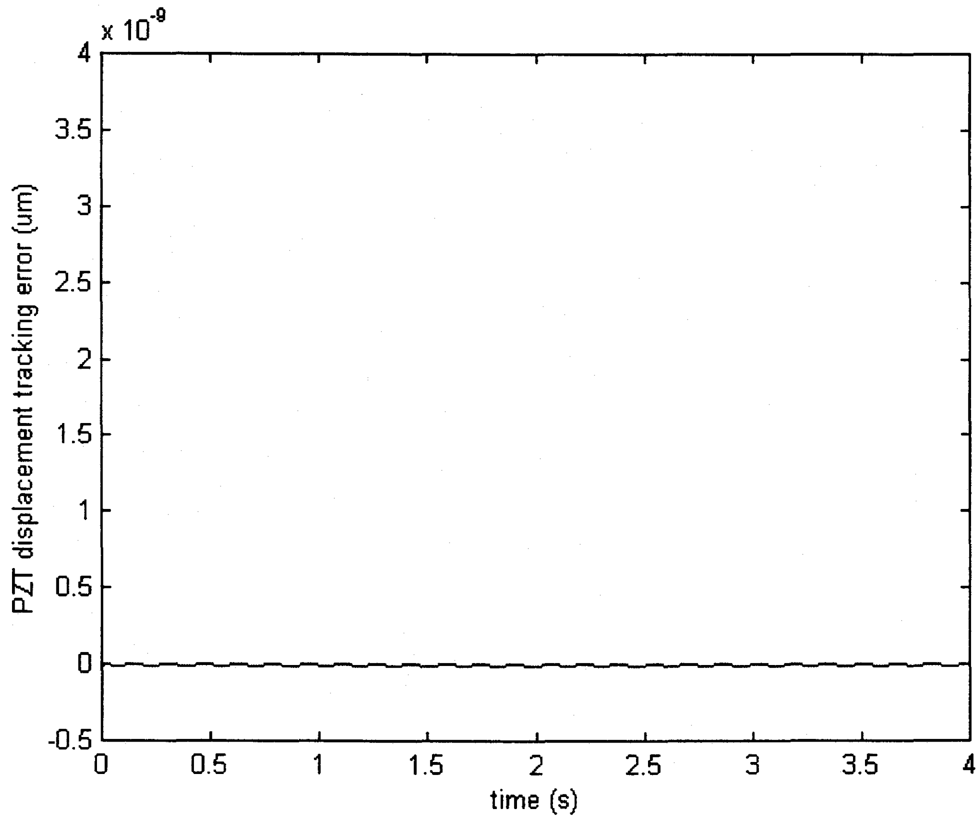

Figure 5.5 Displacement tracking error of PZT actuator 1

The driving force in PZT actuators is also a design concern. The theoretical maximal force versus the displacement is represented by (Tokin, 1996)

$$Q = 833(V/150 - \Delta l/16) \tag{5.9}$$

where Q is the force generated by a PZT actuator, in newtons,

V is the voltage applied on a PZT actuator, in volts, and

Δl is the elongation of a PZT actuator, in µm.

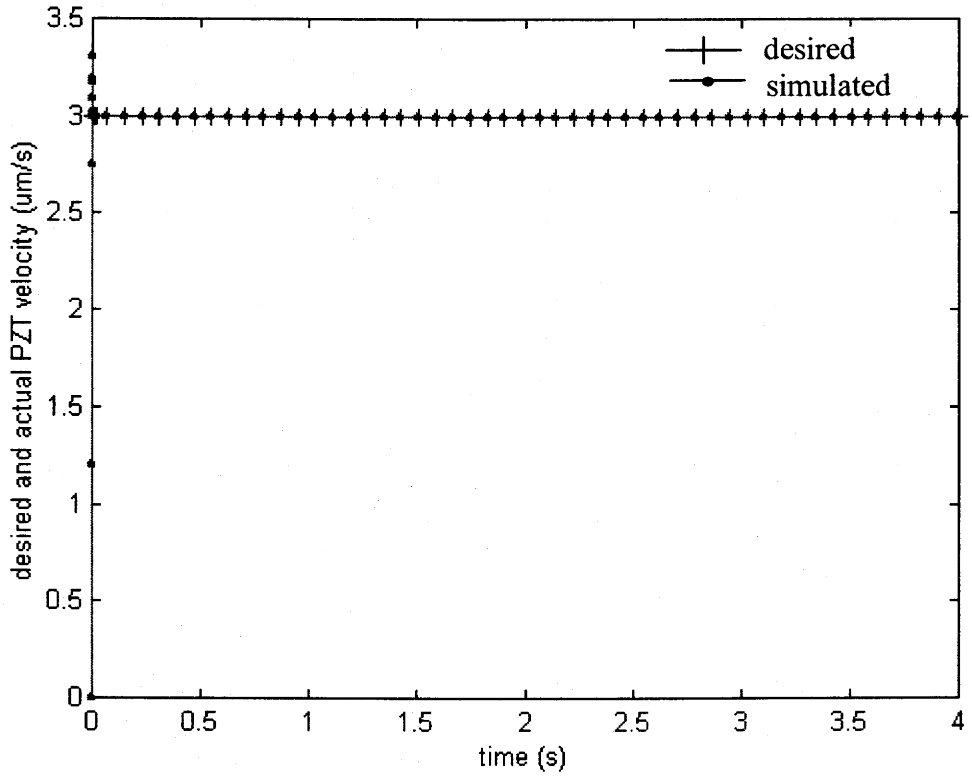

Figure 5.6 Desired and simulated velocity of PZT actuator 1

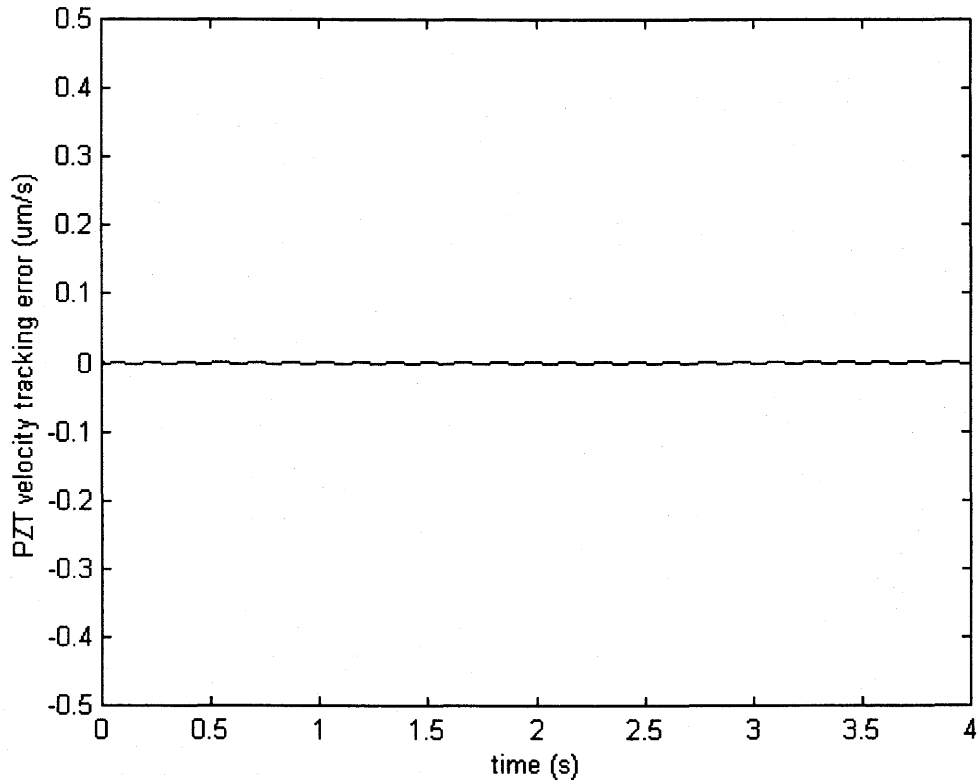

Figure 5.7 Velocity tracking error of PZT actuator 1

This relationship is plotted in Figure 5.8 (V is taken to be 150 V). The actual force generated by the actuator driving the RRR compliant mechanism is computed based on the dynamic model, i.e., equation (5.8), and is plotted in Figure 5.8 too. It can be seen from this figure that the actual force generated by the actuator is less than the maximal theoretical force. From this figure, it is also seen that the fluctuation of the actual driving force is very small and this is very conducive to the smooth operation of the actuator.

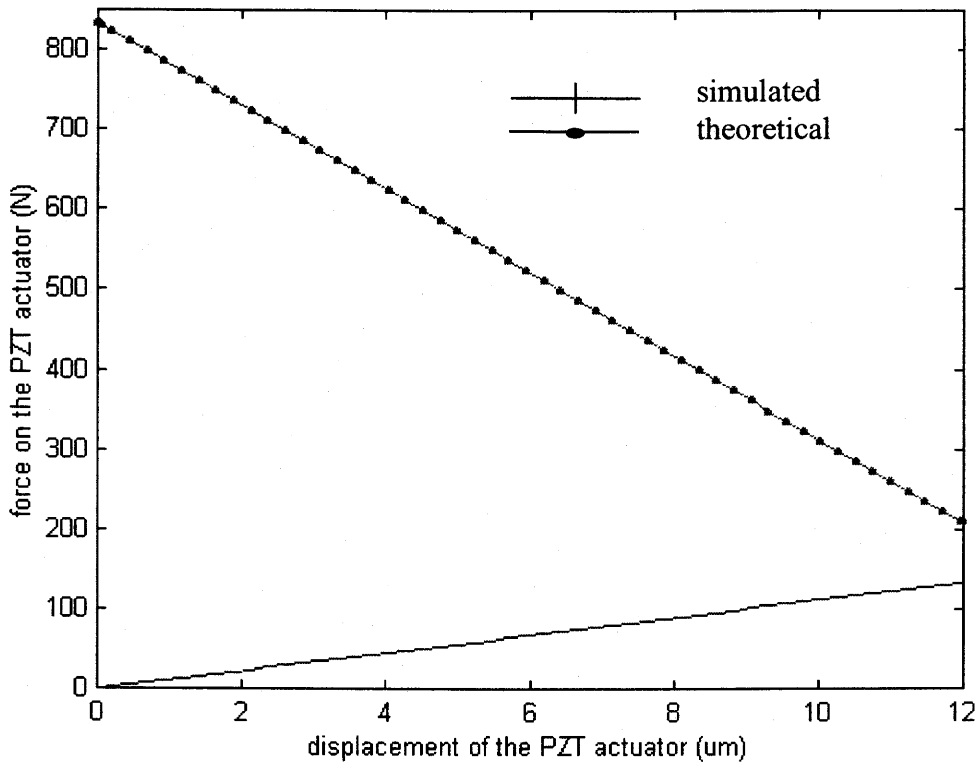

Figure 5.8 Simulated and theoretical maximum generation force of PZT actuator 1

5.5 Conclusion

Independent-joint PD controller may not work for the RRR compliant mechanism, as the dynamic model of this system is highly non-linear and coupled. It is necessary to apply more advanced control methods for this system, such as the CTC method. It has been shown from the simulation results that the CTC law works well with this system. However, the CTC method used here is an idealized and theoretical control strategy that assumes perfect modeling of dynamics of the compliant mechanism. Furthermore, it is assumed here that the feedback compensation term is calculated instantaneously. These assumptions are not valid in practical control applications, and modifications to this control law to compensate for such effects have been proposed (Craig, 1986).

Chapter 6
Conclusion

6.1 Introduction

The research described in this thesis aims to develop an understanding of and a design tool for a particular planar micro-motion mechanism system which is constructed based on the compliant mechanism concept. This system consists of three PZT actuators and a specially shaped member of compliant material. The structure of this system is symmetrical to the center of the system which serves as the end-effector of the system. Two external collaborators, City University of Hong Kong (MEEM, 1999) and Beijing University of Aeronautics & Astronautics of China (Zhao et al., 2000), of the Advanced Engineering Design Laboratory (AEDL), where this thesis work was performed, have physically built this system which provided a test-bed for verifying all theories and methods described in this thesis. Particular research objectives which were discussed in Chapter 1 are repeated here for the convenience of readers:

> **Objective 1**: To develop an accurate and computationally efficient kinematic model for the RRR compliant mechanism based on the PRBM approach.

Objective 2: To develop a computationally efficient dynamic model for the RRR compliant mechanism based on the PRBM approach.

Objective 3: To perform a preliminary study of control methods for the RRR compliant mechanism based on the PRBM approach.

The general contribution of this thesis is that the research developed has achieved these objectives. In this closing chapter, a number of conclusions already drawn in the previous chapters and some new ones are brought together (Section 6.2) in light of specific contributions of this thesis work. Future work is also identified and discussed (Section 6.3).

6.2 Research Findings and Further Discussion

6.2.1 Constant-Jacobian Method

One of the important findings of this research is that in analysis of micro-motion systems (in this research the motion range of the actuator is less than 12 μm), the mathematically exact method may not offer better accuracy in modeling the kinematic behavior of these systems based on a comparison of this method with the experiment. Instead, the Constant-Jacobian method, which keeps the first order term of the Taylor series expansion (for the actuator displacement Δl), shows a satisfactory result. The computation procedure for the mathematically exact method (for the forward kinematics) requires an iterative procedure to solve the system of three non-linear equations, whereas the Constant-Jacobian method presents an explicit solution for the forward kinematics of the RRR compliant mechanism.

It is an important observation that in analysis of micro-motion systems, because conventional analysis methods, including the finite element analysis method, are not capable of modeling the manufacturing and measuring errors and, on the other hand, the quantity of the end-effector displacement is very close to the quantity of the manufacturing and measuring errors. None of these methods has shown an overwhelming advantage in terms of accuracy in predicting the kinematic behavior. Therefore, it is necessary to perform the kinematic calibration which is not a usual case for macro-motion systems analysis. The kinematic calibrated model based on the Constant-Jacobian method offers as good accuracy as the finite element method at predicating the kinematic behavior of micro-motion systems and takes 50 times less than the finite element method. This feature of computational efficiency with the Constant-Jacobian method provides the foundation for developing a computationally efficient dynamic model for real-time control of the RRR compliant mechanism.

6.2.2 Novel Dynamic Model for Real-time Control Applications

The dynamic model developed in this thesis work, which is based on the PRBM of the RRR compliant mechanism, has some unique features. *First*, the model is sufficiently accurate because the model is based on the experimentally verified Constant-Jacobian method (in Chapter 2) and the appropriate approximations (in Chapter 4) which is in essence to neglect the $o(\Delta l^2)$ term and the above. *Second*, the model is highly computationally efficient due to the introduction of the appropriate approximations and a subsequent replacement of trigonometric items by the coordinates of corresponding nodes (at the kinematic joints).

For giving an impression of efficiency of this dynamic model, the simulation for a defined case is performed (in Chapter 5). The trajectory tracking task in this case is such that the actuators operate at a constant velocity of **3** μm/s for **4** seconds. In the Matlab (Ver.5.3) environment, the time for completion of this task is less than **2** seconds with **74** discrete time steps. It is useful to note that in a simulation study of the kinematics of the RRR compliant mechanism using the ANSYS program, one step of actuator motion takes **3** seconds; the time for completion of 74 time steps will then be **222** seconds which are far longer than **4** seconds. Therefore, it is impossible to apply the finite element approach to the real-time control of the RRR compliant mechanism.

It is further noted that the work performed by Ryu et al. (1997), though very close to the work reported here, has not studied the real-time motion tracking problem; their analysis is, in general, static.

6.2.3 Finite Element Method for Compliant Mechanisms

In this thesis, the application of a general-purpose finite element program, i.e., ANSYS, to the kinematic analysis of the compliant mechanism, is demonstrated. This ANSYS model is of high accuracy, compared with other analytical approaches, though it needs to be further improved. One of the strong features of this model is its parametric nature. In total, nine parameters determine the configurations of the system (see Chapter 2 and Chapter 3), which makes it possible to perform optimal selection of these parameters to achieve, for example, a maximal yaw angle. It should be noted that in the literature, some special finite element techniques were used for the design of compliant mechanisms in the field of topology optimization (see the literature review in Chapter 1). This thesis has shown a useful exploration of using a general-purpose finite element program as a tool for the design of compliant mechanisms.

6.2.4 Unique Planar Micro-Motion Device

As a result, this thesis has contributed to the development of a promising system which can produce planar micro-motion, i.e., two translations and one rotation. A set of tools for kinematic analysis (including both the method based on the pseudo rigid body model and finite element method), dynamic analysis, and control has been developed. The experiment has verified the reliability of the kinematic analysis tools.

Through simulation, the system developed, i.e., the RRR compliant mechanism, is found to have the following properties: a total range of 77.28 μm (when Δl_1=12 μm, Δl_2=12 μm, and Δl_3=0 μm) and 71.02 μm (when Δl_1=12 μm, Δl_2=0 μm, and Δl_3=12 μm) along the x- and y- axis, respectively, and a maximal yaw motion range of 2.16 mrad. (when Δl_1=12 μm, Δl_2=12 μm, and Δl_3=12 μm). When the resolution of the PZT actuator is 0.01 μm, the accuracy of motions at the end-effector is 13.2 nm and 3.4 nm along the x- and y-axis, respectively, and the accuracy of the yaw motion is 0.6 μrad. In the following table, a comparison with a similar system developed by Ryu et al. (1997) is summarized, in terms of range and accuracy of the displacement of the end-effector.

Table 6.1 Comparison of the RRR compliant mechanism with the one developed by Ryu et al. (1997)

	X-R (μm)	Y-R (μm)	Yaw angle (mrad)	X-A (nm)	Y-A (nm)	Yaw-A (μrad)
Ryu et al. (1997)	41.5	47.8	1.565	-	-	-
This thesis	77.28	71.02	2.16	13.2	3.4	0.6

R: range; A: accuracy

6.3 Future Work

A refined finite element analysis is worth studying. Use of the triangular element with one midpoint on each edge for the piece of compliant material would not produce distorted elements, owing to its recognized advantage of modeling complex boundaries, the RRR compliant mechanism in this case (Zettl, 2000). Furthermore, sensitivity analysis of the result of finite element analysis with respect to the number of elements would be useful to ensure the reliability of the finite element analysis.

Experimental verification of the real-time control of the RRR compliant mechanism is a necessary task, as there are many factors which would affect the behavior of the end-effector and have not been considered in the modeling of the system, e.g., the manufacturing and measuring errors and external loading.

Other design issues such as fatigue analysis of the system and system stiffness analysis need to be addressed. Compliant mechanisms operate in a frequently cyclic deformation mode that may easily cause fatigue of the material and eventually affects the performance of the system in terms of precision in particular. It is a challenging issue to understand how fatigue of a compliant mechanism system is quantitatively related to the system performance degrading and, thus, how it is possible to offset this degrading by adjusting a controller. To design a system with high system stiffness is a design goal in micro-motion systems, as the higher system stiffness property of a micro-motion system is useful to the precision of the system operation.

The integration of structure design and control design for micro-motion systems should be of interest to further improving and maintaining system performance. This should be incorporated into optimal selection of the shape and configuration of the compliant material. The advantage of such an integrated design and control methodology has already been verified in macro-motion systems (Zhang et al., 1999; Zhang and Li, 1999).

Finally, it is noted that the physical behavior of the PZT actuator has not been considered in the research described in this thesis, which is a limitation. Further studies in the finite element modeling for kinematic behavior can be performed by making use of the PZT element in the ANSYS program. The contact between the PZT actuator and the compliant piece needs some attention. In dynamic modeling, it is possible to integrate the dynamic model of the PZT actuator with the dynamic model developed in this thesis. As a result of this integration, one can expect that for each actuator, there will be two ordinary differential equations (instead of one in the current case) which describe the dynamics of the actuator with consideration of the physics of the PZT actuator.

References

An, C. H., Atkeson, C. G., and Hollerbach, J. M., 1988. *Model-Based Control of a Robot Manipulator*, The MIT Press, Cambridge, Massachusetts.

Bi, S. S., 1999. "Dynamics and Control of Compliant Mechanisms," *Private Communication.*

Cai, C. Y., Ge, Z. K., and Bai, J. Z., 1979. *Machine Component Design Handbook* (in Chinese) (2^{nd}), Vol. 1, Steel Industry Publisher, China.

Craig, J. J., 1986. *Introduction to Robotics Mechanics & Control*, Addison-Wesley Publishing Company.

Derderian, J. M., Howell, L. L., Murphy, M. D., Lyon, S. M., and Pack, S. D., 1996. "Compliant Parallel-Guiding Mechanisms," *Proceedings of the 1996 ASME Design Engineering Technical Conferences and Computers in Engineering conference,* August 18-22, pp. 1-12.

Frecker, M., Kikuchi, N., and Kota, S., 1999. "Topology Optimization of Compliant Mechanism with Multiple Outputs," *Structural Optimization,* Vol. 17, pp. 269-278.

Furukawa, E. and Mizuno, M., 1992. "Piezo-Driven Translation Mechanisms Utilizing Linkages," *Int. J. Japan Soc. Prec. Eng.*, Vol. 26, No. 1, pp. 54-59.

Gosselin, C. M. and Merlet, J. P., 1994. "The Direct Kinematics of Planar Parallel Manipulators: Special Architectures and Number of Solutions," *Mech. Mach. Theory*, Vol. 29, No. 8, pp. 1083-1097.

Gosselin, C. M. and Sefrioui, J., 1991. "Polynomial Solutions for the Direct Kinematic Problem of Planar Three-Degree-of-Freedom Parallel Manipulators," *Proceedings of IEEE Int. Conf. on Robotics and Automation,* pp. 1124-1129.

Guo, L. S., Zhang, W. J., Li, Y. F., and Li, Q., 1999. "Design, Modeling and Control of a Hybrid Machine," *IEEE/ASME Trans on Mechatronics* (submitted).

Guo, L. S., Li, Y. F., and Zhang, W. J., 2000. "Trajectory Control of Two DOF Closed-Chain Mechanical Sysytem," *Proceedings of the 2000 ASME Design Engineering Technical Conference*, Paper Number: DETC'00/MECH-14158, pages: 12 (to appear).

Hayes, M. John, Husty, Manfred L., and Zsombor-Murray, Paul L., 1999. "Kinematic Mapping of Planar Stewart-Gough Platforms," *Proceedings of 17th CANCAM 99*, Hamilton, Ontario, pp. 319-320.

Hara, A. and Sugimoto, K., 1989. "Synthesis of Parallel Micromanipulators," *ASME Trans Journal of Mechanisms, Transmissions, and Automation in Design,* Vol. 111, pp. 34-39.

Her, I. and Chang, J. C., 1994. "A linear Scheme for the Displacement Analysis of Micropositioning Stages With Flexure Hinges," *ASME Trans Journal of Mechanical Design,* Vol. 116, pp. 770-776.

Howell, L. L. and Midha, A., 1994. "The Development of Force-Deflection Relationships for Compliant Mechanisms," *Machine Elements and Machine Dynamics,* DE-Vol. 71, ASME, pp. 501-508.

Jensen, B. D., Howell, L. L., Gunyan, D. B., and Salmon, L. G., 1997. "The Design and Analysis of Compliant MEM Using the Pseudo-Rigid-Body Model," *Micro-electromechanical Systems (MEMS), ASME 1997*, DSC-Vol. 62/HTD-Vol. 354, pp. 119-126.

Jouaneh, M. and Ping, Ge., 1997. "Modeling and Control of a Micro-Positioning Tower," *Mechatronics,* Vol. 7, No. 5, pp. 465-478.

Lee, K. M and Arjunan, S., 1991. "A Three-Degrees-of-Freedom Micromotion In-Parallel Actuated Manipulator," *IEEE Trans on Robotics and Automation,* Vol. 7, No. 5, pp.634-641.

Lee, K. M. and Shah, D. K., 1988a. "Kinematic Analysis of a Three-Degrees-of-Freedom In-Parallel Actuated Manipulator," *IEEE Journal of Robotics and Automation*, Vol. 4, No. 3, pp. 334-360.

Ma, O. and Angele, J., 1989. "Direct Kinematics and Dynamics of a Planar Three-DOF Parallel Manipulator," *ASME Design and Automation Conf., Montreal, September, 17-20,* Vol. 3, pp. 313-320

MEEM, 1999. "Micro-Motion Generation System," *Technical Report (Final Year Student Mechatronics Group Project)*, Department of Manufacturing Engineering, City University of Hong Kong, Hong Kong.

Millar, A. J., Howell, L. L., and Leonard, J. N., 1996. "Design and Evaluation of Compliant Constant-Force Mechanism," *Proceedings of the 1996 ASME Design Engineering Technical Conference and Computers in Engineering Conference*, August 18-22, Irvine, California, pp. 1-12.

Nishiwaki, S., Frecker, M. I., Min, S., and Kikuchi, N., 1998. "Topology Optimization of Compliant Mechanisms Using the Homogenization Method," *International Journal For Numerical Methods in Engineering,* Vol. 42 , pp.535-559.

Paros, J. M. and Weisbord, L., 1965. "How to Design Flexure Hinges," *Machine Design,* Vol. 37, pp.151-156.

Ryu, J. W., Gweon, D. G., and Moon, K. S., 1997. "Optimal Design of a Flexure Hinge Based XYθ Wafer Stage," *Precision Engineering,* Vol. 21, pp.18-28.

Scire, F. E. and Teague, E. C., 1978. "Piezodriven 50-μm Range Stage with ubnanometer Resolution," *Rev. Sci. Instrum.,* Vol. 49, No. 12, pp.1735-1740.

Tokin, 1996. *Multilayer Piezoelectic Actuators: User's Manual*, Tokin Corporate Publisher.

Zettl, B., 2000. "Optimization of a Particular Micro-motion System Using ANSYS," *Technical Report for Optimization Class*, Department of Mechanical Engineering, University of Saskatchewan.

Zhang, W. J., Li, Q., and Guo, S. L., 1999. "Integrated Design of Mechanical Structure and Control Algorithm for a Programmable Four-Bar Linkage," *IEEE/ASME Trans. on Mechatronics*, Vol. 4, No. 4, pp. 354-362.

Zhang, W. J. and Li, Q., 1999. "Design for Control: a New Principle for Technical Systems Development," *13th International Conference on Engineering Design*, August 24-26, Munich, Germany, pp. 135-139.

Zhao, Wei, Bi, S. S., and Zong, G. H., 2000. "Experimental Study of a Series-Parallel Micro Manipulator," *Journal of Beijing Univ. of Aero. & Astr.* (submitted).

Zong, G.H., Zhang, W. J., Xu, W. L., and Bi S. S., 1997. "A Hybrid Serial-Parallel Mechanism for Micro-Manipulation," *The 5th Applied Mechanisms and Robotics Conference, USA, October,* AMR97-050, pages: 8.

Appendix A: Experiment Set-up

The two collaborators of AEDL, where this thesis work is primarily performed, conducted the experiment. These two collaborators are: The Department of Manufacturing Engineering, City University of Hong Kong (MEEM, 1999) and The Institute of Robotics Research, BUAA, China (Zhao et al., 2000). Figure A.1 shows an assembled RRR compliant mechanism system for performing planar micro-motions. Figure A.2 shows a manufactured compliant piece. Figure A.3 shows the experiment set-up (MEEM, 1999). There are two methods to measure the displacements of the end-effector: through the microscope with CCD camera and through the capacity sensor. The experimental data measured by the capacity sensor are used for this thesis work. The displacement of the PZT actuator was measured by the strain gauge. Therefore, the major sensors include the strain gauge and the capacitor sensor, and their data, together with the data of the PZT actuator, are presented below:

Capacitor sensor:

Model name:	BHCWY-1
Maker:	8271 Inc., Beijing, China
Resolution:	5 nm
Range:	100 μm

Strain gauge:

Model name:	YD-15 Dynamic Strain Gauge
Maker:	Hua Dong Electronic Instrument Inc., China
Resolution:	12-bit A/D (equivalent to appro. 4.2 nm/LBS)
Range:	(±) 10000 μm

PZT actuator:

Model name:	AE0505D16
Maker:	Tokin (Japan)
Max deformation:	16 $\pm$ 2 μm

Max generation force:	834 N
Resolution:	0.01 μm
Max driving voltage:	150 V
Dimension:	5 ×5 × 20 mm

The principle of using the capacitor sensor is shown in Figure A4, where the capacitor sensor is deployed at points A, B, and C of a calibrated block. The radius of the circle (of the calibrated block) passing A, B, and C, respectively, as shown in Figure A.4, should be at least greater than 3 mm. The formulae to compute the displacements of the end-effector based on the measured data at points A, B, and C, respectively, are given below:

$$\Delta x = \frac{\Delta x_2 + \Delta x_3}{2} \tag{A.1}$$

$$\Delta y = AO \times \Delta\gamma + \Delta x_1 \tag{A.2}$$

$$\Delta\gamma = \tan^{-1}(\frac{\Delta x_2 - \Delta x_3}{BC}) \tag{A.3}$$

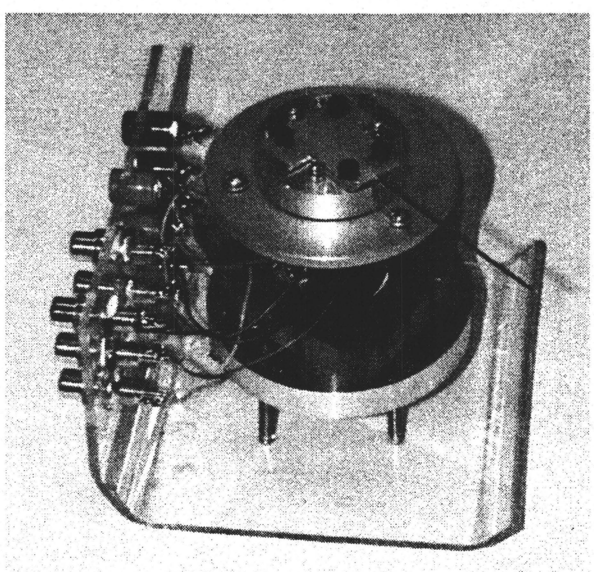

Figure A.1 Assembled RRR compliant mechanism

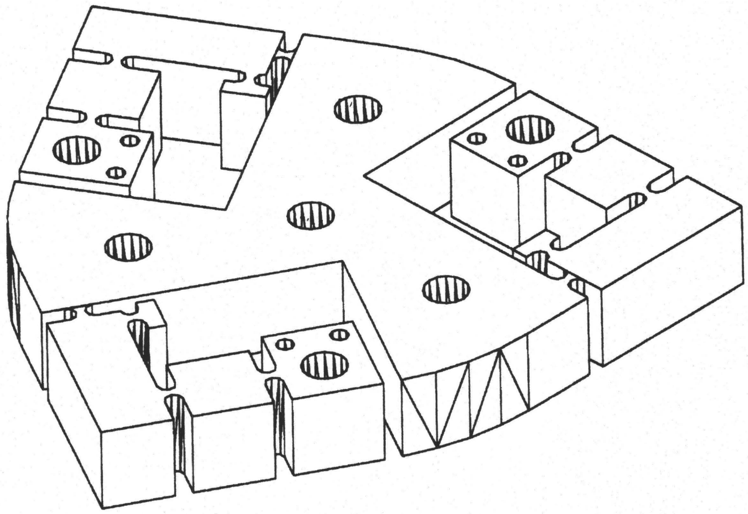

Figure A.2 Manufactured compliant piece

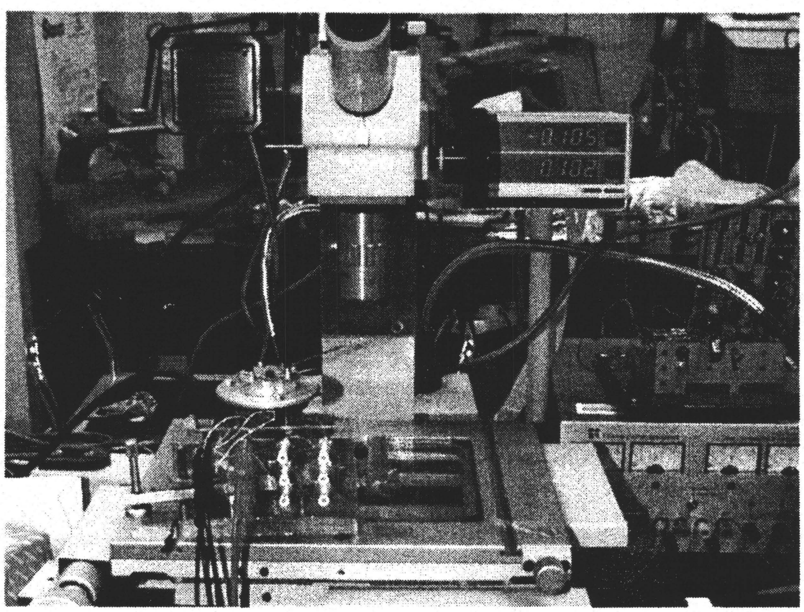

Figure A.3 Experimental setup

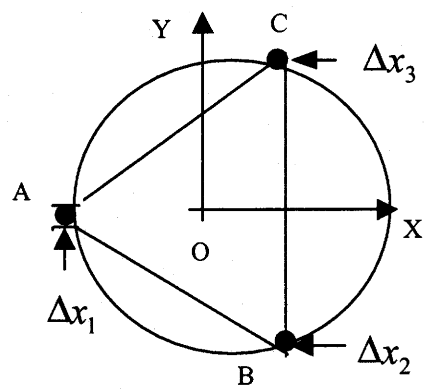

Figure A.4 Measuring method for the motion of the end-effector

In total, 50 points of time step were measured for the displacement of the PZT actuators versus the displacements of the end-effector. The least square method was used to correlate the experimental data, which resulted in a Jacobian matrix as follows:

$$J_{\text{exp}} = \begin{bmatrix} 1.610797127 & -1.298942876 & -0.164324634 \\ -0.6056938677 & -1.42884239 & 1.37702048 \\ -3.269206385\text{e}-005 & -2.830203574\text{e}-005 & -2.019743117\text{e}-005 \end{bmatrix},$$

i.e., $$\begin{bmatrix} x \\ y \\ \gamma \end{bmatrix}_{\text{exp}} \cong J_{\text{exp}} \begin{bmatrix} \Delta l_1 \\ \Delta l_2 \\ \Delta l_3 \end{bmatrix}_{\text{exp}}$$

where the subscript 'exp' means experimentally obtained quantities.

Appendix B: Program for the Kinematic Calibration

The optimization program consists of several sub-programs and functions. A brief instruction to operate the program is as follows:

1. In Matlab (Version 5.3) workspace, type '**findmaxbak_con**.' This is to execute the m-file '**findmaxbak_con.m**' to determine the elongations of the PZT actuators (L1, L2, L3) at which the maximal error between the Constant-Jacobian results and the experimental results occurs. Note that L1, L2, and L3 are used in the Matlab program for the elongation of the PZT actuator. For the program studied in this thesis work, the maximal error occur at L1=12 μm, L2=0 μm, and L3=12 μm.
2. Type '**concalibak_con**.' This is to execute the m-file '**concalibak_con.m**' to obtain the calibrated values for the five parameters: R, ψ_1, ψ_2, L_{AB}, and L_{BC}.

A list of source codes for the program '**findmaxbak_con.m**' is given below:

```
The text after the symbol "%" is the comment of a program.

x0=[ 1,1,-0.001, 5, 5, 5 ];
% initial guess of x, y, r (unit is in μm and rad), L1, L2 and L3
(unit % is in mm)
options=optimset('largescale', 'off','LevenbergMarquardt',
'on','LineSearchType','on');
options = optimset(options,'maxFunEvals',1500);
% Termination tolerance on F
options = optimset(options,'Tolfun',1e-20);
% Termination tolerance on F
options = optimset(options,'Tolx',1e-10);
% Termination tolerance on F
options = optimset(options,'Diagnostics','on');
lb = [-100, -100,-0.1,  0, 0, 0];
% lower bound of x, y, r,L1, L2 and L3 (unit is in μm and rad)
ub = [ 100,  100,  0,  12, 12, 12];
```

```
% upper bound x, y, r, L1, L2 and L3 (unit is in µm and rad)
[x,fval,exitflag,output] = fmin-
con('findmaxbak_obj',x0,[],[],[],[],lb,ub,'findmax_fun',options)

% execute the optimization command making use of the objective
% function: findmaxbak_obj.m, and the Constant-Jacobian function:
% findmax_fun.m to find the maximal difference between the Constant-
% Jacobian results and the experimental results.

==================================
```

A list of source codes for the objective function **'findmaxbak_obj.m'** is given below:

```
function f= findmaxbak_obj(x)
angle = 53.961*pi/180;     % coordinate transformation angle
coordinate_transform = [ cos(angle), -sin(angle), 0;
                        sin(angle), cos(angle), 0;
                             0,      0,          1 ] ;
% coordinate transformation matrix
jlca = [ 1.610797127, -1.298942876,-0.164324634;
   -0.6056938677, -1.42884239, 1.37702048;
   -3.269206385e-5, -2.830203574e-5 ,-2.019743117e-5 ];
% experimental matrix
inca = [ x(4); x(5); x(6)];    % input motion of L1, L2 and L3
outjca=jlca*inca;    % experimental result
outme_transform = inv(coordinate_transform) * [x(1);x(2);x(3)] ;
% constant-Jacobian solution in global coordinate system (unit is in
um % and rad)
f=1/( (outme_transform(1)-outjca(1))^2 + (outme_transform(2)-
outjca(2))^2 + ((outme_transform(3)-outjca(3))*1e4)^2 )

% objective is to find at which elongations of the PZT actuators,the
% difference between the experimental and constant Jacobian results
are % maximal.

========================================
```

A list of source codes for the function **'findmax_fun.m'** is given below:

```
function [c,ceq,GC] = findmax_fun(x)
l1=-x(4);
l2=-x(5);
l3=-x(6);
Rs = 29.546;        % parameter R
lab=17.720;         % parameter $L_{AB}$
f1=1.1733;          % parameter $\psi_1$
f2=0.81569;         % parameter $\psi_2$
n=11;               % parameter $L_{BC}$
fai=f1+f2;
fa=f2+asin( n*sin(f2)/lab );
co = lab*sin(fa);
R0=3.5;
tt = [cos(fai+2*pi/3), sin(fai+2*pi/3), sin(fai)*Rs*1e3;
   cos(fai), sin(fai), sin(fai)*Rs*1e3;
   cos(fai+4*pi/3), sin(fai+4*pi/3), sin(fai)*Rs*1e3];
% constant-Jacobian Matrix
jme = (co/R0) .* inv(tt);
% constant-Jacobian solution
ceq = [ x(1)+jme(1,1)*x(4)+jme(1,2)*x(5)+jme(1,3)*x(6) ;
   x(2)+jme(2,1)*x(4)+jme(2,2)*x(5)+jme(2,3)*x(6) ;
   x(3)+jme(3,1)*x(4)+jme(3,2)*x(5)+jme(3,3)*x(6) ]
% equivalent constraints
c=[];
% no non-equivalent constraints
```

===================================

A list of source codes for the program '**concalibak_con.m**.' is given below:

```
x0=[ 1,1,-0.001,29.546, 17.720, 11, 1.1733, 0.81569 ];
% initial guess of x, y, r (transnational and rotational displacements
% of the end-effector, unit in μm and rad), R, $L_{AB}$, $L_{BC}$, $\psi_1$, $\psi_2$, (unit
in % mm, and rad)
options=optimset('largescale', 'off','LevenbergMarquardt',
'on','LineSearchType','on');
```

```
options = optimset(options,'maxFunEvals',1000);
% Termination tolerance on F
options = optimset(options,'Diagnostics','on'
lb = [-100, -100,-0.1, 20, 10, 10, 0.6, 0.2];
% lower bound of x, y, r, R, L_AB, L_BC, ψ1, ψ2
ub = [ 100,  100, 0,  35,  20, 20, 2.0, 1.5];
% upper bound of x, y, r, R, L_AB, L_BC, ψ1, ψ2
[x,fval,exitflag,output] = fmin-
con('concalibak_obj',x0,[],[],[],[],lb,ub,'concalibak_fun',options,L1,
L2,L3)

% execute the optimization command making use of the objective
% function: concalibak_obj.m, and the Constant-Jacobian function:
% concalibak_fun.m.
```

===============================

A list of source codes for the objective function '**concalibak_obj.m**,' which is defined as minimization of the error between the calibrated results and experimental results minimal, is given below:

```
function f= concalibak_obj(x,L1,L2,L3)
angle = 53.961*pi/180; % coordinate transform angle
coordinate_transform = [ cos(angle), -sin(angle), 0;
                         sin(angle), cos(angle), 0;
                              0,      0,          1 ] ;
% Coordinate transformation matrix
jlca = [ 1.610797127, -1.298942876,-0.164324634;
   -0.6056938677, -1.42884239, 1.37702048;
   -3.269206385e-5, -2.830203574e-5 ,-2.019743117e-5 ];
% Experimental matrix
inca = [ L1; L2; L3];
% input motion
outjca=jlca*inca;  % experimental results in global coordinate system
outme_transform = inv(coordinate_transform) * [ x(1);x(2); x(3) ] ;
% calibrated results in global coordinate system
```

```
f=(outme_transform(1)-outjca(1))^2 + (outme_transform(2)-outjca(2))^2
+ ( (outme_transform(3)-outjca(3))*1e4 )^2

% objective function is to make calibrated results as close as possi-
ble to experimental results
```

A list of source codes for the program '**concalibak_fun.m**,' which is used to obtain the Constant-Jacobian solution, is given below:

```
function [c,ceq] = concalibak_fun(x,L1,L2,L3)
% input displacements: L1, L2 and L3 (unit is in µm)
Rs=x(4)      % parameter R
lab=x(5)     % parameter L_AB
n=x(6)       % parameter L_BC
f1=x(7)      % parameter ψ1
f2=x(8)      % parameter ψ2
l1=-L1;
l2=-L2;
l3=-L3;
R0=3.5;
fai=f1+f2;
fa=f2+asin( n*sin(f2)/lab );
co = lab*sin(fa);
tt = [cos(fai+2*pi/3), sin(fai+2*pi/3), sin(fai)*Rs*1e3;
   cos(fai), sin(fai), sin(fai)*Rs*1e3;
   cos(fai+4*pi/3), sin(fai+4*pi/3), sin(fai)*Rs*1e3];
jme = (co/R0) .* inv(tt);  %Constant-Jacobian Matrix
ceq = [ x(1)-jme(1,1)*l1-jme(1,2)*l2-jme(1,3)*l3 ;
   x(2)-jme(2,1)*l1-jme(2,2)*l2-jme(2,3)*l3 ;
   x(3)-jme(3,1)*l1-jme(3,2)*l2-jme(3,3)*l3 ]
% equivalent constraints
c=[];    % no non-equivalent constraints
```

Appendix C: FEM Modeling

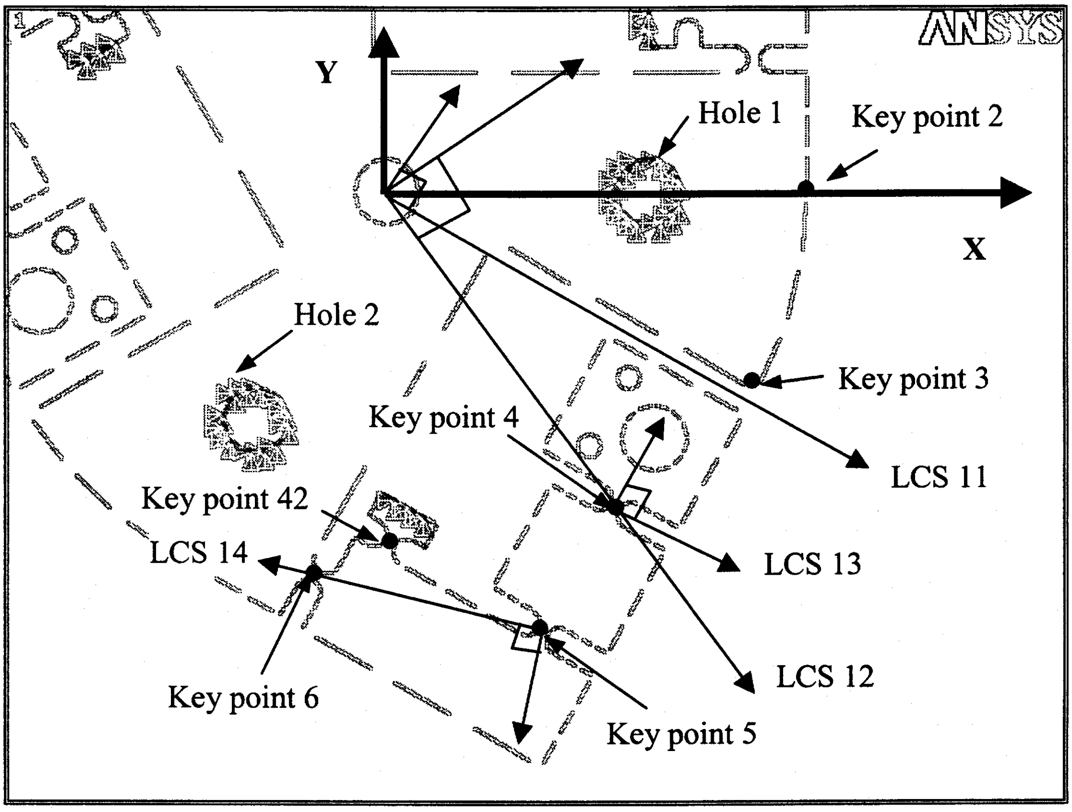

LCS: Local Coordinate System and its pictorial representation is:

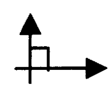

Figure C.1 Local coordinate system (LCS) and the positioning key points in the modeling of the RRR compliant mechanism

```
!**********************************************************************
!       Geometric modeling of the RRR compliant mechanism
!**********************************************************************
/prep7

! Set parameters

*SET,pi,acos(-1)          ! set value for π
!************** Set five parameter to determine the configuration
*SET,Lab,17.720
```

```
*SET,Lbc,11 of the compliant piece
*SET,R,29.546
*SET,fai1,1.1733*180/pi
*SET,fai2,0.81569*180/pi
!*****************************************************************
*SET,faim,asin( (Lbc*sin(fai2*pi/180))/Lab )*180/pi

FAIB      = 180-fai2-faim
*SET,faic,fai1+fai2-90
!************** Set four parameters to determine the shape of flexure
*SET,radius,1
*SET,t,0.8        hinges
*SET,b,10
*SET,h,10
!********************************************************************
*SET,R0,3.5
!****** ! set the coefficient in X and Y directions for PZT actuators
LOAD2X    = -0.5
LOAD2Y    = -0.866025404

LOAD3X    = -0.5
LOAD3Y    = 0.866025404
!*********************************************************************
*

/prep7
k,    !create key point 1 at the global coordinate system (XY) origin
wpstyle,0.5,1,0,35,,0,0,1
k,,32 !key point 2 at coordinate (0,32) in global coordinate system
wprota,-30        !rotate the global coordinate clockwise for 30
degree
csys,4
cswpla,11         !define this coordinate system: local cs 11
k,,32,1           !key point 3
wpstyle,0.5,1,0,35,,1,0,1
csys,4
l,2,3
wpstyle,0.5,1,0,35,,0,0,1
```

```
wprota,-faic        ! rotate local cs 11 clockwise for faic degrees
cswpla,12           !define this coordinate system as local cs 12
k,,R                !creat key point 4 in local cs 12

kwpave,4            !move the working plane origin to key point 4
wprota,faic-90      !rotate the work plane to cs 13
cswpla,13           !local cs 13, its  origin is at key point 4
k,,lbc              !creat key point 5
kwpave,5            !move the working plane origin to key point 5
wprota,faib-180     !rotate the work plane to cs 14
cswpla,14           !local 14, its origin is at key point 5

k,,lab              !create key point 6
wpcsys,,11
/VIEW, 1 ,,,1
/ANG, 1
/REP,FAST
csys,4
k,,9,1              !key point 7
l,7,3

kwpave,4
cswpla,13           !local cs 13
csys,4
k,,-0.5*t
k,,-0.5*t-radius,-radius
k,,-0.5*t-radius,radius
k,,-0.5*t-radius
kwpave,11
wpstyle,0.5,1,0,35,,1,0,1
csys,4
l,9,8
l,8,10              !left half of the flexure hinge at key point 4
wpstyle,0.5,1,0,35,,0,0,1
kwpave,4
k,,0.5*t
k,,0.5*t+radius,radius
k,,0.5*t+radius,-radius
```

```
k,,0.5*t+radius
kwpave,15
wpstyle,0.5,1,0,35,,1,0,1
l,13,12
l,12,14            !right half of the flexure hinge at key point 4


wpstyle,0.5,1,0,35,,0,0,1

kwpave,4
k,,0.5*h,radius
k,,0.5*h,-radius
k,,-7,radius
k,,-5,-radius
l,13,16
l,14,17
l,10,18
l,9,19
k,,-(2+0.5*h),radius+10
k,,0.5*h,radius+10
l,18,20
l,20,21
l,21,16            !block above key point 4

kwpave,5
csys,4
k,,-0.5*t
k,,-0.5*t-radius
k,,-0.5*t-radius,radius
k,,-0.5*t-radius,-radius
kwpave,23
wpstyle,0.5,1,0,35,,1,0,1
l,22,24
l,25,22
wpstyle,0.5,1,0,35,,0,0,1     ! right half of the flexure hinge at key
                              ! point 5
kwpave,5
k,,0.5*t
```

```
k,,0.5*t+radius
k,,0.5*t+radius,radius
k,,0.5*t+radius,-radius
kwpave,27
wpstyle,0.5,1,0,35,,1,0,1
l,28,26
l,26,29                  !right half of the flexure hinge at key point
5
wpstyle,0.5,1,0,35,,0,0,1
kwpave,5
k,,0.5*h,radius
k,,-(0.5*h),radius
k,,5,-radius
l,28,30
l,32,29
l,24,31    !block above key point 5
k,,5,-radius-8

kwpave,6
k,,0,0.5*t
k,,0,-0.5*t
k,,radius,0.5*t+radius
k,,radius,-(0.5*t+radius)
k,,-radius,0.5*t+radius
k,,-radius,-(0.5*t+radius)
kbetw,36,38
kbetw,37,39
kwpave,40
wpstyle,0.5,1,0,35,,1,0,1
l,38,34
l,34,36      ! upper half of the flexure hinge at key point 6
kwpave,41
l,37,35
l,35,39
wpstyle,0.5,1,0,35,,0,0,1   ! lower half of the flexure hinge at key
point 6
kwpave,6
k,,R0,4+radius  ! create key point 42
```

```
kwpave,42
k,,0.5*t
k,,-0.5*t
k,,0.5*t+radius,radius
k,,0.5*t+radius,-radius
k,,-(0.5*t+radius),radius
k,,-(0.5*t+radius),-radius
kbetw,45,46
kbetw,47,48
kwpave,49
wpstyle,0.5,1,0,35,,1,0,1
l,45,43
l,43,46      !left half of the flexure hinge at key point 42
kwpave,50
l,48,44
l,44,47      !right half of the flexure hinge at key point 42

wpstyle,0.5,1,0,35,,0,0,1
kwpave,42
k,,2.5,radius
k,,-2.5,radius
k,,-2.5,radius+2
k,,2.5,radius+2
l,45,51
l,51,54
l,54,53
l,53,52
l,52,47
k,,-2.5,-radius
l,55,36            !block contact with PZT 2

l,7,38
l,48,55
l,46,25
l,19,31
l,17,30
l,32,33
l,2,1              !connect the lines
```

```
kwpave,6
k,,radius,-4
k,,-radius,-4
l,37,56
l,39,57
l,56,33
kwpave,1
k,,0,-32
l,57,58
l,1,58              !finish all the lines

al,all
wprota,150          !create the first part
cswpla,21           !local cs 21
csys,0
atran,21,1          !create the second part
wproat,120
cswpla,31           !local cs 31
csys,0
atran,31,1          !create the third part

aadd,1,2,3          !add the 3 parts to be 1 piece
cyl4,0,0,2.5
asba,4,1            !subtract the center circle
wpcsys,,11

kwpave,4
csys,4
k,,0,radius+5
cyl4,0,radius+5,2.5   !r2.5 circle
kwpave,149
k,,-4,-3
k,,-4,3
cyl4,-4,-3,0.9          ! two r0.9 circles
cyl4,-4,3,0.9

csys,0
```

```
asel,s,,,3,4
asel,a,,,1
atran,21,all            !create 3 circles on second part
asel,s,,,3,4
asel,a,,,1
atran,31,all            !create 3 circles on second part
asel,all
asba,2,all

wpcsys,0
cyl4,20,0,2.5           !fixed circle at 0 degree
csys,0
atran,21,1
atran,31,1
alist
asba,11,all             !subtract 3 circles

aplot

!***************ELEMENT PROPERTY
et,1,plane82            ! specify the first element type to be plane82
mp,ex,1,1.21e4          ! specify the young's modulus for the first
                        ! element type
mp,nuxy,1,0.3
r,1,10

et,2,plane42      ! specify the second element type to be plane42
KEYOPT,2,1,0
KEYOPT,2,2,0
KEYOPT,2,3,3

KEYOPT,2,3,3
mp,ex,2,20e       ! specify the young's modulus for the second
                  ! element type
mp,nuxy,2,0.3
r,2,50

type,1            ! specify the element type to be 1
```

```
real,1              ! specity the real constant number to be 1
mat,1               ! specity the matrial number to be 1
!***********mesh the mechanism

esize,,3            ! specify the number of line divisions to be 3

amesh,4             ! mesh area 4 (the compliant piece)
kbetw,165,167       !center of hole 2
kbetw,176,178
nkpt,3060,200       !create nodes coincident with center
nkpt,3061,149
nkpt,3062,201

mat,2               ! specify the material number to be 2
e,889,891,892,3060        ! create the elements around the perimeter of
hole 1
e,894,893,892,3060
e,894,895,890,3060
e,898,897,890,3060
e,898,899,900,3060
e,896,901,900,3060
e,896,903,904,3060
e,906,905,904,3060
e,906,907,902,3060
e,909,908,902,3060
e,909,910,911,3060
e,889,912,911,3060

e,832,833,834,3061        ! create the elements around the perimeter of
hole 2
e,830,835,834,3061
e,830,836,837,3061
e,839,838,837,3061
e,839,840,817,3061
e,820,819,817,3061
e,820,821,822,3061
e,818,823,822,3061
e,818,825,826,3061
```

```
e,828,827,826,3061
e,828,829,824,3061
e,832,831,824,3061
e,832,833,834,3061

e,983,984,961,3062          ! create the elements around the perimeter of
hole 3
e,964,963,961,3062
e,964,965,966,3062
e,962,967,966,3062
e,962,969,970,3062
e,972,971,970,3062
e,976,975,968,3062
e,976,977,978,3062
e,974,979,978,3062
e,974,980,981,3062
e,983,982,981,3062
e,972,973,968,3062

type,2                      ! specify the element type number to be 2
mat,2
real,2
! kbetw,200,149             ! create key point 202
! kbetw,201,149             ! create key point 203
! kbetw,201,200             ! create key point 204
! nkpt,3063,202
! nkpt,3064,203
! nkpt,3065,204
n,3066,
! e,3066,3060,3063
! e,3066,3061,3063
! e,3066,3061,3064
! e,3066,3062,3064
! e,3066,3062,3065
! e,3066,3060,3065

e,3066,3060,3061            ! create the three element on the rigid
                            ! triangular piece
```

```
e,3066,3061,3062
e,3066,3062,3060
FINISH

!********************** Add bounday conditions

/solu

lsel,s,,,173,184
dl,all,,all             !fix the 3 holes
allsel

!*****************************************************************
!           Input file for different load condition
!*******************************************************************

! *************apply input displacements to PZT 1 form 1um to 12 um

/solu

*dim,dx,,12        ! define an array dx (1*12) to store ux of node 3066
*dim,dy,,12        ! define an array dy (1*12) to store uy of node 3066
*dim,d1x,,12       ! define an array dx (1*12) to store ux of node 3061
*dim,d1y,,12       ! define an array dy (1*12) to store ux of node 3061
*dim,h,,12         ! define an array h (1*12) to store orientation of
                   ! the rigid piece

*set,l2,0          ! set the elogantion of PZT 2 zero
*set,l3,0          ! set the elogantion of PZT 3 zero

*DO,l1,1,12        ! the input motion to PZT is from 1 um to 12 um

dl,58,,ux,l1       !apply input motion on PZT 1 on  X direction
dl,58,,uy,0 !apply input motion on PZT 1 on  Y direction

dl,31,,ux,l2*load2x     !apply input motion on PZT 2 on X direction
dl,31,,uy,l2*load2y     !apply input motion on PZT 2 on Y direction
```

```
dl,104,,uy,l3*load3y    !apply input motion on PZT 3  on Y direction


solve                   !solve the problem at the corresponding l1
(Line 1) input

*get,c1y,node,3061,loc,y      !get uy of node 3061: c1y
*get,c1x,node,3061,loc,x      !get ux of node 3061: c1x
*get,cy,node,3066,loc,y       !get uy of node 3066: cy
*get,cx,node,3066,loc,x       !get ux of node 3066: cx


*vget,dx(l1),node,3066,u,x    !set ux of node 3066 as an array dx
*vget,dy(l1),node,3066,u,y    !set uy of node 3066 as an array dy
*vget,d1x(l1),node,3061,u,x   !set ux of node 3061 as an array d1x
*vget,d1y(l1),node,3061,u,y   !set ux of node 3061 as an array d1y


*set,h(l1),atan(((c1y+d1y(l1)*1e-3)-(cy+dy(l1)*1e-
3))/((c1x+d1x(l1)*1e-3)-(cx+dx(l1)*1e-3)))-atan(c1y/c1x)

!set the orientation of the rigid piece as an array parameter h

*ENDDO

fini


/solu             ! solve the problem


!-------------apply input displacements to PZT 2 from 1 um to 12 um


*dim,dx0a0,,12    !define an array dx0a0 (1*12) to store ux of node
3066
*dim,dy0a0,,12  !define an array dy0a0 (1*12) to store uy of node 3066
*dim,d1x0a0,,12  !define an array d1x0a0 (1*12) to store ux of node
```

```
                  !3061
*dim,d1y0a0,,12  ! define an array d1y0a0 (1*12) to store ux of node
                  !3061
*dim,h0a0,,12

*set,l1,0
*set,l3,0

*DO,l2,1,12        ! the input motion to PZT 2 is from 1 um to 12 um

dl,58,,ux,l1       !apply input motion on PZT 1 on X direction
dl,58,,uy,0        !apply input motion on PZT 1 on Y direction

dl,31,,ux,l2*load2x     !apply input motion on PZT 2 on X direction
dl,31,,uy,l2*load2y     !apply input motion on PZT 2 on Y direction

dl,104,,ux,l3*load3x    !apply input motion on PZT 3 on X direction
dl,104,,uy,l3*load3y    !apply input motion on PZT 3 on Y direction


solve                   !solve the problem



*vget,dx0a0(l2),node,3066,u,x !set ux of node 3066 as an array dx0a0
*vget,dy0a0(l2),node,3066,u,y !set uy of node 3066 as an array r dy0a0
*vget,d1x0a0(l2),node,3061,u,x      !set ux of node 3061 as an array
                                    !d1x0a0
*vget,d1y0a0(l2),node,3061,u,y      !set uy of node 3061 as an array
                                    !d1y0a0


*set,h0a0(l2),atan(((c1y+d1y0a0(l2)*1e-3)-(cy+dy0a0(l2)*1e-
3))/((c1x+d1x0a0(l2)*1e-3)-(cx+dx0a0(l2)*1e-3)))-atan(c1y/c1x)

*ENDDO
fini
```

```
!***************apply input displacements to PZT 3 from 1 um to 12 um

/solu

*dim,dx00a,,12     !define an array dx00a (1*12) to store ux of node
3066
*dim,dy00a,,12     !define an array dy00a (1*12) to store uy of node
3066
*dim,d1x00a,,12    ! define an array d1x00a (1*12) to store ux of node
3061
*dim,d1y00a,,12    !define an array d1y00a (1*12) to store ux of node
                   !3061
*dim,h00a,,12      ! define an array h00a (1*12) to store orientation of
                   !the rigid piece
*set,l1,0          ! set the elongation of PZT 1 zero
*set,l2,0          ! set the elongation of PZT 2 zero

*DO,l3,1,12        ! the input motion to PZT 3 is from 1 um to 12 um

dl,58,,ux,l1       !apply input motion on PZT 1 on X direction
dl,58,,uy,0        !apply input motion on PZT 1 on y direction
dl,31,,ux,l2*load2x      !apply input motion on PZT2 on X direction
dl,31,,uy,l2*load2y      !apply input motion on PZT 2 on Y direction

dl,104,,ux,l3*load3x     !apply input motion on PZT 3 on X direction
dl,104,,uy,l3*load3y     !apply input motion on PZT 3 on Y direction

solve                    !solve the problem

*vget,dx00a(l3),node,3066,u,x !set ux of node 3066 as an array dx00a
*vget,dy00a(l3),node,3066,u,y !set uy of node 3066 as an array dy00a
*vget,d1x00a(l3),node,3061,u,x      !set ux of node 3061 as an array
                                    !d1x00a
*vget,d1y00a(l3),node,3061,u,y      !set uy of node 3061 as an array
                                    !d1y00a

*set,h00a(l3),atan(((c1y+d1y00a(l3)*1e-3)-(cy+dy00a(l3)*1e-
3))/((c1x+d1x00a(l3)*1e-3)-(cx+dx00a(l3)*1e-3)))-atan(c1y/c1x)
```

```
*ENDDO

fini

!******apply input displacements to PZT 1,2 and 3 simultaneously from
!******1 um to 12 um

/solu

*dim,dxaaa,,12     !define an array dxaaa (1*12) to store ux of node
3066
*dim,dyaaa,,12     !define an array dyaaa (1*12) to store uy of node
3066
*dim,d1xaaa,,12 !define an array d1xaaa (1*12) to store ux of node
3061
*dim,d1yaaa,,12 !define an array d1yaaa (1*12) to store uy of node
3061
*dim,haaa,,12      !define an array haaa (1*12) to store the
                   !orientation of the rigid piece


*DO,l,1,12  !input motions to the three PZT are from 1 um to 12 um
dl,58,,ux,l        !apply input motion on PZT 1
dl,58,,uy,0

dl,31,,ux,l*load2x      !apply input motion on PZT 2
dl,31,,uy,l*load2y

dl,104,,ux,l*load3x     !apply input motion on PZT 3
dl,104,,uy,l*load3y


solve                   !solve the problem


*vget,dxaaa(l),node,3066,u,x  !set ux of node 3066 as an array dxaaa
*vget,dyaaa(l),node,3066,u,y  !set uy of node 3066 as an array dyaaa
```

```
*vget,d1xaaa(1),node,3061,u,x !set ux of node 3061 as an array d1xaaa
*vget,d1yaaa(1),node,3061,u,y !set uy of node 3061 as an array d1yaaa

*set,haaa(1),atan(((c1y+d1yaaa(1)*1e-3)-(cy+dyaaa(1)*1e-
3))/((c1x+d1xaaa(1)*1e-3)-(cx+dxaaa(1)*1e-3)))-atan(c1y/c1x)

*ENDDO

fini


!***********************
! Write to File
!*********************
/post1

*cfopen,FEM,dat,H:\      ! open a file in H: drive named FEM.dat

*vwrite,dx(1),dy(1),h(1)
(3e14.6)
*vwrite,dx0a0(1),dy0a0(1),h0a0(1)
(3e14.6)
*vwrite,dx00a(1),dy00a(1),h00a(1)
(3e14.6)
*vwrite,dxaaa(1),dyaaa(1),haaa(1)   ! write all the array into the
file FEM.dat
(3e14.6)
*cfclos                  ! close the file

fini                     ! end of the program
```

Appendix D: Dynamic Model

D.1: Parametric form

The parametric form of the dynamic model consists of the following matrices: $\mathbf{W}_i(\mathbf{l})$, $\mathbf{V}_i(\mathbf{l})$, i=1,2,3, $\mathbf{K}(\mathbf{l})$, $\mathbf{C}(\mathbf{l},\dot{\mathbf{l}})$, and $\mathbf{H}(\mathbf{l})$, see Chapter 4. These matrices are all 3×3. In the following, these matrices are presented in their form of Maple V.

D.1.1 $\mathbf{W}_i(\mathbf{l})$ and $\mathbf{V}_i(\mathbf{l})$, i=1,2,3

For each of these matrices, there are nine elements. The following notations in Maple V for representing these elements apply:

Wijk (Vijk): W and V represent matrices $\mathbf{W}_i(\mathbf{l})$ and $\mathbf{V}_i(\mathbf{l})$, respectively;
i represents the actuator identifer, i=1,2,3;
j represents the row number;
k represents the column number.

Also, for the Constant-Jacobian matrix, the following notations in Maple V apply:

JLjk: JL represents the Constant-Jacobian matrix, i.e., J_l^0;
j represents the row number;
k represents the column number.

$$VI11 := \left(\left(\left(\frac{1}{4}(-2\,JL11 + Rs\sqrt{3}\,JL31)\,A1yo + \frac{1}{4}(2\,JL21 - Rs\,JL31)\,A1xo\right.\right.\right.$$

$$\left.\left.+\frac{1}{4}(-Rs\sqrt{3}\,JL31 + 2\,JL11)\,B1yo + \frac{1}{4}(Rs\,JL31 - 2\,JL21)\,B1xo\right)\cos\left(\frac{L1}{Ro}\right)\right)/\,Ro + \left(\left(\right.\right.$$

$$\frac{1}{4}(-Rs\sqrt{3}\,JL31 + 2\,JL11)\,A1xo + \frac{1}{4}(Rs\,JL31 - 2\,JL21)\,B1yo + \frac{1}{4}(-2\,JL11 + Rs\sqrt{3}\,JL31)\,B1xo$$

$$\left.\left.+\frac{1}{4}(2\,JL21 - Rs\,JL31)\,A1yo\right)\sin\left(\frac{L1}{Ro}\right)\right)/\,Ro - \frac{1}{4}JL11\,Rs\sqrt{3}\,JL31 + \frac{1}{4}Rs^2\,JL31^2$$

$$-\frac{1}{4}JL21\,Rs\,JL31 + \frac{1}{4}JL21^2 + \frac{1}{4}JL11^2$$

$$+\frac{\frac{1}{4}A1xo^2 - \frac{1}{2}B1xo\,A1xo + \frac{1}{4}B1yo^2 + \frac{1}{4}B1xo^2 + \frac{1}{4}A1yo^2 - \frac{1}{2}B1yo\,A1yo}{Ro^2}$$

$$VI22 := \frac{1}{4}Rs^2\,JL32^2 - \frac{1}{4}JL22\,Rs\,JL32 + \frac{1}{4}JL12^2 + \frac{1}{4}JL22^2 - \frac{1}{4}JL12\,Rs\sqrt{3}\,JL32$$

$$VI33 := \frac{1}{4}Rs^2\,JL33^2 - \frac{1}{4}JL23\,Rs\,JL33 + \frac{1}{4}JL13^2 + \frac{1}{4}JL23^2 - \frac{1}{4}JL13\,Rs\sqrt{3}\,JL33$$

$$VI12 := \left(\left(\left(\frac{1}{8}(-2\,JL12 + Rs\sqrt{3}\,JL32)\,A1yo + \frac{1}{8}(-2\,JL22 + Rs\,JL32)\,B1xo\right.\right.\right.$$

$$\left.\left.+\frac{1}{8}(2\,JL12 - Rs\sqrt{3}\,JL32)\,B1yo + \frac{1}{8}(2\,JL22 - Rs\,JL32)\,A1xo\right)\cos\left(\frac{L1}{Ro}\right)\right)/\,Ro + \left(\left(\right.\right.$$

$$\frac{1}{8}(-2\,JL12 + Rs\sqrt{3}\,JL32)\,B1xo + \frac{1}{8}(-2\,JL22 + Rs\,JL32)\,B1yo + \frac{1}{8}(2\,JL12 - Rs\sqrt{3}\,JL32)\,A1xo$$

$$\left.\left.+\frac{1}{8}(2\,JL22 - Rs\,JL32)\,A1yo\right)\sin\left(\frac{L1}{Ro}\right)\right)/\,Ro + \frac{1}{4}JL11\,JL12 + \frac{1}{4}JL21\,JL22 - \frac{1}{8}JL22\,Rs\,JL31$$

$$+\frac{1}{4}Rs^2\,JL31\,JL32 - \frac{1}{8}JL11\,Rs\sqrt{3}\,JL32 - \frac{1}{8}JL12\,Rs\sqrt{3}\,JL31 - \frac{1}{8}JL21\,Rs\,JL32$$

$$VI13 := \left(\left(\left(\frac{1}{8}(-2\,JL13 + Rs\sqrt{3}\,JL33)\,A1yo + \frac{1}{8}(-2\,JL23 + Rs\,JL33)\,B1xo\right.\right.\right.$$

$$\left.\left.+\frac{1}{8}(-Rs\sqrt{3}\,JL33 + 2\,JL13)\,B1yo + \frac{1}{8}(2\,JL23 - Rs\,JL33)\,A1xo\right)\cos\left(\frac{L1}{Ro}\right)\right)/\,Ro + \left(\left(\right.\right.$$

$$\frac{1}{8}(-2\,JL13 + Rs\sqrt{3}\,JL33)\,B1xo + \frac{1}{8}(-2\,JL23 + Rs\,JL33)\,B1yo + \frac{1}{8}(-Rs\sqrt{3}\,JL33 + 2\,JL13)\,A1xo$$

$$\left.\left.+\frac{1}{8}(2\,JL23 - Rs\,JL33)\,A1yo\right)\sin\left(\frac{L1}{Ro}\right)\right)/\,Ro + \frac{1}{4}JL11\,JL13 + \frac{1}{4}JL21\,JL23 + \frac{1}{4}Rs^2\,JL31\,JL33$$

$$-\frac{1}{8}JL21\,Rs\,JL33 - \frac{1}{8}JL11\,Rs\sqrt{3}\,JL33 - \frac{1}{8}JL13\,Rs\sqrt{3}\,JL31 - \frac{1}{8}JL23\,Rs\,JL31$$

$$VI23 := \frac{1}{4}Rs^2\,JL32\,JL33 - \frac{1}{8}JL22\,Rs\,JL33 - \frac{1}{8}JL23\,Rs\,JL32 + \frac{1}{4}JL12\,JL13 + \frac{1}{4}JL22\,JL23 - \frac{1}{8}JL12\,Rs\sqrt{3}\,JL33$$

$$-\frac{1}{8} JL13\, Rs \sqrt{3}\, JL32$$

$$V211 := \frac{1}{4} Rs^2\, JL31^2 + \frac{1}{2} JL21\, Rs\, JL31 + \frac{1}{4} JL21^2 + \frac{1}{4} JL11^2$$

$$V222 := \Bigg(\left(-\frac{1}{2} JL12\, A2yo + \frac{1}{4} (2\, JL22 + 2\, Rs\, JL32)\, A2xo + \frac{1}{2} JL12\, B2yo + \frac{1}{4} (-2\, JL22 - 2\, Rs\, JL32)\, B2xo \right) \cos\left(\frac{L2}{Ro}\right) \Bigg) / Ro + \Bigg(\left(\frac{1}{2} JL12\, A2xo + \frac{1}{4} (-2\, JL22 - 2\, Rs\, JL32)\, B2yo - \frac{1}{2} JL12\, B2xo + \frac{1}{4} (2\, JL22 + 2\, Rs\, JL32)\, A2yo \right) \sin\left(\frac{L2}{Ro}\right) \Bigg) / Ro + \frac{1}{4} JL22^2 + \frac{1}{4} JL12^2 + \frac{1}{4} Rs^2\, JL32^2 + \frac{1}{2} JL22\, Rs\, JL32 + \frac{\frac{1}{4} A2xo^2 - \frac{1}{2} B2xo\, A2xo + \frac{1}{4} B2yo^2 + \frac{1}{4} B2xo^2 + \frac{1}{4} A2yo^2 - \frac{1}{2} B2yo\, A2yo}{Ro^2}$$

$$V233 := \frac{1}{4} Rs^2\, JL33^2 + \frac{1}{4} JL23^2 + \frac{1}{2} JL23\, Rs\, JL33 + \frac{1}{4} JL13^2$$

$$V212 := \Bigg(\left(\frac{1}{8} (2\, Rs\, JL31 + 2\, JL21)\, A2xo - \frac{1}{4} JL11\, A2yo + \frac{1}{8} (-2\, Rs\, JL31 - 2\, JL21)\, B2xo + \frac{1}{4} JL11\, B2yo \right) \cos\left(\frac{L2}{Ro}\right) \Bigg) / Ro + \Bigg(\left(\frac{1}{8} (2\, Rs\, JL31 + 2\, JL21)\, A2yo - \frac{1}{4} JL11\, B2xo + \frac{1}{8} (-2\, Rs\, JL31 - 2\, JL21)\, B2yo + \frac{1}{4} JL11\, A2xo \right) \sin\left(\frac{L2}{Ro}\right) \Bigg) / Ro + \frac{1}{4} Rs^2\, JL31\, JL32 + \frac{1}{4} JL21\, Rs\, JL32 + \frac{1}{4} JL22\, Rs\, JL31 + \frac{1}{4} JL11\, JL12 + \frac{1}{4} JL21\, JL22$$

$$V213 := \frac{1}{4} Rs^2\, JL31\, JL33 + \frac{1}{4} JL21\, JL23 + \frac{1}{4} JL21\, Rs\, JL33 + \frac{1}{4} JL23\, Rs\, JL31 + \frac{1}{4} JL11\, JL13$$

$$V223 := \Bigg(\left(\frac{1}{8} (2\, JL23 + 2\, Rs\, JL33)\, A2xo - \frac{1}{4} JL13\, A2yo + \frac{1}{8} (-2\, JL23 - 2\, Rs\, JL33)\, B2xo + \frac{1}{4} JL13\, B2yo \right) \cos\left(\frac{L2}{Ro}\right) \Bigg) / Ro + \Bigg($$

$$\left(\frac{1}{8}(2\,JL23+2\,Rs\,JL33)\,A2yo-\frac{1}{4}JL13\,B2xo+\frac{1}{8}(-2\,JL23-2\,Rs\,JL33)\,B2yo+\frac{1}{4}JL13\,A2xo\right)$$
$$\sin\left(\frac{L2}{Ro}\right)\Bigg)\Big/\,Ro+\frac{1}{4}JL23\,Rs\,JL32+\frac{1}{4}Rs^2\,JL32\,JL33+\frac{1}{4}JL22\,JL23+\frac{1}{4}JL22\,Rs\,JL33+\frac{1}{4}JL12\,JL13$$

$$V311:=\frac{1}{4}Rs^2\,JL31^2-\frac{1}{4}JL21\,Rs\,JL31+\frac{1}{4}JL21^2+\frac{1}{4}JL11^2+\frac{1}{4}JL11\,Rs\sqrt{3}\,JL31$$

$$V322:=\frac{1}{4}JL12\,Rs\sqrt{3}\,JL32+\frac{1}{4}Rs^2\,JL32^2+\frac{1}{4}JL22^2-\frac{1}{4}JL22\,Rs\,JL32+\frac{1}{4}JL12^2$$

$$V333:=\frac{1}{4}\Bigg(-JL23\,Ro^2\,Rs\,JL33+2\sin\left(\frac{L3}{Ro}\right)A3xo\,JL13\,Ro-2\cos\left(\frac{L3}{Ro}\right)A3yo\,JL13\,Ro$$
$$-2\sin\left(\frac{L3}{Ro}\right)B3yo\,JL23\,Ro+2\cos\left(\frac{L3}{Ro}\right)B3yo\,JL13\,Ro-2\sin\left(\frac{L3}{Ro}\right)B3xo\,JL13\,Ro$$
$$+2\sin\left(\frac{L3}{Ro}\right)A3yo\,JL23\,Ro+2\cos\left(\frac{L3}{Ro}\right)A3xo\,JL23\,Ro-2\cos\left(\frac{L3}{Ro}\right)B3xo\,JL23\,Ro+JL13^2\,Ro^2$$
$$+Rs^2\,Ro^2\,JL33^2+B3xo^2+A3yo^2+A3xo^2+B3yo^2-\sin\left(\frac{L3}{Ro}\right)A3yo\,Rs\,Ro\,JL33+JL23^2\,Ro^2$$
$$-2\,B3yo\,A3yo-2\,B3xo\,A3xo-\cos\left(\frac{L3}{Ro}\right)A3xo\,Rs\,Ro\,JL33+\cos\left(\frac{L3}{Ro}\right)B3xo\,Rs\,Ro\,JL33$$
$$+\sin\left(\frac{L3}{Ro}\right)B3yo\,Rs\,Ro\,JL33+\sin\left(\frac{L3}{Ro}\right)A3xo\,Rs\,Ro\,JL33\sqrt{3}-\sin\left(\frac{L3}{Ro}\right)B3xo\,Rs\,Ro\,JL33\sqrt{3}$$
$$-\cos\left(\frac{L3}{Ro}\right)A3yo\,Rs\,Ro\,JL33\sqrt{3}+\cos\left(\frac{L3}{Ro}\right)B3yo\,Rs\,Ro\,JL33\sqrt{3}+JL13\,Ro^2\,Rs\,JL33\sqrt{3}\Bigg)\Big/\,Ro^2$$

$$V312:=\frac{1}{8}JL11\,Rs\sqrt{3}\,JL32+\frac{1}{8}JL12\,Rs\sqrt{3}\,JL31+\frac{1}{4}Rs^2\,JL31\,JL32+\frac{1}{4}JL21\,JL22+\frac{1}{4}JL11\,JL12$$
$$-\frac{1}{8}JL21\,Rs\,JL32-\frac{1}{8}JL22\,Rs\,JL31$$

$$V313:=\Bigg(\Bigg(-\frac{1}{8}(Rs\,JL31-2\,JL21)\,A3yo-\frac{1}{8}(Rs\sqrt{3}\,JL31+2\,JL11)\,B3xo$$
$$-\frac{1}{8}(2\,JL21-Rs\,JL31)\,B3yo-\frac{1}{8}(-Rs\sqrt{3}\,JL31-2\,JL11)\,A3xo\Bigg)\sin\left(\frac{L3}{Ro}\right)\Bigg)\Big/\,Ro+\Bigg(\Bigg($$
$$-\frac{1}{8}(2\,JL21-Rs\,JL31)\,B3xo-\frac{1}{8}(-Rs\sqrt{3}\,JL31-2\,JL11)\,B3yo-\frac{1}{8}(Rs\,JL31-2\,JL21)\,A3xo$$
$$-\frac{1}{8}(Rs\sqrt{3}\,JL31+2\,JL11)\,A3yo\Bigg)\cos\left(\frac{L3}{Ro}\right)\Bigg)\Big/\,Ro+\frac{1}{4}JL21\,JL23+\frac{1}{4}Rs^2\,JL31\,JL33$$
$$-\frac{1}{8}JL23\,Rs\,JL31-\frac{1}{8}JL21\,Rs\,JL33+\frac{1}{4}JL11\,JL13+\frac{1}{8}JL11\,Rs\sqrt{3}\,JL33+\frac{1}{8}JL13\,Rs\sqrt{3}\,JL31$$

$$V323:=\Bigg(\Bigg(-\frac{1}{8}(-2\,JL22+Rs\,JL32)\,A3yo-\frac{1}{8}(Rs\sqrt{3}\,JL32+2\,JL12)\,B3xo$$

$$-\frac{1}{8}(2\,JL22 - Rs\,JL32)\,B3yo - \frac{1}{8}(-2\,JL12 - Rs\sqrt{3}\,JL32)\,A3xo\Bigg)\sin\left(\frac{L3}{Ro}\right)\Bigg)/\,Ro + \Bigg(\Bigg($$

$$-\frac{1}{8}(2\,JL22 - Rs\,JL32)\,B3xo - \frac{1}{8}(-2\,JL12 - Rs\sqrt{3}\,JL32)\,B3yo - \frac{1}{8}(-2\,JL22 + Rs\,JL32)\,A3xo$$

$$-\frac{1}{8}(Rs\sqrt{3}\,JL32 + 2\,JL12)\,A3yo\Bigg)\cos\left(\frac{L3}{Ro}\right)\Bigg)/\,Ro + \frac{1}{8}JL12\,Rs\sqrt{3}\,JL33 + \frac{1}{4}JL12\,JL13$$

$$-\frac{1}{8}JL23\,Rs\,JL32 + \frac{1}{4}Rs^2\,JL32\,JL33 + \frac{1}{4}JL22\,JL23 + \frac{1}{8}JL13\,Rs\sqrt{3}\,JL32 - \frac{1}{8}JL22\,Rs\,JL33$$

$$w111 := \Bigg(((-Rs\sqrt{3}\,JL31 + 2\,JL11)\,A1yo + (Rs\,JL31 - 2\,JL21)\,A1xo$$

$$+ (-2\,JL11 + Rs\sqrt{3}\,JL31)\,B1yo + (2\,JL21 - Rs\,JL31)\,B1xo)\cos\left(\frac{L1}{Ro}\right)\Bigg)\Big/(Lbc^2\,Ro) + \Bigg(($$

$$(-2\,JL11 + Rs\sqrt{3}\,JL31)\,A1xo + (2\,JL21 - Rs\,JL31)\,B1yo + (-Rs\sqrt{3}\,JL31 + 2\,JL11)\,B1xo$$

$$+ (Rs\,JL31 - 2\,JL21)\,A1yo)\sin\left(\frac{L1}{Ro}\right)\Bigg)\Big/(Lbc^2\,Ro)$$

$$+ \frac{-JL11\,Rs\sqrt{3}\,JL31 + JL11^2 - JL21\,Rs\,JL31 + Rs^2\,JL31^2 + JL21^2}{Lbc^2}$$

$$+ \frac{A1xo^2 - 2\,B1xo\,A1xo + B1yo^2 + B1xo^2 + A1yo^2 - 2\,B1yo\,A1yo}{Lbc^2\,Ro^2}$$

$$w122 := \frac{Rs^2\,JL32^2 + JL22^2 + JL12^2 - JL22\,Rs\,JL32 - JL12\,Rs\sqrt{3}\,JL32}{Lbc^2}$$

$$w133 := \frac{Rs^2\,JL33^2 + JL23^2 + JL13^2 - JL23\,Rs\,JL33 - JL13\,Rs\sqrt{3}\,JL33}{Lbc^2}$$

$$w112 := \Bigg(\Bigg(\frac{1}{2}(-2\,JL22 + Rs\,JL32)\,A1xo + \frac{1}{2}(2\,JL12 - Rs\sqrt{3}\,JL32)\,A1yo$$

$$+ \frac{1}{2}(2\,JL22 - Rs\,JL32)\,B1xo + \frac{1}{2}(-2\,JL12 + Rs\sqrt{3}\,JL32)\,B1yo\Bigg)\cos\left(\frac{L1}{Ro}\right)\Bigg)\Big/(Lbc^2\,Ro) + \Bigg(\Bigg($$

$$\frac{1}{2}(-2\,JL22 + Rs\,JL32)\,A1yo + \frac{1}{2}(2\,JL12 - Rs\sqrt{3}\,JL32)\,B1xo + \frac{1}{2}(2\,JL22 - Rs\,JL32)\,B1yo$$

$$+ \frac{1}{2}(-2\,JL12 + Rs\sqrt{3}\,JL32)\,A1xo\Bigg)\sin\left(\frac{L1}{Ro}\right)\Bigg)\Big/(Lbc^2\,Ro) + \Bigg(-\frac{1}{2}JL11\,Rs\sqrt{3}\,JL32$$

$$-\frac{1}{2}JL12\,Rs\sqrt{3}\,JL31 + JL21\,JL22 + JL11\,JL12 - \frac{1}{2}JL22\,Rs\,JL31 - \frac{1}{2}JL21\,Rs\,JL32$$

$$+ Rs^2\,JL31\,JL32\Bigg)\Big/\,Lbc^2$$

$$w113 := \Bigg(\Bigg(\frac{1}{2}(-2\,JL23 + Rs\,JL33)\,A1xo + \frac{1}{2}(-Rs\sqrt{3}\,JL33 + 2\,JL13)\,A1yo$$

$$+\frac{1}{2}(2\,JL23 - Rs\,JL33)\,B1xo + \frac{1}{2}(-2\,JL13 + Rs\sqrt{3}\,JL33)\,B1yo\Bigg)\cos\left(\frac{L1}{Ro}\right)\Bigg)\Big/(Lbc^2\,Ro) + \Bigg(\Bigg(\Bigg($$

$$\frac{1}{2}(-2\,JL23 + Rs\,JL33)\,A1yo + \frac{1}{2}(-Rs\sqrt{3}\,JL33 + 2\,JL13)\,B1xo + \frac{1}{2}(2\,JL23 - Rs\,JL33)\,B1yo$$

$$+\frac{1}{2}(-2\,JL13 + Rs\sqrt{3}\,JL33)\,A1xo\Bigg)\sin\left(\frac{L1}{Ro}\right)\Bigg)\Big/(Lbc^2\,Ro) + \Bigg(-\frac{1}{2}JL11\,Rs\sqrt{3}\,JL33$$

$$-\frac{1}{2}JL13\,Rs\sqrt{3}\,JL31 + JL21\,JL23 - \frac{1}{2}JL21\,Rs\,JL33 + JL11\,JL13 + Rs^2\,JL31\,JL33$$

$$-\frac{1}{2}JL23\,Rs\,JL31\Bigg)\Big/Lbc^2$$

$$w123 := \frac{1}{2}(2\,JL12\,JL13 + 2\,JL22\,JL23 - JL22\,Rs\,JL33 - JL23\,Rs\,JL32 + 2\,Rs^2\,JL32\,JL33$$

$$-JL12\,Rs\sqrt{3}\,JL33 - JL13\,Rs\sqrt{3}\,JL32)\Big/Lbc^2$$

$$w211 := \frac{2\,JL21\,Rs\,JL31 + Rs^2\,JL31^2 + JL21^2 + JL11^2}{Lbc^2}$$

$$w222 := \Bigg($$

$$(2\,JL12\,A2yo + (-2\,JL22 - 2\,Rs\,JL32)\,A2xo - 2\,JL12\,B2yo + (2\,JL22 + 2\,Rs\,JL32)\,B2xo)$$

$$\cos\left(\frac{L2}{Ro}\right)\Bigg)\Big/(Lbc^2\,Ro) + \Bigg($$

$$(-2\,JL12\,A2xo + (2\,JL22 + 2\,Rs\,JL32)\,B2yo + 2\,JL12\,B2xo + (-2\,JL22 - 2\,Rs\,JL32)\,A2yo)$$

$$\sin\left(\frac{L2}{Ro}\right)\Bigg)\Big/(Lbc^2\,Ro) + \frac{Rs^2\,JL32^2 + JL22^2 + 2\,JL22\,Rs\,JL32 + JL12^2}{Lbc^2}$$

$$+\frac{A2xo^2 - 2\,B2xo\,A2xo + B2yo^2 + B2xo^2 + A2yo^2 - 2\,B2yo\,A2yo}{Lbc^2\,Ro^2}$$

$$w233 := \frac{Rs^2\,JL33^2 + JL23^2 + JL13^2 + 2\,JL23\,Rs\,JL33}{Lbc^2}$$

$$w212 := \Bigg($$

$$\left(\frac{1}{2}(-2\,Rs\,JL31 - 2\,JL21)\,A2xo + JL11\,A2yo + \frac{1}{2}(2\,Rs\,JL31 + 2\,JL21)\,B2xo - JL11\,B2yo\right)$$

$$\cos\left(\frac{L2}{Ro}\right)\Bigg)\Big/(Lbc^2\,Ro) + \Bigg($$

$$\left(\frac{1}{2}(-2\,Rs\,JL31 - 2\,JL21)\,A2yo + JL11\,B2xo + \frac{1}{2}(2\,Rs\,JL31 + 2\,JL21)\,B2yo - JL11\,A2xo\right)$$

$$\sin\left(\frac{L2}{Ro}\right)\Bigg)\Big/(Lbc^2\,Ro) + \frac{JL21\,JL22 + JL21\,Rs\,JL32 + Rs^2\,JL31\,JL32 + JL22\,Rs\,JL31 + JL11\,JL12}{Lbc^2}$$

$$w213 := \frac{JL21\ JL23 + JL21\ Rs\ JL33 + JL11\ JL13 + JL23\ Rs\ JL31 + Rs^2\ JL31\ JL33}{Lbc^2}$$

$$w223 := \Bigg(\left(\frac{1}{2}(-2\ JL23 - 2\ Rs\ JL33)\ A2xo + JL13\ A2yo + \frac{1}{2}(2\ JL23 + 2\ Rs\ JL33)\ B2xo - JL13\ B2yo\right) \cos\left(\frac{L2}{Ro}\right)\Bigg) \Big/ (Lbc^2\ Ro) + \Bigg(\left(\frac{1}{2}(-2\ JL23 - 2\ Rs\ JL33)\ A2yo + JL13\ B2xo + \frac{1}{2}(2\ JL23 + 2\ Rs\ JL33)\ B2yo - JL13\ A2xo\right) \sin\left(\frac{L2}{Ro}\right)\Bigg) \Big/ (Lbc^2\ Ro) + \frac{JL12\ JL13 + JL23\ Rs\ JL32 + Rs^2\ JL32\ JL33 + JL22\ Rs\ JL33 + JL22\ JL23}{Lbc^2}$$

$$w311 := \frac{-JL21\ Rs\ JL31 + Rs^2\ JL31^2 + JL21^2 + JL11^2 + JL11\ Rs\sqrt{3}\ JL31}{Lbc^2}$$

$$w322 := \frac{Rs^2\ JL32^2 + JL22^2 + JL12^2 - JL22\ Rs\ JL32 + JL12\ Rs\sqrt{3}\ JL32}{Lbc^2}$$

$$w333 := \Bigg(((2\ JL23 - Rs\ JL33)\ B3yo + (2\ JL13 + Rs\sqrt{3}\ JL33)\ B3xo + (-2\ JL23 + Rs\ JL33)\ A3yo + (-Rs\sqrt{3}\ JL33 - 2\ JL13)\ A3xo) \sin\left(\frac{L3}{Ro}\right)\Bigg) \Big/ (Lbc^2\ Ro) + \Bigg(((2\ JL23 - Rs\ JL33)\ B3xo + (2\ JL13 + Rs\sqrt{3}\ JL33)\ A3yo + (-2\ JL23 + Rs\ JL33)\ A3xo + (-Rs\sqrt{3}\ JL33 - 2\ JL13)\ B3yo) \cos\left(\frac{L3}{Ro}\right)\Bigg) \Big/ (Lbc^2\ Ro) + \frac{JL23^2 - JL23\ Rs\ JL33 + JL13\ Rs\sqrt{3}\ JL33 + JL13^2 + Rs^2\ JL33^2}{Lbc^2} + \frac{B3xo^2 - 2\ B3xo\ A3xo + A3yo^2 + A3xo^2 + B3yo^2 - 2\ B3yo\ A3yo}{Lbc^2\ Ro^2}$$

$$w312 := \frac{1}{2}(JL11\ Rs\sqrt{3}\ JL32 + JL12\ Rs\sqrt{3}\ JL31 + 2\ JL21\ JL22 - JL21\ Rs\ JL32 + 2\ JL11\ JL12 + 2\ Rs^2\ JL31\ JL32 - JL22\ Rs\ JL31) \Big/ Lbc^2$$

$$w313 := \Bigg(\bigg(\frac{1}{2}(Rs\sqrt{3}\ JL31 + 2\ JL11)\ B3xo + \frac{1}{2}(2\ JL21 - Rs\ JL31)\ B3yo + \frac{1}{2}(-Rs\sqrt{3}\ JL31 - 2\ JL11)\ A3xo + \frac{1}{2}(Rs\ JL31 - 2\ JL21)\ A3yo\bigg) \sin\left(\frac{L3}{Ro}\right)\Bigg) \Big/ (Lbc^2\ Ro) + \Bigg(\bigg(\frac{1}{2}(-Rs\sqrt{3}\ JL31 - 2\ JL11)\ B3yo + \frac{1}{2}(Rs\ JL31 - 2\ JL21)\ A3xo + \frac{1}{2}(Rs\sqrt{3}\ JL31 + 2\ JL11)\ A3yo + \frac{1}{2}(2\ JL21 - Rs\ JL31)\ B3xo\bigg) \cos\left(\frac{L3}{Ro}\right)\Bigg) \Big/ (Lbc^2\ Ro) + \bigg(\frac{1}{2} JL11\ Rs\sqrt{3}\ JL33 + JL21\ JL23$$

$$-\frac{1}{2} JL21\, Rs\, JL33+\frac{1}{2} JL13\, Rs \sqrt{3}\, JL31+Rs^2\, JL31\, JL33+JL11\, JL13-\frac{1}{2} JL23\, Rs\, JL31 \Big) \Big/ Lbc^2$$

$$w323 := \Bigg(\Bigg(\frac{1}{2}(Rs\sqrt{3}\, JL32+2\, JL12)\, B3xo+\frac{1}{2}(2\, JL22-Rs\, JL32)\, B3yo$$
$$+\frac{1}{2}(-2\, JL12-Rs\sqrt{3}\, JL32)\, A3xo+\frac{1}{2}(-2\, JL22+Rs\, JL32)\, A3yo\Bigg)\sin\left(\frac{L3}{Ro}\right)\Bigg) \Big/ (Lbc^2\, Ro)+\Bigg(\Bigg($$
$$\frac{1}{2}(-2\, JL12-Rs\sqrt{3}\, JL32)\, B3yo+\frac{1}{2}(-2\, JL22+Rs\, JL32)\, A3xo+\frac{1}{2}(Rs\sqrt{3}\, JL32+2\, JL12)\, A3yo$$
$$+\frac{1}{2}(2\, JL22-Rs\, JL32)\, B3xo\Bigg)\cos\left(\frac{L3}{Ro}\right)\Bigg) \Big/ (Lbc^2\, Ro)+\Big(JL12\, JL13+JL22\, JL23$$
$$-\frac{1}{2} JL22\, Rs\, JL33-\frac{1}{2} JL23\, Rs\, JL32+Rs^2\, JL32\, JL33+\frac{1}{2} JL12\, Rs\sqrt{3}\, JL33+\frac{1}{2} JL13\, Rs\sqrt{3}\, JL32\Big)$$
$$\Big/ Lbc^2$$

D.1.2 $\mathbf{K(l)}$, $\mathbf{C(l,\dot{l})}$, and $\mathbf{H(l)}$

The following notations in Maple V apply:

Ldot represents $\dot{L}$;

LDDOT represents $\ddot{L}$;

Lidot (i=1,2,3) represents $\dot{L}_i$;

LiDDOT (i=1,2,3) represents $\ddot{L}_i$.

$$K\_11 := \Big(Ibc\, ((-Rs\sqrt{3}\, JL31 + 2\, JL11)\, A1yo + (Rs\, JL31 - 2\, JL21)\, A1xo$$

$$+ (-2\, JL11 + Rs\sqrt{3}\, JL31)\, B1yo + (2\, JL21 - Rs\, JL31)\, B1xo) \,/\, (Lbc^2\, Ro) + Mbc\Big($$

$$\frac{1}{4}(-2\, JL11 + Rs\sqrt{3}\, JL31)\, A1yo + \frac{1}{4}(2\, JL21 - Rs\, JL31)\, A1xo + \frac{1}{4}(-Rs\sqrt{3}\, JL31 + 2\, JL11)\, B1yo$$

$$+ \frac{1}{4}(Rs\, JL31 - 2\, JL21)\, B1xo\Big) / Ro\Big) \cos\left(\frac{L1}{Ro}\right) + \Big(Ibc\, ((-2\, JL11 + Rs\sqrt{3}\, JL31)\, A1xo$$

$$+ (2\, JL21 - Rs\, JL31)\, B1yo + (-Rs\sqrt{3}\, JL31 + 2\, JL11)\, B1xo + (Rs\, JL31 - 2\, JL21)\, A1yo) \,/\, ($$

$$Lbc^2\, Ro) + Mbc\Big(\frac{1}{4}(-Rs\sqrt{3}\, JL31 + 2\, JL11)\, A1xo + \frac{1}{4}(Rs\, JL31 - 2\, JL21)\, B1yo$$

$$+ \frac{1}{4}(-2\, JL11 + Rs\sqrt{3}\, JL31)\, B1xo + \frac{1}{4}(2\, JL21 - Rs\, JL31)\, A1yo\Big) / Ro\Big) \sin\left(\frac{L1}{Ro}\right)$$

$$+ Me\, (JL11^2 + JL21^2) + Ie\, JL31^2 + \frac{Iab}{Ro^2} + Ibc\Big(\frac{2\, JL21\, Rs\, JL31 + Rs^2\, JL31^2 + JL21^2 + JL11^2}{Lbc^2}$$

$$+ \frac{-JL11\, Rs\sqrt{3}\, JL31 + JL11^2 - JL21\, Rs\, JL31 + Rs^2\, JL31^2 + JL21^2}{Lbc^2}$$

$$+ \frac{A1xo^2 - 2\, B1xo\, A1xo + B1yo^2 + B1xo^2 + A1yo^2 - 2\, B1yo\, A1yo}{Lbc^2\, Ro^2}$$

$$+ \frac{-JL21\, Rs\, JL31 + Rs^2\, JL31^2 + JL21^2 + JL11^2 + JL11\, Rs\sqrt{3}\, JL31}{Lbc^2}\Big) + Mbc\Big(\frac{3}{4} JL21^2 + \frac{3}{4} Rs^2\, JL31^2$$

$$+ \frac{3}{4} JL11^2 + \frac{\frac{1}{4} A1xo^2 - \frac{1}{2} B1xo\, A1xo + \frac{1}{4} B1yo^2 + \frac{1}{4} B1xo^2 + \frac{1}{4} A1yo^2 - \frac{1}{2} B1yo\, A1yo}{Ro^2}\Big)$$

$$K\_12 := \Big($$

$$\frac{Ibc\left(\frac{1}{2}(-2\, JL21 - 2\, Rs\, JL31)\, A2xo + JL11\, A2yo + \frac{1}{2}(2\, Rs\, JL31 + 2\, JL21)\, B2xo - JL11\, B2yo\right)}{Lbc^2\, Ro} +$$

$$Mbc\left(\frac{1}{8}(2\, Rs\, JL31 + 2\, JL21)\, A2xo - \frac{1}{4} JL11\, A2yo + \frac{1}{8}(-2\, JL21 - 2\, Rs\, JL31)\, B2xo + \frac{1}{4} JL11\, B2yo\right)$$

$$/ Ro\Big) \cos\left(\frac{L2}{Ro}\right) + \Big(Ibc\Big(\frac{1}{2}(Rs\, JL32 - 2\, JL22)\, A1xo + \frac{1}{2}(2\, JL12 - Rs\sqrt{3}\, JL32)\, A1yo$$

$$+ \frac{1}{2}(-Rs\, JL32 + 2\, JL22)\, B1xo + \frac{1}{2}(Rs\sqrt{3}\, JL32 - 2\, JL12)\, B1yo\Big) / (Lbc^2\, Ro) + Mbc\Big($$

$$\frac{1}{8}(-Rs\, JL32 + 2\, JL22)\, A1xo + \frac{1}{8}(Rs\sqrt{3}\, JL32 - 2\, JL12)\, A1yo + \frac{1}{8}(Rs\, JL32 - 2\, JL22)\, B1xo$$

$$+ \frac{1}{8}(2\, JL12 - Rs\sqrt{3}\, JL32)\, B1yo\Big) / Ro\Big) \cos\left(\frac{L1}{Ro}\right) + \Big($$

$$\frac{Ibc\left(\frac{1}{2}(-2\,JL21-2\,Rs\,JL31)\,A2yo+JL11\,B2xo+\frac{1}{2}(2\,Rs\,JL31+2\,JL21)\,B2yo-JL11\,A2xo\right)}{Lbc^2\,Ro}+$$

$$Mbc\left(\frac{1}{8}(2\,Rs\,JL31+2\,JL21)\,A2yo-\frac{1}{4}JL11\,B2xo+\frac{1}{8}(-2\,JL21-2\,Rs\,JL31)\,B2yo+\frac{1}{4}JL11\,A2xo\right)$$

$$/\,Ro\Bigg)\sin\left(\frac{L2}{Ro}\right)+\Bigg(Ibc\Bigg(\frac{1}{2}(Rs\,JL32-2\,JL22)\,A1yo+\frac{1}{2}(2\,JL12-Rs\sqrt{3}\,JL32)\,B1xo$$

$$+\frac{1}{2}(-Rs\,JL32+2\,JL22)\,B1yo+\frac{1}{2}(Rs\sqrt{3}\,JL32-2\,JL12)\,A1xo\Bigg)\Big/(Lbc^2\,Ro)+Mbc\Bigg($$

$$\frac{1}{8}(-Rs\,JL32+2\,JL22)\,A1yo+\frac{1}{8}(Rs\sqrt{3}\,JL32-2\,JL12)\,B1xo+\frac{1}{8}(Rs\,JL32-2\,JL22)\,B1yo$$

$$+\frac{1}{8}(2\,JL12-Rs\sqrt{3}\,JL32)\,A1xo\Bigg)/\,Ro\Bigg)\sin\left(\frac{L1}{Ro}\right)+Me\,(JL11\,JL12+JL21\,JL22)+Ie\,JL31\,JL32$$

$$+Ibc\Bigg(\frac{JL21\,JL22+JL21\,Rs\,JL32+Rs^2\,JL31\,JL32+JL22\,Rs\,JL31+JL11\,JL12}{Lbc^2}+\Bigg($$

$$-\frac{1}{2}JL11\,Rs\sqrt{3}\,JL32-\frac{1}{2}JL12\,Rs\sqrt{3}\,JL31+JL21\,JL22+JL11\,JL12-\frac{1}{2}JL22\,Rs\,JL31$$

$$-\frac{1}{2}JL21\,Rs\,JL32+Rs^2\,JL31\,JL32\Bigg)\Big/Lbc^2+\frac{1}{2}(JL11\,Rs\sqrt{3}\,JL32+JL12\,Rs\sqrt{3}\,JL31$$

$$+2\,JL21\,JL22-JL21\,Rs\,JL32+2\,JL11\,JL12+2\,Rs^2\,JL31\,JL32-JL22\,Rs\,JL31)\Big/Lbc^2\Bigg)$$

$$+Mbc\left(\frac{3}{4}JL11\,JL12+\frac{3}{4}JL21\,JL22+\frac{3}{4}Rs^2\,JL31\,JL32\right)$$

$$K\_13:=\Bigg(Ibc\Bigg(\frac{1}{2}(-Rs\sqrt{3}\,JL31-2\,JL11)\,B3yo+\frac{1}{2}(Rs\,JL31-2\,JL21)\,A3xo$$

$$+\frac{1}{2}(Rs\sqrt{3}\,JL31+2\,JL11)\,A3yo+\frac{1}{2}(2\,JL21-Rs\,JL31)\,B3xo\Bigg)\Big/(Lbc^2\,Ro)+Mbc\Bigg($$

$$\frac{1}{8}(Rs\sqrt{3}\,JL31+2\,JL11)\,B3yo+\frac{1}{8}(2\,JL21-Rs\,JL31)\,A3xo+\frac{1}{8}(-Rs\sqrt{3}\,JL31-2\,JL11)\,A3yo$$

$$+\frac{1}{8}(Rs\,JL31-2\,JL21)\,B3xo\Bigg)/\,Ro\Bigg)\cos\left(\frac{L3}{Ro}\right)+\Bigg(Ibc\Bigg(\frac{1}{2}(Rs\,JL33-2\,JL23)\,A1xo$$

$$+\frac{1}{2}(-Rs\sqrt{3}\,JL33+2\,JL13)\,A1yo+\frac{1}{2}(-Rs\,JL33+2\,JL23)\,B1xo+\frac{1}{2}(-2\,JL13+Rs\sqrt{3}\,JL33)\,B1yo\Bigg)$$

$$\Big/(Lbc^2\,Ro)+Mbc\Bigg(\frac{1}{8}(-Rs\,JL33+2\,JL23)\,A1xo+\frac{1}{8}(-2\,JL13+Rs\sqrt{3}\,JL33)\,A1yo$$

$$+\frac{1}{8}(Rs\,JL33-2\,JL23)\,B1xo+\frac{1}{8}(-Rs\sqrt{3}\,JL33+2\,JL13)\,B1yo\Bigg)/\,Ro\Bigg)\cos\left(\frac{L1}{Ro}\right)+\Bigg(Ibc\Bigg($$

$$\frac{1}{2}(Rs\sqrt{3}\,JL31+2\,JL11)\,B3xo+\frac{1}{2}(2\,JL21-Rs\,JL31)\,B3yo+\frac{1}{2}(-Rs\sqrt{3}\,JL31-2\,JL11)\,A3xo$$

$$+\frac{1}{2}(Rs\,JL31-2\,JL21)\,A3yo\Bigg)\Big/(Lbc^2\,Ro)+Mbc\Bigg(\frac{1}{8}(-Rs\sqrt{3}\,JL31-2\,JL11)\,B3xo$$

$$+\frac{1}{8}(Rs\,JL31-2\,JL21)\,B3yo+\frac{1}{8}(Rs\sqrt{3}\,JL31+2\,JL11)\,A3xo+\frac{1}{8}(2\,JL21-Rs\,JL31)\,A3yo\Bigg)/\,Ro\Bigg)$$

$$\sin\left(\frac{L3}{Ro}\right)+\Bigg(Ibc\Bigg(\frac{1}{2}(Rs\,JL33-2\,JL23)\,A1yo+\frac{1}{2}(-Rs\sqrt{3}\,JL33+2\,JL13)\,B1xo$$

$$+\frac{1}{2}(-Rs\,JL33+2\,JL23)\,B1yo+\frac{1}{2}(-2\,JL13+Rs\sqrt{3}\,JL33)\,A1xo\Bigg)\Big/(Lbc^2\,Ro)+Mbc\Bigg($$

$$\frac{1}{8}(-Rs\,JL33+2\,JL23)\,A1yo+\frac{1}{8}(-2\,JL13+Rs\sqrt{3}\,JL33)\,B1xo+\frac{1}{8}(Rs\,JL33-2\,JL23)\,B1yo$$

$$+\frac{1}{8}(-Rs\sqrt{3}\,JL33+2\,JL13)\,A1xo\Bigg)/Ro\Bigg)\sin\left(\frac{L1}{Ro}\right)+Me\,(JL11\,JL13+JL21\,JL23)+Ie\,JL31\,JL33+$$

$$Ibc\Bigg(\Bigg(\frac{1}{2}JL11\,Rs\sqrt{3}\,JL33+JL21\,JL23-\frac{1}{2}JL21\,Rs\,JL33+\frac{1}{2}JL13\,Rs\sqrt{3}\,JL31+Rs^2\,JL31\,JL33$$

$$+JL11\,JL13-\frac{1}{2}JL23\,Rs\,JL31\Bigg)\Big/Lbc^2+\Bigg(-\frac{1}{2}JL11\,Rs\sqrt{3}\,JL33-\frac{1}{2}JL13\,Rs\sqrt{3}\,JL31+JL21\,JL23$$

$$-\frac{1}{2}JL21\,Rs\,JL33+JL11\,JL13+Rs^2\,JL31\,JL33-\frac{1}{2}JL23\,Rs\,JL31\Bigg)\Big/Lbc^2$$

$$+\frac{JL21\,JL23+JL21\,Rs\,JL33+JL11\,JL13+JL23\,Rs\,JL31+Rs^2\,JL31\,JL33}{Lbc^2}\Bigg)$$

$$+Mbc\left(\frac{3}{4}JL21\,JL23+\frac{3}{4}Rs^2\,JL31\,JL33+\frac{3}{4}JL11\,JL13\right)$$

>

$$K\_21:=\Bigg($$

$$\frac{Ibc\left(\frac{1}{2}(-2\,JL21-2\,Rs\,JL31)\,A2xo+JL11\,A2yo+\frac{1}{2}(2\,Rs\,JL31+2\,JL21)\,B2xo-JL11\,B2yo\right)}{Lbc^2\,Ro}+$$

$$Mbc\left(\frac{1}{8}(2\,Rs\,JL31+2\,JL21)\,A2xo-\frac{1}{4}JL11\,A2yo+\frac{1}{8}(-2\,JL21-2\,Rs\,JL31)\,B2xo+\frac{1}{4}JL11\,B2yo\right)$$

$$/Ro\Bigg)\cos\left(\frac{L2}{Ro}\right)+\Bigg(Ibc\Bigg(\frac{1}{2}(Rs\,JL32-2\,JL22)\,A1xo+\frac{1}{2}(2\,JL12-Rs\sqrt{3}\,JL32)\,A1yo$$

$$+\frac{1}{2}(-Rs\,JL32+2\,JL22)\,B1xo+\frac{1}{2}(Rs\sqrt{3}\,JL32-2\,JL12)\,B1yo\Bigg)\Big/(Lbc^2\,Ro)+Mbc\Bigg($$

$$\frac{1}{8}(-Rs\,JL32+2\,JL22)\,A1xo+\frac{1}{8}(Rs\sqrt{3}\,JL32-2\,JL12)\,A1yo+\frac{1}{8}(Rs\,JL32-2\,JL22)\,B1xo$$

$$+\frac{1}{8}(2\,JL12-Rs\sqrt{3}\,JL32)\,B1yo\Bigg)/Ro\Bigg)\cos\left(\frac{L1}{Ro}\right)+\Bigg($$

$$\frac{Ibc\left(\frac{1}{2}(-2\,JL21-2\,Rs\,JL31)\,A2yo+JL11\,B2xo+\frac{1}{2}(2\,Rs\,JL31+2\,JL21)\,B2yo-JL11\,A2xo\right)}{Lbc^2\,Ro}+$$

$$Mbc\left(\frac{1}{8}(2\,Rs\,JL31+2\,JL21)\,A2yo-\frac{1}{4}JL11\,B2xo+\frac{1}{8}(-2\,JL21-2\,Rs\,JL31)\,B2yo+\frac{1}{4}JL11\,A2xo\right)$$

$$/Ro\Bigg)\sin\left(\frac{L2}{Ro}\right)+\Bigg(Ibc\Bigg(\frac{1}{2}(Rs\,JL32-2\,JL22)\,A1yo+\frac{1}{2}(2\,JL12-Rs\sqrt{3}\,JL32)\,B1xo$$

$$+\frac{1}{2}(-Rs\,JL32+2\,JL22)\,B1yo+\frac{1}{2}(Rs\sqrt{3}\,JL32-2\,JL12)\,A1xo\Bigg)\Big/(Lbc^2\,Ro)+Mbc\Bigg($$

$$\frac{1}{8}(-Rs\,JL32+2\,JL22)\,A1yo+\frac{1}{8}(Rs\sqrt{3}\,JL32-2\,JL12)\,B1xo+\frac{1}{8}(Rs\,JL32-2\,JL22)\,B1yo$$

$$+\frac{1}{8}(2\,JL12-Rs\sqrt{3}\,JL32)\,A1xo\Bigg)/Ro\Bigg)\sin\left(\frac{L1}{Ro}\right)+Me\,(JL11\,JL12+JL21\,JL22)+Ie\,JL31\,JL32$$

$$+Ibc\left(\frac{JL21\,JL22+JL21\,Rs\,JL32+Rs^2\,JL31\,JL32+JL22\,Rs\,JL31+JL11\,JL12}{Lbc^2}+\Bigg(\right.$$

$$-\frac{1}{2}JL11\,Rs\sqrt{3}\,JL32-\frac{1}{2}JL12\,Rs\sqrt{3}\,JL31+JL21\,JL22+JL11\,JL12-\frac{1}{2}JL22\,Rs\,JL31$$

$$-\frac{1}{2}JL21\,Rs\,JL32+Rs^2\,JL31\,JL32\Bigg)\Big/Lbc^2+\frac{1}{2}(JL11\,Rs\sqrt{3}\,JL32+JL12\,Rs\sqrt{3}\,JL31$$

$$\left.+2\,JL21\,JL22-JL21\,Rs\,JL32+2\,JL11\,JL12+2\,Rs^2\,JL31\,JL32-JL22\,Rs\,JL31)\Big/Lbc^2\right)$$

$$+Mbc\left(\frac{3}{4}JL11\,JL12+\frac{3}{4}JL21\,JL22+\frac{3}{4}Rs^2\,JL31\,JL32\right)$$

$$K\_22:=\Bigg($$

$$\frac{Ibc\,(2\,JL12\,A2yo+(-2\,Rs\,JL32-2\,JL22)\,A2xo-2\,JL12\,B2yo+(2\,JL22+2\,Rs\,JL32)\,B2xo)}{Lbc^2\,Ro}+$$

$$Mbc$$

$$\left(-\frac{1}{2}JL12\,A2yo+\frac{1}{4}(2\,JL22+2\,Rs\,JL32)\,A2xo+\frac{1}{2}JL12\,B2yo+\frac{1}{4}(-2\,Rs\,JL32-2\,JL22)\,B2xo\right)/$$

$$Ro\Bigg)\cos\left(\frac{L2}{Ro}\right)+\Bigg($$

$$\frac{Ibc\,(-2\,JL12\,A2xo+(2\,JL22+2\,Rs\,JL32)\,B2yo+2\,JL12\,B2xo+(-2\,Rs\,JL32-2\,JL22)\,A2yo)}{Lbc^2\,Ro}+$$

$$Mbc\left(\frac{1}{2}JL12\,A2xo+\frac{1}{4}(-2\,Rs\,JL32-2\,JL22)\,B2yo-\frac{1}{2}JL12\,B2xo+\frac{1}{4}(2\,JL22+2\,Rs\,JL32)\,A2yo\right)$$

$$/Ro\Bigg)\sin\left(\frac{L2}{Ro}\right)+Me\,(JL12^2+JL22^2)+Ie\,JL32^2+\frac{Iab}{Ro^2}+Ibc\Bigg($$

$$\frac{Rs^2\,JL32^2+JL22^2+JL12^2-JL22\,Rs\,JL32-JL12\,Rs\sqrt{3}\,JL32}{Lbc^2}$$

$$+\frac{Rs^2\,JL32^2+JL22^2+JL12^2-JL22\,Rs\,JL32+JL12\,Rs\sqrt{3}\,JL32}{Lbc^2}$$

$$+\frac{Rs^2\,JL32^2+JL22^2+2\,JL22\,Rs\,JL32+JL12^2}{Lbc^2}$$

$$+\frac{A2xo^2-2\,B2xo\,A2xo+B2yo^2+B2xo^2+A2yo^2-2\,B2yo\,A2yo}{Lbc^2\,Ro^2}\Bigg)+Mbc\Bigg(\frac{3}{4}JL12^2+\frac{3}{4}Rs^2\,JL32^2$$

$$+\frac{3}{4}JL22^2+\frac{\frac{1}{4}A2xo^2-\frac{1}{2}B2xo\,A2xo+\frac{1}{4}B2yo^2+\frac{1}{4}B2xo^2+\frac{1}{4}A2yo^2-\frac{1}{2}B2yo\,A2yo}{Ro^2}\Bigg)$$

$$K\_23 := \Bigg($$

$$\frac{Ibc \left(\frac{1}{2} (-2\, JL23 - 2\, Rs\, JL33)\, A2xo + JL13\, A2yo + \frac{1}{2} (2\, JL23 + 2\, Rs\, JL33)\, B2xo - JL13\, B2yo \right)}{Lbc^2\, Ro}$$

$$+ \frac{Mbc \left(\frac{1}{8} (2\, JL23 + 2\, Rs\, JL33)\, A2xo - \frac{1}{4} JL13\, A2yo + \frac{1}{8} (-2\, JL23 - 2\, Rs\, JL33)\, B2xo + \frac{1}{4} JL13\, B2yo \right)}{Ro}$$

$$\Bigg) \cos\left(\frac{L2}{Ro} \right) + \Bigg(Ibc \Big(\frac{1}{2} (-2\, JL12 - Rs \sqrt{3}\, JL32)\, B3yo + \frac{1}{2} (Rs\, JL32 - 2\, JL22)\, A3xo$$

$$+ \frac{1}{2} (Rs \sqrt{3}\, JL32 + 2\, JL12)\, A3yo + \frac{1}{2} (-Rs\, JL32 + 2\, JL22)\, B3xo \Big) \Big/ (Lbc^2\, Ro) + Mbc \Big($$

$$- \frac{1}{8} (-2\, JL12 - Rs \sqrt{3}\, JL32)\, B3yo - \frac{1}{8} (Rs\, JL32 - 2\, JL22)\, A3xo - \frac{1}{8} (Rs \sqrt{3}\, JL32 + 2\, JL12)\, A3yo$$

$$- \frac{1}{8} (-Rs\, JL32 + 2\, JL22)\, B3xo \Big) / Ro \Bigg) \cos\left(\frac{L3}{Ro} \right) + \Bigg(Ibc \Big(\frac{1}{2} (Rs \sqrt{3}\, JL32 + 2\, JL12)\, B3xo$$

$$+ \frac{1}{2} (-Rs\, JL32 + 2\, JL22)\, B3yo + \frac{1}{2} (-2\, JL12 - Rs \sqrt{3}\, JL32)\, A3xo + \frac{1}{2} (Rs\, JL32 - 2\, JL22)\, A3yo \Big) \Big/ ($$

$$Lbc^2\, Ro) + Mbc \Big(- \frac{1}{8} (Rs \sqrt{3}\, JL32 + 2\, JL12)\, B3xo - \frac{1}{8} (-Rs\, JL32 + 2\, JL22)\, B3yo$$

$$- \frac{1}{8} (-2\, JL12 - Rs \sqrt{3}\, JL32)\, A3xo - \frac{1}{8} (Rs\, JL32 - 2\, JL22)\, A3yo \Big) / Ro \Bigg) \sin\left(\frac{L3}{Ro} \right) + \Bigg($$

$$\frac{Ibc \left(\frac{1}{2} (-2\, JL23 - 2\, Rs\, JL33)\, A2yo + JL13\, B2xo + \frac{1}{2} (2\, JL23 + 2\, Rs\, JL33)\, B2yo - JL13\, A2xo \right)}{Lbc^2\, Ro}$$

$$+ \frac{Mbc \left(\frac{1}{8} (2\, JL23 + 2\, Rs\, JL33)\, A2yo - \frac{1}{4} JL13\, B2xo + \frac{1}{8} (-2\, JL23 - 2\, Rs\, JL33)\, B2yo + \frac{1}{4} JL13\, A2xo \right)}{Ro}$$

$$\Bigg) \sin\left(\frac{L2}{Ro} \right) + Me\, (JL12\, JL13 + JL22\, JL23) + Ie\, JL32\, JL33 + Ibc \Bigg(\frac{1}{2} (2\, JL12\, JL13 + 2\, JL22\, JL23$$

$$- JL22\, Rs\, JL33 - JL23\, Rs\, JL32 + 2\, Rs^2\, JL32\, JL33 - JL12\, Rs \sqrt{3}\, JL33 - JL13\, Rs \sqrt{3}\, JL32) \Big/ Lbc^2$$

$$+ \Big(JL12\, JL13 + JL22\, JL23 - \frac{1}{2} JL22\, Rs\, JL33 - \frac{1}{2} JL23\, Rs\, JL32 + Rs^2\, JL32\, JL33 + \frac{1}{2} JL12\, Rs \sqrt{3}\, JL33$$

$$+ \frac{1}{2} JL13\, Rs \sqrt{3}\, JL32 \Big) \Big/ Lbc^2$$

$$+ \frac{JL12\, JL13 + JL23\, Rs\, JL32 + Rs^2\, JL32\, JL33 + JL22\, Rs\, JL33 + JL22\, JL23}{Lbc^2} \Bigg)$$

$$+ Mbc \left(\frac{3}{4} JL12\, JL13 + \frac{3}{4} JL22\, JL23 + \frac{3}{4} Rs^2\, JL32\, JL33 \right)$$

$$K\_31 := \Bigg(Ibc \Big(\frac{1}{2} (-Rs \sqrt{3}\, JL31 - 2\, JL11)\, B3yo + \frac{1}{2} (Rs\, JL31 - 2\, JL21)\, A3xo$$

$$+ \frac{1}{2} (Rs \sqrt{3}\, JL31 + 2\, JL11)\, A3yo + \frac{1}{2} (2\, JL21 - Rs\, JL31)\, B3xo \Big) \Big/ (Lbc^2\, Ro) + Mbc \Big($$

$$\frac{1}{8}(Rs\sqrt{3}\ JL31+2\ JL11)\ B3yo+\frac{1}{8}(2\ JL21-Rs\ JL31)\ A3xo+\frac{1}{8}(-Rs\sqrt{3}\ JL31-2\ JL11)\ A3yo$$
$$+\frac{1}{8}(Rs\ JL31-2\ JL21)\ B3xo\Bigg)\Bigg/ Ro\Bigg)\cos\left(\frac{L3}{Ro}\right)+\Bigg(Ibc\left(\frac{1}{2}(Rs\ JL33-2\ JL23)\ A1xo\right.$$
$$+\frac{1}{2}(-Rs\sqrt{3}\ JL33+2\ JL13)\ A1yo+\frac{1}{2}(-Rs\ JL33+2\ JL23)\ B1xo$$
$$\left.+\frac{1}{2}(-2\ JL13+Rs\sqrt{3}\ JL33)\ B1yo\right)\Big/ (Lbc^2\ Ro)+Mbc\left(\frac{1}{8}(-Rs\ JL33+2\ JL23)\ A1xo\right.$$
$$+\frac{1}{8}(-2\ JL13+Rs\sqrt{3}\ JL33)\ A1yo+\frac{1}{8}(Rs\ JL33-2\ JL23)\ B1xo$$
$$\left.+\frac{1}{8}(-Rs\sqrt{3}\ JL33+2\ JL13)\ B1yo\right)\Big/ Ro\Bigg)\cos\left(\frac{L1}{Ro}\right)+\Bigg(Ibc\left(\frac{1}{2}(Rs\sqrt{3}\ JL31+2\ JL11)\ B3xo\right.$$
$$\left.+\frac{1}{2}(2\ JL21-Rs\ JL31)\ B3yo+\frac{1}{2}(-Rs\sqrt{3}\ JL31-2\ JL11)\ A3xo+\frac{1}{2}(Rs\ JL31-2\ JL21)\ A3yo\right)\Big/$$
$$(Lbc^2\ Ro)+Mbc\left(\frac{1}{8}(-Rs\sqrt{3}\ JL31-2\ JL11)\ B3xo+\frac{1}{8}(Rs\ JL31-2\ JL21)\ B3yo\right.$$
$$\left.+\frac{1}{8}(Rs\sqrt{3}\ JL31+2\ JL11)\ A3xo+\frac{1}{8}(2\ JL21-Rs\ JL31)\ A3yo\right)\Big/ Ro\Bigg)\sin\left(\frac{L3}{Ro}\right)+\Bigg(Ibc\Bigg($$
$$\frac{1}{2}(Rs\ JL33-2\ JL23)\ A1yo+\frac{1}{2}(-Rs\sqrt{3}\ JL33+2\ JL13)\ B1xo+\frac{1}{2}(-Rs\ JL33+2\ JL23)\ B1yo$$
$$+\frac{1}{2}(-2\ JL13+Rs\sqrt{3}\ JL33)\ A1xo\Bigg)\Big/ (Lbc^2\ Ro)+Mbc\left(\frac{1}{8}(-Rs\ JL33+2\ JL23)\ A1yo\right.$$
$$+\frac{1}{8}(-2\ JL13+Rs\sqrt{3}\ JL33)\ B1xo+\frac{1}{8}(Rs\ JL33-2\ JL23)\ B1yo$$
$$\left.+\frac{1}{8}(-Rs\sqrt{3}\ JL33+2\ JL13)\ A1xo\right)\Big/ Ro\Bigg)\sin\left(\frac{L1}{Ro}\right)+Me\ (JL11\ JL13+JL21\ JL23)+Ie\ JL31\ JL33$$
$$+Ibc\Bigg(\Bigg(\frac{1}{2}JL11\ Rs\sqrt{3}\ JL33+JL21\ JL23-\frac{1}{2}JL21\ Rs\ JL33+\frac{1}{2}JL13\ Rs\sqrt{3}\ JL31+Rs^2\ JL31\ JL33$$
$$+JL11\ JL13-\frac{1}{2}JL23\ Rs\ JL31\Bigg)\Big/ Lbc^2+\Bigg(-\frac{1}{2}JL11\ Rs\sqrt{3}\ JL33-\frac{1}{2}JL13\ Rs\sqrt{3}\ JL31$$
$$+JL21\ JL23-\frac{1}{2}JL21\ Rs\ JL33+JL11\ JL13+Rs^2\ JL31\ JL33-\frac{1}{2}JL23\ Rs\ JL31\Bigg)\Big/ Lbc^2$$
$$+\frac{JL21\ JL23+JL21\ Rs\ JL33+JL11\ JL13+JL23\ Rs\ JL31+Rs^2\ JL31\ JL33}{Lbc^2}\Bigg)$$
$$+Mbc\left(\frac{3}{4}JL21\ JL23+\frac{3}{4}Rs^2\ JL31\ JL33+\frac{3}{4}JL11\ JL13\right)$$

$$K\_32:=\Bigg($$
$$\frac{Ibc\left(\frac{1}{2}(-2\ JL23-2\ Rs\ JL33)\ A2xo+JL13\ A2yo+\frac{1}{2}(2\ JL23+2\ Rs\ JL33)\ B2xo-JL13\ B2yo\right)}{Lbc^2\ Ro}+$$
$$Mbc\left(\frac{1}{8}(2\ JL23+2\ Rs\ JL33)\ A2xo-\frac{1}{4}JL13\ A2yo+\frac{1}{8}(-2\ JL23-2\ Rs\ JL33)\ B2xo+\frac{1}{4}JL13\ B2yo\right)$$

$$\Big/ Ro \Bigg) \cos\left(\frac{L2}{Ro}\right) + \Bigg(Ibc \left(\frac{1}{2} (-2\, JL12 - Rs \sqrt{3}\, JL32)\, B3yo + \frac{1}{2} (Rs\, JL32 - 2\, JL22)\, A3xo \right.$$

$$\left. + \frac{1}{2} (Rs \sqrt{3}\, JL32 + 2\, JL12)\, A3yo + \frac{1}{2} (-Rs\, JL32 + 2\, JL22)\, B3xo \right) \Big/ (Lbc^2\, Ro) + Mbc \Bigg($$

$$- \frac{1}{8} (-2\, JL12 - Rs \sqrt{3}\, JL32)\, B3yo - \frac{1}{8} (Rs\, JL32 - 2\, JL22)\, A3xo - \frac{1}{8} (Rs \sqrt{3}\, JL32 + 2\, JL12)\, A3yo$$

$$- \frac{1}{8} (-Rs\, JL32 + 2\, JL22)\, B3xo \Bigg) \Big/ Ro \Bigg) \cos\left(\frac{L3}{Ro}\right) + \Bigg(Ibc \left(\frac{1}{2} (Rs \sqrt{3}\, JL32 + 2\, JL12)\, B3xo \right.$$

$$\left. + \frac{1}{2} (-Rs\, JL32 + 2\, JL22)\, B3yo + \frac{1}{2} (-2\, JL12 - Rs \sqrt{3}\, JL32)\, A3xo + \frac{1}{2} (Rs\, JL32 - 2\, JL22)\, A3yo \right)$$

$$\Big/ (Lbc^2\, Ro) + Mbc \Bigg(- \frac{1}{8} (Rs \sqrt{3}\, JL32 + 2\, JL12)\, B3xo - \frac{1}{8} (-Rs\, JL32 + 2\, JL22)\, B3yo$$

$$- \frac{1}{8} (-2\, JL12 - Rs \sqrt{3}\, JL32)\, A3xo - \frac{1}{8} (Rs\, JL32 - 2\, JL22)\, A3yo \Bigg) \Big/ Ro \Bigg) \sin\left(\frac{L3}{Ro}\right) + \Bigg($$

$$\frac{Ibc \left(\frac{1}{2} (-2\, JL23 - 2\, Rs\, JL33)\, A2yo + JL13\, B2xo + \frac{1}{2} (2\, JL23 + 2\, Rs\, JL33)\, B2yo - JL13\, A2xo \right)}{Lbc^2\, Ro} +$$

$$Mbc \left(\frac{1}{8} (2\, JL23 + 2\, Rs\, JL33)\, A2yo - \frac{1}{4} JL13\, B2xo + \frac{1}{8} (-2\, JL23 - 2\, Rs\, JL33)\, B2yo + \frac{1}{4} JL13\, A2xo \right)$$

$$\Big/ Ro \Bigg) \sin\left(\frac{L2}{Ro}\right) + Me\, (JL12\, JL13 + JL22\, JL23) + Ie\, JL32\, JL33 + Ibc \Bigg(\frac{1}{2} (2\, JL12\, JL13$$

$$+ 2\, JL22\, JL23 - JL22\, Rs\, JL33 - JL23\, Rs\, JL32 + 2\, Rs^2\, JL32\, JL33 - JL12\, Rs \sqrt{3}\, JL33$$

$$- JL13\, Rs \sqrt{3}\, JL32) \Big/ Lbc^2 + \Bigg(JL12\, JL13 + JL22\, JL23 - \frac{1}{2} JL22\, Rs\, JL33 - \frac{1}{2} JL23\, Rs\, JL32$$

$$+ Rs^2\, JL32\, JL33 + \frac{1}{2} JL12\, Rs \sqrt{3}\, JL33 + \frac{1}{2} JL13\, Rs \sqrt{3}\, JL32 \Bigg) \Big/ Lbc^2$$

$$+ \frac{JL12\, JL13 + JL23\, Rs\, JL32 + Rs^2\, JL32\, JL33 + JL22\, Rs\, JL33 + JL22\, JL23}{Lbc^2} \Bigg)$$

$$+ Mbc \left(\frac{3}{4} JL12\, JL13 + \frac{3}{4} JL22\, JL23 + \frac{3}{4} Rs^2\, JL32\, JL33 \right)$$

$$K\_33 := \Bigg(Ibc\, ((-Rs\, JL33 + 2\, JL23)\, B3xo + (2\, JL13 + Rs \sqrt{3}\, JL33)\, A3yo + (Rs\, JL33 - 2\, JL23)\, A3xo$$

$$+ (-Rs \sqrt{3}\, JL33 - 2\, JL13)\, B3yo) \Big/ (Lbc^2\, Ro) + \frac{1}{4} Mbc\, (-A3xo\, Rs\, Ro\, JL33 - 2\, B3xo\, JL23\, Ro$$

$$- 2\, A3yo\, JL13\, Ro + 2\, A3xo\, JL23\, Ro + B3xo\, Rs\, Ro\, JL33 - A3yo\, Rs\, Ro\, JL33 \sqrt{3}$$

$$+ B3yo\, Rs\, Ro\, JL33 \sqrt{3} + 2\, B3yo\, JL13\, Ro) \Big/ Ro^2 \Bigg) \cos\left(\frac{L3}{Ro}\right) + \Bigg(Ibc\, ((-Rs\, JL33 + 2\, JL23)\, B3yo$$

$$+ (2\, JL13 + Rs \sqrt{3}\, JL33)\, B3xo + (Rs\, JL33 - 2\, JL23)\, A3yo + (-Rs \sqrt{3}\, JL33 - 2\, JL13)\, A3xo) \Big/ ($$

$$Lbc^2\, Ro) + \frac{1}{4} Mbc\, (-B3xo\, Rs\, Ro\, JL33 \sqrt{3} + B3yo\, Rs\, Ro\, JL33 - 2\, B3yo\, JL23\, Ro - 2\, B3xo\, JL13\, Ro$$

$$+ 2\, A3yo\, JL23\, Ro + 2\, A3xo\, JL13\, Ro + A3xo\, Rs\, Ro\, JL33 \sqrt{3} - A3yo\, Rs\, Ro\, JL33) \Big/ Ro^2 \Bigg) \sin\left(\frac{L3}{Ro}\right)$$

$$
\begin{aligned}
&+ Me\,(JL13^2 + JL23^2) + Ie\,JL33^2 + \frac{Iab}{Ro^2} + Ibc\Bigg(\\
&\frac{Rs^2\,JL33^2 + JL23^2 + JL13^2 - JL23\,Rs\,JL33 - JL13\,Rs\sqrt{3}\,JL33}{Lbc^2} \\
&+ \frac{Rs^2\,JL33^2 + JL23^2 + JL13^2 + 2\,JL23\,Rs\,JL33}{Lbc^2} \\
&+ \frac{JL23^2 - JL23\,Rs\,JL33 + JL13\,Rs\sqrt{3}\,JL33 + JL13^2 + Rs^2\,JL33^2}{Lbc^2} \\
&+ \frac{B3xo^2 - 2\,B3xo\,A3xo + A3yo^2 + A3xo^2 + B3yo^2 - 2\,B3yo\,A3yo}{Lbc^2\,Ro^2}\Bigg) + Mbc\Bigg(\frac{1}{4}JL23\,Rs\,JL33 \\
&+ \frac{1}{2}Rs^2\,JL33^2 + \frac{1}{2}JL13^2 + \frac{1}{2}JL23^2 - \frac{1}{4}JL13\,Rs\sqrt{3}\,JL33 + \frac{1}{4}(B3yo^2 + B3xo^2 + A3yo^2 + A3xo^2 \\
&- 2\,B3xo\,A3xo - JL23\,Ro^2\,Rs\,JL33 - 2\,B3yo\,A3yo + JL23^2\,Ro^2 + Rs^2\,Ro^2\,JL33^2 + JL13^2\,Ro^2 \\
&+ JL13\,Ro^2\,Rs\,JL33\sqrt{3}\,) \Big/ Ro^2\Bigg)
\end{aligned}
$$

$$
\begin{aligned}
C\_11 :={}& \Bigg(\Bigg(\frac{1}{2} Ibc\,((-2\,JL11 + Rs\sqrt{3}\,JL31)\,A1xo + (2\,JL21 - Rs\,JL31)\,B1yo \\
&+ (-Rs\sqrt{3}\,JL31 + 2\,JL11)\,B1xo + (Rs\,JL31 - 2\,JL21)\,A1yo) \Big/ (Lbc^2\,Ro^2) + \frac{1}{2} Mbc\Bigg(\\
&\frac{1}{4}(-Rs\sqrt{3}\,JL31 + 2\,JL11)\,A1xo + \frac{1}{4}(Rs\,JL31 - 2\,JL21)\,B1yo + \frac{1}{4}(-2\,JL11 + Rs\sqrt{3}\,JL31)\,B1xo \\
&+ \frac{1}{4}(2\,JL21 - Rs\,JL31)\,A1yo\Bigg) \Big/ Ro^2\Bigg) L1dot + \Bigg(-\frac{1}{2} Ibc\Bigg(\frac{1}{2}(Rs\,JL32 - 2\,JL22)\,A1yo \\
&+ \frac{1}{2}(2\,JL12 - Rs\sqrt{3}\,JL32)\,B1xo + \frac{1}{2}(-Rs\,JL32 + 2\,JL22)\,B1yo + \frac{1}{2}(Rs\sqrt{3}\,JL32 - 2\,JL12)\,A1xo\Bigg) \\
&\Big/ (Lbc^2\,Ro^2) - \frac{1}{2} Mbc\Bigg(\frac{1}{8}(-Rs\,JL32 + 2\,JL22)\,A1yo + \frac{1}{8}(Rs\sqrt{3}\,JL32 - 2\,JL12)\,B1xo \\
&+ \frac{1}{8}(Rs\,JL32 - 2\,JL22)\,B1yo + \frac{1}{8}(2\,JL12 - Rs\sqrt{3}\,JL32)\,A1xo\Bigg) \Big/ Ro^2\Bigg) L2dot + \Bigg(-\frac{1}{2} Ibc\Bigg(\\
&\frac{1}{2}(Rs\,JL33 - 2\,JL23)\,A1yo + \frac{1}{2}(-Rs\sqrt{3}\,JL33 + 2\,JL13)\,B1xo + \frac{1}{2}(-Rs\,JL33 + 2\,JL23)\,B1yo \\
&+ \frac{1}{2}(-2\,JL13 + Rs\sqrt{3}\,JL33)\,A1xo\Bigg) \Big/ (Lbc^2\,Ro^2) - \frac{1}{2} Mbc\Bigg(\frac{1}{8}(-Rs\,JL33 + 2\,JL23)\,A1yo \\
&+ \frac{1}{8}(-2\,JL13 + Rs\sqrt{3}\,JL33)\,B1xo + \frac{1}{8}(Rs\,JL33 - 2\,JL23)\,B1yo \\
&+ \frac{1}{8}(-Rs\sqrt{3}\,JL33 + 2\,JL13)\,A1xo\Bigg) \Big/ Ro^2\Bigg) L3dot\Bigg)\cos\left(\frac{L1}{Ro}\right) + \Bigg(\Bigg(-\frac{1}{2} Ibc\,(\\
&(-Rs\sqrt{3}\,JL31 + 2\,JL11)\,A1yo + (Rs\,JL31 - 2\,JL21)\,A1xo + (-2\,JL11 + Rs\sqrt{3}\,JL31)\,B1yo \\
&+ (2\,JL21 - Rs\,JL31)\,B1xo) \Big/ (Lbc^2\,Ro^2) - \frac{1}{2} Mbc\Bigg(\frac{1}{4}(-2\,JL11 + Rs\sqrt{3}\,JL31)\,A1yo \\
&+ \frac{1}{4}(2\,JL21 - Rs\,JL31)\,A1xo + \frac{1}{4}(-Rs\sqrt{3}\,JL31 + 2\,JL11)\,B1yo + \frac{1}{4}(Rs\,JL31 - 2\,JL21)\,B1xo\Bigg) \Big/ \\
&Ro^2\Bigg) L1dot + \Bigg(\frac{1}{2} Ibc\Bigg(\frac{1}{2}(Rs\,JL32 - 2\,JL22)\,A1xo + \frac{1}{2}(2\,JL12 - Rs\sqrt{3}\,JL32)\,A1yo \\
&+ \frac{1}{2}(-Rs\,JL32 + 2\,JL22)\,B1xo + \frac{1}{2}(Rs\sqrt{3}\,JL32 - 2\,JL12)\,B1yo\Bigg) \Big/ (Lbc^2\,Ro^2) + \frac{1}{2} Mbc\Bigg(\\
&\frac{1}{8}(-Rs\,JL32 + 2\,JL22)\,A1xo + \frac{1}{8}(Rs\sqrt{3}\,JL32 - 2\,JL12)\,A1yo + \frac{1}{8}(Rs\,JL32 - 2\,JL22)\,B1xo \\
&+ \frac{1}{8}(2\,JL12 - Rs\sqrt{3}\,JL32)\,B1yo\Bigg) \Big/ Ro^2\Bigg) L2dot + \Bigg(\frac{1}{2} Ibc\Bigg(\frac{1}{2}(Rs\,JL33 - 2\,JL23)\,A1xo \\
&+ \frac{1}{2}(-Rs\sqrt{3}\,JL33 + 2\,JL13)\,A1yo + \frac{1}{2}(-Rs\,JL33 + 2\,JL23)\,B1xo \\
&+ \frac{1}{2}(-2\,JL13 + Rs\sqrt{3}\,JL33)\,B1yo\Bigg) \Big/ (Lbc^2\,Ro^2) + \frac{1}{2} Mbc\Bigg(\frac{1}{8}(-Rs\,JL33 + 2\,JL23)\,A1xo \\
&+ \frac{1}{8}(-2\,JL13 + Rs\sqrt{3}\,JL33)\,A1yo + \frac{1}{8}(Rs\,JL33 - 2\,JL23)\,B1xo \\
&+ \frac{1}{8}(-Rs\sqrt{3}\,JL33 + 2\,JL13)\,B1yo\Bigg) \Big/ Ro^2\Bigg) L3dot\Bigg)\sin\left(\frac{L1}{Ro}\right)
\end{aligned}
$$

$$
\begin{aligned}
C\_12 := {} & L2dot\Bigg(\frac{Ibc\left(\frac{1}{2}(-2\,JL21 - 2\,Rs\,JL31)\,A2yo + JL11\,B2xo + \frac{1}{2}(2\,Rs\,JL31 + 2\,JL21)\,B2yo - JL11\,A2xo\right)}{Lbc^2\,Ro^2} + \\
& Mbc\left(\frac{1}{8}(2\,Rs\,JL31 + 2\,JL21)\,A2yo - \frac{1}{4}JL11\,B2xo + \frac{1}{8}(-2\,JL21 - 2\,Rs\,JL31)\,B2yo + \frac{1}{4}JL11\,A2xo\right) \\
& \Big/ Ro^2 \Bigg)\cos\left(\frac{L2}{Ro}\right) + \Bigg(\frac{1}{2}Ibc\left(\frac{1}{2}(Rs\,JL32 - 2\,JL22)\,A1yo + \frac{1}{2}(2\,JL12 - Rs\sqrt{3}\,JL32)\,B1xo\right. \\
& \left. + \frac{1}{2}(-Rs\,JL32 + 2\,JL22)\,B1yo + \frac{1}{2}(Rs\sqrt{3}\,JL32 - 2\,JL12)\,A1xo\right) \Big/ (Lbc^2\,Ro^2) + \frac{1}{2}Mbc\Bigg(\\
& \frac{1}{8}(-Rs\,JL32 + 2\,JL22)\,A1yo + \frac{1}{8}(Rs\sqrt{3}\,JL32 - 2\,JL12)\,B1xo + \frac{1}{8}(Rs\,JL32 - 2\,JL22)\,B1yo \\
& + \frac{1}{8}(2\,JL12 - Rs\sqrt{3}\,JL32)\,A1xo\Bigg) \Big/ Ro^2\Bigg) L1dot\cos\left(\frac{L1}{Ro}\right) + L2dot\Bigg(\\
& -\frac{Ibc\left(\frac{1}{2}(-2\,JL21 - 2\,Rs\,JL31)\,A2xo + JL11\,A2yo + \frac{1}{2}(2\,Rs\,JL31 + 2\,JL21)\,B2xo - JL11\,B2yo\right)}{Lbc^2\,Ro^2} - \\
& Mbc\left(\frac{1}{8}(2\,Rs\,JL31 + 2\,JL21)\,A2xo - \frac{1}{4}JL11\,A2yo + \frac{1}{8}(-2\,JL21 - 2\,Rs\,JL31)\,B2xo + \frac{1}{4}JL11\,B2yo\right) \\
& \Big/ Ro^2 \Bigg)\sin\left(\frac{L2}{Ro}\right) + \Bigg(-\frac{1}{2}Ibc\left(\frac{1}{2}(Rs\,JL32 - 2\,JL22)\,A1xo + \frac{1}{2}(2\,JL12 - Rs\sqrt{3}\,JL32)\,A1yo\right. \\
& \left. + \frac{1}{2}(-Rs\,JL32 + 2\,JL22)\,B1xo + \frac{1}{2}(Rs\sqrt{3}\,JL32 - 2\,JL12)\,B1yo\right) \Big/ (Lbc^2\,Ro^2) - \frac{1}{2}Mbc\Bigg(\\
& \frac{1}{8}(-Rs\,JL32 + 2\,JL22)\,A1xo + \frac{1}{8}(Rs\sqrt{3}\,JL32 - 2\,JL12)\,A1yo + \frac{1}{8}(Rs\,JL32 - 2\,JL22)\,B1xo \\
& + \frac{1}{8}(2\,JL12 - Rs\sqrt{3}\,JL32)\,B1yo\Bigg) \Big/ Ro^2\Bigg) L1dot\sin\left(\frac{L1}{Ro}\right)
\end{aligned}
$$

$$
\begin{aligned}
C\_13 := {} & L3dot\Bigg(Ibc\left(\frac{1}{2}(Rs\sqrt{3}\,JL31 + 2\,JL11)\,B3xo + \frac{1}{2}(2\,JL21 - Rs\,JL31)\,B3yo\right. \\
& \left. + \frac{1}{2}(-Rs\sqrt{3}\,JL31 - 2\,JL11)\,A3xo + \frac{1}{2}(Rs\,JL31 - 2\,JL21)\,A3yo\right) \Big/ (Lbc^2\,Ro^2) + Mbc\Bigg(\\
& \frac{1}{8}(-Rs\sqrt{3}\,JL31 - 2\,JL11)\,B3xo + \frac{1}{8}(Rs\,JL31 - 2\,JL21)\,B3yo + \frac{1}{8}(Rs\sqrt{3}\,JL31 + 2\,JL11)\,A3xo \\
& + \frac{1}{8}(2\,JL21 - Rs\,JL31)\,A3yo\Bigg) \Big/ Ro^2\Bigg)\cos\left(\frac{L3}{Ro}\right) + \Bigg(\frac{1}{2}Ibc\left(\frac{1}{2}(Rs\,JL33 - 2\,JL23)\,A1yo\right. \\
& \left. + \frac{1}{2}(-Rs\sqrt{3}\,JL33 + 2\,JL13)\,B1xo + \frac{1}{2}(-Rs\,JL33 + 2\,JL23)\,B1yo + \frac{1}{2}(-2\,JL13 + Rs\sqrt{3}\,JL33)\,A1xo\right) \\
& \Big/ (Lbc^2\,Ro^2) + \frac{1}{2}Mbc\left(\frac{1}{8}(-Rs\,JL33 + 2\,JL23)\,A1yo + \frac{1}{8}(-2\,JL13 + Rs\sqrt{3}\,JL33)\,B1xo\right.
\end{aligned}
$$

$$+\frac{1}{8}(Rs\,JL33-2\,JL23)\,B1yo+\frac{1}{8}(-Rs\sqrt{3}\,JL33+2\,JL13)\,A1xo\Bigg)\Bigg/Ro^2\Bigg)L1dot\cos\left(\frac{L1}{Ro}\right)+L3dot\Bigg(-$$

$$Ibc\left(\frac{1}{2}(-Rs\sqrt{3}\,JL31-2\,JL11)\,B3yo+\frac{1}{2}(Rs\,JL31-2\,JL21)\,A3xo+\frac{1}{2}(Rs\sqrt{3}\,JL31+2\,JL11)\,A3yo\right.$$

$$\left.+\frac{1}{2}(2\,JL21-Rs\,JL31)\,B3xo\right)\Bigg/(Lbc^2\,Ro^2)-Mbc\left(\frac{1}{8}(Rs\sqrt{3}\,JL31+2\,JL11)\,B3yo\right.$$

$$\left.+\frac{1}{8}(2\,JL21-Rs\,JL31)\,A3xo+\frac{1}{8}(-Rs\sqrt{3}\,JL31-2\,JL11)\,A3yo+\frac{1}{8}(Rs\,JL31-2\,JL21)\,B3xo\right)\Bigg/$$

$$Ro^2\Bigg)\sin\left(\frac{L3}{Ro}\right)+\Bigg(-\frac{1}{2}Ibc\left(\frac{1}{2}(Rs\,JL33-2\,JL23)\,A1xo+\frac{1}{2}(-Rs\sqrt{3}\,JL33+2\,JL13)\,A1yo\right.$$

$$\left.+\frac{1}{2}(-Rs\,JL33+2\,JL23)\,B1xo+\frac{1}{2}(-2\,JL13+Rs\sqrt{3}\,JL33)\,B1yo\right)\Bigg/(Lbc^2\,Ro^2)-\frac{1}{2}Mbc\Bigg($$

$$\frac{1}{8}(-Rs\,JL33+2\,JL23)\,A1xo+\frac{1}{8}(-2\,JL13+Rs\sqrt{3}\,JL33)\,A1yo+\frac{1}{8}(Rs\,JL33-2\,JL23)\,B1xo$$

$$+\frac{1}{8}(-Rs\sqrt{3}\,JL33+2\,JL13)\,B1yo\Bigg)\Bigg/Ro^2\Bigg)L1dot\sin\left(\frac{L1}{Ro}\right)$$

$$C\_21:=\Bigg($$

$$\frac{1}{2}\frac{Ibc\left(\frac{1}{2}(-2\,JL21-2\,Rs\,JL31)\,A2yo+JL11\,B2xo+\frac{1}{2}(2\,Rs\,JL31+2\,JL21)\,B2yo-JL11\,A2xo\right)}{Lbc^2\,Ro^2}+$$

$$\frac{1}{2}$$

$$Mbc\left(\frac{1}{8}(2\,Rs\,JL31+2\,JL21)\,A2yo-\frac{1}{4}JL11\,B2xo+\frac{1}{8}(-2\,JL21-2\,Rs\,JL31)\,B2yo+\frac{1}{4}JL11\,A2xo\right)$$

$$\Bigg/Ro^2\Bigg)L2dot\cos\left(\frac{L2}{Ro}\right)+L1dot\Bigg(Ibc\left(\frac{1}{2}(Rs\,JL32-2\,JL22)\,A1yo\right.$$

$$\left.+\frac{1}{2}(2\,JL12-Rs\sqrt{3}\,JL32)\,B1xo+\frac{1}{2}(-Rs\,JL32+2\,JL22)\,B1yo+\frac{1}{2}(Rs\sqrt{3}\,JL32-2\,JL12)\,A1xo\right)$$

$$\Bigg/(Lbc^2\,Ro^2)+Mbc\left(\frac{1}{8}(-Rs\,JL32+2\,JL22)\,A1yo+\frac{1}{8}(Rs\sqrt{3}\,JL32-2\,JL12)\,B1xo\right.$$

$$\left.+\frac{1}{8}(Rs\,JL32-2\,JL22)\,B1yo+\frac{1}{8}(2\,JL12-Rs\sqrt{3}\,JL32)\,A1xo\right)\Bigg/Ro^2\Bigg)\cos\left(\frac{L1}{Ro}\right)+\Bigg($$

$$-\frac{1}{2}\frac{Ibc\left(\frac{1}{2}(-2\,JL21-2\,Rs\,JL31)\,A2xo+JL11\,A2yo+\frac{1}{2}(2\,Rs\,JL31+2\,JL21)\,B2xo-JL11\,B2yo\right)}{Lbc^2\,Ro^2}$$

$$-\frac{1}{2}$$

$$Mbc\left(\frac{1}{8}(2\,Rs\,JL31+2\,JL21)\,A2xo-\frac{1}{4}JL11\,A2yo+\frac{1}{8}(-2\,JL21-2\,Rs\,JL31)\,B2xo+\frac{1}{4}JL11\,B2yo\right)$$

$$\left. \Big/ Ro^2 \right) L2dot \sin\left(\frac{L2}{Ro}\right) + L1dot \left(- Ibc \left(\frac{1}{2} (Rs\, JL32 - 2\, JL22)\, A1xo \right.\right.$$

$$\left. + \frac{1}{2} (2\, JL12 - Rs \sqrt{3}\, JL32)\, A1yo + \frac{1}{2} (-Rs\, JL32 + 2\, JL22)\, B1xo + \frac{1}{2} (Rs \sqrt{3}\, JL32 - 2\, JL12)\, B1yo \right)$$

$$\Big/ (Lbc^2\, Ro^2) - Mbc \left(\frac{1}{8} (-Rs\, JL32 + 2\, JL22)\, A1xo + \frac{1}{8} (Rs \sqrt{3}\, JL32 - 2\, JL12)\, A1yo \right.$$

$$\left.\left. + \frac{1}{8} (Rs\, JL32 - 2\, JL22)\, B1xo + \frac{1}{8} (2\, JL12 - Rs \sqrt{3}\, JL32)\, B1yo \right) \Big/ Ro^2 \right) \sin\left(\frac{L1}{Ro}\right)$$

$$C\_22 := \left(\left(\left(\right.\right.\right.$$

$$-\frac{1}{2} \frac{Ibc \left(\frac{1}{2} (-2\, JL21 - 2\, Rs\, JL31)\, A2yo + JL11\, B2xo + \frac{1}{2} (2\, Rs\, JL31 + 2\, JL21)\, B2yo - JL11\, A2xo \right)}{Lbc^2\, Ro^2}$$

$$-\frac{1}{2}$$

$$Mbc \left(\frac{1}{8} (2\, Rs\, JL31 + 2\, JL21)\, A2yo - \frac{1}{4} JL11\, B2xo + \frac{1}{8} (-2\, JL21 - 2\, Rs\, JL31)\, B2yo + \frac{1}{4} JL11\, A2xo \right)$$

$$\left. \Big/ Ro^2 \right) L1dot + \left(\right.$$

$$\frac{1}{2} \frac{Ibc\, (-2\, JL12\, A2xo + (2\, JL22 + 2\, Rs\, JL32)\, B2yo + 2\, JL12\, B2xo + (-2\, Rs\, JL32 - 2\, JL22)\, A2yo)}{Lbc^2\, Ro^2}$$

$$+\frac{1}{2}$$

$$Mbc \left(\frac{1}{2} JL12\, A2xo + \frac{1}{4} (-2\, Rs\, JL32 - 2\, JL22)\, B2yo - \frac{1}{2} JL12\, B2xo + \frac{1}{4} (2\, JL22 + 2\, Rs\, JL32)\, A2yo \right)$$

$$\left. \Big/ Ro^2 \right) L2dot + \left(\right.$$

$$-\frac{1}{2} \frac{Ibc \left(\frac{1}{2} (-2\, JL23 - 2\, Rs\, JL33)\, A2yo + JL13\, B2xo + \frac{1}{2} (2\, JL23 + 2\, Rs\, JL33)\, B2yo - JL13\, A2xo \right)}{Lbc^2\, Ro^2}$$

$$-\frac{1}{2}$$

$$Mbc \left(\frac{1}{8} (2\, JL23 + 2\, Rs\, JL33)\, A2yo - \frac{1}{4} JL13\, B2xo + \frac{1}{8} (-2\, JL23 - 2\, Rs\, JL33)\, B2yo + \frac{1}{4} JL13\, A2xo \right)$$

$$\left.\left.\left. \Big/ Ro^2 \right) L3dot \right) \cos\left(\frac{L2}{Ro}\right) + \left(\left(\left(\right.\right.\right.$$

$$\frac{1}{2} \frac{Ibc \left(\frac{1}{2} (-2\, JL21 - 2\, Rs\, JL31)\, A2xo + JL11\, A2yo + \frac{1}{2} (2\, Rs\, JL31 + 2\, JL21)\, B2xo - JL11\, B2yo \right)}{Lbc^2\, Ro^2} +$$

$$\frac{1}{2}$$

$$Mbc\left(\frac{1}{8}(2\,Rs\,JL31+2\,JL21)\,A2xo-\frac{1}{4}JL11\,A2yo+\frac{1}{8}(-2\,JL21-2\,Rs\,JL31)\,B2xo+\frac{1}{4}JL11\,B2yo\right)$$

$$\left.\Big/\,Ro^2\right)L1dot+\Bigg($$

$$-\frac{1}{2}\frac{Ibc\,(2\,JL12\,A2yo+(-2\,Rs\,JL32-2\,JL22)\,A2xo-2\,JL12\,B2yo+(2\,JL22+2\,Rs\,JL32)\,B2xo)}{Lbc^2\,Ro^2}$$

$$-\frac{1}{2}Mbc$$

$$\left(-\frac{1}{2}JL12\,A2yo+\frac{1}{4}(2\,JL22+2\,Rs\,JL32)\,A2xo+\frac{1}{2}JL12\,B2yo+\frac{1}{4}(-2\,Rs\,JL32-2\,JL22)\,B2xo\right)$$

$$\left.\Big/\,Ro^2\right)L2dot+\Bigg($$

$$\frac{1}{2}\frac{Ibc\left(\frac{1}{2}(-2\,JL23-2\,Rs\,JL33)\,A2xo+JL13\,A2yo+\frac{1}{2}(2\,JL23+2\,Rs\,JL33)\,B2xo-JL13\,B2yo\right)}{Lbc^2\,Ro^2}+$$

$$\frac{1}{2}$$

$$Mbc\left(\frac{1}{8}(2\,JL23+2\,Rs\,JL33)\,A2xo-\frac{1}{4}JL13\,A2yo+\frac{1}{8}(-2\,JL23-2\,Rs\,JL33)\,B2xo+\frac{1}{4}JL13\,B2yo\right)$$

$$\left.\left.\Big/\,Ro^2\right)L3dot\right)\sin\left(\frac{L2}{Ro}\right)$$

$$C\_23:=\Bigg($$

$$\frac{1}{2}\frac{Ibc\left(\frac{1}{2}(-2\,JL23-2\,Rs\,JL33)\,A2yo+JL13\,B2xo+\frac{1}{2}(2\,JL23+2\,Rs\,JL33)\,B2yo-JL13\,A2xo\right)}{Lbc^2\,Ro^2}+\frac{1}{2}$$

$$\left.\frac{Mbc\left(\frac{1}{8}(2\,JL23+2\,Rs\,JL33)\,A2yo-\frac{1}{4}JL13\,B2xo+\frac{1}{8}(-2\,JL23-2\,Rs\,JL33)\,B2yo+\frac{1}{4}JL13\,A2xo\right)}{Ro^2}\right)$$

$$L2dot\cos\left(\frac{L2}{Ro}\right)+L3dot\left(Ibc\left(\frac{1}{2}(Rs\sqrt{3}\,JL32+2\,JL12)\,B3xo+\frac{1}{2}(-Rs\,JL32+2\,JL22)\,B3yo\right.\right.$$

$$\left.+\frac{1}{2}(-2\,JL12-Rs\sqrt{3}\,JL32)\,A3xo+\frac{1}{2}(Rs\,JL32-2\,JL22)\,A3yo\right)\Big/(Lbc^2\,Ro^2)+Mbc\Bigg($$

$$-\frac{1}{8}(Rs\sqrt{3}\,JL32+2\,JL12)\,B3xo-\frac{1}{8}(-Rs\,JL32+2\,JL22)\,B3yo-\frac{1}{8}(-2\,JL12-Rs\sqrt{3}\,JL32)\,A3xo$$

$$\left.\left.-\frac{1}{8}(Rs\,JL32-2\,JL22)\,A3yo\right)\Big/\,Ro^2\right)\cos\left(\frac{L3}{Ro}\right)+L3dot\left(-Ibc\left(\frac{1}{2}(-2\,JL12-Rs\sqrt{3}\,JL32)\,B3yo\right.\right.$$

$$+\frac{1}{2}(Rs\,JL32-2\,JL22)\,A3xo+\frac{1}{2}(Rs\sqrt{3}\,JL32+2\,JL12)\,A3yo+\frac{1}{2}(-Rs\,JL32+2\,JL22)\,B3xo\Bigg)\Bigg/($$

$$Lbc^2\,Ro^2)-Mbc\left(-\frac{1}{8}(-2\,JL12-Rs\sqrt{3}\,JL32)\,B3yo-\frac{1}{8}(Rs\,JL32-2\,JL22)\,A3xo\right.$$

$$\left.-\frac{1}{8}(Rs\sqrt{3}\,JL32+2\,JL12)\,A3yo-\frac{1}{8}(-Rs\,JL32+2\,JL22)\,B3xo\right)\Bigg/Ro^2\Bigg)\sin\left(\frac{L3}{Ro}\right)+\Bigg($$

$$-\frac{1}{2}\frac{Ibc\left(\frac{1}{2}(-2\,JL23-2\,Rs\,JL33)\,A2xo+JL13\,A2yo+\frac{1}{2}(2\,JL23+2\,Rs\,JL33)\,B2xo-JL13\,B2yo\right)}{Lbc^2\,Ro^2}-$$

$$\frac{1}{2}\frac{Mbc\left(\frac{1}{8}(2\,JL23+2\,Rs\,JL33)\,A2xo-\frac{1}{4}JL13\,A2yo+\frac{1}{8}(-2\,JL23-2\,Rs\,JL33)\,B2xo+\frac{1}{4}JL13\,B2yo\right)}{Ro^2}$$

$$\Bigg)L2dot\,\sin\left(\frac{L2}{Ro}\right)$$

$$C\_31:=\left(\frac{1}{2}Ibc\left(\frac{1}{2}(Rs\sqrt{3}\,JL31+2\,JL11)\,B3xo+\frac{1}{2}(2\,JL21-Rs\,JL31)\,B3yo\right.\right.$$

$$\left.+\frac{1}{2}(-Rs\sqrt{3}\,JL31-2\,JL11)\,A3xo+\frac{1}{2}(Rs\,JL31-2\,JL21)\,A3yo\right)\Bigg/(Lbc^2\,Ro^2)+\frac{1}{2}Mbc\Bigg($$

$$\frac{1}{8}(-Rs\sqrt{3}\,JL31-2\,JL11)\,B3xo+\frac{1}{8}(Rs\,JL31-2\,JL21)\,B3yo+\frac{1}{8}(Rs\sqrt{3}\,JL31+2\,JL11)\,A3xo$$

$$+\frac{1}{8}(2\,JL21-Rs\,JL31)\,A3yo\Bigg)\Bigg/Ro^2\Bigg)L3dot\,\cos\left(\frac{L3}{Ro}\right)+L1dot\left(Ibc\left(\frac{1}{2}(Rs\,JL33-2\,JL23)\,A1yo\right.\right.$$

$$+\frac{1}{2}(-Rs\sqrt{3}\,JL33+2\,JL13)\,B1xo+\frac{1}{2}(-Rs\,JL33+2\,JL23)\,B1yo$$

$$\left.+\frac{1}{2}(-2\,JL13+Rs\sqrt{3}\,JL33)\,A1xo\right)\Bigg/(Lbc^2\,Ro^2)+Mbc\left(\frac{1}{8}(-Rs\,JL33+2\,JL23)\,A1yo\right.$$

$$+\frac{1}{8}(-2\,JL13+Rs\sqrt{3}\,JL33)\,B1xo+\frac{1}{8}(Rs\,JL33-2\,JL23)\,B1yo$$

$$\left.+\frac{1}{8}(-Rs\sqrt{3}\,JL33+2\,JL13)\,A1xo\right)\Bigg/Ro^2\Bigg)\cos\left(\frac{L1}{Ro}\right)+\left(-\frac{1}{2}Ibc\left(\frac{1}{2}(-Rs\sqrt{3}\,JL31-2\,JL11)\,B3yo\right.\right.$$

$$\left.+\frac{1}{2}(Rs\,JL31-2\,JL21)\,A3xo+\frac{1}{2}(Rs\sqrt{3}\,JL31+2\,JL11)\,A3yo+\frac{1}{2}(2\,JL21-Rs\,JL31)\,B3xo\right)\Bigg/($$

$$Lbc^2\,Ro^2)-\frac{1}{2}Mbc\left(\frac{1}{8}(Rs\sqrt{3}\,JL31+2\,JL11)\,B3yo+\frac{1}{8}(2\,JL21-Rs\,JL31)\,A3xo\right.$$

$$\left.+\frac{1}{8}(-Rs\sqrt{3}\,JL31-2\,JL11)\,A3yo+\frac{1}{8}(Rs\,JL31-2\,JL21)\,B3xo\right)\Bigg/Ro^2\Bigg)L3dot\,\sin\left(\frac{L3}{Ro}\right)+L1dot$$

$$\left(-Ibc\left(\frac{1}{2}(Rs\,JL33-2\,JL23)\,A1xo+\frac{1}{2}(-Rs\sqrt{3}\,JL33+2\,JL13)\,A1yo\right.\right.$$

$$\left.+\frac{1}{2}(-Rs\,JL33+2\,JL23)\,B1xo+\frac{1}{2}(-2\,JL13+Rs\sqrt{3}\,JL33)\,B1yo\right)\Bigg/(Lbc^2\,Ro^2)-Mbc\Bigg($$

$$\frac{1}{8}(-Rs\,JL33+2\,JL23)\,A1xo+\frac{1}{8}(-2\,JL13+Rs\sqrt{3}\,JL33)\,A1yo+\frac{1}{8}(Rs\,JL33-2\,JL23)\,B1xo$$

$$+\frac{1}{8}(-Rs\sqrt{3}\,JL33+2\,JL13)\,B1yo\Bigg)\Bigg/ Ro^2\Bigg)\sin\left(\frac{L1}{Ro}\right)$$

$$C\_32 := L2dot\Bigg($$

$$\frac{Ibc\left(\frac{1}{2}(-2\,JL23-2\,Rs\,JL33)\,A2yo+JL13\,B2xo+\frac{1}{2}(2\,JL23+2\,Rs\,JL33)\,B2yo-JL13\,A2xo\right)}{Lbc^2\,Ro^2}+$$

$$Mbc\left(\frac{1}{8}(2\,JL23+2\,Rs\,JL33)\,A2yo-\frac{1}{4}JL13\,B2xo+\frac{1}{8}(-2\,JL23-2\,Rs\,JL33)\,B2yo+\frac{1}{4}JL13\,A2xo\right)$$

$$\Bigg/ Ro^2\Bigg)\cos\left(\frac{L2}{Ro}\right)+\Bigg(\frac{1}{2}\,Ibc\Bigg(\frac{1}{2}(Rs\sqrt{3}\,JL32+2\,JL12)\,B3xo+\frac{1}{2}(-Rs\,JL32+2\,JL22)\,B3yo$$

$$+\frac{1}{2}(-2\,JL12-Rs\sqrt{3}\,JL32)\,A3xo+\frac{1}{2}(Rs\,JL32-2\,JL22)\,A3yo\Bigg)\Bigg/(Lbc^2\,Ro^2)+\frac{1}{2}\,Mbc\Bigg($$

$$-\frac{1}{8}(Rs\sqrt{3}\,JL32+2\,JL12)\,B3xo-\frac{1}{8}(-Rs\,JL32+2\,JL22)\,B3yo-\frac{1}{8}(-2\,JL12-Rs\sqrt{3}\,JL32)\,A3xo$$

$$-\frac{1}{8}(Rs\,JL32-2\,JL22)\,A3yo\Bigg)\Bigg/ Ro^2\Bigg)L3dot\cos\left(\frac{L3}{Ro}\right)+\Bigg(-\frac{1}{2}\,Ibc\Bigg($$

$$\frac{1}{2}(-2\,JL12-Rs\sqrt{3}\,JL32)\,B3yo+\frac{1}{2}(Rs\,JL32-2\,JL22)\,A3xo+\frac{1}{2}(Rs\sqrt{3}\,JL32+2\,JL12)\,A3yo$$

$$+\frac{1}{2}(-Rs\,JL32+2\,JL22)\,B3xo\Bigg)\Bigg/(Lbc^2\,Ro^2)-\frac{1}{2}\,Mbc\Bigg(-\frac{1}{8}(-2\,JL12-Rs\sqrt{3}\,JL32)\,B3yo$$

$$-\frac{1}{8}(Rs\,JL32-2\,JL22)\,A3xo-\frac{1}{8}(Rs\sqrt{3}\,JL32+2\,JL12)\,A3yo-\frac{1}{8}(-Rs\,JL32+2\,JL22)\,B3xo\Bigg)\Bigg/$$

$$Ro^2\Bigg)L3dot\sin\left(\frac{L3}{Ro}\right)+L2dot\Bigg($$

$$-\frac{Ibc\left(\frac{1}{2}(-2\,JL23-2\,Rs\,JL33)\,A2xo+JL13\,A2yo+\frac{1}{2}(2\,JL23+2\,Rs\,JL33)\,B2xo-JL13\,B2yo\right)}{Lbc^2\,Ro^2}-$$

$$Mbc\left(\frac{1}{8}(2\,JL23+2\,Rs\,JL33)\,A2xo-\frac{1}{4}JL13\,A2yo+\frac{1}{8}(-2\,JL23-2\,Rs\,JL33)\,B2xo+\frac{1}{4}JL13\,B2yo\right)$$

$$\Bigg/ Ro^2\Bigg)\sin\left(\frac{L2}{Ro}\right)$$

$$C\_33 := \Bigg(\Bigg(-\frac{1}{2}\,Ibc\Bigg(\frac{1}{2}(Rs\sqrt{3}\,JL31+2\,JL11)\,B3xo+\frac{1}{2}(2\,JL21-Rs\,JL31)\,B3yo$$

$$+\frac{1}{2}(-Rs\sqrt{3}\,JL31-2\,JL11)\,A3xo+\frac{1}{2}(Rs\,JL31-2\,JL21)\,A3yo\Bigg)\Bigg/(Lbc^2\,Ro^2)-\frac{1}{2}\,Mbc\Bigg($$

$$\frac{1}{8}(-Rs\sqrt{3}\,JL31-2\,JL11)\,B3xo+\frac{1}{8}(Rs\,JL31-2\,JL21)\,B3yo+\frac{1}{8}(Rs\sqrt{3}\,JL31+2\,JL11)\,A3xo$$

$$+\frac{1}{8}(2\,JL21 - Rs\,JL31)\,A3yo\bigg)\Big/ Ro^2\bigg)L1dot + \bigg(-\frac{1}{2}\,Ibc\bigg(\frac{1}{2}(Rs\sqrt{3}\,JL32 + 2\,JL12)\,B3xo$$

$$+\frac{1}{2}(-Rs\,JL32 + 2\,JL22)\,B3yo + \frac{1}{2}(-2\,JL12 - Rs\sqrt{3}\,JL32)\,A3xo + \frac{1}{2}(Rs\,JL32 - 2\,JL22)\,A3yo\bigg)\Big/ ($$

$$Lbc^2\,Ro^2) - \frac{1}{2}\,Mbc\bigg(-\frac{1}{8}(Rs\sqrt{3}\,JL32 + 2\,JL12)\,B3xo - \frac{1}{8}(-Rs\,JL32 + 2\,JL22)\,B3yo$$

$$-\frac{1}{8}(-2\,JL12 - Rs\sqrt{3}\,JL32)\,A3xo - \frac{1}{8}(Rs\,JL32 - 2\,JL22)\,A3yo\bigg)\Big/ Ro^2\bigg)L2dot + \bigg(\frac{1}{2}\,Ibc\,($$

$$(-Rs\,JL33 + 2\,JL23)\,B3yo + (2\,JL13 + Rs\sqrt{3}\,JL33)\,B3xo + (Rs\,JL33 - 2\,JL23)\,A3yo$$

$$+(-Rs\sqrt{3}\,JL33 - 2\,JL13)\,A3xo)\Big/(Lbc^2\,Ro^2) + \frac{1}{8}\,Mbc\,(2\,A3yo\,JL23 + 2\,A3xo\,JL13$$

$$-A3yo\,Rs\,JL33 + A3xo\,Rs\,JL33\sqrt{3} - B3xo\,Rs\,JL33\sqrt{3} - 2\,B3xo\,JL13 + B3yo\,Rs\,JL33$$

$$-2\,B3yo\,JL23)\Big/ Ro^2\bigg)L3dot\bigg)\cos\left(\frac{L3}{Ro}\right) + \bigg(\bigg(\frac{1}{2}\,Ibc\bigg(\frac{1}{2}(-Rs\sqrt{3}\,JL31 - 2\,JL11)\,B3yo$$

$$+\frac{1}{2}(Rs\,JL31 - 2\,JL21)\,A3xo + \frac{1}{2}(Rs\sqrt{3}\,JL31 + 2\,JL11)\,A3yo + \frac{1}{2}(2\,JL21 - Rs\,JL31)\,B3xo\bigg)\Big/ ($$

$$Lbc^2\,Ro^2) + \frac{1}{2}\,Mbc\bigg(\frac{1}{8}(Rs\sqrt{3}\,JL31 + 2\,JL11)\,B3yo + \frac{1}{8}(2\,JL21 - Rs\,JL31)\,A3xo$$

$$+\frac{1}{8}(-Rs\sqrt{3}\,JL31 - 2\,JL11)\,A3yo + \frac{1}{8}(Rs\,JL31 - 2\,JL21)\,B3xo\bigg)\Big/ Ro^2\bigg)L1dot + \bigg(\frac{1}{2}\,Ibc\bigg($$

$$\frac{1}{2}(-2\,JL12 - Rs\sqrt{3}\,JL32)\,B3yo + \frac{1}{2}(Rs\,JL32 - 2\,JL22)\,A3xo + \frac{1}{2}(Rs\sqrt{3}\,JL32 + 2\,JL12)\,A3yo$$

$$+\frac{1}{2}(-Rs\,JL32 + 2\,JL22)\,B3xo\bigg)\Big/(Lbc^2\,Ro^2) + \frac{1}{2}\,Mbc\bigg(-\frac{1}{8}(-2\,JL12 - Rs\sqrt{3}\,JL32)\,B3yo$$

$$-\frac{1}{8}(Rs\,JL32 - 2\,JL22)\,A3xo - \frac{1}{8}(Rs\sqrt{3}\,JL32 + 2\,JL12)\,A3yo - \frac{1}{8}(-Rs\,JL32 + 2\,JL22)\,B3xo\bigg)\Big/$$

$$Ro^2\bigg)L2dot + \bigg(-\frac{1}{2}\,Ibc\,((-Rs\,JL33 + 2\,JL23)\,B3xo + (2\,JL13 + Rs\sqrt{3}\,JL33)\,A3yo$$

$$+(Rs\,JL33 - 2\,JL23)\,A3xo + (-Rs\sqrt{3}\,JL33 - 2\,JL13)\,B3yo)\Big/(Lbc^2\,Ro^2) + \frac{1}{8}\,Mbc\,($$

$$A3yo\,Rs\,JL33\sqrt{3} - 2\,A3xo\,JL23 - B3yo\,Rs\,JL33\sqrt{3} + A3xo\,Rs\,JL33 + 2\,A3yo\,JL13 - B3xo\,Rs\,JL33$$

$$+2\,B3xo\,JL23 - 2\,B3yo\,JL13)\Big/ Ro^2\bigg)L3dot\bigg)\sin\left(\frac{L3}{Ro}\right)$$

$$H\_11 := \frac{1}{2} Kb \Big(2 (((A2yo - B2yo)(C2xo - B2xo) - (A2xo - B2xo)(C2yo - B2yo))$$

$$(JL21 (C2xo - B2xo) - JL11 (C2yo - B2yo))) / Lbc^4 + \frac{1}{18} ((6\, B2xo\, C2yo\, Rs - 6\, B2yo\, C2xo\, Rs$$

$$- 6\, A2xo\, C2yo\, Rs - 6\, A2yo\, B2xo\, Rs + 6\, A2xo\, B2yo\, Rs + 6\, A2yo\, C2xo\, Rs)$$

$$(6\, JL21\, C2xo\, Rs + 6\, JL11\, B2yo\, Rs - 6\, JL21\, B2xo\, Rs - 6\, JL11\, C2yo\, Rs)) / (Lbc^4\, Rs^2) \Big) \cos\left(\frac{L2}{Ro}\right) +$$

$$\frac{1}{2} Kb \Big(\frac{1}{2} ((-2\, B3yo\, C3xo\, Lab^2 + 2\, A3yo\, C3xo\, Lab^2 - 2\, A3yo\, B3xo\, Lab^2 - 2\, A3xo\, C3yo\, Lab^2$$

$$+ 2\, B3xo\, C3yo\, Lab^2 + 2\, A3xo\, B3yo\, Lab^2)$$

$$(-2\, JL21\, B3xo\, Lab^2 + 2\, JL21\, C3xo\, Lab^2 + 2\, JL11\, B3yo\, Lab^2 - 2\, JL11\, C3yo\, Lab^2)) \Big/ (Lab^4\, Lbc^4)$$

$$+ \frac{1}{18} ((-6\, B3yo\, C3xo\, Rs + 6\, B3xo\, C3yo\, Rs - 6\, A3yo\, B3xo\, Rs + 6\, A3xo\, B3yo\, Rs + 6\, A3yo\, C3xo\, Rs$$

$$- 6\, A3xo\, C3yo\, Rs)(-6\, JL11\, C3yo\, Rs + 6\, JL21\, C3xo\, Rs - 6\, JL21\, B3xo\, Rs + 6\, JL11\, B3yo\, Rs)) / ($$

$$Lbc^4\, Rs^2) \Big) \cos\left(\frac{L3}{Ro}\right) + \frac{1}{2} Kb \Big(\frac{1}{18} \Big((-6\, B1xo\, C1yo\, Rs + 6\, A1yo\, B1xo\, Rs + 6\, A1xo\, C1yo\, Rs$$

$$- 6\, A1xo\, B1yo\, Rs + 6\, B1yo\, C1xo\, Rs - 6\, A1yo\, C1xo\, Rs) \Big(-6 \frac{A1xo\, B1xo\, Rs}{Ro} + 6 \frac{B1xo^2\, Rs}{Ro}$$

$$+ 6 \frac{B1yo^2\, Rs}{Ro} + 6 \frac{A1yo\, C1yo\, Rs}{Ro} - 6 \frac{A1yo\, B1yo\, Rs}{Ro} - 6 \frac{B1xo\, C1xo\, Rs}{Ro} + 6 \frac{A1xo\, C1xo\, Rs}{Ro}$$

$$- 6 \frac{B1yo\, C1yo\, Rs}{Ro} \Big) \Big) \Big/ (Lbc^4\, Rs^2) + \frac{1}{2} \Big((2\, A1yo\, B1xo\, Lab^2 - 2\, B1xo\, C1yo\, Lab^2$$

$$+ 2\, A1xo\, C1yo\, Lab^2 - 2\, A1yo\, C1xo\, Lab^2 - 2\, A1xo\, B1yo\, Lab^2 + 2\, B1yo\, C1xo\, Lab^2) \Big($$

$$4 \frac{B1xo\, A1xo\, Lbc^2}{Ro} - 2 \frac{A1xo^2\, Lbc^2}{Ro} + 2 \frac{B1yo^2\, Lab^2}{Ro} - 2 \frac{A1yo^2\, Lbc^2}{Ro} + 2 \frac{A1yo\, C1yo\, Lab^2}{Ro}$$

$$+ 2 \frac{A1xo\, C1xo\, Lab^2}{Ro} + 4 \frac{B1yo\, A1yo\, Lbc^2}{Ro} - 2 \frac{B1xo\, A1xo\, Lab^2}{Ro} - 2 \frac{B1xo\, C1xo\, Lab^2}{Ro}$$

$$- 2 \frac{B1yo^2\, Lbc^2}{Ro} - 2 \frac{B1yo\, C1yo\, Lab^2}{Ro} - 2 \frac{B1xo^2\, Lbc^2}{Ro} - 2 \frac{B1yo\, A1yo\, Lab^2}{Ro} + 2 \frac{B1xo^2\, Lab^2}{Ro} \Big) \Big) \Big/ ($$

$$Lbc^4\, Lab^4) \Big) \cos\left(\frac{L1}{Ro}\right)^2 + \Big(\frac{1}{2} Kb \Big(\frac{1}{18} \Big((6\, B1yo^2\, Rs + 6\, B1xo^2\, Rs - 6\, B1yo\, C1yo\, Rs - 6\, A1yo\, B1yo\, Rs$$

$$- 6\, B1xo\, C1xo\, Rs - 6\, A1xo\, B1xo\, Rs + 6\, A1yo\, C1yo\, Rs + 6\, A1xo\, C1xo\, Rs) \Big(-6 \frac{A1xo\, B1xo\, Rs}{Ro}$$

$$+ 6 \frac{B1xo^2\, Rs}{Ro} + 6 \frac{B1yo^2\, Rs}{Ro} + 6 \frac{A1yo\, C1yo\, Rs}{Ro} - 6 \frac{A1yo\, B1yo\, Rs}{Ro} - 6 \frac{B1xo\, C1xo\, Rs}{Ro}$$

$$+ 6 \frac{A1xo\, C1xo\, Rs}{Ro} - 6 \frac{B1yo\, C1yo\, Rs}{Ro} \Big) \Big) \Big/ (Lbc^4\, Rs^2) + \frac{1}{18} \Big((-6\, B1xo\, C1yo\, Rs + 6\, A1yo\, B1xo\, Rs$$

$$+ 6\, A1xo\, C1yo\, Rs - 6\, A1xo\, B1yo\, Rs + 6\, B1yo\, C1xo\, Rs - 6\, A1yo\, C1xo\, Rs) \Big(-6 \frac{A1yo\, B1xo\, Rs}{Ro}$$

$$+ 6 \frac{B1xo\, C1yo\, Rs}{Ro} - 6 \frac{B1yo\, C1xo\, Rs}{Ro} - 6 \frac{A1xo\, C1yo\, Rs}{Ro} + 6 \frac{A1yo\, C1xo\, Rs}{Ro} + 6 \frac{A1xo\, B1yo\, Rs}{Ro} \Big) \Big)$$

$$\Big/ (Lbc^4\, Rs^2) + \frac{1}{2} \Big((-2\, A1yo^2\, Lbc^2 + 2\, B1xo^2\, Lab^2 - 2\, A1xo^2\, Lbc^2 + 2\, B1yo^2\, Lab^2 - 2\, B1yo^2\, Lbc^2$$

$$+ 4\, B1yo\, A1yo\, Lbc^2 - 2\, B1xo\, A1xo\, Lab^2 - 2\, B1xo\, C1xo\, Lab^2 - 2\, B1xo^2\, Lbc^2 + 4\, B1xo\, A1xo\, Lbc^2$$

$$- 2\, B1yo\, A1yo\, Lab^2 + 2\, A1yo\, C1yo\, Lab^2 + 2\, A1xo\, C1xo\, Lab^2 - 2\, B1yo\, C1yo\, Lab^2) \Big($$

$$4 \frac{B1xo\, A1xo\, Lbc^2}{Ro} - 2 \frac{A1xo^2\, Lbc^2}{Ro} + 2 \frac{B1yo^2\, Lab^2}{Ro} - 2 \frac{A1yo^2\, Lbc^2}{Ro} + 2 \frac{A1yo\, C1yo\, Lab^2}{Ro}$$

$$+2\frac{A1xo\,C1xo\,Lab^2}{Ro}+4\frac{B1yo\,A1yo\,Lbc^2}{Ro}-2\frac{B1xo\,A1xo\,Lab^2}{Ro}-2\frac{B1xo\,C1xo\,Lab^2}{Ro}$$

$$-2\frac{B1yo^2\,Lbc^2}{Ro}-2\frac{B1yo\,C1yo\,Lab^2}{Ro}-2\frac{B1xo^2\,Lbc^2}{Ro}-2\frac{B1yo\,A1yo\,Lab^2}{Ro}+2\frac{B1xo^2\,Lab^2}{Ro}\Bigg)\Bigg)\Big/($$

$$Lbc^4\,Lab^4)+\frac{1}{2}\Bigg((2\,A1yo\,B1xo\,Lab^2-2\,B1xo\,C1yo\,Lab^2+2\,A1xo\,C1yo\,Lab^2-2\,A1yo\,C1xo\,Lab^2$$

$$-2\,A1xo\,B1yo\,Lab^2+2\,B1yo\,C1xo\,Lab^2)\Bigg(-2\frac{B1yo\,C1xo\,Lab^2}{Ro}-2\frac{A1yo\,B1xo\,Lab^2}{Ro}$$

$$+2\frac{B1yo\,A1xo\,Lab^2}{Ro}+2\frac{B1xo\,C1yo\,Lab^2}{Ro}-2\frac{A1xo\,C1yo\,Lab^2}{Ro}+2\frac{A1yo\,C1xo\,Lab^2}{Ro}\Bigg)\Bigg)\Big/($$

$$Lbc^4\,Lab^4)\Bigg)\sin\left(\frac{L1}{Ro}\right)+\frac{1}{2}Kb\left(\frac{1}{18}\Bigg((-6\,A1xo\,C1yo\,Rs+6\,A1xo\,B1yo\,Rs+3\,Rs^2\,B1yo\right.$$

$$+6\,A1yo\,C1xo\,Rs-6\,A1yo\,B1xo\,Rs-6\,JL21\,L1\,C1xo\,Rs+6\,JL21\,L1\,B1xo\,Rs-3\,Rs^2\,C1yo$$
$$+6\,JL22\,L2\,B1xo\,Rs-6\,JL23\,L3\,C1xo\,Rs+6\,JL23\,L3\,B1xo\,Rs-6\,JL11\,L1\,B1yo\,Rs$$
$$+6\,JL11\,L1\,C1yo\,Rs-6\,JL22\,L2\,C1xo\,Rs+6\,JL12\,L2\,C1yo\,Rs-6\,JL12\,L2\,B1yo\,Rs$$
$$+6\,JL13\,L3\,C1yo\,Rs-6\,JL13\,L3\,B1yo\,Rs+3\,C1yo\,Lbc^2-3\,C2yo\,Lbc^2+\sqrt{3}\,C1xo\,Lbc^2$$

$$-\sqrt{3}\,C2xo\,Lbc^2-3\,Rs^2\sqrt{3}\,C1xo+3\,Rs^2\sqrt{3}\,B1xo)\Bigg(-6\frac{A1xo\,B1xo\,Rs}{Ro}+6\frac{B1xo^2\,Rs}{Ro}$$

$$+6\frac{B1yo^2\,Rs}{Ro}+6\frac{A1yo\,C1yo\,Rs}{Ro}-6\frac{A1yo\,B1yo\,Rs}{Ro}-6\frac{B1xo\,C1xo\,Rs}{Ro}+6\frac{A1xo\,C1xo\,Rs}{Ro}$$

$$-6\frac{B1yo\,C1yo\,Rs}{Ro}\Bigg)\Bigg)\Big/(Lbc^4\,Rs^2)+\frac{1}{18}((-6\,B1xo\,C1yo\,Rs+6\,A1yo\,B1xo\,Rs+6\,A1xo\,C1yo\,Rs$$
$$-6\,A1xo\,B1yo\,Rs+6\,B1yo\,C1xo\,Rs-6\,A1yo\,C1xo\,Rs)$$

$$(6\,JL21\,B1xo\,Rs-6\,JL11\,B1yo\,Rs+6\,JL11\,C1yo\,Rs-6\,JL21\,C1xo\,Rs))/(Lbc^4\,Rs^2)+\frac{1}{2}\Bigg(($$

$$-2\,A1yo\,B1xo\,Lab^2+2\,JL13\,L3\,C1yo\,Lab^2-2\,JL13\,L3\,B1yo\,Lab^2-2\,A1xo\,C1yo\,Lab^2$$
$$+2\,A1xo\,B1yo\,Lab^2-2\,JL11\,L1\,B1yo\,Lab^2+2\,JL12\,L2\,C1yo\,Lab^2+Rs\,B1yo\,Lab^2$$
$$-2\,JL12\,L2\,B1yo\,Lab^2-Rs\,C1yo\,Lab^2+2\,JL23\,L3\,B1xo\,Lab^2+2\,JL22\,L2\,B1xo\,Lab^2$$
$$+2\,JL11\,L1\,C1yo\,Lab^2-2\,JL22\,L2\,C1xo\,Lab^2-2\,JL23\,L3\,C1xo\,Lab^2-2\,JL21\,L1\,C1xo\,Lab^2$$

$$+2\,JL21\,L1\,B1xo\,Lab^2+2\,A1yo\,C1xo\,Lab^2+Rs\sqrt{3}\,B1xo\,Lab^2-Rs\sqrt{3}\,C1xo\,Lab^2)\Bigg($$

$$4\frac{B1xo\,A1xo\,Lbc^2}{Ro}-2\frac{A1xo^2\,Lbc^2}{Ro}+2\frac{B1yo^2\,Lab^2}{Ro}-2\frac{A1yo^2\,Lbc^2}{Ro}+2\frac{A1yo\,C1yo\,Lab^2}{Ro}$$

$$+2\frac{A1xo\,C1xo\,Lab^2}{Ro}+4\frac{B1yo\,A1yo\,Lbc^2}{Ro}-2\frac{B1xo\,A1xo\,Lab^2}{Ro}-2\frac{B1xo\,C1xo\,Lab^2}{Ro}$$

$$-2\frac{B1yo^2\,Lbc^2}{Ro}-2\frac{B1yo\,C1yo\,Lab^2}{Ro}-2\frac{B1xo^2\,Lbc^2}{Ro}-2\frac{B1yo\,A1yo\,Lab^2}{Ro}+2\frac{B1xo^2\,Lab^2}{Ro}\Bigg)\Bigg)\Big/($$

$$Lbc^4\,Lab^4)+\frac{1}{2}((2\,A1yo\,B1xo\,Lab^2-2\,B1xo\,C1yo\,Lab^2+2\,A1xo\,C1yo\,Lab^2-2\,A1yo\,C1xo\,Lab^2$$
$$-2\,A1xo\,B1yo\,Lab^2+2\,B1yo\,C1xo\,Lab^2)$$
$$(-2\,JL21\,C1xo\,Lab^2-2\,JL11\,B1yo\,Lab^2+2\,JL11\,C1yo\,Lab^2+2\,JL21\,B1xo\,Lab^2))\Big/(Lbc^4\,Lab^4)$$

$$\Bigg)\Bigg)\cos\left(\frac{L1}{Ro}\right)+\frac{1}{2}Kb\Bigg(\frac{1}{2}((2\,B3xo^2\,Lbc^2-2\,B3yo^2\,Lab^2-2\,B3xo^2\,Lab^2+2\,B3yo^2\,Lbc^2$$
$$+2\,A3xo^2\,Lbc^2+2\,B3yo\,A3yo\,Lab^2+2\,A3yo^2\,Lbc^2-2\,A3yo\,C3yo\,Lab^2-2\,A3xo\,C3xo\,Lab^2$$
$$-4\,B3yo\,A3yo\,Lbc^2+2\,B3yo\,C3yo\,Lab^2+2\,B3xo\,A3xo\,Lab^2+2\,B3xo\,C3xo\,Lab^2$$
$$-4\,B3xo\,A3xo\,Lbc^2)$$
$$(-2\,JL21\,B3xo\,Lab^2+2\,JL21\,C3xo\,Lab^2+2\,JL11\,B3yo\,Lab^2-2\,JL11\,C3yo\,Lab^2))\Big/(Lab^4\,Lbc^4)$$

$$+\frac{1}{18}((-6\,A3yo\,C3yo\,Rs+6\,B3yo\,C3yo\,Rs+6\,A3yo\,B3yo\,Rs+6\,A3xo\,B3xo\,Rs-6\,B3yo^2\,Rs$$
$$+6\,B3xo\,C3xo\,Rs-6\,A3xo\,C3xo\,Rs-6\,B3xo^2\,Rs)$$

$$(-6\,JL11\,C3yo\,Rs + 6\,JL21\,C3xo\,Rs - 6\,JL21\,B3xo\,Rs + 6\,JL11\,B3yo\,Rs)) \Big/ (Lbc^4\,Rs^2)\Bigg)\sin\left(\frac{L3}{Ro}\right)$$

$$+\frac{1}{2}\,Kb\left(-2\left(\left(\frac{2\,B2xo\,A2xo - B2xo^2 - A2xo^2 + 2\,B2yo\,A2yo - B2yo^2 - A2yo^2}{Lab^2}\right.\right.\right.$$

$$\left.- \frac{(B2xo - A2xo)(C2xo - B2xo) - (A2yo - B2yo)(C2yo - B2yo)}{Lbc^2}\right)$$

$$(JL21\,(C2xo - B2xo) - JL11\,(C2yo - B2yo))\Bigg) \Big/ Lbc^2 + \frac{1}{18}((6\,B2xo\,C2xo\,Rs + 6\,B2yo\,A2yo\,Rs$$

$$- 6\,B2yo^2\,Rs + 6\,B2yo\,C2yo\,Rs - 6\,A2xo\,C2xo\,Rs - 6\,A2yo\,C2yo\,Rs - 6\,B2xo^2\,Rs$$

$$+ 6\,B2xo\,A2xo\,Rs)(6\,JL21\,C2xo\,Rs + 6\,JL11\,B2yo\,Rs - 6\,JL21\,B2xo\,Rs - 6\,JL11\,C2yo\,Rs)) \Big/ ($$

$$Lbc^4\,Rs^2)\Bigg)\sin\left(\frac{L2}{Ro}\right) + \frac{1}{2}\,Kb\left(\frac{1}{18}\left((6\,B1yo^2\,Rs + 6\,B1xo^2\,Rs - 6\,B1yo\,C1yo\,Rs - 6\,A1yo\,B1yo\,Rs\right.\right.$$

$$- 6\,B1xo\,C1xo\,Rs - 6\,A1xo\,B1xo\,Rs + 6\,A1yo\,C1yo\,Rs + 6\,A1xo\,C1xo\,Rs)\left(-6\,\frac{A1yo\,B1xo\,Rs}{Ro}\right.$$

$$\left.\left.\left. + 6\,\frac{B1xo\,C1yo\,Rs}{Ro} - 6\,\frac{B1yo\,C1xo\,Rs}{Ro} - 6\,\frac{A1xo\,C1yo\,Rs}{Ro} + 6\,\frac{A1yo\,C1xo\,Rs}{Ro} + 6\,\frac{A1xo\,B1yo\,Rs}{Ro}\right)\right)\right)$$

$$\Big/ (Lbc^4\,Rs^2) + \frac{1}{2}\Big((-2\,A1yo^2\,Lbc^2 + 2\,B1xo^2\,Lab^2 - 2\,A1xo^2\,Lbc^2 + 2\,B1yo^2\,Lab^2 - 2\,B1yo^2\,Lbc^2$$

$$+ 4\,B1yo\,A1yo\,Lbc^2 - 2\,B1xo\,A1xo\,Lab^2 - 2\,B1xo\,C1xo\,Lab^2 - 2\,B1xo^2\,Lbc^2 + 4\,B1xo\,A1xo\,Lbc^2$$

$$- 2\,B1yo\,A1yo\,Lab^2 + 2\,A1yo\,C1yo\,Lab^2 + 2\,A1xo\,C1xo\,Lab^2 - 2\,B1yo\,C1yo\,Lab^2)\Big($$

$$-2\,\frac{B1yo\,C1xo\,Lab^2}{Ro} - 2\,\frac{A1yo\,B1xo\,Lab^2}{Ro} + 2\,\frac{B1yo\,A1xo\,Lab^2}{Ro} + 2\,\frac{B1xo\,C1yo\,Lab^2}{Ro}$$

$$\left.\left. - 2\,\frac{A1xo\,C1yo\,Lab^2}{Ro} + 2\,\frac{A1yo\,C1xo\,Lab^2}{Ro}\right)\right) \Big/ (Lbc^4\,Lab^4)\Bigg)\sin\left(\frac{L1}{Ro}\right)^2 + \frac{1}{2}\,Kb\left(\frac{1}{2}\Big((\right.$$

$$-2\,A1yo\,B1xo\,Lab^2 + 2\,JL13\,L3\,C1yo\,Lab^2 - 2\,JL13\,L3\,B1yo\,Lab^2 - 2\,A1xo\,C1yo\,Lab^2$$

$$+ 2\,A1xo\,B1yo\,Lab^2 - 2\,JL11\,L1\,B1yo\,Lab^2 + 2\,JL12\,L2\,C1yo\,Lab^2 + Rs\,B1yo\,Lab^2$$

$$- 2\,JL12\,L2\,B1yo\,Lab^2 - Rs\,C1yo\,Lab^2 + 2\,JL23\,L3\,B1xo\,Lab^2 + 2\,JL22\,L2\,B1xo\,Lab^2$$

$$+ 2\,JL11\,L1\,C1yo\,Lab^2 - 2\,JL22\,L2\,C1xo\,Lab^2 - 2\,JL23\,L3\,C1xo\,Lab^2 - 2\,JL21\,L1\,C1xo\,Lab^2$$

$$+ 2\,JL21\,L1\,B1xo\,Lab^2 + 2\,A1yo\,C1xo\,Lab^2 + Rs\sqrt{3}\,B1xo\,Lab^2 - Rs\sqrt{3}\,C1xo\,Lab^2)\Big($$

$$-2\,\frac{B1yo\,C1xo\,Lab^2}{Ro} - 2\,\frac{A1yo\,B1xo\,Lab^2}{Ro} + 2\,\frac{B1yo\,A1xo\,Lab^2}{Ro} + 2\,\frac{B1xo\,C1yo\,Lab^2}{Ro}$$

$$\left.\left. - 2\,\frac{A1xo\,C1yo\,Lab^2}{Ro} + 2\,\frac{A1yo\,C1xo\,Lab^2}{Ro}\right)\right) \Big/ (Lbc^4\,Lab^4) + \frac{1}{2}((-2\,A1yo^2\,Lbc^2 + 2\,B1xo^2\,Lab^2$$

$$- 2\,A1xo^2\,Lbc^2 + 2\,B1yo^2\,Lab^2 - 2\,B1yo^2\,Lbc^2 + 4\,B1yo\,A1yo\,Lbc^2 - 2\,B1xo\,A1xo\,Lab^2$$

$$- 2\,B1xo\,C1xo\,Lab^2 - 2\,B1xo^2\,Lbc^2 + 4\,B1xo\,A1xo\,Lbc^2 - 2\,B1yo\,A1yo\,Lab^2 + 2\,A1yo\,C1yo\,Lab^2$$

$$+ 2\,A1xo\,C1xo\,Lab^2 - 2\,B1yo\,C1yo\,Lab^2)$$

$$(-2\,JL21\,C1xo\,Lab^2 - 2\,JL11\,B1yo\,Lab^2 + 2\,JL11\,C1yo\,Lab^2 + 2\,JL21\,B1xo\,Lab^2)) \Big/ (Lbc^4\,Lab^4)$$

$$+ \frac{1}{18}\Big((-6\,A1xo\,C1yo\,Rs + 6\,A1xo\,B1yo\,Rs + 3\,Rs^2\,B1yo + 6\,A1yo\,C1xo\,Rs - 6\,A1yo\,B1xo\,Rs$$

$$- 6\,JL21\,L1\,C1xo\,Rs + 6\,JL21\,L1\,B1xo\,Rs - 3\,Rs^2\,C1yo + 6\,JL22\,L2\,B1xo\,Rs - 6\,JL23\,L3\,C1xo\,Rs$$

$$+ 6\,JL23\,L3\,B1xo\,Rs - 6\,JL11\,L1\,B1yo\,Rs + 6\,JL11\,L1\,C1yo\,Rs - 6\,JL22\,L2\,C1xo\,Rs$$

$$+ 6\,JL12\,L2\,C1yo\,Rs - 6\,JL12\,L2\,B1yo\,Rs + 6\,JL13\,L3\,C1yo\,Rs - 6\,JL13\,L3\,B1yo\,Rs$$

$$+ 3\,C1yo\,Lbc^2 - 3\,C2yo\,Lbc^2 + \sqrt{3}\,C1xo\,Lbc^2 - \sqrt{3}\,C2xo\,Lbc^2 - 3\,Rs^2\sqrt{3}\,C1xo + 3\,Rs^2\sqrt{3}\,B1xo)$$

$$\left(-6\,\frac{A1yo\,B1xo\,Rs}{Ro} + 6\,\frac{B1xo\,C1yo\,Rs}{Ro} - 6\,\frac{B1yo\,C1xo\,Rs}{Ro} - 6\,\frac{A1xo\,C1yo\,Rs}{Ro} + 6\,\frac{A1yo\,C1xo\,Rs}{Ro}\right.$$

$$\left.\left. + 6\,\frac{A1xo\,B1yo\,Rs}{Ro}\right)\right) \Big/ (Lbc^4\,Rs^2) + \frac{1}{18}((6\,B1yo^2\,Rs + 6\,B1xo^2\,Rs - 6\,B1yo\,C1yo\,Rs$$

$$- 6\,A1yo\,B1yo\,Rs - 6\,B1xo\,C1xo\,Rs - 6\,A1xo\,B1xo\,Rs + 6\,A1yo\,C1yo\,Rs + 6\,A1xo\,C1xo\,Rs)$$

$$(6\,JL21\,B1xo\,Rs - 6\,JL11\,B1yo\,Rs + 6\,JL11\,C1yo\,Rs - 6\,JL21\,C1xo\,Rs))\Big/(Lbc^4\,Rs^2)\Bigg)\sin\left(\frac{L1}{Ro}\right)$$

$$+\frac{1}{2}\,Kb\left(\frac{1}{2}((-2\,A1yo\,B1xo\,Lab^2 + 2\,JL13\,L3\,C1yo\,Lab^2 - 2\,JL13\,L3\,B1yo\,Lab^2\right.$$

$$- 2\,A1xo\,C1yo\,Lab^2 + 2\,A1xo\,B1yo\,Lab^2 - 2\,JL11\,L1\,B1yo\,Lab^2 + 2\,JL12\,L2\,C1yo\,Lab^2$$

$$+ Rs\,B1yo\,Lab^2 - 2\,JL12\,L2\,B1yo\,Lab^2 - Rs\,C1yo\,Lab^2 + 2\,JL23\,L3\,B1xo\,Lab^2$$

$$+ 2\,JL22\,L2\,B1xo\,Lab^2 + 2\,JL11\,L1\,C1yo\,Lab^2 - 2\,JL22\,L2\,C1xo\,Lab^2 - 2\,JL23\,L3\,C1xo\,Lab^2$$

$$- 2\,JL21\,L1\,C1xo\,Lab^2 + 2\,JL21\,L1\,B1xo\,Lab^2 + 2\,A1yo\,C1xo\,Lab^2 + Rs\sqrt{3}\,B1xo\,Lab^2$$

$$- Rs\sqrt{3}\,C1xo\,Lab^2)$$

$$(-2\,JL21\,C1xo\,Lab^2 - 2\,JL11\,B1yo\,Lab^2 + 2\,JL11\,C1yo\,Lab^2 + 2\,JL21\,B1xo\,Lab^2))\Big/(Lbc^4\,Lab^4)$$

$$+\frac{1}{3}\left(\left(\frac{1}{6}\,\frac{2\sqrt{3}\,C3xo - 2\sqrt{3}\,C1xo}{Rs}\right.\right.$$

$$+\frac{1}{6}\,\frac{(-6\,JL11\,C3yo\,Rs + 6\,JL21\,C3xo\,Rs - 6\,JL21\,B3xo\,Rs + 6\,JL11\,B3yo\,Rs)\,L1}{Lbc^2\,Rs}$$

$$+\frac{1}{6}\,\frac{(6\,JL12\,B3yo\,Rs - 6\,JL12\,C3yo\,Rs + 6\,JL22\,C3xo\,Rs - 6\,JL22\,B3xo\,Rs)\,L2}{Lbc^2\,Rs}$$

$$+\frac{1}{6}\,\frac{(6\,JL23\,C3xo\,Rs - 6\,JL23\,B3xo\,Rs + 6\,JL13\,B3yo\,Rs - 6\,JL13\,C3yo\,Rs)\,L3}{Lbc^2\,Rs} + \frac{1}{6}($$

$$6\,A3xo\,C3yo\,Rs - 3\,Rs^2\,B3yo + 3\,Rs^2\,C3yo - 3\,Rs^2\sqrt{3}\,C3xo + 3\,Rs^2\sqrt{3}\,B3xo - 6\,A3xo\,B3yo\,Rs$$

$$\left.- 6\,A3yo\,C3xo\,Rs + 6\,A3yo\,B3xo\,Rs)\Big/(Rs\,Lbc^2)\right)$$

$$\left.(-6\,JL11\,C3yo\,Rs + 6\,JL21\,C3xo\,Rs - 6\,JL21\,B3xo\,Rs + 6\,JL11\,B3yo\,Rs)\right)\Big/(Lbc^2\,Rs) + 2\,\frac{L1}{Ro^2} +$$

$$\frac{1}{18}((-6\,A1xo\,C1yo\,Rs + 6\,A1xo\,B1yo\,Rs + 3\,Rs^2\,B1yo + 6\,A1yo\,C1xo\,Rs - 6\,A1yo\,B1xo\,Rs$$

$$- 6\,JL21\,L1\,C1xo\,Rs + 6\,JL21\,L1\,B1xo\,Rs - 3\,Rs^2\,C1yo + 6\,JL22\,L2\,B1xo\,Rs - 6\,JL23\,L3\,C1xo\,Rs$$

$$+ 6\,JL23\,L3\,B1xo\,Rs - 6\,JL11\,L1\,B1yo\,Rs + 6\,JL11\,L1\,C1yo\,Rs - 6\,JL22\,L2\,C1xo\,Rs$$

$$+ 6\,JL12\,L2\,C1yo\,Rs - 6\,JL12\,L2\,B1yo\,Rs + 6\,JL13\,L3\,C1yo\,Rs - 6\,JL13\,L3\,B1yo\,Rs$$

$$+ 3\,C1yo\,Lbc^2 - 3\,C2yo\,Lbc^2 + \sqrt{3}\,C1xo\,Lbc^2 - \sqrt{3}\,C2xo\,Lbc^2 - 3\,Rs^2\sqrt{3}\,C1xo + 3\,Rs^2\sqrt{3}\,B1xo)$$

$$(6\,JL21\,B1xo\,Rs - 6\,JL11\,B1yo\,Rs + 6\,JL11\,C1yo\,Rs - 6\,JL21\,C1xo\,Rs))\Big/(Lbc^4\,Rs^2) + \frac{1}{2}(($$

$$-2\,JL13\,L3\,C3yo\,Lab^2 + 2\,JL12\,L2\,B3yo\,Lab^2 + 2\,JL22\,L2\,C3xo\,Lab^2 - 2\,JL21\,L1\,B3xo\,Lab^2$$

$$+ 2\,JL21\,L1\,C3xo\,Lab^2 - 2\,A3yo\,C3xo\,Lab^2 - 2\,JL23\,L3\,B3xo\,Lab^2 + 2\,JL23\,L3\,C3xo\,Lab^2$$

$$- 2\,JL22\,L2\,B3xo\,Lab^2 + 2\,A3yo\,B3xo\,Lab^2 - 2\,JL12\,L2\,C3yo\,Lab^2 + 2\,JL11\,L1\,B3yo\,Lab^2$$

$$- 2\,JL11\,L1\,C3yo\,Lab^2 - 2\,A3xo\,B3yo\,Lab^2 + 2\,A3xo\,C3yo\,Lab^2 - Rs\,B3yo\,Lab^2 + Rs\,C3yo\,Lab^2$$

$$+ 2\,JL13\,L3\,B3yo\,Lab^2 + Rs\sqrt{3}\,B3xo\,Lab^2 - Rs\sqrt{3}\,C3xo\,Lab^2)$$

$$(-2\,JL21\,B3xo\,Lab^2 + 2\,JL21\,C3xo\,Lab^2 + 2\,JL11\,B3yo\,Lab^2 - 2\,JL11\,C3yo\,Lab^2))\Big/(Lab^4\,Lbc^4)$$

$$+\frac{1}{3}\left(\left(\frac{1}{6}\,\frac{-\sqrt{3}\,C2xo + 3\,C2yo - 3\,C3yo + \sqrt{3}\,C3xo}{Rs}\right.\right.$$

$$+\frac{1}{6}\,\frac{(6\,JL21\,C2xo\,Rs + 6\,JL11\,B2yo\,Rs - 6\,JL21\,B2xo\,Rs - 6\,JL11\,C2yo\,Rs)\,L1}{Lbc^2\,Rs}$$

$$+\frac{1}{6}\,\frac{(6\,JL22\,C2xo\,Rs + 6\,JL12\,B2yo\,Rs - 6\,JL22\,B2xo\,Rs - 6\,JL12\,C2yo\,Rs)\,L2}{Lbc^2\,Rs}$$

$$+\frac{1}{6}\,\frac{(6\,JL23\,C2xo\,Rs + 6\,JL13\,B2yo\,Rs - 6\,JL23\,B2xo\,Rs - 6\,JL13\,C2yo\,Rs)\,L3}{Lbc^2\,Rs} + \frac{1}{6}$$

$$\frac{-6\,Rs^2\,C2yo - 6\,A2xo\,B2yo\,Rs + 6\,A2yo\,B2xo\,Rs + 6\,Rs^2\,B2yo - 6\,A2yo\,C2xo\,Rs + 6\,A2xo\,C2yo\,Rs}{Rs\,Lbc^2}$$

$$\left.\left.\right)(6\,JL21\,C2xo\,Rs + 6\,JL11\,B2yo\,Rs - 6\,JL21\,B2xo\,Rs - 6\,JL11\,C2yo\,Rs)\right)\Big/(Lbc^2\,Rs) - 2\left(\left(\right.\right.$$

$$
-\frac{(JL23\,(C2xo-B2xo)-JL13\,(C2yo-B2yo))\,L3}{Lbc^2}
$$
$$
-\frac{-A2yo\,(C2xo-B2xo)-(-A2xo+Rs)\,(C2yo-B2yo)}{Lbc^2}
$$
$$
-\frac{(JL21\,(C2xo-B2xo)-JL11\,(C2yo-B2yo))\,L1}{Lbc^2}
$$
$$
\left.-\frac{(JL22\,(C2xo-B2xo)-JL12\,(C2yo-B2yo))\,L2}{Lbc^2}\right)
$$
$$
\left.(JL21\,(C2xo-B2xo)-JL11\,(C2yo-B2yo))\right)\Big/\left.Lbc^2\right)
$$

$$
H\_21:=\frac{1}{2}\,Kb\left(-2\left(((A2yo-B2yo)\,(C2xo-B2xo)-(A2xo-B2xo)\,(C2yo-B2yo))\right(\right.\right.
$$
$$
\frac{2\,B2xo\,A2xo-B2xo^2-A2xo^2+2\,B2yo\,A2yo-B2yo^2-A2yo^2}{Ro\,Lab^2}
$$
$$
\left.\left.\left.-\frac{(B2xo-A2xo)\,(C2xo-B2xo)-(A2yo-B2yo)\,(C2yo-B2yo)}{Lbc^2\,Ro}\right)\right)\right)\Big/Lbc^2+\frac{1}{18}((
$$
$$
6\,B2xo\,C2yo\,Rs-6\,B2yo\,C2xo\,Rs-6\,A2xo\,C2yo\,Rs-6\,A2yo\,B2xo\,Rs+6\,A2xo\,B2yo\,Rs
$$
$$
+6\,A2yo\,C2xo\,Rs)\,(6\,B2xo\,C2xo\,Rs+6\,B2yo\,A2yo\,Rs-6\,B2yo^2\,Rs+6\,B2yo\,C2yo\,Rs
$$
$$
\left.-6\,A2xo\,C2xo\,Rs-6\,A2yo\,C2yo\,Rs-6\,B2xo^2\,Rs+6\,B2xo\,A2xo\,Rs))\Big/(Lbc^4\,Rs^2\,Ro)\right)
$$
$$
\cos\left(\frac{L2}{Ro}\right)^2+\left(\frac{1}{2}\,Kb\left(\frac{1}{18}(6\,B2xo\,C2xo\,Rs+6\,B2yo\,A2yo\,Rs-6\,B2yo^2\,Rs+6\,B2yo\,C2yo\,Rs\right.\right.
$$
$$
-6\,A2xo\,C2xo\,Rs-6\,A2yo\,C2yo\,Rs-6\,B2xo^2\,Rs+6\,B2xo\,A2xo\,Rs)^2\Big/(Lbc^4\,Rs^2\,Ro)-\frac{1}{18}(
$$
$$
6\,B2xo\,C2yo\,Rs-6\,B2yo\,C2xo\,Rs-6\,A2xo\,C2yo\,Rs-6\,A2yo\,B2xo\,Rs+6\,A2xo\,B2yo\,Rs
$$
$$
+6\,A2yo\,C2xo\,Rs)^2\Big/(Lbc^4\,Rs^2\,Ro)+2\Big(
$$
$$
\frac{2\,B2xo\,A2xo-B2xo^2-A2xo^2+2\,B2yo\,A2yo-B2yo^2-A2yo^2}{Lab^2}
$$
$$
\left.-\frac{(B2xo-A2xo)\,(C2xo-B2xo)-(A2yo-B2yo)\,(C2yo-B2yo)}{Lbc^2}\right)\Big(
$$
$$
\frac{2\,B2xo\,A2xo-B2xo^2-A2xo^2+2\,B2yo\,A2yo-B2yo^2-A2yo^2}{Ro\,Lab^2}
$$
$$
\left.-\frac{(B2xo-A2xo)\,(C2xo-B2xo)-(A2yo-B2yo)\,(C2yo-B2yo)}{Lbc^2\,Ro}\right)
$$
$$
\left.-2\,\frac{((A2yo-B2yo)\,(C2xo-B2xo)-(A2xo-B2xo)\,(C2yo-B2yo))^2}{Lbc^4\,Ro}\right)\sin\left(\frac{L2}{Ro}\right)+\frac{1}{2}\,Kb\left(\frac{1}{3}\Big(\Big(\right.
$$
$$
\frac{1}{6}\,\frac{-\sqrt{3}\,C2xo+3\,C2yo-3\,C3yo+\sqrt{3}\,C3xo}{Rs}
$$
$$
+\frac{1}{6}\,\frac{(6\,JL21\,C2xo\,Rs+6\,JL11\,B2yo\,Rs-6\,JL21\,B2xo\,Rs-6\,JL11\,C2yo\,Rs)\,L1}{Lbc^2\,Rs}
$$
$$
+\frac{1}{6}\,\frac{(6\,JL22\,C2xo\,Rs+6\,JL12\,B2yo\,Rs-6\,JL22\,B2xo\,Rs-6\,JL12\,C2yo\,Rs)\,L2}{Lbc^2\,Rs}
$$
$$
+\frac{1}{6}\,\frac{(6\,JL23\,C2xo\,Rs+6\,JL13\,B2yo\,Rs-6\,JL23\,B2xo\,Rs-6\,JL13\,C2yo\,Rs)\,L3}{Lbc^2\,Rs}+\frac{1}{6}
$$

$$\frac{-6\,Rs^2\,C2yo - 6\,A2xo\,B2yo\,Rs + 6\,A2yo\,B2xo\,Rs + 6\,Rs^2\,B2yo - 6\,A2yo\,C2xo\,Rs + 6\,A2xo\,C2yo\,Rs}{Rs\,Lbc^2}$$

$$\Bigg)(6\,B2xo\,C2xo\,Rs + 6\,B2yo\,A2yo\,Rs - 6\,B2yo^2\,Rs + 6\,B2yo\,C2yo\,Rs - 6\,A2xo\,C2xo\,Rs$$

$$- 6\,A2yo\,C2yo\,Rs - 6\,B2xo^2\,Rs + 6\,B2xo\,A2xo\,Rs)\Bigg) \Big/ (Lbc^2\,Rs\,Ro) + \frac{1}{18}((6\,B2xo\,C2yo\,Rs$$

$$- 6\,B2yo\,C2xo\,Rs - 6\,A2xo\,C2yo\,Rs - 6\,A2yo\,B2xo\,Rs + 6\,A2xo\,B2yo\,Rs + 6\,A2yo\,C2xo\,Rs)$$

$$(6\,JL22\,C2xo\,Rs + 6\,JL12\,B2yo\,Rs - 6\,JL22\,B2xo\,Rs - 6\,JL12\,C2yo\,Rs))\,/\,(Lbc^4\,Rs^2) + 2\Bigg($$

$$-\frac{(JL23\,(C2xo - B2xo) - JL13\,(C2yo - B2yo))\,L3}{Lbc^2}$$

$$-\frac{-A2yo\,(C2xo - B2xo) - (-A2xo + Rs)\,(C2yo - B2yo)}{Lbc^2}$$

$$-\frac{(JL21\,(C2xo - B2xo) - JL11\,(C2yo - B2yo))\,L1}{Lbc^2}$$

$$-\frac{(JL22\,(C2xo - B2xo) - JL12\,(C2yo - B2yo))\,L2}{Lbc^2}\Bigg)\Bigg($$

$$\frac{2\,B2xo\,A2xo - B2xo^2 - A2xo^2 + 2\,B2yo\,A2yo - B2yo^2 - A2yo^2}{Ro\,Lab^2}$$

$$-\frac{(B2xo - A2xo)\,(C2xo - B2xo) - (A2yo - B2yo)\,(C2yo - B2yo)}{Lbc^2\,Ro}\Bigg) + 2\,($$

$$((A2yo - B2yo)\,(C2xo - B2xo) - (A2xo - B2xo)\,(C2yo - B2yo))$$

$$(JL22\,(C2xo - B2xo) - JL12\,(C2yo - B2yo)))\,/\,Lbc^4\Bigg)\Bigg)\cos\left(\frac{L2}{Ro}\right) + \frac{1}{2}\,Kb\left(\frac{1}{2}((-2\,B3yo\,C3xo\,Lab^2\right.$$

$$+ 2\,A3yo\,C3xo\,Lab^2 - 2\,A3yo\,B3xo\,Lab^2 - 2\,A3xo\,C3yo\,Lab^2 + 2\,B3xo\,C3yo\,Lab^2$$

$$+ 2\,A3xo\,B3yo\,Lab^2)$$

$$(-2\,JL22\,B3xo\,Lab^2 + 2\,JL12\,B3yo\,Lab^2 + 2\,JL22\,C3xo\,Lab^2 - 2\,JL12\,C3yo\,Lab^2)) \Big/ (Lab^4\,Lbc^4)$$

$$+ \frac{1}{18}((-6\,B3yo\,C3xo\,Rs + 6\,B3xo\,C3yo\,Rs - 6\,A3yo\,B3xo\,Rs + 6\,A3xo\,B3yo\,Rs + 6\,A3yo\,C3xo\,Rs$$

$$- 6\,A3xo\,C3yo\,Rs)\,(6\,JL12\,B3yo\,Rs - 6\,JL12\,C3yo\,Rs + 6\,JL22\,C3xo\,Rs - 6\,JL22\,B3xo\,Rs))\,/\,($$

$$\left.Lbc^4\,Rs^2)\right)\cos\left(\frac{L3}{Ro}\right) + \frac{1}{2}\,Kb\left(\frac{1}{2}((2\,A1yo\,B1xo\,Lab^2 - 2\,B1xo\,C1yo\,Lab^2 + 2\,A1xo\,C1yo\,Lab^2\right.$$

$$- 2\,A1yo\,C1xo\,Lab^2 - 2\,A1xo\,B1yo\,Lab^2 + 2\,B1yo\,C1xo\,Lab^2)$$

$$(-2\,JL12\,B1yo\,Lab^2 + 2\,JL12\,C1yo\,Lab^2 + 2\,JL22\,B1xo\,Lab^2 - 2\,JL22\,C1xo\,Lab^2)) \Big/ (Lbc^4\,Lab^4)$$

$$+ \frac{1}{18}((-6\,B1xo\,C1yo\,Rs + 6\,A1yo\,B1xo\,Rs + 6\,A1xo\,C1yo\,Rs - 6\,A1xo\,B1yo\,Rs + 6\,B1yo\,C1xo\,Rs$$

$$- 6\,A1yo\,C1xo\,Rs)\,(6\,JL22\,B1xo\,Rs - 6\,JL12\,B1yo\,Rs - 6\,JL22\,C1xo\,Rs + 6\,JL12\,C1yo\,Rs))\,/\,($$

$$\left.Lbc^4\,Rs^2)\right)\cos\left(\frac{L1}{Ro}\right) + \frac{1}{2}\,Kb\left(\frac{1}{2}((2\,B3xo^2\,Lbc^2 - 2\,B3yo^2\,Lab^2 - 2\,B3xo^2\,Lab^2 + 2\,B3yo^2\,Lbc^2\right.$$

$$+ 2\,A3xo^2\,Lbc^2 + 2\,B3yo\,A3yo\,Lab^2 + 2\,A3yo^2\,Lbc^2 - 2\,A3yo\,C3yo\,Lab^2 - 2\,A3xo\,C3xo\,Lab^2$$

$$- 4\,B3yo\,A3yo\,Lbc^2 + 2\,B3yo\,C3yo\,Lab^2 + 2\,B3xo\,A3xo\,Lab^2 + 2\,B3xo\,C3xo\,Lab^2$$

$$- 4\,B3xo\,A3xo\,Lbc^2)$$

$$(-2\,JL22\,B3xo\,Lab^2 + 2\,JL12\,B3yo\,Lab^2 + 2\,JL22\,C3xo\,Lab^2 - 2\,JL12\,C3yo\,Lab^2)) \Big/ (Lab^4\,Lbc^4)$$

$$+ \frac{1}{18}((-6\,A3yo\,C3yo\,Rs + 6\,B3yo\,C3yo\,Rs + 6\,A3yo\,B3yo\,Rs + 6\,A3xo\,B3xo\,Rs - 6\,B3yo^2\,Rs$$

$$+ 6\,B3xo\,C3xo\,Rs - 6\,A3xo\,C3xo\,Rs - 6\,B3xo^2\,Rs)$$

$$\left.(6\,JL12\,B3yo\,Rs - 6\,JL12\,C3yo\,Rs + 6\,JL22\,C3xo\,Rs - 6\,JL22\,B3xo\,Rs)) \Big/ (Lbc^4\,Rs^2)\right)\sin\left(\frac{L3}{Ro}\right)$$

$$+\frac{1}{2} Kb \Bigg(-\frac{1}{18} ((6\, B2xo\, C2yo\, Rs - 6\, B2yo\, C2xo\, Rs - 6\, A2xo\, C2yo\, Rs - 6\, A2yo\, B2xo\, Rs$$

$$+ 6\, A2xo\, B2yo\, Rs + 6\, A2yo\, C2xo\, Rs)(6\, B2xo\, C2xo\, Rs + 6\, B2yo\, A2yo\, Rs - 6\, B2yo^2\, Rs$$

$$+ 6\, B2yo\, C2yo\, Rs - 6\, A2xo\, C2xo\, Rs - 6\, A2yo\, C2yo\, Rs - 6\, B2xo^2\, Rs + 6\, B2xo\, A2xo\, Rs)) \big/ ($$

$$Lbc^4\, Rs^2\, Ro) + 2 \Bigg(\Bigg(\frac{2\, B2xo\, A2xo - B2xo^2 - A2xo^2 + 2\, B2yo\, A2yo - B2yo^2 - A2yo^2}{Lab^2}$$

$$- \frac{(B2xo - A2xo)(C2xo - B2xo) - (A2yo - B2yo)(C2yo - B2yo)}{Lbc^2} \Bigg)$$

$$((A2yo - B2yo)(C2xo - B2xo) - (A2xo - B2xo)(C2yo - B2yo)) \Bigg) \Big/ (Lbc^2\, Ro) \Bigg) \sin\left(\frac{L2}{Ro}\right)^2 + \frac{1}{2} Kb$$

$$\Bigg(2 \Bigg(\Bigg(-\frac{(JL23\, (C2xo - B2xo) - JL13\, (C2yo - B2yo))\, L3}{Lbc^2}$$

$$- \frac{-A2yo\, (C2xo - B2xo) - (-A2xo + Rs)(C2yo - B2yo)}{Lbc^2}$$

$$- \frac{(JL21\, (C2xo - B2xo) - JL11\, (C2yo - B2yo))\, L1}{Lbc^2}$$

$$- \frac{(JL22\, (C2xo - B2xo) - JL12\, (C2yo - B2yo))\, L2}{Lbc^2} \Bigg)$$

$$((A2yo - B2yo)(C2xo - B2xo) - (A2xo - B2xo)(C2yo - B2yo)) \Bigg) \Big/ (Lbc^2\, Ro) - 2 \Bigg(\Bigg($$

$$\frac{2\, B2xo\, A2xo - B2xo^2 - A2xo^2 + 2\, B2yo\, A2yo - B2yo^2 - A2yo^2}{Lab^2}$$

$$- \frac{(B2xo - A2xo)(C2xo - B2xo) - (A2yo - B2yo)(C2yo - B2yo)}{Lbc^2} \Bigg)$$

$$(JL22\, (C2xo - B2xo) - JL12\, (C2yo - B2yo)) \Bigg) \Big/ Lbc^2 - \frac{1}{3} \Bigg(\Bigg($$

$$\frac{1}{6} \frac{-\sqrt{3}\, C2xo + 3\, C2yo - 3\, C3yo + \sqrt{3}\, C3xo}{Rs}$$

$$+ \frac{1}{6} \frac{(6\, JL21\, C2xo\, Rs + 6\, JL11\, B2yo\, Rs - 6\, JL21\, B2xo\, Rs - 6\, JL11\, C2yo\, Rs)\, L1}{Lbc^2\, Rs}$$

$$+ \frac{1}{6} \frac{(6\, JL22\, C2xo\, Rs + 6\, JL12\, B2yo\, Rs - 6\, JL22\, B2xo\, Rs - 6\, JL12\, C2yo\, Rs)\, L2}{Lbc^2\, Rs}$$

$$+ \frac{1}{6} \frac{(6\, JL23\, C2xo\, Rs + 6\, JL13\, B2yo\, Rs - 6\, JL23\, B2xo\, Rs - 6\, JL13\, C2yo\, Rs)\, L3}{Lbc^2\, Rs} + \frac{1}{6}$$

$$\frac{-6\, Rs^2\, C2yo - 6\, A2xo\, B2yo\, Rs + 6\, A2yo\, B2xo\, Rs + 6\, Rs^2\, B2yo - 6\, A2yo\, C2xo\, Rs + 6\, A2xo\, C2yo\, Rs}{Rs\, Lbc^2}$$

$$\Bigg)(6\, B2xo\, C2yo\, Rs - 6\, B2yo\, C2xo\, Rs - 6\, A2xo\, C2yo\, Rs - 6\, A2yo\, B2xo\, Rs + 6\, A2xo\, B2yo\, Rs$$

$$+ 6\, A2yo\, C2xo\, Rs) \Bigg) \Big/ (Lbc^2\, Rs\, Ro) + \frac{1}{18} ((6\, B2xo\, C2xo\, Rs + 6\, B2yo\, A2yo\, Rs - 6\, B2yo^2\, Rs$$

$$+ 6\, B2yo\, C2yo\, Rs - 6\, A2xo\, C2xo\, Rs - 6\, A2yo\, C2yo\, Rs - 6\, B2xo^2\, Rs + 6\, B2xo\, A2xo\, Rs)$$

$$(6\, JL22\, C2xo\, Rs + 6\, JL12\, B2yo\, Rs - 6\, JL22\, B2xo\, Rs - 6\, JL12\, C2yo\, Rs)) \big/ (Lbc^4\, Rs^2) \Bigg) \sin\left(\frac{L2}{Ro}\right)$$

$$+ \frac{1}{2} Kb \Bigg(\frac{1}{2} ((-2\, A1yo^2\, Lbc^2 + 2\, B1xo^2\, Lab^2 - 2\, A1xo^2\, Lbc^2 + 2\, B1yo^2\, Lab^2 - 2\, B1yo^2\, Lbc^2$$

$$+ 4\, B1yo\, A1yo\, Lbc^2 - 2\, B1xo\, A1xo\, Lab^2 - 2\, B1xo\, C1xo\, Lab^2 - 2\, B1xo^2\, Lbc^2 + 4\, B1xo\, A1xo\, Lbc^2$$

$$- 2\, B1yo\, A1yo\, Lab^2 + 2\, A1yo\, C1yo\, Lab^2 + 2\, A1xo\, C1xo\, Lab^2 - 2\, B1yo\, C1yo\, Lab^2)$$

$$(-2\,JL12\,B1yo\,Lab^2 + 2\,JL12\,C1yo\,Lab^2 + 2\,JL22\,B1xo\,Lab^2 - 2\,JL22\,C1xo\,Lab^2))\,/\,(Lbc^4\,Lab^4)$$

$$+\frac{1}{18}((6\,B1yo^2\,Rs + 6\,B1xo^2\,Rs - 6\,B1yo\,C1yo\,Rs - 6\,A1yo\,B1yo\,Rs - 6\,B1xo\,C1xo\,Rs$$

$$- 6\,A1xo\,B1xo\,Rs + 6\,A1yo\,C1yo\,Rs + 6\,A1xo\,C1xo\,Rs)$$

$$(6\,JL22\,B1xo\,Rs - 6\,JL12\,B1yo\,Rs - 6\,JL22\,C1xo\,Rs + 6\,JL12\,C1yo\,Rs))\,/\,(Lbc^4\,Rs^2)\Bigg)\sin\left(\frac{L1}{Ro}\right)$$

$$+\frac{1}{2}\,Kb\Bigg(\frac{1}{2}((-2\,A1yo\,B1xo\,Lab^2 + 2\,JL13\,L3\,C1yo\,Lab^2 - 2\,JL13\,L3\,B1yo\,Lab^2$$

$$- 2\,A1xo\,C1yo\,Lab^2 + 2\,A1xo\,B1yo\,Lab^2 - 2\,JL11\,L1\,B1yo\,Lab^2 + 2\,JL12\,L2\,C1yo\,Lab^2$$

$$+ Rs\,B1yo\,Lab^2 - 2\,JL12\,L2\,B1yo\,Lab^2 - Rs\,C1yo\,Lab^2 + 2\,JL23\,L3\,B1xo\,Lab^2$$

$$+ 2\,JL22\,L2\,B1xo\,Lab^2 + 2\,JL11\,L1\,C1yo\,Lab^2 - 2\,JL22\,L2\,C1xo\,Lab^2 - 2\,JL23\,L3\,C1xo\,Lab^2$$

$$- 2\,JL21\,L1\,C1xo\,Lab^2 + 2\,JL21\,L1\,B1xo\,Lab^2 + 2\,A1yo\,C1xo\,Lab^2 + Rs\sqrt{3}\,B1xo\,Lab^2$$

$$- Rs\sqrt{3}\,C1xo\,Lab^2)$$

$$(-2\,JL12\,B1yo\,Lab^2 + 2\,JL12\,C1yo\,Lab^2 + 2\,JL22\,B1xo\,Lab^2 - 2\,JL22\,C1xo\,Lab^2))\,/\,(Lbc^4\,Lab^4)$$

$$+\frac{1}{2}((-2\,JL13\,L3\,C3yo\,Lab^2 + 2\,JL12\,L2\,B3yo\,Lab^2 + 2\,JL22\,L2\,C3xo\,Lab^2$$

$$- 2\,JL21\,L1\,B3xo\,Lab^2 + 2\,JL21\,L1\,C3xo\,Lab^2 - 2\,A3yo\,C3xo\,Lab^2 - 2\,JL23\,L3\,B3xo\,Lab^2$$

$$+ 2\,JL23\,L3\,C3xo\,Lab^2 - 2\,JL22\,L2\,B3xo\,Lab^2 + 2\,A3yo\,B3xo\,Lab^2 - 2\,JL12\,L2\,C3yo\,Lab^2$$

$$+ 2\,JL11\,L1\,B3yo\,Lab^2 - 2\,JL11\,L1\,C3yo\,Lab^2 - 2\,A3xo\,B3yo\,Lab^2 + 2\,A3xo\,C3yo\,Lab^2$$

$$- Rs\,B3yo\,Lab^2 + Rs\,C3yo\,Lab^2 + 2\,JL13\,L3\,B3yo\,Lab^2 + Rs\sqrt{3}\,B3xo\,Lab^2 - Rs\sqrt{3}\,C3xo\,Lab^2)$$

$$(-2\,JL22\,B3xo\,Lab^2 + 2\,JL12\,B3yo\,Lab^2 + 2\,JL22\,C3xo\,Lab^2 - 2\,JL12\,C3yo\,Lab^2))\,/\,(Lab^4\,Lbc^4)$$

$$+\frac{1}{18}((-6\,A1xo\,C1yo\,Rs + 6\,A1xo\,B1yo\,Rs + 3\,Rs^2\,B1yo + 6\,A1yo\,C1xo\,Rs - 6\,A1yo\,B1xo\,Rs$$

$$- 6\,JL21\,L1\,C1xo\,Rs + 6\,JL21\,L1\,B1xo\,Rs - 3\,Rs^2\,C1yo + 6\,JL22\,L2\,B1xo\,Rs - 6\,JL23\,L3\,C1xo\,Rs$$

$$+ 6\,JL23\,L3\,B1xo\,Rs - 6\,JL11\,L1\,B1yo\,Rs + 6\,JL11\,L1\,C1yo\,Rs - 6\,JL22\,L2\,C1xo\,Rs$$

$$+ 6\,JL12\,L2\,C1yo\,Rs - 6\,JL12\,L2\,B1yo\,Rs + 6\,JL13\,L3\,C1yo\,Rs - 6\,JL13\,L3\,B1yo\,Rs$$

$$+ 3\,C1yo\,Lbc^2 - 3\,C2yo\,Lbc^2 + \sqrt{3}\,C1xo\,Lbc^2 - \sqrt{3}\,C2xo\,Lbc^2 - 3\,Rs^2\sqrt{3}\,C1xo + 3\,Rs^2\sqrt{3}\,B1xo)$$

$$(6\,JL22\,B1xo\,Rs - 6\,JL12\,B1yo\,Rs - 6\,JL22\,C1xo\,Rs + 6\,JL12\,C1yo\,Rs))\,/\,(Lbc^4\,Rs^2) + \frac{1}{3}\Bigg(\Bigg($$

$$\frac{1}{6}\,\frac{2\sqrt{3}\,C3xo - 2\sqrt{3}\,C1xo}{Rs}$$

$$+\frac{1}{6}\,\frac{(-6\,JL11\,C3yo\,Rs + 6\,JL21\,C3xo\,Rs - 6\,JL21\,B3xo\,Rs + 6\,JL11\,B3yo\,Rs)\,L1}{Lbc^2\,Rs}$$

$$+\frac{1}{6}\,\frac{(6\,JL12\,B3yo\,Rs - 6\,JL12\,C3yo\,Rs + 6\,JL22\,C3xo\,Rs - 6\,JL22\,B3xo\,Rs)\,L2}{Lbc^2\,Rs}$$

$$+\frac{1}{6}\,\frac{(6\,JL23\,C3xo\,Rs - 6\,JL23\,B3xo\,Rs + 6\,JL13\,B3yo\,Rs - 6\,JL13\,C3yo\,Rs)\,L3}{Lbc^2\,Rs} + \frac{1}{6}($$

$$6\,A3xo\,C3yo\,Rs - 3\,Rs^2\,B3yo + 3\,Rs^2\,C3yo - 3\,Rs^2\sqrt{3}\,C3xo + 3\,Rs^2\sqrt{3}\,B3xo - 6\,A3xo\,B3yo\,Rs$$

$$- 6\,A3yo\,C3xo\,Rs + 6\,A3yo\,B3xo\,Rs)\,/\,(Rs\,Lbc^2)\Bigg)$$

$$(6\,JL12\,B3yo\,Rs - 6\,JL12\,C3yo\,Rs + 6\,JL22\,C3xo\,Rs - 6\,JL22\,B3xo\,Rs)\Bigg)\,/\,(Lbc^2\,Rs) - 2\Bigg(\Bigg($$

$$-\frac{(JL23\,(C2xo - B2xo) - JL13\,(C2yo - B2yo))\,L3}{Lbc^2}$$

$$-\frac{-A2yo\,(C2xo - B2xo) - (-A2xo + Rs)\,(C2yo - B2yo)}{Lbc^2}$$

$$-\frac{(JL21\,(C2xo - B2xo) - JL11\,(C2yo - B2yo))\,L1}{Lbc^2}$$

$$- \frac{(JL22\,(C2xo - B2xo) - JL12\,(C2yo - B2yo))\,L2}{Lbc^2} \Bigg)$$

$$(JL22\,(C2xo - B2xo) - JL12\,(C2yo - B2yo))\Bigg) \Big/ Lbc^2 + \frac{1}{3}\Bigg(\Bigg($$

$$\frac{1}{6}\,\frac{-\sqrt{3}\,C2xo + 3\,C2yo - 3\,C3yo + \sqrt{3}\,C3xo}{Rs}$$

$$+ \frac{1}{6}\,\frac{(6\,JL21\,C2xo\,Rs + 6\,JL11\,B2yo\,Rs - 6\,JL21\,B2xo\,Rs - 6\,JL11\,C2yo\,Rs)\,L1}{Lbc^2\,Rs}$$

$$+ \frac{1}{6}\,\frac{(6\,JL22\,C2xo\,Rs + 6\,JL12\,B2yo\,Rs - 6\,JL22\,B2xo\,Rs - 6\,JL12\,C2yo\,Rs)\,L2}{Lbc^2\,Rs}$$

$$+ \frac{1}{6}\,\frac{(6\,JL23\,C2xo\,Rs + 6\,JL13\,B2yo\,Rs - 6\,JL23\,B2xo\,Rs - 6\,JL13\,C2yo\,Rs)\,L3}{Lbc^2\,Rs} + \frac{1}{6}$$

$$\frac{-6\,Rs^2\,C2yo - 6\,A2xo\,B2yo\,Rs + 6\,A2yo\,B2xo\,Rs + 6\,Rs^2\,B2yo - 6\,A2yo\,C2xo\,Rs + 6\,A2xo\,C2yo\,Rs}{Rs\,Lbc^2}$$

$$\Bigg)(6\,JL22\,C2xo\,Rs + 6\,JL12\,B2yo\,Rs - 6\,JL22\,B2xo\,Rs - 6\,JL12\,C2yo\,Rs)\Bigg) \Big/ (Lbc^2\,Rs) + 2\,\frac{L2}{Ro^2}\Bigg)$$

$$H\_31 := \frac{1}{2}\,Kb\Bigg(2\,(((A2yo - B2yo)\,(C2xo - B2xo) - (A2xo - B2xo)\,(C2yo - B2yo))$$

$$(JL23\,(C2xo - B2xo) - JL13\,(C2yo - B2yo)))\,/\,Lbc^4 + \frac{1}{18}((6\,B2xo\,C2yo\,Rs - 6\,B2yo\,C2xo\,Rs$$

$$- 6\,A2xo\,C2yo\,Rs - 6\,A2yo\,B2xo\,Rs + 6\,A2xo\,B2yo\,Rs + 6\,A2yo\,C2xo\,Rs)$$

$$(6\,JL23\,C2xo\,Rs + 6\,JL13\,B2yo\,Rs - 6\,JL23\,B2xo\,Rs - 6\,JL13\,C2yo\,Rs))\,/\,(Lbc^4\,Rs^2)\Bigg)\cos\left(\frac{L2}{Ro}\right) +$$

$$\frac{1}{2}\,Kb\Bigg(\frac{1}{2}\Bigg((-2\,B3yo\,C3xo\,Lab^2 + 2\,A3yo\,C3xo\,Lab^2 - 2\,A3yo\,B3xo\,Lab^2 - 2\,A3xo\,C3yo\,Lab^2$$

$$+ 2\,B3xo\,C3yo\,Lab^2 + 2\,A3xo\,B3yo\,Lab^2)\Bigg(2\,\frac{B3yo\,C3yo\,Lab^2}{Ro} - 2\,\frac{A3xo\,C3xo\,Lab^2}{Ro}$$

$$- 2\,\frac{A3yo\,C3yo\,Lab^2}{Ro} + 2\,\frac{B3yo\,A3yo\,Lab^2}{Ro} + 2\,\frac{B3xo\,A3xo\,Lab^2}{Ro} + 2\,\frac{B3xo\,C3xo\,Lab^2}{Ro}$$

$$+ 2\,\frac{B3xo^2\,Lbc^2}{Ro} - 2\,\frac{B3yo^2\,Lab^2}{Ro} - 2\,\frac{B3xo^2\,Lab^2}{Ro} - 4\,\frac{B3yo\,A3yo\,Lbc^2}{Ro} + 2\,\frac{B3yo^2\,Lbc^2}{Ro}$$

$$+ 2\,\frac{A3xo^2\,Lbc^2}{Ro} - 4\,\frac{B3xo\,A3xo\,Lbc^2}{Ro} + 2\,\frac{A3yo^2\,Lbc^2}{Ro}\Bigg)\Bigg) \Big/ (Lab^4\,Lbc^4) + \frac{1}{18}((-6\,B3yo\,C3xo\,Rs$$

$$+ 6\,B3xo\,C3yo\,Rs - 6\,A3yo\,B3xo\,Rs + 6\,A3xo\,B3yo\,Rs + 6\,A3yo\,C3xo\,Rs - 6\,A3xo\,C3yo\,Rs)\,($$

$$-6\,A3yo\,C3yo\,Rs + 6\,B3yo\,C3yo\,Rs + 6\,A3yo\,B3yo\,Rs + 6\,A3xo\,B3xo\,Rs - 6\,B3yo^2\,Rs$$

$$+ 6\,B3xo\,C3xo\,Rs - 6\,A3xo\,C3xo\,Rs - 6\,B3xo^2\,Rs)) \Big/ (Lbc^4\,Rs^2\,Ro)\Bigg)\cos\left(\frac{L3}{Ro}\right)^2 + \Bigg(\frac{1}{2}\,Kb\Bigg(\frac{1}{18}($$

$$-6\,A3yo\,C3yo\,Rs + 6\,B3yo\,C3yo\,Rs + 6\,A3yo\,B3yo\,Rs + 6\,A3xo\,B3xo\,Rs - 6\,B3yo^2\,Rs$$

$$+ 6\,B3xo\,C3xo\,Rs - 6\,A3xo\,C3xo\,Rs - 6\,B3xo^2\,Rs)^2 \Big/ (Lbc^4\,Rs^2\,Ro) - \frac{1}{18}(-6\,B3yo\,C3xo\,Rs$$

$$+ 6\,B3xo\,C3yo\,Rs - 6\,A3yo\,B3xo\,Rs + 6\,A3xo\,B3yo\,Rs + 6\,A3yo\,C3xo\,Rs - 6\,A3xo\,C3yo\,Rs)^2 \Big/ ($$

$$Lbc^4\,Rs^2\,Ro) + \frac{1}{2}\Bigg((2\,B3xo^2\,Lbc^2 - 2\,B3yo^2\,Lab^2 - 2\,B3xo^2\,Lab^2 + 2\,B3yo^2\,Lbc^2 + 2\,A3xo^2\,Lbc^2$$

$$+ 2\,B3yo\,A3yo\,Lab^2 + 2\,A3yo^2\,Lbc^2 - 2\,A3yo\,C3yo\,Lab^2 - 2\,A3xo\,C3xo\,Lab^2 - 4\,B3yo\,A3yo\,Lbc^2$$

$$+ 2\,B3yo\,C3yo\,Lab^2 + 2\,B3xo\,A3xo\,Lab^2 + 2\,B3xo\,C3xo\,Lab^2 - 4\,B3xo\,A3xo\,Lbc^2)\Bigg($$

$$2\frac{B3yo\ C3yo\ Lab^2}{Ro}-2\frac{A3xo\ C3xo\ Lab^2}{Ro}-2\frac{A3yo\ C3yo\ Lab^2}{Ro}+2\frac{B3yo\ A3yo\ Lab^2}{Ro}$$

$$+2\frac{B3xo\ A3xo\ Lab^2}{Ro}+2\frac{B3xo\ C3xo\ Lab^2}{Ro}+2\frac{B3xo^2\ Lbc^2}{Ro}-2\frac{B3yo^2\ Lab^2}{Ro}-2\frac{B3xo^2\ Lab^2}{Ro}$$

$$-4\frac{B3yo\ A3yo\ Lbc^2}{Ro}+2\frac{B3yo^2\ Lbc^2}{Ro}+2\frac{A3xo^2\ Lbc^2}{Ro}-4\frac{B3xo\ A3xo\ Lbc^2}{Ro}+2\frac{A3yo^2\ Lbc^2}{Ro}\Bigg)\Bigg)\Big/ ($$

$$Lab^4\ Lbc^4)+\frac{1}{2}\Bigg((-2\ B3yo\ C3xo\ Lab^2+2\ A3yo\ C3xo\ Lab^2-2\ A3yo\ B3xo\ Lab^2-2\ A3xo\ C3yo\ Lab^2$$

$$+2\ B3xo\ C3yo\ Lab^2+2\ A3xo\ B3yo\ Lab^2)\Bigg(-2\frac{B3xo\ C3yo\ Lab^2}{Ro}+2\frac{A3yo\ B3xo\ Lab^2}{Ro}$$

$$+2\frac{A3xo\ C3yo\ Lab^2}{Ro}-2\frac{A3yo\ C3xo\ Lab^2}{Ro}+2\frac{B3yo\ C3xo\ Lab^2}{Ro}-2\frac{B3yo\ A3xo\ Lab^2}{Ro}\Bigg)\Bigg)\Big/ ($$

$$Lab^4\ Lbc^4)\Bigg)\sin\left(\frac{L3}{Ro}\right)+\frac{1}{2}Kb\Bigg(\frac{1}{3}\Bigg(\Bigg(\frac{1}{6}\frac{2\sqrt{3}\ C3xo-2\sqrt{3}\ C1xo}{Rs}$$

$$+\frac{1}{6}\frac{(-6\ JL11\ C3yo\ Rs+6\ JL21\ C3xo\ Rs-6\ JL21\ B3xo\ Rs+6\ JL11\ B3yo\ Rs)\ L1}{Lbc^2\ Rs}$$

$$+\frac{1}{6}\frac{(6\ JL12\ B3yo\ Rs-6\ JL12\ C3yo\ Rs+6\ JL22\ C3xo\ Rs-6\ JL22\ B3xo\ Rs)\ L2}{Lbc^2\ Rs}$$

$$+\frac{1}{6}\frac{(6\ JL23\ C3xo\ Rs-6\ JL23\ B3xo\ Rs+6\ JL13\ B3yo\ Rs-6\ JL13\ C3yo\ Rs)\ L3}{Lbc^2\ Rs}+\frac{1}{6}($$

$$6\ A3xo\ C3yo\ Rs-3\ Rs^2\ B3yo+3\ Rs^2\ C3yo-3\ Rs^2\sqrt{3}\ C3xo+3\ Rs^2\sqrt{3}\ B3xo-6\ A3xo\ B3yo\ Rs$$

$$-6\ A3yo\ C3xo\ Rs+6\ A3yo\ B3xo\ Rs)\Big/(Rs\ Lbc^2)\Bigg)(-6\ A3yo\ C3yo\ Rs+6\ B3yo\ C3yo\ Rs$$

$$+6\ A3yo\ B3yo\ Rs+6\ A3xo\ B3xo\ Rs-6\ B3yo^2\ Rs+6\ B3xo\ C3xo\ Rs-6\ A3xo\ C3xo\ Rs$$

$$-6\ B3xo^2\ Rs)\Bigg)\Big/(Lbc^2\ Rs\ Ro)+\frac{1}{18}((-6\ B3yo\ C3xo\ Rs+6\ B3xo\ C3yo\ Rs-6\ A3yo\ B3xo\ Rs$$

$$+6\ A3xo\ B3yo\ Rs+6\ A3yo\ C3xo\ Rs-6\ A3xo\ C3yo\ Rs)$$

$$(6\ JL23\ C3xo\ Rs-6\ JL23\ B3xo\ Rs+6\ JL13\ B3yo\ Rs-6\ JL13\ C3yo\ Rs))/(Lbc^4\ Rs^2)+\frac{1}{2}\Bigg(($$

$$-2\ JL13\ L3\ C3yo\ Lab^2+2\ JL12\ L2\ B3yo\ Lab^2+2\ JL22\ L2\ C3xo\ Lab^2-2\ JL21\ L1\ B3xo\ Lab^2$$

$$+2\ JL21\ L1\ C3xo\ Lab^2-2\ A3yo\ C3xo\ Lab^2-2\ JL23\ L3\ B3xo\ Lab^2+2\ JL23\ L3\ C3xo\ Lab^2$$

$$-2\ JL22\ L2\ B3xo\ Lab^2+2\ A3yo\ B3xo\ Lab^2-2\ JL12\ L2\ C3yo\ Lab^2+2\ JL11\ L1\ B3yo\ Lab^2$$

$$-2\ JL11\ L1\ C3yo\ Lab^2-2\ A3xo\ B3yo\ Lab^2+2\ A3xo\ C3yo\ Lab^2-Rs\ B3yo\ Lab^2+Rs\ C3yo\ Lab^2$$

$$+2\ JL13\ L3\ B3yo\ Lab^2+Rs\sqrt{3}\ B3xo\ Lab^2-Rs\sqrt{3}\ C3xo\ Lab^2)\Bigg(2\frac{B3yo\ C3yo\ Lab^2}{Ro}$$

$$-2\frac{A3xo\ C3xo\ Lab^2}{Ro}-2\frac{A3yo\ C3yo\ Lab^2}{Ro}+2\frac{B3yo\ A3yo\ Lab^2}{Ro}+2\frac{B3xo\ A3xo\ Lab^2}{Ro}$$

$$+2\frac{B3xo\ C3xo\ Lab^2}{Ro}+2\frac{B3xo^2\ Lbc^2}{Ro}-2\frac{B3yo^2\ Lab^2}{Ro}-2\frac{B3xo^2\ Lab^2}{Ro}-4\frac{B3yo\ A3yo\ Lbc^2}{Ro}$$

$$+2\frac{B3yo^2\ Lbc^2}{Ro}+2\frac{A3xo^2\ Lbc^2}{Ro}-4\frac{B3xo\ A3xo\ Lbc^2}{Ro}+2\frac{A3yo^2\ Lbc^2}{Ro}\Bigg)\Bigg)\Big/(Lab^4\ Lbc^4)+\frac{1}{2}(($$

$$-2\ B3yo\ C3xo\ Lab^2+2\ A3yo\ C3xo\ Lab^2-2\ A3yo\ B3xo\ Lab^2-2\ A3xo\ C3yo\ Lab^2$$

$$+2\ B3xo\ C3yo\ Lab^2+2\ A3xo\ B3yo\ Lab^2)$$

$$(-2\ JL13\ C3yo\ Lab^2-2\ JL23\ B3xo\ Lab^2+2\ JL23\ C3xo\ Lab^2+2\ JL13\ B3yo\ Lab^2))\Big/(Lab^4\ Lbc^4)$$

$$\Bigg)\Bigg)\cos\left(\frac{L3}{Ro}\right)+\frac{1}{2}Kb\Bigg(\frac{1}{2}((2\ A1yo\ B1xo\ Lab^2-2\ B1xo\ C1yo\ Lab^2+2\ A1xo\ C1yo\ Lab^2$$

$$-2\ A1yo\ C1xo\ Lab^2-2\ A1xo\ B1yo\ Lab^2+2\ B1yo\ C1xo\ Lab^2)$$

$$(2\ JL13\ C1yo\ Lab^2-2\ JL13\ B1yo\ Lab^2+2\ JL23\ B1xo\ Lab^2-2\ JL23\ C1xo\ Lab^2))\Big/(Lbc^4\ Lab^4)$$

$$+\frac{1}{18}((-6\, B1xo\, C1yo\, Rs+6\, A1yo\, B1xo\, Rs+6\, A1xo\, C1yo\, Rs-6\, A1xo\, B1yo\, Rs+6\, B1yo\, C1xo\, Rs$$
$$-6\, A1yo\, C1xo\, Rs)\,(-6\, JL23\, C1xo\, Rs+6\, JL23\, B1xo\, Rs+6\, JL13\, C1yo\, Rs-6\, JL13\, B1yo\, Rs))\,/\,($$
$$Lbc^4\, Rs^2)\Big)\cos\left(\frac{L1}{Ro}\right)+\frac{1}{2}\, Kb\Big(-\frac{1}{18}((-6\, B3yo\, C3xo\, Rs+6\, B3xo\, C3yo\, Rs-6\, A3yo\, B3xo\, Rs$$
$$+6\, A3xo\, B3yo\, Rs+6\, A3yo\, C3xo\, Rs-6\, A3xo\, C3yo\, Rs)\,(-6\, A3yo\, C3yo\, Rs+6\, B3yo\, C3yo\, Rs$$
$$+6\, A3yo\, B3yo\, Rs+6\, A3xo\, B3xo\, Rs-6\, B3yo^2\, Rs+6\, B3xo\, C3xo\, Rs-6\, A3xo\, C3xo\, Rs$$
$$-6\, B3xo^2\, Rs))\,\Big/\,(Lbc^4\, Rs^2\, Ro)+\frac{1}{2}\Big((2\, B3xo^2\, Lbc^2-2\, B3yo^2\, Lab^2-2\, B3xo^2\, Lab^2+2\, B3yo^2\, Lbc^2$$
$$+2\, A3xo^2\, Lbc^2+2\, B3yo\, A3yo\, Lab^2+2\, A3yo^2\, Lbc^2-2\, A3yo\, C3yo\, Lab^2-2\, A3xo\, C3xo\, Lab^2$$
$$-4\, B3yo\, A3yo\, Lbc^2+2\, B3yo\, C3yo\, Lab^2+2\, B3xo\, A3xo\, Lab^2+2\, B3xo\, C3xo\, Lab^2$$
$$-4\, B3xo\, A3xo\, Lbc^2)\Big(-2\,\frac{B3xo\, C3yo\, Lab^2}{Ro}+2\,\frac{A3yo\, B3xo\, Lab^2}{Ro}+2\,\frac{A3xo\, C3yo\, Lab^2}{Ro}$$
$$-2\,\frac{A3yo\, C3xo\, Lab^2}{Ro}+2\,\frac{B3yo\, C3xo\, Lab^2}{Ro}-2\,\frac{B3yo\, A3xo\, Lab^2}{Ro}\Big)\Big)\Big/\,(Lab^4\, Lbc^4)\Big)\sin\left(\frac{L3}{Ro}\right)^2+\frac{1}{2}$$
$$Kb\Big(\frac{1}{2}\Big((-2\, JL13\, L3\, C3yo\, Lab^2+2\, JL12\, L2\, B3yo\, Lab^2+2\, JL22\, L2\, C3xo\, Lab^2$$
$$-2\, JL21\, L1\, B3xo\, Lab^2+2\, JL21\, L1\, C3xo\, Lab^2-2\, A3yo\, C3xo\, Lab^2-2\, JL23\, L3\, B3xo\, Lab^2$$
$$+2\, JL23\, L3\, C3xo\, Lab^2-2\, JL22\, L2\, B3xo\, Lab^2+2\, A3yo\, B3xo\, Lab^2-2\, JL12\, L2\, C3yo\, Lab^2$$
$$+2\, JL11\, L1\, B3yo\, Lab^2-2\, JL11\, L1\, C3yo\, Lab^2-2\, A3xo\, B3yo\, Lab^2+2\, A3xo\, C3yo\, Lab^2$$
$$-Rs\, B3yo\, Lab^2+Rs\, C3yo\, Lab^2+2\, JL13\, L3\, B3yo\, Lab^2+Rs\sqrt{3}\, B3xo\, Lab^2-Rs\sqrt{3}\, C3xo\, Lab^2)\Big($$
$$-2\,\frac{B3xo\, C3yo\, Lab^2}{Ro}+2\,\frac{A3yo\, B3xo\, Lab^2}{Ro}+2\,\frac{A3xo\, C3yo\, Lab^2}{Ro}-2\,\frac{A3yo\, C3xo\, Lab^2}{Ro}$$
$$+2\,\frac{B3yo\, C3xo\, Lab^2}{Ro}-2\,\frac{B3yo\, A3xo\, Lab^2}{Ro}\Big)\Big)\Big/\,(Lab^4\, Lbc^4)+\frac{1}{2}((2\, B3xo^2\, Lbc^2-2\, B3yo^2\, Lab^2$$
$$-2\, B3xo^2\, Lab^2+2\, B3yo^2\, Lbc^2+2\, A3xo^2\, Lbc^2+2\, B3yo\, A3yo\, Lab^2+2\, A3yo^2\, Lbc^2$$
$$-2\, A3yo\, C3yo\, Lab^2-2\, A3xo\, C3xo\, Lab^2-4\, B3yo\, A3yo\, Lbc^2+2\, B3yo\, C3yo\, Lab^2$$
$$+2\, B3xo\, A3xo\, Lab^2+2\, B3xo\, C3xo\, Lab^2-4\, B3xo\, A3xo\, Lbc^2)$$
$$(-2\, JL13\, C3yo\, Lab^2-2\, JL23\, B3xo\, Lab^2+2\, JL23\, C3xo\, Lab^2+2\, JL13\, B3yo\, Lab^2))\,\Big/\,(Lab^4\, Lbc^4)$$
$$-\frac{1}{3}\Big(\Big(\Big(\frac{1}{6}\,\frac{2\sqrt{3}\, C3xo-2\sqrt{3}\, C1xo}{Rs}$$
$$+\frac{1}{6}\,\frac{(-6\, JL11\, C3yo\, Rs+6\, JL21\, C3xo\, Rs-6\, JL21\, B3xo\, Rs+6\, JL11\, B3yo\, Rs)\, L1}{Lbc^2\, Rs}$$
$$+\frac{1}{6}\,\frac{(6\, JL12\, B3yo\, Rs-6\, JL12\, C3yo\, Rs+6\, JL22\, C3xo\, Rs-6\, JL22\, B3xo\, Rs)\, L2}{Lbc^2\, Rs}$$
$$+\frac{1}{6}\,\frac{(6\, JL23\, C3xo\, Rs-6\, JL23\, B3xo\, Rs+6\, JL13\, B3yo\, Rs-6\, JL13\, C3yo\, Rs)\, L3}{Lbc^2\, Rs}+\frac{1}{6}($$
$$6\, A3xo\, C3yo\, Rs-3\, Rs^2\, B3yo+3\, Rs^2\, C3yo-3\, Rs^2\sqrt{3}\, C3xo+3\, Rs^2\sqrt{3}\, B3xo-6\, A3xo\, B3yo\, Rs$$
$$-6\, A3yo\, C3xo\, Rs+6\, A3yo\, B3xo\, Rs)\,\Big/\,(Rs\, Lbc^2)\Big)(-6\, B3yo\, C3xo\, Rs+6\, B3xo\, C3yo\, Rs$$
$$-6\, A3yo\, B3xo\, Rs+6\, A3xo\, B3yo\, Rs+6\, A3yo\, C3xo\, Rs-6\, A3xo\, C3yo\, Rs)\Big)\Big/\,(Lbc^2\, Rs\, Ro)+\frac{1}{18}(($$
$$-6\, A3yo\, C3yo\, Rs+6\, B3yo\, C3yo\, Rs+6\, A3yo\, B3yo\, Rs+6\, A3xo\, B3xo\, Rs-6\, B3yo^2\, Rs$$
$$+6\, B3xo\, C3xo\, Rs-6\, A3xo\, C3xo\, Rs-6\, B3xo^2\, Rs)$$
$$(6\, JL23\, C3xo\, Rs-6\, JL23\, B3xo\, Rs+6\, JL13\, B3yo\, Rs-6\, JL13\, C3yo\, Rs))\,\Big/\,(Lbc^4\, Rs^2)\Big)\sin\left(\frac{L3}{Ro}\right)$$
$$+\frac{1}{2}\, Kb\Big(\frac{1}{18}((6\, B2xo\, C2xo\, Rs+6\, B2yo\, A2yo\, Rs-6\, B2yo^2\, Rs+6\, B2yo\, C2yo\, Rs-6\, A2xo\, C2xo\, Rs$$

$- 6\ A2yo\ C2yo\ Rs - 6\ B2xo^2\ Rs + 6\ B2xo\ A2xo\ Rs)$

$(6\ JL23\ C2xo\ Rs + 6\ JL13\ B2yo\ Rs - 6\ JL23\ B2xo\ Rs - 6\ JL13\ C2yo\ Rs)) \Big/ (Lbc^4\ Rs^2) - 2\Bigg(\Bigg($

$$\frac{2\ B2xo\ A2xo - B2xo^2 - A2xo^2 + 2\ B2yo\ A2yo - B2yo^2 - A2yo^2}{Lab^2}$$

$$- \frac{(B2xo - A2xo)(C2xo - B2xo) - (A2yo - B2yo)(C2yo - B2yo)}{Lbc^2}\Bigg)$$

$(JL23\ (C2xo - B2xo) - JL13\ (C2yo - B2yo))\Bigg) \Big/ Lbc^2\Bigg) \sin\left(\frac{L2}{Ro}\right) + \frac{1}{2} Kb \left(\frac{1}{2}((-2\ A1yo^2\ Lbc^2\right.$

$+ 2\ B1xo^2\ Lab^2 - 2\ A1xo^2\ Lbc^2 + 2\ B1yo^2\ Lab^2 - 2\ B1yo^2\ Lbc^2 + 4\ B1yo\ A1yo\ Lbc^2$

$- 2\ B1xo\ A1xo\ Lab^2 - 2\ B1xo\ C1xo\ Lab^2 - 2\ B1xo^2\ Lbc^2 + 4\ B1xo\ A1xo\ Lbc^2 - 2\ B1yo\ A1yo\ Lab^2$

$+ 2\ A1yo\ C1yo\ Lab^2 + 2\ A1xo\ C1xo\ Lab^2 - 2\ B1yo\ C1yo\ Lab^2)$

$(2\ JL13\ C1yo\ Lab^2 - 2\ JL13\ B1yo\ Lab^2 + 2\ JL23\ B1xo\ Lab^2 - 2\ JL23\ C1xo\ Lab^2)) \Big/ (Lbc^4\ Lab^4)$

$+ \frac{1}{18}((6\ B1yo^2\ Rs + 6\ B1xo^2\ Rs - 6\ B1yo\ C1yo\ Rs - 6\ A1yo\ B1yo\ Rs - 6\ B1xo\ C1xo\ Rs$

$- 6\ A1xo\ B1xo\ Rs + 6\ A1yo\ C1yo\ Rs + 6\ A1xo\ C1xo\ Rs)$

$(-6\ JL23\ C1xo\ Rs + 6\ JL23\ B1xo\ Rs + 6\ JL13\ C1yo\ Rs - 6\ JL13\ B1yo\ Rs)) \Big/ (Lbc^4\ Rs^2)\Bigg) \sin\left(\frac{L1}{Ro}\right)$

$+ \frac{1}{2} Kb \left(\frac{1}{2}((-2\ A1yo\ B1xo\ Lab^2 + 2\ JL13\ L3\ C1yo\ Lab^2 - 2\ JL13\ L3\ B1yo\ Lab^2\right.$

$- 2\ A1xo\ C1yo\ Lab^2 + 2\ A1xo\ B1yo\ Lab^2 - 2\ JL11\ L1\ B1yo\ Lab^2 + 2\ JL12\ L2\ C1yo\ Lab^2$

$+ Rs\ B1yo\ Lab^2 - 2\ JL12\ L2\ B1yo\ Lab^2 - Rs\ C1yo\ Lab^2 + 2\ JL23\ L3\ B1xo\ Lab^2$

$+ 2\ JL22\ L2\ B1xo\ Lab^2 + 2\ JL11\ L1\ C1yo\ Lab^2 - 2\ JL22\ L2\ C1xo\ Lab^2 - 2\ JL23\ L3\ C1xo\ Lab^2$

$- 2\ JL21\ L1\ C1xo\ Lab^2 + 2\ JL21\ L1\ B1xo\ Lab^2 + 2\ A1yo\ C1xo\ Lab^2 + Rs\sqrt{3}\ B1xo\ Lab^2$

$- Rs\sqrt{3}\ C1xo\ Lab^2)$

$(2\ JL13\ C1yo\ Lab^2 - 2\ JL13\ B1yo\ Lab^2 + 2\ JL23\ B1xo\ Lab^2 - 2\ JL23\ C1xo\ Lab^2)) \Big/ (Lbc^4\ Lab^4)$

$$+ \frac{1}{3}\Bigg(\Bigg(\frac{1}{6}\frac{2\sqrt{3}\ C3xo - 2\sqrt{3}\ C1xo}{Rs}$$

$$+ \frac{1}{6}\frac{(-6\ JL11\ C3yo\ Rs + 6\ JL21\ C3xo\ Rs - 6\ JL21\ B3xo\ Rs + 6\ JL11\ B3yo\ Rs)\ L1}{Lbc^2\ Rs}$$

$$+ \frac{1}{6}\frac{(6\ JL12\ B3yo\ Rs - 6\ JL12\ C3yo\ Rs + 6\ JL22\ C3xo\ Rs - 6\ JL22\ B3xo\ Rs)\ L2}{Lbc^2\ Rs}$$

$$+ \frac{1}{6}\frac{(6\ JL23\ C3xo\ Rs - 6\ JL23\ B3xo\ Rs + 6\ JL13\ B3yo\ Rs - 6\ JL13\ C3yo\ Rs)\ L3}{Lbc^2\ Rs} + \frac{1}{6}($$

$6\ A3xo\ C3yo\ Rs - 3\ Rs^2\ B3yo + 3\ Rs^2\ C3yo - 3\ Rs^2\sqrt{3}\ C3xo + 3\ Rs^2\sqrt{3}\ B3xo - 6\ A3xo\ B3yo\ Rs$

$- 6\ A3yo\ C3xo\ Rs + 6\ A3yo\ B3xo\ Rs) \Big/ (Rs\ Lbc^2)\Bigg)$

$(6\ JL23\ C3xo\ Rs - 6\ JL23\ B3xo\ Rs + 6\ JL13\ B3yo\ Rs - 6\ JL13\ C3yo\ Rs)\Bigg) \Big/ (Lbc^2\ Rs) + \frac{1}{18}(($

$-6\ A1xo\ C1yo\ Rs + 6\ A1xo\ B1yo\ Rs + 3\ Rs^2\ B1yo + 6\ A1yo\ C1xo\ Rs - 6\ A1yo\ B1xo\ Rs$

$- 6\ JL21\ L1\ C1xo\ Rs + 6\ JL21\ L1\ B1xo\ Rs - 3\ Rs^2\ C1yo + 6\ JL22\ L2\ B1xo\ Rs - 6\ JL23\ L3\ C1xo\ Rs$

$+ 6\ JL23\ L3\ B1xo\ Rs - 6\ JL11\ L1\ B1yo\ Rs + 6\ JL11\ L1\ C1yo\ Rs - 6\ JL22\ L2\ C1xo\ Rs$

$+ 6\ JL12\ L2\ C1yo\ Rs - 6\ JL12\ L2\ B1yo\ Rs + 6\ JL13\ L3\ C1yo\ Rs - 6\ JL13\ L3\ B1yo\ Rs$

$+ 3\ C1yo\ Lbc^2 - 3\ C2yo\ Lbc^2 + \sqrt{3}\ C1xo\ Lbc^2 - \sqrt{3}\ C2xo\ Lbc^2 - 3\ Rs^2\sqrt{3}\ C1xo + 3\ Rs^2\sqrt{3}\ B1xo)$

$(-6\ JL23\ C1xo\ Rs + 6\ JL23\ B1xo\ Rs + 6\ JL13\ C1yo\ Rs - 6\ JL13\ B1yo\ Rs)) \Big/ (Lbc^4\ Rs^2) + \frac{1}{3}\Bigg(\Bigg($

$$\frac{1}{6}\frac{-\sqrt{3}\ C2xo + 3\ C2yo - 3\ C3yo + \sqrt{3}\ C3xo}{Rs}$$

$$+\frac{1}{6}\,\frac{(6\,JL21\,C2xo\,Rs+6\,JL11\,B2yo\,Rs-6\,JL21\,B2xo\,Rs-6\,JL11\,C2yo\,Rs)\,L1}{Lbc^2\,Rs}$$

$$+\frac{1}{6}\,\frac{(6\,JL22\,C2xo\,Rs+6\,JL12\,B2yo\,Rs-6\,JL22\,B2xo\,Rs-6\,JL12\,C2yo\,Rs)\,L2}{Lbc^2\,Rs}$$

$$+\frac{1}{6}\,\frac{(6\,JL23\,C2xo\,Rs+6\,JL13\,B2yo\,Rs-6\,JL23\,B2xo\,Rs-6\,JL13\,C2yo\,Rs)\,L3}{Lbc^2\,Rs}+\frac{1}{6}$$

$$\frac{-6\,Rs^2\,C2yo-6\,A2xo\,B2yo\,Rs+6\,A2yo\,B2xo\,Rs+6\,Rs^2\,B2yo-6\,A2yo\,C2xo\,Rs+6\,A2xo\,C2yo\,Rs}{Rs\,Lbc^2}$$

$$\Bigg)(6\,JL23\,C2xo\,Rs+6\,JL13\,B2yo\,Rs-6\,JL23\,B2xo\,Rs-6\,JL13\,C2yo\,Rs)\Bigg)\Big/(Lbc^2\,Rs)-2\Bigg(\Bigg(\Bigg($$

$$-\frac{(JL23\,(C2xo-B2xo)-JL13\,(C2yo-B2yo))\,L3}{Lbc^2}$$

$$-\frac{-A2yo\,(C2xo-B2xo)-(-A2xo+Rs)\,(C2yo-B2yo)}{Lbc^2}$$

$$-\frac{(JL21\,(C2xo-B2xo)-JL11\,(C2yo-B2yo))\,L1}{Lbc^2}$$

$$-\frac{(JL22\,(C2xo-B2xo)-JL12\,(C2yo-B2yo))\,L2}{Lbc^2}\Bigg)$$

$$(JL23\,(C2xo-B2xo)-JL13\,(C2yo-B2yo))\Bigg)\Big/Lbc^2+\frac{1}{2}((-2\,JL13\,L3\,C3yo\,Lab^2$$

$$+2\,JL12\,L2\,B3yo\,Lab^2+2\,JL22\,L2\,C3xo\,Lab^2-2\,JL21\,L1\,B3xo\,Lab^2+2\,JL21\,L1\,C3xo\,Lab^2$$

$$-2\,A3yo\,C3xo\,Lab^2-2\,JL23\,L3\,B3xo\,Lab^2+2\,JL23\,L3\,C3xo\,Lab^2-2\,JL22\,L2\,B3xo\,Lab^2$$

$$+2\,A3yo\,B3xo\,Lab^2-2\,JL12\,L2\,C3yo\,Lab^2+2\,JL11\,L1\,B3yo\,Lab^2-2\,JL11\,L1\,C3yo\,Lab^2$$

$$-2\,A3xo\,B3yo\,Lab^2+2\,A3xo\,C3yo\,Lab^2-Rs\,B3yo\,Lab^2+Rs\,C3yo\,Lab^2+2\,JL13\,L3\,B3yo\,Lab^2$$

$$+Rs\sqrt{3}\,B3xo\,Lab^2-Rs\sqrt{3}\,C3xo\,Lab^2)$$

$$(-2\,JL13\,C3yo\,Lab^2-2\,JL23\,B3xo\,Lab^2+2\,JL23\,C3xo\,Lab^2+2\,JL13\,B3yo\,Lab^2))\Big/(Lab^4\,Lbc^4)$$

$$+2\,\frac{L3}{Ro^2}\Bigg)$$

D.2 Non-parametric Form of the Dynamic Model

The non-parametric form of the dynamic model is formulated by substantiation of all the parameters in the model presented in Appendix D.1. After the substantiation, the matrices $\mathbf{K(l)}$, $\mathbf{C(l,\dot{l})}$ and $\mathbf{H(l)}$ of the non-parametric forms of are obtained. The following tables show this substantiation process. It is noted that for clarity, all the values shown in these tables keep 4 effective digits.

Table D.1 Initial coordinates (unit in m) of all the joint points: A_i, B_i and C_i (i=1,2,3)

A1xo	A1yo	B1xo	B1yo	A2xo	A2yo	B2xo	B2yo	A3xo
.008386	.02852	-.008301	.03448	.02051	-.02153	.03401	-.01005	-.02889
A3yo	B3xo	B3yo	C1xo	C1yo	C2xo	C2yo	C3xo	C3yo
-.006998	-.02571	-.02443	-.01477	.02559	.029546	0	-.01477	-.02559

Table D.2 Mass (unit in Kg) and moment of inertia (unit in KgM^2) of the end-effector and all the links

Me (mass of end-effector)	Mab (mass of bar A_iB_i, i=1,2,3)	Mbc (mass of bar B_iC_i, i=1,2,3)
.1323	.1416e-1	.7628e-2
Ie (moment of inertia of end-effector)	Iab (moment of inertia of link A_iB_i, i=1,2,3)	Ibc (moment of inertia of link B_iC_i, i=1,2,3)
.9622e-5	.1483e-5	.3077e-6

Table D.3 Other parameter values

rou (density of the material)	Ro (shown in Figure 2.3)	Kb (spring stiffness)
8.25e3 (Kg/m^3)	3.5 (mm)	40.8963 (N/m)

$K\_11 := 1.711619836 + .02652829408 \sin(285.7142857\, L1) + .05737063933 \cos(285.7142857\, L1)$

$K\_12 := -.6748959083 - .006399691688 \cos(285.7142857\, L1) + .02175882715 \sin(285.7142857\, L1)$
$+ .003786205208 \cos(285.7142857\, L2) - .01287302405 \sin(285.7142857\, L2)$

$K\_13 := -.6748959083 + .003786205219 \cos(285.7142857\, L1) - .01287302403 \sin(285.7142857\, L1)$
$- .006399691686 \cos(285.7142857\, L3) + .02175882716 \sin(285.7142857\, L3)$

$K\_21 := -.6748959083 - .006399691688 \cos(285.7142857\, L1) + .02175882715 \sin(285.7142857\, L1)$
$+ .003786205208 \cos(285.7142857\, L2) - .01287302405 \sin(285.7142857\, L2)$

$K\_22 := 1.711619836 + .02652829408 \sin(285.7142857\, L2) + .05737063933 \cos(285.7142857\, L2)$

$K\_23 := -.6748959081 - .006399691676 \cos(285.7142857\, L2) + .02175882716 \sin(285.7142857\, L2)$
$+ .003786205207 \cos(285.7142857\, L3) - .01287302405 \sin(285.7142857\, L3)$

$K\_31 := -.6748959083 + .003786205219 \cos(285.7142857\, L1) - .01287302403 \sin(285.7142857\, L1)$
$- .006399691686 \cos(285.7142857\, L3) + .02175882716 \sin(285.7142857\, L3)$

$K\_32 := -.6748959081 - .006399691676 \cos(285.7142857\, L2) + .02175882716 \sin(285.7142857\, L2)$
$+ .003786205207 \cos(285.7142857\, L3) - .01287302405 \sin(285.7142857\, L3)$

$K\_33 := 1.711619835 + .05737063933 \cos(285.7142857\, L3) + .02652829405 \sin(285.7142857\, L3)$

$C\_11 := 3.789756297\, L1dot \cos(285.7142857\, L1) - 8.195805620\, L1dot \sin(285.7142857\, L1)$
$- .9142416695 \sin(285.7142857\, L1)\, L2dot - 3.108403879 \cos(285.7142857\, L1)\, L2dot$
$+ .5408864600 \sin(285.7142857\, L1)\, L3dot + 1.839003433 \cos(285.7142857\, L1)\, L3dot$

$C\_12 := .9142416695\, L1dot \sin(285.7142857\, L1) + 3.108403879\, L1dot \cos(285.7142857\, L1)$
$- 1.081772917\, L2dot \sin(285.7142857\, L2) - 3.678006871\, L2dot \cos(285.7142857\, L2)$

$C\_13 := -.5408864600\, L1dot \sin(285.7142857\, L1) - 1.839003433\, L1dot \cos(285.7142857\, L1)$
$+ 1.828483339\, L3dot \sin(285.7142857\, L3) + 6.216807760\, L3dot \cos(285.7142857\, L3)$

$C\_21 := 1.828483339\, L1dot \sin(285.7142857\, L1) + 6.216807757\, L1dot \cos(285.7142857\, L1)$
$- .5408864585\, L2dot \sin(285.7142857\, L2) - 1.839003436\, L2dot \cos(285.7142857\, L2)$

$C\_22 := 3.789756297\, L2dot \cos(285.7142857\, L2) - 8.195805620\, L2dot \sin(285.7142857\, L2)$
$+ .5408864585 \sin(285.7142857\, L2)\, L1dot + 1.839003436 \cos(285.7142857\, L2)\, L1dot$
$- .9142416680 \sin(285.7142857\, L2)\, L3dot - 3.108403880 \cos(285.7142857\, L2)\, L3dot$

$C\_23 := .9142416680\, L2dot \sin(285.7142857\, L2) + 3.108403880\, L2dot \cos(285.7142857\, L2)$
$- 1.081772916\, L3dot \sin(285.7142857\, L3) - 3.678006871\, L3dot \cos(285.7142857\, L3)$

$C\_31 := -1.081772920\, L1dot \sin(285.7142857\, L1) - 3.678006866\, L1dot \cos(285.7142857\, L1)$
$+ .9142416695\, L3dot \sin(285.7142857\, L3) + 3.108403880\, L3dot \cos(285.7142857\, L3)$

$C\_32 := 1.828483336\, L2dot \sin(285.7142857\, L2) + 6.216807760\, L2dot \cos(285.7142857\, L2)$
$- .5408864580\, L3dot \sin(285.7142857\, L3) - 1.839003436\, L3dot \cos(285.7142857\, L3)$

$C\_33 := -8.195805620\, L3dot \sin(285.7142857\, L3) + 3.789756293\, L3dot \cos(285.7142857\, L3)$
$- .9142416695\, L1dot \sin(285.7142857\, L3) - 3.108403880\, L1dot \cos(285.7142857\, L3)$
$+ .5408864580\, L2dot \sin(285.7142857\, L3) + 1.839003436\, L2dot \cos(285.7142857\, L3)$

$$
\begin{aligned}
H\_11 := {} & 34474.50308 \cos(285.7142857\, L1) + 55815.62208 \sin(285.7142857\, L1) \\
& - 19903.86364 \sin(285.7142857\, L2) + 32225.16448 \cos(285.7142857\, L2) \\
& + .5686818183\ 10^7 \cos(285.7142857\, L1)\, L2 - .5686818177\ 10^7 \cos(285.7142857\, L1)\, L3 \\
& - 28680.12737 \sin(285.7142857\, L1) \cos(285.7142857\, L1) \\
& + .9207189840\ 10^7 \sin(285.7142857\, L1)\, L2 - .9207189834\ 10^7 \sin(285.7142857\, L1)\, L3 \\
& + .1397002006\ 10^8\, L1 - .5315773540\ 10^7\, L2 - .5315773540\ 10^7\, L3 \\
& - 68949.00616 \cos(285.7142857\, L1)^2 + 34474.50308 + 19903.86364 \sin(285.7142857\, L3) \\
& - 32225.16448 \cos(285.7142857\, L3)
\end{aligned}
$$

$$
\begin{aligned}
H\_21 := {} & 55815.62217 \sin(285.7142857\, L2) + 34474.50308 \cos(285.7142857\, L2) \\
& - .5686818183\ 10^7 \cos(285.7142857\, L2)\, L1 + .5686818180\ 10^7 \cos(285.7142857\, L2)\, L3 \\
& + .9207189851\ 10^7 \sin(285.7142857\, L2)\, L3 \\
& - 28680.12743 \cos(285.7142857\, L2) \sin(285.7142857\, L2) + 34474.50308 \\
& - 68949.00616 \cos(285.7142857\, L2)^2 - .9207189851\ 10^7 \sin(285.7142857\, L2)\, L1 \\
& + 19903.86364 \sin(285.7142857\, L1) - 32225.16444 \cos(285.7142857\, L1) - .5315773540\ 10^7\, L1 \\
& + .1397002006\ 10^8\, L2 - .5315773530\ 10^7\, L3 - 19903.86364 \sin(285.7142857\, L3) \\
& + 32225.16448 \cos(285.7142857\, L3)
\end{aligned}
$$

$$
\begin{aligned}
H\_31 := {} & 55815.62217 \sin(285.7142857\, L3) + 34474.50308 \cos(285.7142857\, L3) \\
& + 19903.86363 \sin(285.7142857\, L2) - 32225.16448 \cos(285.7142857\, L2) \\
& - 19903.86362 \sin(285.7142857\, L1) - 68949.00616 \cos(285.7142857\, L3)^2 + 34474.50308 \\
& + .1397002005\ 10^8\, L3 + 32225.16442 \cos(285.7142857\, L1) - .5315773540\ 10^7\, L1 \\
& - .5315773530\ 10^7\, L2 - .5686818183\ 10^7 \cos(285.7142857\, L3)\, L2 \\
& + .5686818183\ 10^7 \cos(285.7142857\, L3)\, L1 \\
& - 28680.12746 \sin(285.7142857\, L3) \cos(285.7142857\, L3) \\
& - .9207189851\ 10^7 \sin(285.7142857\, L3)\, L2 + .9207189851\ 10^7 \sin(285.7142857\, L3)\, L1
\end{aligned}
$$

Appendix E: Control Simulation Program

The simulation of the control of the RRR compliant mechanism is performed using the SIMULINK tool in Matlab (Ver.5.3). The simulation program is put into the attached floppy disk. The operation of this simulation program is as follows:

1. Open Matlab and enter its command window.

2. Type '**dy_pa**' (execute the m-file '**dy_pa.m**') to load the initial condition (needed for solving the ordinary differential equation) for L_i and $\dot{L}_i$ (i=1,2,3), which are the initial displacement and velocity of the three PZT actuators, respectively.

3. Open a file '**dynamics_modelbase.mdl**' in the command window, and a window named '**dynamics_modelbase**' appears. In this window, there is a block named subsystem. Double click this block, and a window named '**dynamics_modelbase/subsystem**' appears.

4. In the window named '**dynamics_modelbase/subsystem**', there are three subsystem blocks named '**subsystem: L1**', '**subsystem: L2**', and '**subsystem: L3**' at the top of this window. Each subsystem is to control the corresponding PZT actuator 1, 2 and 3, respectively.

5. Double click the block '**subsystem: L1**'. A window named '**dynamics_modelbase/subsystem/ subsystem: L1**' appears. A model-based PD control block named '**PD controller 1**' is designed in this window. For demonstration purpose, the operation of '**subsystem: L1**' is explained here. The other two subsystems follow the same procedures. In this block, 'L1_e' and 'L1DOT_e' denote the displacement and velocity error of PZT actuator 1. 'Kp_1' and 'Kv_1' denote the proportional and derivative gain for this controller. The block named '**numerator_1**' and '**denominator**' are to implement the dynamic model to get the results of L1, L1_DOT ($\dot{L}_1$) and L1DDOT ($\ddot{L}_1$), respectively.

6. Find the icon '**simulation**' in the tool bar of the window, click and hold on this icon. A menu appears below this icon. Click on '**start**' command to start the simulation.
7. The results can be seen in the corresponding scope. The displacement and velocity error of PZT 1 can be seen in the scopes: '**L1_e**' and '**L1dot_e**'. The actual displacement, velocity and generating force of PZT actuator 1 can be seen in the scopes: '**L1**', '**L1_DOT**' and '**Q1**', respectively.